

CHARACTERIZATION OF AUTOANTIBODIES TO ADAMTS13 IN HIV-ASSOCIATED THROMBOTIC THROMBOCYTOPENIC PURPURA

By

MMAKGABU MARTHA KHEMISI

Submitted in fulfilment of the requirements in respect of the Doctoral Degree in Haematology in the Department of Haematology and Cell Biology in the Faculty of Health Sciences at the University of the Free State.

JANUARY 2020

Promotor: PROF MURIEL S. MEIRING

Department of Haematology and Cell Biology, University of the Free State

Co-promoter: Dr SUSAN LOUW

Department of Haematology and Molecular Medicine, University of the Witwatersrand

Faculty of Health Sciences

University of the Free State

Bloemfontein

South Africa



Declarations

I, Mmakgabu Martha Khemisi, declare that the thesis that I herewith submit for the Doctoral Degree in Haematology at the University of the Free State, is my independent work, and that I have not previously submitted it for a qualification at another institution of higher education.



Mmakgabu M. Khemisi

Acknowledgements

Firstly, I would like to extend many thanks to GOD and my family for their great support, motivation and patience throughout my studies and many challenges we conquered together.

Secondly, I would like to express my sincere gratitude for all guidance and assistance provided by the following persons and institutions:

Prof Muriel Meiring, it has been a privilege to learn and work alongside you.

Dr Susan Louw, for her dedication and unconditional support to this study.

The Department of Haematology and Cell Biology for their facilities, with greatest thanks to the Haemostasis team for all their support.

The National Health Laboratory Services for funding this project and making their facilities available for this study.

The Next Generation Sequencing Unit and the Department of Virology for making their facilities available for laboratory work and training.

Lastly, to everyone who opened their doors to assist me, either with teaching and or training, their contribution is highly appreciated.

“This Thesis is dedicated to my late father, Thabiso Simon Khemisi, for he is my rock and motivation in life.”

“Our greatest weakness lies in giving up.

The most certain way to succeed is always to try just one more time...”

Thomas A Adison

Table of contents

| | |
|---|-----|
| Declaration | i |
| Acknowledgements | ii |
| Table of contents | iii |
| Abbreviations and acronyms | a |
| List of figures | f |
| List of tables | h |
| ABSTRACT | 1 |
| CHAPTER 1: Introduction | 3 |
| CHAPTER 2: Literature review | 6 |
| 2.1 Introduction to ADAMTS13: Structure, function, biosynthesis and secretion | 7 |
| 2.2 Function of von Willebrand factor (WVF) | 15 |
| 2.3 Interactions of VWF and ADAMTS13 | 17 |
| 2.4 Regulation of ADAMTS13 | 19 |
| 2.4.1 Factors that enhance the proteolytic activity of ADAMTS13 | 20 |
| 2.4.2 Factors that inhibit the proteolytic activity of ADAMTS13 | 22 |
| 2.4.3 Endothelial dysfunction | 26 |
| 2.4.4. Microparticles (MPs) and ADAMTS13 | 27 |
| 2.5 Deficiency of ADAMTS13 | 28 |
| 2.5.1 Congenital ADAMTS13 deficiency (cTTP) | 28 |
| 2.5.2 Acquired ADAMTS13 deficiency | 30 |
| 2.5.2.1. Loss of immune tolerance in acquired TTP | 32 |
| 2.5.2.1.1. T-cell tolerance | 32 |
| 2.5.2.1.2. B-cell tolerance | 33 |
| 2.5.2.2. ADAMTS13 antigen presentation to CD4 ⁺ T-cell | 34 |
| 2.5.2.3. ADAMTS13-antibody Immune complexes | 35 |
| 2.5.2.4 Epitope mapping studies | 36 |
| 2.5.3. Subtypes of TTP | 40 |
| 2.5.3.1 HIV-associated TTP | 41 |
| 2.6 HIV-associated thrombotic microangiopathies (TMA's) | 46 |
| 2.6.1. Other systemic conditions | 47 |
| 2.7 ADAMTS13 assays for acquired TTP diagnosis | 49 |

| | |
|--|-----------|
| 2.8 Treatment of TTP | 52 |
| 2.9 Relapses | 54 |
| 2.10 Rationale of the study | 54 |
| 2.11 Aim and objectives | 55 |
| CHAPTER 3: Methodology | 56 |
| 3.1. Ethics | 56 |
| 3.2. Study design | 56 |
| 3.3. Study participants | 56 |
| 3.3.1. HIV-associated TTP patients..... | 56 |
| 3.3.2. HIV positive control non-TTP patients..... | 56 |
| 3.4. Inclusion criteria | 57 |
| 3.4.1. HIV-associated TTP plasma samples..... | 57 |
| 3.4.2. HIV positive control plasma samples..... | 59 |
| 3.4.3. De-identification of samples | 59 |
| 3.4.4. Specimen collection, processing and storage | 59 |
| 3.4.5. Pooled human normal plasma | 60 |
| 3.5. Materials and methods | 60 |
| 3.5.1. The HIV status of collected patient plasma samples | 60 |
| 3.5.2. Measurement of ADAMTS13 antigen and ADAMTS13 activity levels..... | 61 |
| 3.5.3. Measurement of autoantibodies to ADAMTS13..... | 62 |
| 3.5.3.1. Anti-ADAMTS13 IgG antibodies | 62 |
| 3.5.3.1.1. Mixing studies..... | 63 |
| 3.5.3.2. IgM and IgA antibodies..... | 64 |
| 3.5.3.2.1. Total IgM and IgA antibodies in plasma..... | 64 |
| 3.5.3.2.2. Anti-ADAMTS13 IgM and IgA antibodies..... | 65 |
| 3.5.4. VWF analysis..... | 66 |
| 3.5.4.1. VWF antigen (VWF:Ag) levels..... | 66 |
| 3.5.4.2. VWF propeptide (VWFpp) levels..... | 67 |
| 3.5.4.3. VWF multimer analysis..... | 68 |
| 3.5.5. Extraction of IgG autoantibodies | 69 |
| 3.5.5.1. Antibody IgG extraction..... | 69 |
| 3.5.5.2. Quantification of purified IgG..... | 70 |
| 3.5.5.3. The SDS-PAGE analysis of purified IgG..... | 70 |

| | | |
|---------------------------|---|-----------|
| 3.5.5.4. | Dialysis of purified IgG protein | 71 |
| 3.5.6. | Epitope mapping studies of anti-ADAMTS13 IgG antibodies in HIV-associated TTP..... | 72 |
| 3.5.6.1. | Synthetic peptides | 72 |
| 3.5.6.2. | Development of a Peptide ELISA..... | 76 |
| 3.5.6.3. | Plate viability assay..... | 77 |
| 3.5.6.4. | Peptide ELISA..... | 78 |
| 3.5.6.5. | Monitoring binding of purified IgG antibodies to linear overlapping peptides of ADAMTS13 using Peptide ELISA..... | 82 |
| 3.6. | Statistical analysis | 83 |
| CHAPTER 4: Results | | 84 |
| 4.1. | ADAMTS13 antigen and activity levels..... | 84 |
| 4.2. | Autoantibodies to ADAMTS13..... | 85 |
| 4.2.1. | Anti-ADAMTS13 IgG antibodies | 85 |
| 4.2.1.1. | Mixing studies..... | 87 |
| 4.2.2. | IgM and IgA antibodies | 88 |
| 4.2.2.1. | Total IgM and IgA antibodies in plasma..... | 88 |
| 4.2.2.2. | Anti-ADAMTS13 IgM and IgA antibodies..... | 89 |
| 4.3. | VWF analysis..... | 91 |
| 4.3.1. | VWF antigen (VWF:Ag) levels..... | 91 |
| 4.3.2. | VWF propeptide (VWFpp) levels..... | 92 |
| 4.3.3. | VWF multimers analysis..... | 93 |
| 4.4. | Extraction of IgG autoantibodies..... | 94 |
| 4.4.1. | Quantification of purified IgG..... | 94 |
| 4.4.2. | The SDS-PAGE analysis of purified IgG..... | 95 |
| 4.5. | Epitope mapping studies of anti-ADAMTS13 IgG antibodies in HIV-associated TTP patient samples..... | 97 |
| 4.5.1. | Peptide library..... | 97 |
| 4.5.2. | Development of a peptide ELISA..... | 97 |
| 4.5.2.1. | Plate viability assay..... | 97 |
| 4.5.2.2. | Peptide ELISA..... | 98 |
| 4.5.2.3. | Binding of purified IgG antibodies to linear overlapping peptides of ADMATS13 using Peptide ELISA..... | 101 |

| | |
|--|-----|
| CHAPTER 5: Discussions | 116 |
| CHAPTER 6: Conclusion | 129 |
| Limitations and future studies..... | 130 |
| Impact of the study | 131 |
| REFERENCES | 132 |
| Appendix A: The full-length ADAMTS13 nucleotide sequence | 159 |
| Appendix B: Laboratory data of HIV-associated TTP patients at initial disease presentation. | 161 |
| Appendix C: Laboratory data of HIV positive control plasma samples | 165 |
| <i>Supplementary data 1</i> | 168 |
| <i>Supplementary data 2</i> | 171 |
| <i>Supplementary data 3</i> | 174 |
| <i>Supplementary data 4</i> | 177 |
| <i>Supplementary data 5</i> | 179 |
| <i>Supplementary data 6</i> | 181 |
| <i>Supplementary data 7</i> | 185 |
| <i>Supplementary data 8</i> | 188 |
| <i>Supplementary data 9</i> | 191 |
| <i>Supplementary data 10</i> | 192 |
| <i>Supplementary data 11</i> | 194 |
| <i>Supplementary data 12</i> | 198 |
| <i>Supplementary data 13</i> | 199 |

Abbreviations and acronyms

% - percentage

$\alpha_v\beta^3$ - alpha-v beta-3

$\mu\text{g}/\mu\text{L}$ – microgram/ microliter

$^{\circ}\text{C}$ – degree Celsius

A280/260 – Absorbance ratio at 280/260

aa – amino acid

ADAMTS13 - A Disintegrin and Metalloproteinase with Thrombospondin Motifs member 13

ART – Antiretroviral therapy

BPB – Bromophenol blue

BSA – Bovine serum albumin

BU – Bethesda Unit

Ca^{2+} - Calcium ion

CAMs – cell adhesion molecules

CB – Collagen binding

CD – Cluster of differentiation

Cl^- - Chlorine ion

CLSI – Clinical and Laboratory Standards Institute

CSA – Cyclosporine

cTTP – congenital Thrombotic Thrombocytopenic Purpura

CUB – Complement 1r/s, Uegf [a sea urchin embryonic protein], and Bone morphogenetic protein 1

CV – Coefficient of variation

Cys – Cysteine-rich

dH₂O – distilled water

DIC – Disseminated intravascular coagulation

Dis – Disintegrin-like

dL – decilitre

DMSO – Dimethyl sulfoxide

DTT – dithiothreitol

E. coli – Escherichia coli

EC – Endothelial cell

ELAMs – Endothelial Leukocyte Adhesion Molecules

ELISA – Enzyme-linked immunosorbent assay

EMPs – Endothelial Microparticles

FRETS – Fluorescence Resonance Energy Transfer

FV – Factor five

FVII – Factor seven

FVIII – Factor eight

FS – Free State

FXa – activated Factor ten

g – Gram

Glu/ E – Glutamic acid

GPIb α - glycoprotein Ib α

H₂O₂ – Hydrogen peroxide

H₂SO₄ – Sulphuric acid

HAART – Highly active antiretroviral therapy

Hb – haemoglobin

HCl – Hydrochloric acid

HCV – Hepatitis C virus (HCV)

HEK 293 cells –

HELLP – Elevated liver function and low platelet

HIV – Human Immunodeficiency Virus

HLA - Human leukocyte antigen

HOCL - Hypochlorous acid

HRP – Horseradish peroxidase

HSREC – Health Sciences Research Ethics Committee

HUS – Haemolytic Uremic Syndrome

HUVECs – Human umbilical vein endothelial cells

Ig (A, G, M) – Immunoglobulin (A, G, M)

IL (1b, 6, 8) – Interleukin (1b, 6, 8)

Inc. - Incorporation

Inh – Inhibitor

ISO - International Organization for Standardization

kDa – kilo Delta

L - Litre

LDH – Lactate dehydrogenase

M – Molar

mAb – monoclonal Antibody

MAHA – Microangiopathic haemolytic anaemia

Met1606 – Methionine residue at position 1606

mg – milligram

MHC – Major histocompatibility complex

mL – millilitre

mm³ – millimetre cubic

MP – Metalloprotease

MPO - Myeloperoxidase

MPs – Microparticles

MWCO - Molecular weight cut-off

n – nano

N - Negative

Na₂HPO₄ – disodium ortho-phosphate

NaH₂PO₄ – Sodium hypophosphate

NaCl – Sodium chloride

ND – Not done

NHLS - National Health Laboratory Services

nm – nanometer

OD – Optical density

OPD – Ortho-phnylenediamine

P - Positive

pAb – polyclonal Antibody

PAGE – Polyacrylamide gel

PBS – Phosphate buffered saline

PEX – Plasma exchange

PLT – platelet

PMPs – Platelet microparticles

PNP – Pooled normal plasma

POX – Proline oxidase

Pro1645 – Proline residue at position 1645

PT – Prothrombin time

PTT – Partial thrombin time

rmp – revolutions per minute

RNA – Ribonucleic acid

RSA – Republic of South Africa

SA – Streptavidin

ScFv – Single chain variable fragment

SD – Standard deviation

SDS – Sodium dodecyl sulfate

SHL – Special Haemostasis laboratory

SLE – Systemic lupus erythematosus

SOP – Standard operating procedure

STAS SA – Statistics South Africa

TCR – T-cell receptor

TEMED - Tetramethylethylenediamine

TF – Tissue factor

TMA – Thrombotic microangiopathy

TMB – tetramethylbenzidine

TNF α – Tissue necrosis factor alpha

tPA – tissue Plasminogen Activator

TSP1 – Thrombospondin type -1 motif

TTP – Thrombotic Thrombocytopenic Purpura

Tyr1605 – Tyrosine residue at position 1065

μ - Micro

U/mL – International unit/ millilitre

UFS – University of the Free State

UK – United Kingdom

UL-VWF – Ultra large von Willebrand Factor

USA – United States of America

V – Volt

Viz. - Namely

VWF – Von Willebrand Factor

VWF:Ag – Von Willebrand Factor antigen

VWFpp – von Willebrand factor propeptide

Zn²⁺ - Zinc ion

List of figures

| | |
|--|-----|
| Figure 2.1: Domain organization of ADAMTS13. | 7 |
| Figure 2.2: The molecular model of ADAMTS13 protein. | 7 |
| Figure 2.3: ADAMTS13 MP – Dis-like residue structure. | 9 |
| Figure 2.4: ADAMTS13 TSP1-1 residue structure. | 11 |
| Figure 2.5: ADAMTS13 Cysteine-rich and Spacer domains residue structure. | 12 |
| Figure 2.6: Proposed model for the interaction of ADAMTS13 with unravelled VWF A2 domain. | 13 |
| Figure 2.7: Schematic presentation of a multi-domain organization of a mature VWF. | 16 |
| Figure 2.8: Proteolysis of VWF by ADAMTS13. | 18 |
| Figure 2.9: Summary of factors enhancing the proteolytic activity of ADAMTS13. | 21 |
| Figure 2.10: Summary of factors inhibiting the proteolytic activity of ADAMTS13. | 23 |
| Figure 2.11: Locations of mutations in variable regions of ADATMS13 gene in patients with cTTP. | 29 |
| Figure 2.12. Schematic presentation of the onset of immune-mediated TTP. | 35 |
| Figure 2.13. Contributing factors in HIV-associated TTP development. | 46 |
| Figure 3.1: Schematic presentation of the steps involved in the determination of the ADAMTS13 antigen and activity levels using the Technoclone® assay. | 62 |
| Figure 3.2: Mini floating device with 2mL dialysis cups fitted and placed into a suitable sized beaker. | 72 |
| Figure 3.3. Overlapping linear peptide sequences from the Metalloprotease domain 75-150. | 74 |
| Figure 3.4. A schematic presentation of a Peptide ELISA. | 77 |
| Figure 3.5: Checkerboard titration of peptide antigen and control samples. | 79 |
| Figure 3.6: Checkerboard titration of HRP conjugated detection antibody. | 80 |
| Figure 3.7: Checkerboard titration of blocking conditions. | 81 |
| Figure 4.1: Comparison of ADAMTS13 antigen and ADAMTS13 activity levels results of individual plasma samples between the HIV-associated TTP group (blue circles) and the HIV positive plasma group (red squares). | 84 |
| Figure 4.2: Anti-ADAMTS13 IgG antibody results of the HIV-associate TTP (blue circles) and the HIV positive (red squares) plasma samples. | 86 |
| Figure 4.3: Anti-ADAMTS13 IgM and IgA autoantibody results detected from HIV-associated TTP and HIV positive plasma samples. | 90 |
| Figure 4.4: Analysis of plasma VWF multimer patterns. | 94 |
| Figure 4.4.1: VWF multimer patterns obtained by 1% SDS agarose gel electrophoresis. (<i>Supplementary data 9</i>) | 191 |
| Figure 4.5. SDS-PAGE results of purified IgG antibodies. | 96 |
| Figure 4.6: Standard curve for the streptavidin-biotin binding. | 97 |
| Figure 4.7A - E: Optimization of the Peptide ELISA working conditions. | 98 |

Figure 4.8A - E: IgG autoantibody-binding patterns observed from individual HIV-associated TTP samples.104

Figure 4.9A - C: IgG autoantibody-binding patterns from individual HIV positive samples.107

Figure 4.10A - E: IgG autoantibody-binding patterns from individual HIV-associated TTP samples.111

Figure 4.11: Anti-ADAMTS13 IgG antibody binding to ADAMTS13 proximal domains.115

List of tables

| | |
|---|-----|
| Table 2.1: A summary of IgG autoantibody-ADAMTS13 epitope mapping studies..... | 39 |
| Table 2.2: Systemic conditions presenting with MAHA and thrombocytopenia..... | 48 |
| Table 3.1: Laboratory inclusion criteria for HIV-associated TTP diagnosis..... | 58 |
| Table 3.2: The ADAMTS13 domain groupings selected for designing a peptide library. | 73 |
| Table 3.3: List of peptide sequences of the ADAMTS13 Metalloprotease to disintegrin-like domains..... | 74 |
| Table 3.4: List of peptide sequences from the ADAMTS13 Cysteine-rich to Spacer domains..... | 75 |
| Table 4: The HIV status results. (<i>Supplementary data 1</i>)..... | 168 |
| Table 4.1: - ADAMTS13 antigen levels and ADAMTS13 activity of HIV-associated TTP and HIV positive individual plasma samples. (<i>Supplementary data 2</i>)..... | 171 |
| Table 4.1.1: ADAMTS13 antigen and ADAMTS13 activity levels of HIV-associated TTP and HIV positive plasma samples. | 85 |
| Table 4.2: Anti-ADAMTS13 IgG antibody titer of HIV-associated TTP and HIV positive individual plasma samples. (<i>Supplementary data 3</i>). | 174 |
| Table 4.2.1: Anti-ADAMTS13 IgG autoantibodies in HIV-associated TTP and HIV positive control groups. | 86 |
| Table 4.2.2: ADAMTS13 antigen levels and anti-ADAMTS13 IgG antibody titer results of HIV-associated TTP plasma samples..... | 87 |
| Table 4.3: Mixing studies results and the inhibitory Bethesda units for individual HIV-associated TTP plasma samples. (<i>Supplementary data 4</i>). | 177 |
| Table 4.3.1: Anti-ADAMTS13 IgG antibody concentrations and Bethesda Inhibitory (BU) results in HIV-associated TTP plasma samples. | 88 |
| Table 4.4: The concentrations of IgM and IgA antibodies in plasma samples of HIV-associated TTP and HIV positive patients. (<i>Supplementary data 5</i>). | 178 |
| Table 4.4.1: The mean concentrations of IgM and IgA in HIV-associated TTP and HIV positive groups..... | 89 |
| Table 4.5 A: Anti-ADAMTS13 IgM and anti-ADAMTS13 IgA in HIV-associated TTP and HIV positive plasma samples. (<i>Supplementary data 6</i>). | 181 |
| Table 4.5 B: Anti-ADAMTS13 IgM and IgA ELISA assay precision calculation results. (<i>Supplementary data 6</i>). | 182 |
| Table 4.5 C: Determining the cut-off values for anti-ADAMTS13 IgM and anti-ADAMTS13 IgA. (<i>Supplementary data 6</i>). | 183 |
| Table 4.5.1: Precision results for anti-ADAMTS13 IgM antibody ELISA assay..... | 90 |
| Table 4.5.2: Precision results for anti-ADAMTS13 IgA antibody ELISA assay..... | 91 |
| Table 4.6: VWF antigen levels of HIV-associated TTP plasma samples and HIV positive samples. (<i>Supplementary data 7</i>). | 185 |

| | |
|---|-----|
| Table 4.6.1: von Willebrand factor antigen levels in HIV-associated TTP and HIV positive plasma samples. | 91 |
| Table 4.6.2: The VWF:Ag levels and ADAMTS13 levels in HIV-associated TTP group and HIV positive control group. | 92 |
| Table 4.7: The VWF propeptide levels and VWFpp/VWF:Ag ratio of HIV-associated TTP and HIV positive plasma samples. (<i>Supplementary data 8</i>). | 188 |
| Table 4.7.1: VWFpp levels for the HIV-associated TTP and HIV positive plasma samples. | 93 |
| Table 4.8: Obtained concentrations of purified IgG from individual plasma samples. (<i>Supplementary data 10</i>). | 192 |
| Table 4.8.1: Obtained concentrations of Purified IgG antibody from plasma samples. | 95 |
| Table 4.9: Shows the precision results for anti-ADAMTS13 IgG antibody in Peptide ELISA assay. | 101 |
| Table 4.10: The details of reactive peptides and OD values obtained for each patient IgG antibody sample. (<i>Supplementary data 12</i>). | 198 |
| Table 4.10.1: Summary of ADAMTS13 domains with reactivity towards IgG antibodies of individual HIV-associated TTP and HIV positive control samples. | 103 |
| Table 4.11: Linear peptides with potential antigenic regions in the Metalloprotease (MP) and Disintegrin (Dis)-like domains. | 109 |
| Table 4.12: Table 4.12: Linear peptides with potential antigenic regions detected from the Cysteine-rich (Cys) and Spacer (Spa) domains. | 114 |
| Table 4.13: Shared and non-shared linear ADAMTS13 peptide epitope regions binding IgG autoantibodies isolated from HIV-associated TTP patient and HIV positive control cohort samples. | 115 |

ABSTRACT

Thrombotic thrombocytopenic purpura (TTP) is a potentially fatal thrombotic microangiopathic disorder that can occur secondary to human immunodeficiency virus (HIV) infection and is prevalent in sub-Saharan Africa. The pathogenesis involves deficiency of the von Willebrand factor (VWF) cleaving protease ADAMTS13 and the presence of anti-ADAMTS13 autoantibodies. Insufficient information is however available regarding epitope specificity and reactivity of the ADAMTS13 autoantibodies present in HIV-associated TTP. In this study, epitope-mapping analysis was performed to provide novel insight into the specific antigenic regions (epitopes) on ADAMTS13 domains affected by autoantibodies in patients with HIV-associated TTP. Anti-ADAMTS13 IgG autoantibodies are also present in HIV positive individuals, and their binding specificities were analysed.

Methods: A total of 59 HIV-associated TTP plasma samples with severe ADAMTS13 deficiency of less than 10% were collected prior to plasma therapy and analysed. Hundred (100) plasma samples from HIV positive patients without TTP were included as a control group. We compared the ADAMTS13 parameters i.e. ADAMTS13 antigen and activity levels and autoantibody titers and VWF parameters i.e. antigen levels, propeptide and multimeric patterns between the HIV-associated TTP and the control cohort. To understand the pathogenic mechanisms of anti-ADAMTS13 IgG autoantibodies, a synthetic peptide library comprising of ADAMTS13 proximal domains was used to map potential epitope regions that bind to purified anti-ADAMTS13 IgG antibodies isolated from 53 individual HIV-associated TTP patient samples and 18 control cohort samples using a newly developed Peptide ELISA-based assay.

Results: The HIV-associated TTP patient plasma samples had severely reduced ADAMTS13 antigen (<50%) and activity (<10%) levels compared to the HIV positive control samples (ADAMTS13 antigen and activity levels >25% but <150%), with a statistically significance difference ($p < 0.05$). Anti-ADAMTS13 IgG autoantibodies were detected in 90% of the HIV-associated TTP patient samples, and only in 18% of the HIV infected control cohort plasma samples. About 90% of the HIV-associated TTP patient samples were found to contain clinically significant ADAMTS13 autoantibodies of which 64% were inhibitory as demonstrated with mixing studies. Furthermore, high anti-ADAMTS13 IgG autoantibody titers ($\geq 50 \mu\text{g/mL}$) were detected in samples with a low median ADAMTS13 antigen level of $\sim 4.5\%$ and low anti-ADAMTS13 IgG autoantibody titers ($< 50 \mu\text{g/mL}$) in samples with a high median ADAMTS13 antigen level of $\sim 12.5\%$. Additional anti-ADAMTS13 autoantibodies that were

detected in the HIV-associated TTP patient samples were IgM (30%) and IgA (64%) isotypes in combination with IgG isotype autoantibodies. In 18 out of the 100 HIV positive control patient samples positive for anti-ADAMTS13 IgG autoantibodies, 28% were positive for IgM and 22% for IgA autoantibody isotypes. Both groups presented with normal to significantly increased VWF:Ag and VWFpp levels (>200%), and no statistically significant difference between them ($p>0.05$). The epitope mapping results revealed that the Metalloprotease, Cysteine-rich and Spacer domains were constantly (100%) involved in binding anti-ADAMTS13 IgG antibodies isolated from the 53 patients with HIV-associated TTP samples. 58% of these samples contained anti-ADAMTS13 IgG antibodies that bind to the C-terminal part of ADAMTS13 Disintegrin-like domain. However, in the HIV positive plasma samples, the Metalloprotease and Disintegrin-like domains were the primary targets (100%) for anti-ADAMTS13 IgG antibody binding, while only 61% of samples with IgG antibodies showed binding to the Cysteine-rich and Spacer domains of ADAMTS13. The IgG autoantibodies detected in the control cohort samples shared linear epitopes at various regions of the ADAMTS13 proximal domains investigated with anti-ADAMTS13 IgG antibodies detected in HIV-associated TTP patient samples.

Conclusions: Most (90%) of patients diagnosed with HIV-associated TTP with severe ADAMTS13 activity levels of less than 10% have anti-ADAMTS13 autoantibodies. Thus, highlighting that ADAMTS13 autoantibody-mediated deficiency may be involved in HIV-associated TTP. Both inhibitory and non-inhibitory anti-ADAMTS13 autoantibodies are present in these patients, suggesting that different pathogenic mechanisms may be involved in HIV-associated TTP. The Metalloprotease, Cysteine-rich and Spacer domains are the primary target for anti-ADAMTS13 IgG autoantibodies in patients with HIV-associated TTP. In contrast, HIV positive patients without TTP may have anti-ADAMTS13 IgG autoantibodies, which may even share linear epitopes with those detected in patients with HIV-associated TTP, but their pathological relevance has not been elucidated. The results of this study provides new insight into the pathophysiology of HIV-associated TTP. HIV-associated TTP patients have anti-ADAMTS13 antibodies potentially affecting the proteolytic activity of this enzyme.

Key words: Human immunodeficiency virus, Thrombotic thrombocytopenic purpura, ADAMTS13, ADAMTS13 autoantibodies.

CHAPTER 1: Introduction

Thrombotic Thrombocytopenic Purpura (TTP) is a rare but life-threatening haematological condition classified under thrombotic microangiopathy (TMA) disorders (Moake, 2002). TMAs are a group of diseases characterised by microangiopathic haemolytic anaemia and thrombocytopenia associated with micro-vascular platelet-rich thrombi with ischaemic organ dysfunction that includes renal impairment and neurological abnormalities. In TTP, the systemic occlusion of the microcirculation often affects the central nervous system, and less frequently, the kidneys (Moake, 2002).

Dysfunction of a metalloproteinase enzyme, a Disintegrin and Metalloprotease with Thrombospondin motives member 13 (ADAMTS13), has been identified as playing a pathophysiological role in patients with chronic relapsing TTP (Zheng *et al.* 2001). This enzyme is responsible for regulating the size of ultra large von Willebrand Factor (UL-VWF) multimers that are haemostatically reactive to platelets. Defects or deficiencies of ADAMTS13 leads to the accumulation of UL-VWF multimers in the circulation, eventually forming VWF-platelet-rich thrombi under high shear stress conditions manifesting phenotypically as TTP. TTP is therefore a TMA with an absence or a severe deficiency of ADAMTS13 activity (<10%). These findings further differentiate TTP from other TMA disorders, such as haemolytic uremic syndrome (HUS) (Zheng *et al.* 2001).

Two types of TTP have been identified namely a congenital and acquired form. Congenital TTP is due to inherited mutations within the ADAMTS13 gene that can affect the secretion, expression or the activity of ADAMTS13 protein (Levy *et al.* 2001). Acquired TTP is often associated with severe deficiency of ADAMTS13 activity (<10%) and the presence of autoantibodies to ADAMTS13 (Reese *et al.* 2013; Scully *et al.* 2008; Peyvandi *et al.* 2008). Autoantibodies to ADAMTS13 can either block the activity of ADAMTS13 or promote rapid clearance of ADAMTS13 from the blood (Thomas *et al.* 2015). The acquired form of TTP is much more common than the inherited form, but for unknown reasons, it occurs more frequently in black African females (between the ages of 30 - 40 years) compared to males (Reese *et al.* 2013; Terrell *et al.* 2010).

The classically described forms of TTP are rare but a similar condition is now frequently observed in patients infected with the human immunodeficiency virus (HIV) in Sub-Saharan Africa (Swart *et al.* 2019). Since the discovery of the first case of HIV-associated TTP in the 1980's (Jokela *et al.* 1987), numerous cases of TTP associated with HIV infection have been reported in South Africa which is the sub-Saharan country with the highest HIV infection rate (Masoet *et al.* 2019; George *et al.* 2012; Visagie and Louw 2010; Gunther *et al.* 2007;). According to the 2019 mid-year population statistics

of South Africa, about 7.97 million (13.5%) people are estimated to be infected with HIV (STATS SA 2019) which is a growing health problem. Furthermore, the incidence of TTP related to HIV infection is much higher than the incidence of TTP in non-infected individuals (Masoet *et al.* 2019; George *et al.* 2012). Reports have also shown that relapses are more common occurring in up to 60% of patients with higher mortality rates (10-30%) in HIV vs. non-HIV TTP patients (Swart *et al.* 2019; Boro *et al.* 2011; Rock *et al.* 1991). The high mortality rates probably reflect diagnostic uncertainty coupled with an inability to identify at risk patients and unavailability of resources. Diagnostic and prognostic biomarkers have to be identified in patients with HIV-associated TTP.

TTP is common in patients with advanced HIV disease in whom it is associated with low CD4⁺ counts of below 200 cells per cubic millimetre of blood and high viral loads (Hart *et al.* 2011; Benjamin *et al.* 2009; Miller *et al.* 2005; Gunther *et al.* 2007). The incidence of HIV-associated TTP was expected to decline with widespread access to antiretroviral therapy (ART) (Becker *et al.* 2004). However, cases of TTP in HIV infection are still prevalent in South Africa despite increased access to ART (Masoet *et al.* 2019; Louw *et al.* 2018). Recently, TTP is being observed even in HIV infected patients with viral loads below the detectable limit and on ART (Louw *et al.* 2018; Novitsky *et al.* 2005), but the exact underlying pathogenesis is not clear.

HIV-associated TTP is probably related to heterogeneous mechanisms related to the viral infection. HIV endothelial cell dysfunction has been considered as important in the pathogenesis of HIV-associated TTP (Cruccu *et al.* 1994; Gunther *et al.* 2006; Fujimura and Matsumoto 2010; Pos *et al.* 2011). Although some studies suggested that endothelial dysfunction may not be the primary cause of TTP, rather that vascular perturbation may be the consequence of TTP (de Wit *et al.* 2003). Autoimmune dysfunction with autoantibody production and aberrant T-cell responses may contribute significantly to the depletion of ADAMTS13 in HIV-associated TTP (Boro *et al.* 2011; Massabki *et al.* 1997). HIV infection with a low CD4⁺ lymphocyte count (less than 200/mm³) and a high viral load are associated with an increased incidence of ADAMTS13 autoantibodies (Chen *et al.* 2002; Gunther *et al.* 2007). Furthermore, the presence of ADAMTS13 autoantibodies may contribute to severe ADAMTS13 deficiency and trigger HIV-associated TTP (Boro *et al.* 2011; Coppo *et al.* 2004; Massabki *et al.* 1997). Several studies have confirmed the importance of autoantibodies to ADAMTS13 in the pathogenesis of HIV-associated TTP (Alwan *et al.* 2017; Thomas *et al.* 2015; Scheiflinger *et al.* 2003; Tsai *et al.* 2000; Zheng *et al.* 2001; Furlan *et al.* 1997).

The current literature on HIV-associated TTP is limited and contains mostly case studies and database records of patients. There is also limited data on the presence of ADAMTS13

autoantibodies in HIV-associated TTP. The majority of acquired TTP case studies assessing these parameters, either do not include or specifically excluded HIV-positive patients (Swart *et al.* 2019; Alwan *et al.* 2019). Two previous South African studies have detected autoantibodies to ADAMTS13 in HIV-associated TTP as well as in HIV infected people without TTP (Gunther *et al.* 2007; Meiring *et al.* 2012). The binding specificity of these autoantibodies however remains unknown. The detection of ADAMTS13 autoantibodies and defining their epitopes on the ADAMTS13 protein in HIV-associated TTP patients may be of clinical value with disease prognostication and treatment efficacy assessment.

In some HIV-associated TTP cases, acquired ADAMTS13 deficiency may occur in the absence of detectable autoantibodies/ autoantibodies that inhibit ADAMTS13 (Zheng *et al.* 2004; Gunther *et al.* 2007). The possible mechanism may be the presence of non-neutralizing antibodies that increase clearance or inhibit ADAMTS13 binding to the endothelium without interfering with its activity (Scheiflinger *et al.* 2003; Thomas *et al.* 2015). The biological function of the IgG/IgM/IgA autoantibodies is determined by their specificity, affinity and sub-class designation, which results in different immunologic effector functions (Scheiflinger *et al.* 2003). Thus, the role of ADAMTS13 autoantibodies in the pathophysiology of HIV-associated TTP requires further investigations.

The antigenic determinants of autoantibodies that result in compromised ADAMTS13 activity in HIV-associated TTP need to be determined and will possibly assist in the identification of humoral immune responses which culminate in ADAMTS13 deficiency. Autoantibodies are also considered to be reliable prognostic biomarkers that can predict the severity of a disease (Page *et al.* 2017; Ferrari *et al.* 2007; Tsai and Lian, 1998). Detection, quantification and characterization of ADAMTS13 autoantibodies and subclass distribution may be potentially valuable in HIV patients at risk to develop or suffer from TTP. Important, autoantibody determination can be used to monitor therapeutic interventions.

The aim of this study was to use epitope mapping to provide us with a novel insight into the specific antigenic regions (epitopes) on ADAMTS13 domains affected immunologically by autoantibodies detected in HIV-associated TTP patients and to characterise the autoantibodies to ADAMTS13 that are present in HIV-associated TTP plasma. The results of this study will contribute to a better understanding of the disease, HIV-associated TTP.

CHAPTER 2. Literature review

The ADAMTS13 protein plays a central role in the pathogenesis of thrombotic thrombocytopenic purpura (TTP). With this literature review we will start by explaining the structure-function relationship of ADAMTS13, followed by a brief overview of interactions between the ADAMTS13 enzyme and its substrate, von Willebrand factor (VWF).

2.1. Introduction to ADAMTS13: Structure, function, biosynthesis and secretion

A disintegrin-like metalloproteinase with thrombospondin motif type 1 member 13 (ADAMTS13) is a member of multidomain extracellular protease enzymes (Zheng *et al.* 2001). Primarily synthesized in the hepatic stellate cells, ADAMTS13 is secreted into plasma in its active form (Zhou *et al.* 2005; Soejima *et al.* 2001). From its discovery in 2001, functional ADAMTS13 has been identified as a cleaving protease of ultra large (UL)-VWF multimers (Zheng *et al.* 2001).

The gene coding for ADAMTS13 is located in the long arm of chromosome 9 at position 34, and the mature protein consists of 1427 amino acids (GenBank: AAL11095.1, **Appendix A**). The structure of ADAMTS13 from its N-terminus, consists of a propeptide, metalloprotease domain (MP), a disintegrin-like domain (Dis-like), the first thrombospondin type-1 (TSP1) motif, a Cysteine-rich domain (Cys-rich), a Spacer domain, seven additional TSP1 repeats, and two CUB (Complement 1r/s, Uegf, Bone morphogenic protein 1) domains at the C-terminal (Zheng *et al.* 2001). The ADAMTS13 structure with domain organization is shown in **Figure 2.1**. A depiction of ADAMTS13 molecular structure in its folded and unfolded form is shown in **Figure 2.2**.

ADAMTS13

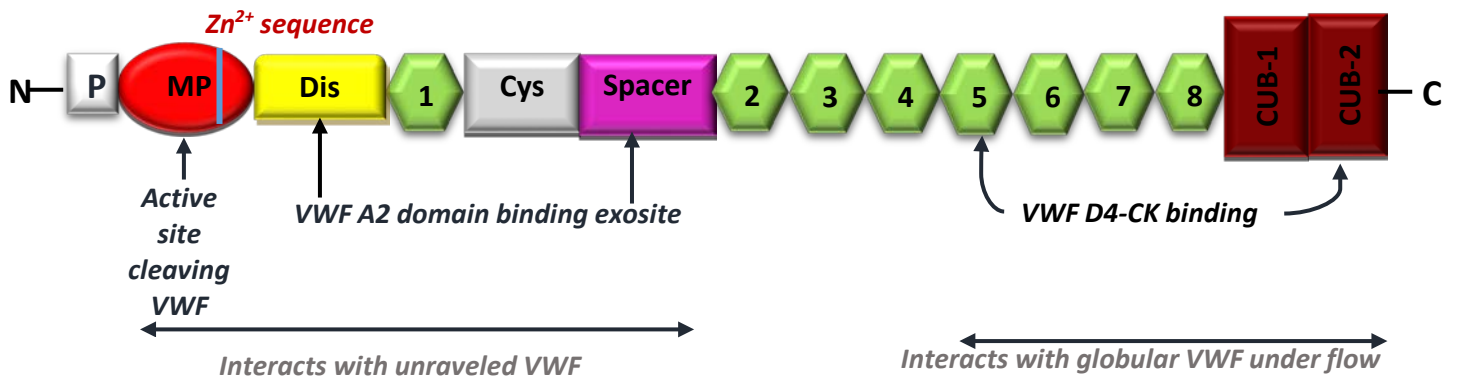


Figure 2.1: Domain organization of ADAMTS13.

From the N-terminal side: (P)- Propeptide, (MP)-Metalloprotease, (Dis)-Disintegrin-like domain, (1)-first thrombospondin type 1 repeat (TSP1), (Cys)-Cysteine-rich domain, (Spacer)-Spacer domain, (2-8)-second to eighth TSP1 repeats, and (CUB1 and CUB2)- CUB domains. The metalloprotease domain contains the active catalytic centre (with the location of the zinc-binding sequence shown in blue) that cleaves VWF. The N-terminal/proximal domains (MP – Spacer) recognize/bind to the unravelled VWF, and the C-terminal/distal domains (TSP2-8 – CUB) interact with globular VWF under high fluid shear stress (Crawley *et al.* 2011).

Molecular model of ADAMTS13

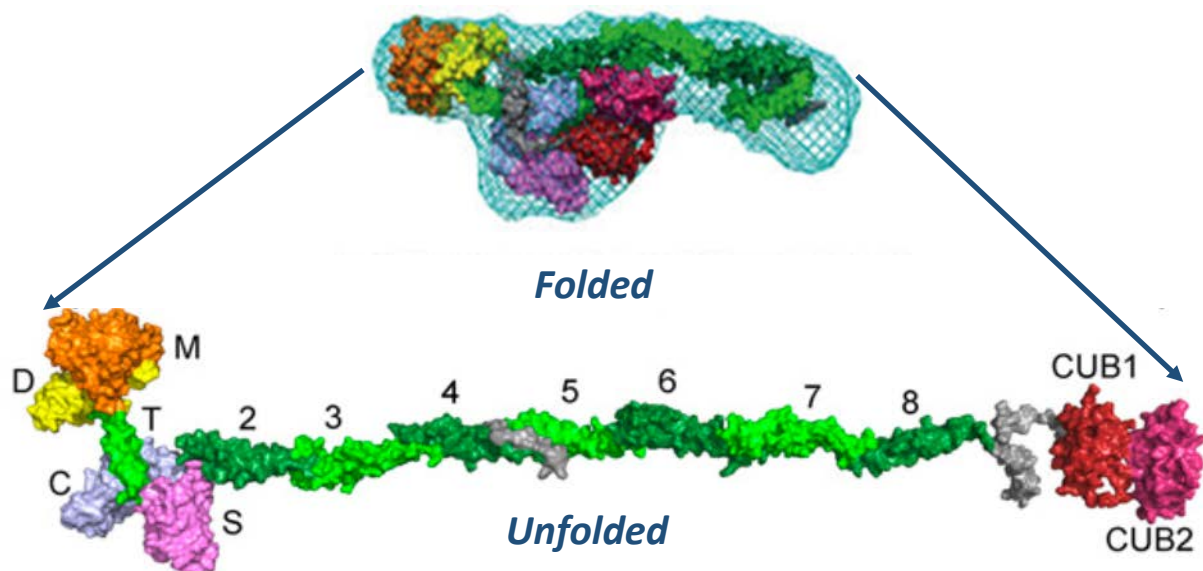


Figure 2.2: The molecular model of ADAMTS13 protein.

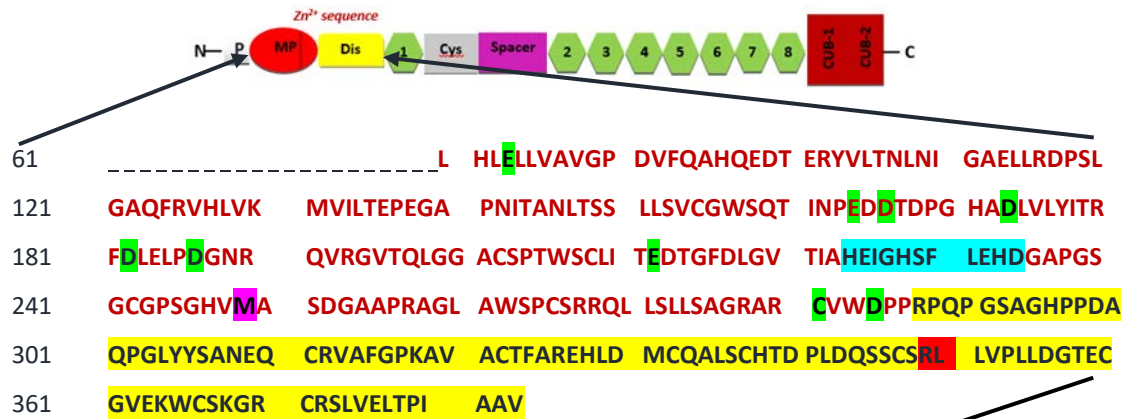
A molecular model of ADAMTS13 in its folded and unfolded conformation using small angle X-ray scattering by *Muia et al.* (2014). In the folded conformation, the distal domains lie in close proximity with the proximal domains implying that distal domains allosterically regulate ADAMTS13's activity and substrate binding.

The ADAMTS13 structure contains a propeptide (from a mature N-terminal side, highlighted in grey in **Figure 2.1**), which functions exclusively as a molecular chaperone and has no effect on the

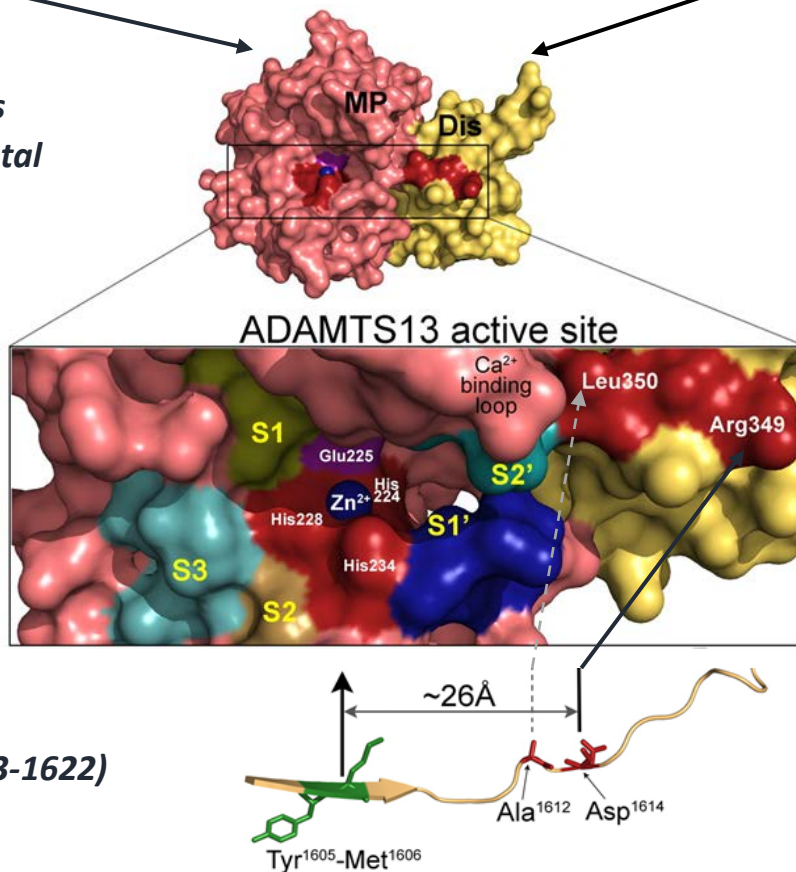
enzymatic function or the expression levels of ADAMTS13 (Majerus *et al.* 2003). The metalloprotease domain (MP) of ADAMTS13, referred to as zinc-dependent hydrolase, contains the active site responsible for hydrolysing the Tyr1605-Met1606 scissile bond of the VWF A2 domain (Zheng, 2013). For proteolysis to occur, the MP domain binds to a zinc ion (Zn^{2+}) with the sequence HEXXHXXGXXHD, highlighted grey in **Figure 2.3A**, and the three underlined histidine residues coordinate the Zn^{2+} ion in the sequence (Zheng *et al.* 2001), with the 'X' in the sequence representing various random amino acid residues. The sequence also contains the catalytic 'E'- glutamic acid residue at position 225 (double underlined in the sequence) that is stabilised by the Zn^{2+} ion and polarizes the water molecule through hydrogen bonding. The Zn^{2+} ion is responsible for the nucleophilic attack on the carbon molecules of the VWF substrate scissile peptide bond, allowing hydrolysis of the bond (Bode *et al.* 1999; Bode *et al.* 1993). Furthermore, each site of the catalytic zinc sequence contains the S1-S' subsites of ADAMTS13 that accommodates the VWF P1-Tyr1605 and Met1606-P1' residues (De Groot *et al.* 2010; Crawley *et al.* 2011). These subsites facilitate the cleavage efficiency and site specificity of ADAMTS13 by allowing it to interact with VWF-substrate in the vicinity of the active-site cleft (**Figure 2.3B**: insert).

A methionine residue at position 249 creates a tight turn (Met-turn) at a short distance from the sequence following the zinc-binding sequence (Bode *et al.* 1999). This tight turn forms a hydrophobic base beneath the catalytic Zn^{2+} contributing to the structural integrity of the metalloprotease, which is vital for the function of ADAMTS13. The ADAMTS13-MP domain also requires divalent cations to perform its enzymatic function. This is modulated by the presence of three functional calcium (Ca^{2+}) binding sites on the MP domain (Crawley *et al.* 2011; Gardner *et al.* 2009; Bode *et al.* 1999; Anderson *et al.* 2006). These Ca^{2+} binding sites are present in residues adjacent to the active site. The two Ca^{2+} binding sites on residues (Glu83, Asp173, Cys281, Asp284) and (Glu164, Asp166) respectively, mediate low affinity Ca^{2+} binding and have no effect on Ca^{2+} -dependent ADAMTS13 activity. The third Ca^{2+} binding site on (Asp182, Asp187 and Glu212) residues is thought to play a critical role in providing high affinity Ca^{2+} binding and proteolytic activity. The Ca^{2+} binding property provides structural integrity to the loop necessary for efficient proteolysis of the VWF substrate by enhancing the proteolytic activity of ADAMTS13 through the conformational change of the active site cleft of the MP domain (Gardner *et al.* 2009). Residue Asp187 is hypothesized to play a critical role by providing a high affinity Ca^{2+} binding site that modulates the shape of the functional loop (Gardner *et al.* 2009). Mutations at the third site can dramatically reduce Ca^{2+} -induced ADAMTS13 activity. **Figure 2.3** shows the constituents of the MP domain that forms an important part of the proteolysis machinery.

A. ADAMTS13 Amino Acid Sequence



B. MP and Dis Domains Crystal structure



C. VWF (A2 1603-1622)

Figure 2.3: ADAMTS13 MP – Dis domains residue structure.

A: The Metalloprotease (MP) domain residue sequence (80-286, in red) with the active site (zinc sequence) highlighted in light blue and the Met-turn methionine (M249) in purple. The residues with calcium binding sites are highlighted in green. The Disintegrin-like (Dis) domain residue sequence is highlighted in yellow (287-383), with exocites highlighted in dark blue within the sequence (GenBank: AAL11095.1). **B:** Depiction of the crystal structure of ADAMTS13 (Crawley *et al.* 2011) with MP domain in red and Dis domain in yellow. Insert: the active site cleft. Active site residues (Zn²⁺ and its 3 coordinating Histidine residues (His224, His228 and His234) and the catalytic (Glu225), with high-affinity binding functional Ca²⁺-binding loop marked. Regions of MP domain predicted to contain the S-sites are labelled and marked in different colours. The Dis domain exosite residues are also indicated in red. **C:** A proposed model by De Groot *et al.* (2015), showing Asp1614 in the VWF domain (located 26 Å from the Tyr1605-Met1606 scissile bond) interacts with Arg349 in ADAMTS13. This, in turn, helps position the scissile bond into the active-site cleft.

It is important to note that ADAMTS13 proteolytic activity does not take place in the absence of the zinc sequence, (Ai *et al.* 2005; Gao *et al.* 2008; Soejima *et al.* 2003; Zheng *et al.* 2003). Moreover, the ability of ADAMTS13 to perform its proteolytic activity is dependent on the presence of other functional domains added to the MP domain. The interaction between the ADAMTS13 and VWF are discussed in the next section. The functions of the different domains present on the ADAMTS13 protein are discussed below as they are sequentially added to the MP domain.

The domain adjacent to the MP domain is the Disintegrin-like (Dis) domain, highlighted in yellow in **Figure 2.3**. The Dis domain significantly increases cleavage efficiency and specificity of ADAMTS13 (Ai *et al.* 2005; De Groot *et al.* 2009; Xiang *et al.* 2011; Crawley *et al.* 2011). It contains exocites at Arg349 and Leu350 residues that form weaker interactions with the unravelled VWF A2 domain residues at Asp1614 and Ala1612 close to the cleavage site. The proposed model by De Groot *et al.* (2009) (**Figure 2.3:C**), demonstrates that the Arg349 residue in ADAMTS13 interacts with the Asp1614 residue in the VWF A2 domain in order to position the VWF Tyr1605-Met1606 scissile bond into the active-site cleft of ADAMTS13. The ADAMTS13 residues Arg349 and Leu350 are located adjacent to the active-site cleft with residue Arg349, in close proximity to the active site. When bound to the VWF residue Asp1614, the scissile bond is orientated towards the active centre of ADAMTS13 for cleavage to occur.

Although the exocites in the Dis domain provide low-affinity binding, these secondary interactions are important for enhancing binding of the MP domain to VWF scissile bond. Using kinetic analysis of point substitutions, De Groot *et al.* (2009) showed how mutations of Arg349 or Leu350 in the Dis domain reduced cleavage efficiency of the VWF substrate, suggesting that both functional substrate binding and substrate turnover are significantly affected. Therefore, the MP and the Dis domains operate as an inseparable functional unit for optimal catalytic activity of ADAMTS13 and without the Dis domain, the catalytic activity of ADAMTS13 is reduced (De Groot *et al.* 2009).

The third domain to be sequentially added after the Dis domain is the first thrombospondin type-1 repeat (TSP1). The role of all TSP1 repeats is still unclear, however, it is suggested to play an important role in cell surface binding and substrate recognition (Zheng *et al.* 2013, Vomund and Majerus, 2009). Moreover, TSP1 repeats have also shown to contain up to 6 cysteine residues (highlighted in coloured pairs in **Figure 2.4**) that may act as free thiols (Xiao and Zheng, 2011; Yeh *et al.* 2010). These free cysteine residues form part of the catalytic active site in an enzyme and are involved in the formation of intra- and inter-molecular disulphide bonds (Trivedi *et al.* 2009). The presence of disulphide bonds in proteins have been shown to impose conformational rigidity of a protein, preventing mis-folding. A cluster of surface exposed free thiols have also been identified on

the ADAMTS13 C-terminal TSP1 repeats and the CUB domains. These free thiols on ADAMTS13 interact with free thiols on the surface of UL-VWF forming disulphide bonds between ADAMTS13 and VWF, and prevent disulphide bond formation between 2 VWF multimers under flow (Bao *et al.* 2014; Xiao and Zheng 2011; Yeh *et al.* 2010). Thus, ADAMTS13 binding to VWF also prevents VWF-mediated platelet adhesion and aggregation.

ADAMTS13 Amino Acid Sequence

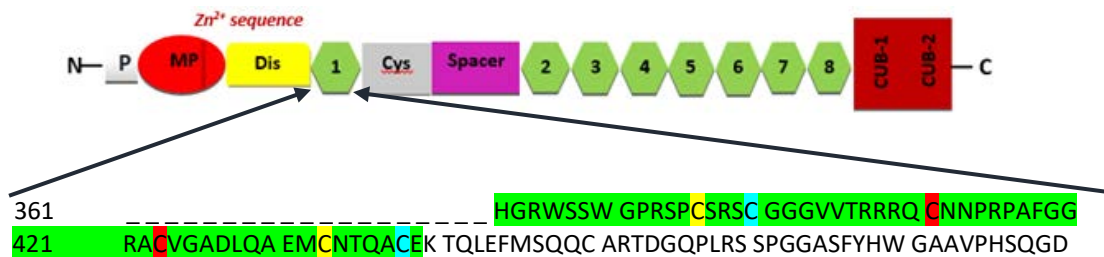


Figure 2.4: ADAMTS13 TSP1-1 domain residue structure.

The 6 cysteine residues that pair to form disulphide bonds are located on the amino acid sequence from 384-439, highlighted within the TSP1-1 sequence (GenBank: AAL11095.1). Cys396 pairs with Cys433 (yellow), Cys400 pairs with Cys438 (light blue), and Cys411 pairs with Cys423 (red).

The fourth and the fifth domains sequentially added in ADAMTS13 protease is the Cysteine-rich (Cys) and Spacer domains, respectively. These 2 domains play a critical role in binding to VWF and promoting proteolysis. The Spacer domain is responsible for the tight binding between ADAMTS13 and the VWF A2 domain (De Groot *et al.* 2015; Jin *et al.* 2010; Gao *et al.* 2008; Gao, 2006; Majerus *et al.* 2005; Akiyama *et al.* 2009). Whereas the Cys domain plays a supporting role by promoting the functional conformation of the Spacer domain so that it can interact with VWF (De Groot *et al.* 2011). As mentioned before, interactions of other domains are required to enhance proteolysis of the VWF A2 domain by the ADAMTS13 MP domain. Extensive interactions by C-terminal non-catalytic domains of ADAMTS13 greatly increases VWF substrate recognition and cleavage efficiency.

The important interactions of functional Cys-rich and Spacer domains are discussed in the next section. The amino-acid sequence of the Cys-rich and Spacer domains of ADAMTS13 is shown in **Figure 2.5.**

ADAMTS13 Amino Acid Sequence

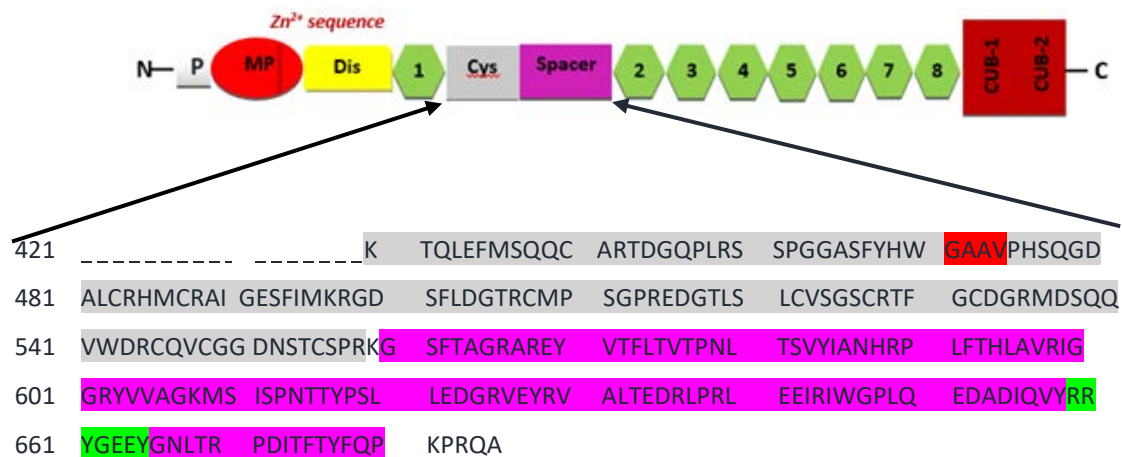


Figure 2.5: ADAMTS13 Cysteine-rich and Spacer domains residue structure.

Cysteine-rich domain sequence (440-558) highlighted in grey with highlighted hydrophobic residues in red. Spacer domain sequence (559-680) highlighted in purple, with exocites (residues Arg659, Tyr660, Tyr661 and Tyr664, highlighted in green) (GenBank: AAL11095.1). These exocites play a significant role in substrate recognition and cleavage.

De Groot *et al.* (2015) demonstrated that the Cys domain contains hydrophobic residues (Gly471-Val474) situated on the same side as the Spacer domain exocites (Arg660-Tyr665) using a 3D crystal structure shown in **Figure 2.6**. The positions of these residues are highlighted in red and green respectively in **Figure 2.5**. These Cys hydrophobic pocket interact directly with hydrophobic residues located on the VWF, causing a conformational change that further enhances binding of the Spacer domain. De Groot *et al.* (2015) employed deletion and substitution mutagenesis to demonstrate that without these interactions, binding of the Spacer domain with VWF is significantly reduced. Furthermore, the Cys hydrophobic pocket is also thought to play a role in opposing interactions between the Spacer and the CUB domain under flow conditions when VWF unfolds (Zheng, 2015). The exact mechanism by which the Cys hydrophobic pockets achieve this effect is still unclear and investigation are still ongoing. It is safe to suggest that binding of the Spacer domain may be dependent on the function of the Cys domain (Zheng, 2015). The CUB domains have a regulatory role by inhibiting the ADAMTS13 activity through interactions with the Spacer domain under flow, as discussed later in the literature review.

The Spacer domain contains residues (Arg659, Arg660, Tyr661 and Tyr665) that form a high-affinity binding site for the C-terminal residues (from Glu1660 to Arg1668) in the VWF A2 domain (Gao *et al.* 2006; Jin *et al.* 2010). Furthermore, kinetic analysis using folded-VWF and wild type unfolded-VWF substrates under various conditions showed that these amino acid residues recognize the

unfolded central VWF-A2 domain 10-fold better than the folded-VWF. The Spacer domain has also been demonstrated to promote cleavage of the VWF by the ADAMTS13 MP domain under high fluid shear stress. **Figure 2.6** shows the proposed model for the interaction of ADAMTS13 with the unravelled VWF A2 domain.

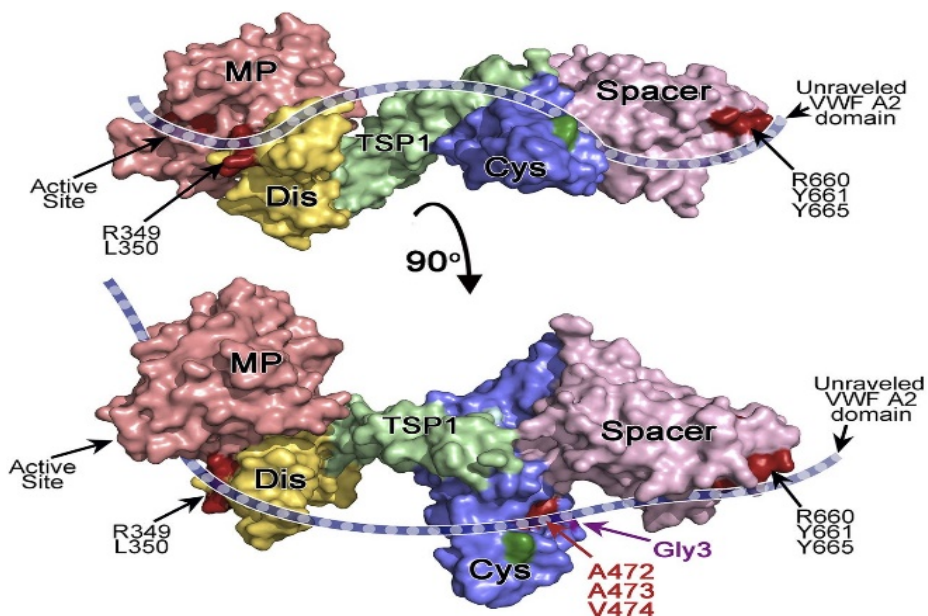


Figure 2.6: Proposed model for the interaction of ADAMTS13 with unravelled VWF A2 domain.

The figure represents the proposed crystal structure of ADAMTS13 DTCS model by Akiyama *et al.* (2009). The ADAMTS13 domains are colour-coded as follows: MP (red), Dis (yellow), TSP1 (green), Cys (blue), and Spacer (pink). The active site, Disintegrin-like exosites (R349 and Leu350), and Spacer exosite (R660, Y661, and Y665) are shown in dark red and are labelled. Unravelled VWF A2 domain (dashed blue ribbon) is shown and demonstrates extension across the ADAMTS13 active site and the exosites in the ancillary Dis, Cys, and Spacer domains. The location of the hydrophobic pocket in the Cys domain involving the A472, A473 and V474 amino acids is shown in red. Mutagenesis studies also revealed that modifying the structure of the Cys domain by addition of a glycan at position 476 (shown in purple) impaired the binding and cleaving function of ADAMTS13 (De Groot *et al.* 2015).

When the UL-VWF multimer changes conformation from a globular form to a string-like form under shear stress, the Spacer domain is the first to recognise residues on VWF (Jin *et al.* 2010). The Spacer domain exosites mediate most of the binding between VWF and ADAMTS13 through its high-affinity binding to VWF residues. When VWF unfolds, the hydrophobic pockets of the Cys domain further enhance the tight binding of the Spacer domain and subsequent proteolysis. These two domains approximate the ADAMTS13 to VWF but are not sufficient for proteolysis to occur. The second exosites of the Dis domain residues provide weaker interactions with VWF residues and are required to position the VWF A2 Tyr1605-Met1606 scissile bonds within the active site-cleft of the ADAMTS13. Then the MP domain S1-S1' pockets adjacent to the cleavage site interact with VWF residues to accommodate the VWF P1-P1' pockets (Tyr1605-Met1606), thus bringing the scissile

bond near the active site. Thereafter, binding between the ADAMTS13 MP domain active site and the VWF A2 domain at Tyr1605-Met1606 bond take place for proteolysis to occur. These interactions work like a molecular zipper presenting the VWF scissile bond to the ADAMTS13 active site through various domains interacting with VWF substrate (Crawley *et al.* 2011; Feys *et al.* 2009), see **Figure 2.8**.

The function of ADAMTS13 is thus dependent on the cooperation between the critically important Spacer domain and Cys domain (De Groot *et al.* 2011). When weaker interactions of the Dis domain to VWF are disrupted, efficient substrate recognition and cleavage are also affected. It is thus clear that interactions between ADAMTS13 and VWF are dependent on the presence of multiple ADAMTS13 domains that initiate direct contact with the complementary exosites in VWF.

The TSP2-8 and the CUB non-catalytic domains of ADAMTS13 does not increase the proteolytic activity of ADAMTS13. Instead, these domains provide secondary interactions between ADAMTS13 and VWF-A2 in a linear fashion, which is critical for the proteolysis of VWF under flow. A small portion (~3%) of ADAMTS13 is suggested to circulate in the blood with the TSP5-CUB domains bound to D4-CK domains of the VWF (**Figure 2.8**) (Feys *et al.* 2009; Zanardelli *et al.* 2009). The binding exosites of the Spacer domain are only revealed when shear forces promote unfolding of VWF, which exposes the A2 domain. Then the Dis domain can position the Tyr1605-Met1606 scissile bond for proteolysis by the active site of the ADAMTS13 MP domain.

The C-terminal of the TSP1 repeats also interact with the endothelial cell surface receptor CD36, which may enhance proteolytic cleavage of UL-VWF under flow conditions (Vomund and Majerus, 2009). The ADAMTS13 C-terminal TSP1 repeats have also been shown to regulate platelet interaction with collagen, which is independent of ADAMTS13 proteolytic activity (Xiao and Zheng, 2011). Under high shear stress conditions, the TSP1 repeats inhibit platelet adhesion to collagen, thereby decreasing platelet adhesion and aggregation, which may contribute to the antithrombotic activity of ADAMTS13 under pathophysiological conditions (Bao *et al.* 2014).

The CUB domains are unique to ADAMTS13 and are not found in other ADAMTS proteases (Tang, 2001; Apte, 2009). Although the role of the CUB domains alone is not yet clear, experimental studies suggest that the CUB domains have a negative regulatory function of ADAMTS13 (South *et al.* 2014; Jin *et al.* 2009; Xiao *et al.* 2011). These studies showed that the proteolytic activity of ADAMTS13 is increased when the CUB domains are removed or blocked, because the CUB domains circulate bound to the Spacer domain under flow, blocking interactions of the Spacer domain with the substrate. This action of the CUB domains can also be viewed as a regulatory mechanism of the

ADAMTS13 enzyme, which prevent unnecessary proteolysis of VWF in the circulation (Tao *et al.* 2005). Other studies showed that ADAMTS13 lacking the CUB domains is unable to cleave platelets-derived UL-VWF under flow in animal models (De Maeyer *et al.* 2010; Tao *et al.* 2005; Tao *et al.* 2005). The results of these studies indicate that the CUB domains are vital to the action of ADAMTS13 under different physiological conditions.

Functionally active ADAMTS13 has also been found in small quantities in vascular and glomerular endothelial cells, megakaryocytes, platelets and glial cells. (Turner *et al.* 2006; Tati *et al.* 2011; Liu *et al.* 2005; Suzuki *et al.* 2004; Tauchi *et al.* 2012). These small quantities of ADAMTS13 detected in vascular endothelial cells are constitutively secreted from these cells and potentially contribute to maintaining a VWF-free endothelial cell surface (Turner *et al.* 2009). The ADAMTS13 produced by glomerular endothelial cells protects the kidneys against thrombosis by preventing platelet aggregation along the capillary lumina where high shear stress is present and proteolytic activity of ADAMTS13 is essential for cleaving unravelled UL-VWF multimers (Tati *et al.* 2011). ADAMTS13 derived from platelets cleaves platelet-derived UL-VWF under static and flow conditions (Liu *et al.* 2005). Furthermore, the expression of ADAMTS13 on platelet surfaces increase significantly when platelets are activated by thrombin and thus counteracts the sudden release of hyperactive UL-VWF multimers from platelets (Liu *et al.* 2005; Pickens *et al.* 2012).

2.2. Function of von Willebrand factor (VWF)

Von Willebrand factor (VWF) is an adhesive plasma glycoprotein that functions as a sensor of vessel wall damage and the initiator of primary haemostasis (Moake *et al.* 1986; Sadler 1998). VWF is synthesized in both vascular endothelial cells and megakaryocytes as a pre-propolypeptide (Sporn *et al.* 1985; Wagner *et al.* 1982). The mature functional VWF is secreted in plasma as ultra large VWF (UL-VWF) multimers (Wagner *et al.* 1991; Sadler 1991). The function of VWF is dependent on its multimeric size, as UL-VWF multimers in plasma are the most adhesive and haemostatically active form of VWF. The UL-VWF multimers contain more ligand binding sites and are thus more conformationally responsive to vascular shear forces (Sadler 1998). The mature VWF contains structural domains that have a variety of specific ligand binding sites (Zhou *et al.* 2011), which allow VWF to interact with platelet surface glycoprotein Iba (GPIba) at the A1 domain, integrin α IIb β III at the C1 domain, extracellular matrix collagen at the A3 domain, and act as carrier for plasma FVIII at the D'-D3 domains. For the latter, VWF protects FVIII from being degraded by activated protein C thereby prolonging its half-life (Federici, 2003; Lenting *et al.* 1998). **Figure 2.7** shows the multi-domain organisation of VWF.

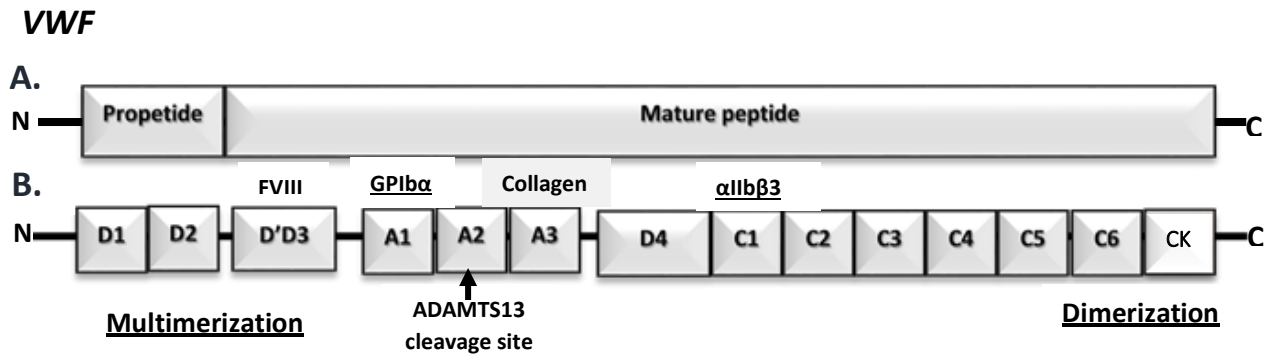


Figure 2.7: Schematic presentation of a multi-domain organization of a mature VWF.

Adapted from Zhou et al. (2011) with slight modifications. **A.** N-terminal side of VWF contains a signal peptide (SP), propeptide and a mature VWF peptide. **B.** VWF A-D domains with sites for multimerization, protein interactions, proteolytic cleavage and dimerization. The 4 D-domains for multimerization and FVIII binding, 3 A-domains with the A1 for platelet GPIb α binding site, A2 for cleavage by ADAMTS13 (indicated by the black arrow), and the A3 for collagen binding and C-domains for platelet α IIb β 3 interaction.

The D1-D2 domains that form the propeptide, are responsible for multimerization of the VWF dimers by forming an interdimer disulphide bond in the Golgi apparatus. The A1 domain of VWF is the only platelet-binding site, which initiates platelet adhesion through GPIb-IX-V complex, ultimately leading to platelet aggregation and thrombus formation (Zhou *et al.* 2011). However, the regulation of platelet adhesion depends upon cleavage by ADAMTS13. The UL-VWF multimers unwind in response to rheological shear stress (Zhang *et al.* 2009), which expose the A1 domain of VWF for platelet binding as well as the A2 domain prone to ADAMTS13 proteolysis activity. The A2 domain on the VWF multimer provides the cleavage site for the ADAMTS13 MP domain at the Tyr1605-Met1606 bond. ADAMTS13 converts UL-VWF into smaller, less haemostatically active fragments. Thus, when the UL-VWF multimers undergo a structural transitioning from a globular to an elongated form, it undergoes cleavage by ADAMTS13, thus regulating VWF function.

During its synthesis, VWF undergoes extensive glycosylation that is essential for its secretion (McKinnon *et al.* 2008; McKinnon *et al.* 2010). Important *N*- and *O*-linked glycans that contain the ABO (H) blood group have been identified to influence VWF plasma levels and proteolysis by ADAMTS13 (O'Donnell *et al.* 2005). In addition, an important *N*-glycan attached to residue Asn1574 within the VWF A2 domain helps to stabilize the unfolding of the VWF A2 domain that is needed for proteolysis to take place (McKinnon *et al.* 2008). The *O*-linked glycans are thought to play a role in stiffening the hinge of adjacent domains in VWF (Schulte *et al.* 2005).

After glycosylation, furin removes the VWF propeptide and transports the mature multimeric VWF to the Weibel-Palade bodies of endothelial cells or α -granules of platelets for storage in their UL

forms (Wagner *et al.* 1991). New UL-VWF is released constitutively from endothelial cells into the circulation or upon stimulation by activated platelets in response to vessel wall injury. Once released, UL-VWF multimers circulate in the blood in its globular form. This shape allows the VWF to survey the vasculature without unnecessary binding to platelets. However, in response to vessel wall damage or shear forces, globular VWF changes to an elongated string-like form which exposes the collagen and the platelet binding sites. This structural transitioning allows the UL-VWF to capture circulating platelets in the blood to the site of injury.

Released UL-VWF are anchored by the D'-D3 domains on endothelial cell surface binding P-Selectin molecules. The P-Selectin molecules are also stored in the Weibel-Palade bodies of endothelial cells and functions as adhesion molecules on the surface of activated endothelial cells (Padilla *et al.* 2004). The interaction between P-Selectin and the VWF D'-D3 domain allows the A2 domain binding site to be exposed to ADAMTS13 for cleavage (Lopez and Dong 2004).

2.3. Interactions of VWF and ADAMTS13

The proteolytic activity of ADAMTS13 is important for maintaining a homeostatic balance between bleeding and thrombosis in the microcirculation. In the absence of functional ADAMTS13, UL-VWF multimers may accumulate and cause spontaneous platelet adhesion that can occlude the microvasculature. Released UL-VWF multimers must therefore be cleaved by ADAMTS13 to less haemostatically active fragments (Dong *et al.* 2002).

Under normal physiological conditions, proteolysis of UL-VWF multimers occurs at three locations: firstly, at the surface of the endothelial cell membrane where the newly anchored UL-VWF multimers are released from the Weibel-Palade bodies; secondly, upon unfolding of the UL-VWF multimers at sites of vessel wall injury; thirdly, in the microcirculation under high fluid shear stress. Endothelial cell membrane-anchored UL-VWF are rapidly broken down by ADAMTS13 almost under no fluid shear stress (Siedlecki *et al.* 1996; Tsai *et al.* 1994). However, the VWF multimers anchored on the endothelial cell membrane remain large in size even after cleavage by the ADAMTS13 (Jin *et al.* 2009). Further proteolytic processing is required to reduce the UL-multimers to sizes that do not bind platelets in the circulation. The VWF conformational changes to string-like elongated forms due to shear force in the circulation, make it prone to ADAMTS13 proteolysis activity.

Once the VWF has undergone proteolysis, it assumes a globular proteolysis-resistant conformation with reduced platelet binding capacity. The proteolytic activity of ADAMTS13 is therefore regulated by the conformational shape of VWF to prevent uncontrolled proteolysis from occurring, which

could lead to haemostatically incompetent plasma VWF pools and haemorrhage. This is observed in patients with type 2A VWD with mutations in the VWF A2 domain that cause unstable unfolding of the A2 domain in the circulation, resulting in excessive proteolysis of VWF by ADAMTS13 (Xu and Springer, 2013). The current understanding of proteolysis of VWF by ADAMTS13 as described by Crawley *et al.* (2011) is shown in **Figure 2.8**. This phenomenon acts much like a molecular zip in terms of substrate recognition and binding, which is very specific until the ADAMTS13's active site cleaves the VWF substrate at the A2 domain.

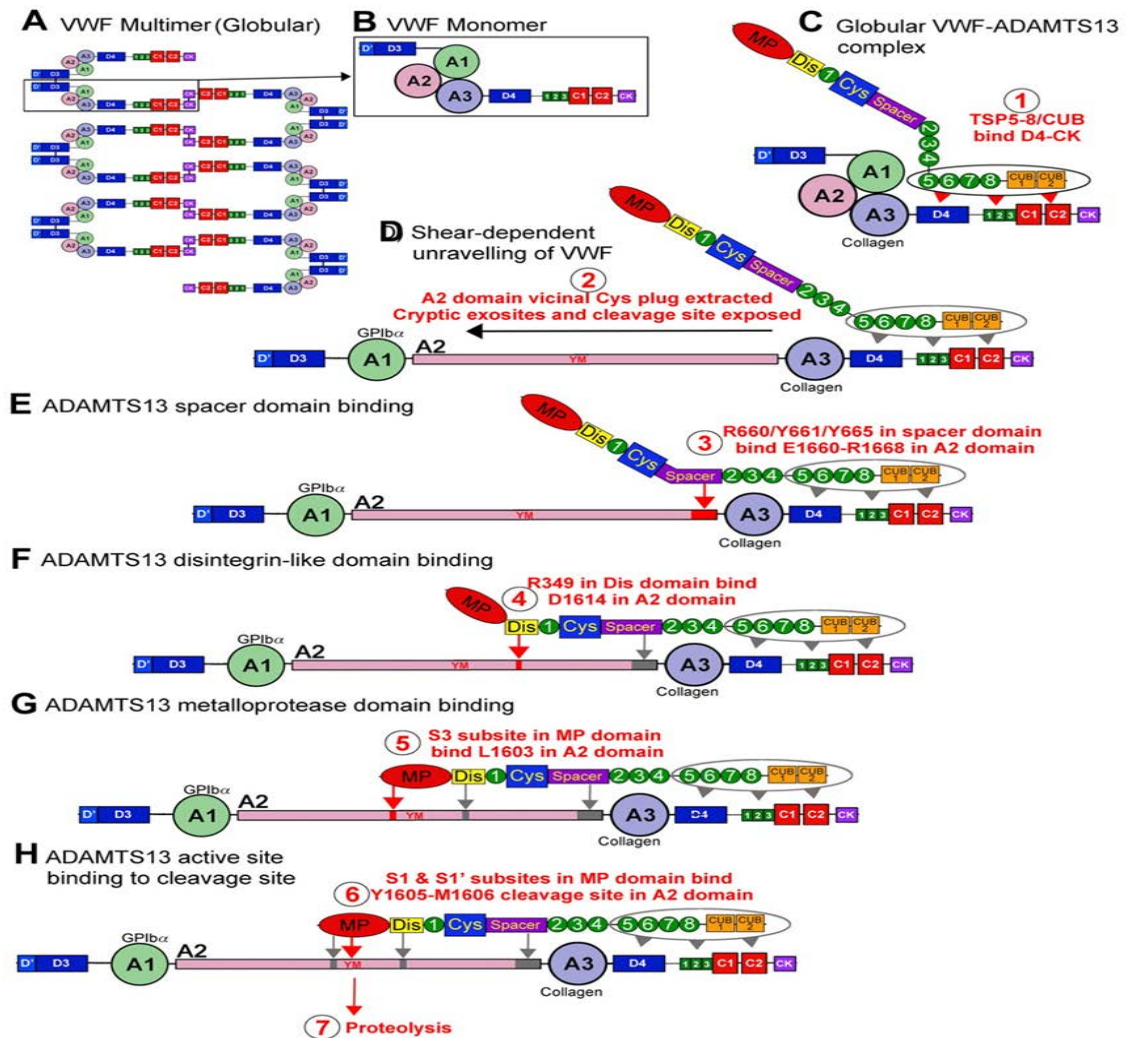


Figure 2.8: Proteolysis of VWF by ADAMTS13 (Crawley *et al.* 2011).

VWF circulates in plasma as a multimeric molecule (A) that adopts a quiescent globular conformation. Each multimer is composed of disulphide linked VWF monomers (B). In its globular conformation, the collagen-binding site on the A3 domain is exposed. ADAMTS13 can bind to this globular VWF via its TSP1 (5-8) and CUB domains (C - step 1). This enables the formation of VWF and ADAMTS13 complexes that circulate in plasma. Under high shear forces, which can occur on secretion, collagen binding, or passage through the microvasculature, VWF unravels to expose the A1 domain binding site for GPIIb/IIIa. These shear forces also remove the molecular plug formed by the vicinal disulphide bond in the A2 domain, which causes A2 domain to unfold (D - step 2). This unfolding reveals cryptic exosites that enable residues in the ADAMTS13 Spacer domain to bind to the unfolded A2 domain (E - step 3). Thereafter, a critical low-affinity interaction between D1614 and the Dis domain helps to approximate and position the cleavage site (F - step 4). This enables further interactions between the MP domain, including an essential interaction via an S3 subsite with L1603 in VWF (G - step 5). All these interactions allow the MP domain to engage via S1 and S1' subsites with the cleavage site (YM; H - step 6), after which proteolysis can occur, (- step 7).

The UL-VWF multimers, which make up ~3% of the circulating VWF are the most haemostatically reactive form of VWF, and circulate in their globular form bound to ADAMTS13 TSP1-5 – CUB domains at the VWF C4 – CK domains (Feys *et al.* 2009). These UL-VWF/ADAMTS13 complexes allow ADAMTS13 to regulate the VWF-platelet binding function. However, this interaction does not cause ADAMTS13 to automatically cleave VWF. The binding sites and the A2 domain scissile bond within the globular VWF are still hidden within the folded VWF (Crawley *et al.* 2011).

Unfolding of the VWF A2 domain is necessary for proteolysis by ADAMTS13 as it contains a vicinal disulphide bond at the C-terminus that bends the peptide backbone to form a molecular plug (Zhang *et al.* 2009). A disulphide bond is formed between two adjacent cysteine residues and provides structural stability of the protein. This molecular plug interacts directly with the hydrophobic residues in the A2 domain core, which stabilizes the VWF A2 domain, making it resistant to proteolysis by ADAMTS13 (Luken *et al.* 2010). The molecular plug is then removed under high fluid shear stress, which allows water molecules to enter and destabilizes the hydrophobic core (Crawley *et al.* 2011). This results in the unfolding of the VWF A2 domain exposing additional binding sites for ADAMTS13 with subsequent VWF proteolysis (Crawley *et al.* 2011).

Refolding of the A2 domain under high-shear stress has also been reported and prevents excessive cleavage (Zhang *et al.* 2009). The VWF A2 domain also contains the residue Pro1645 that can change to *trans*-proline when exposed to shear fluid stress, which can delay refolding of the A2 domain, enhancing proteolysis by ADAMTS13 (Zhang *et al.* 2009). Therefore, the balance between folding and refolding of the VWF A2 domain also regulates interactions between ADAMTS13 and VWF. Furthermore, the A2 domains present in UL-VWF multimers are more prone to unfolding than those present in short multimers, since tensile forces created by shear in the circulation are much higher in the middle of large multimers compared to smaller ones (Zhang *et al.* 2009; Dong *et al.* 2002).

2.4. Regulation of ADAMTS13

Regulation of ADAMTS13 within the vasculature is necessary to prevent haemostatic imbalances. ADAMTS13 is a stable enzyme with a half-life of 2 to 3 days in plasma (Furlan *et al.* 1999). Its ability to cleave VWF efficiently is dependent on the presence of shear stress on, or denaturation of VWF, which promotes unfolding of VWF (Tsai *et al.* 1994). If ADAMTS13 activity is not regulated, it could result in either the presence of excessive hyperactive UL-VWF or haemostatically incompetent small-cleaved fractions with resultant platelet-rich thrombi in the microvasculature or bleeding. Therefore, cleavage of UL-VWF multimers by ADAMTS13 needs to be regulated at the site of vascular injury and at a distant site from thrombin generation in order to control thrombus

formation. Although the exact control of ADAMTS13 activity in the circulation has not been fully elucidated, studies have shown the presence of certain factors can either enhance or inhibit the proteolytic activity of ADAMTS13 as discussed in **2.4.1** and **2.4.2** (Anderson *et al.* 2006; Crawley *et al.* 2005; Bernado *et al.* 2004; Studt *et al.* 2004).

2.4.1. Factors that enhance the proteolytic activity of ADAMTS13

The proteolytic processing of UL-VWF multimers occurs more rapidly in the microcirculation with high flow shear stress, such as in the arterioles and capillaries (Dong *et al.* 2005). Studies by Vincentelli *et al.* (2003) and Tsai, (2003) have shown that patients suffering from aortic stenosis demonstrated increased VWF proteolysis and reduced VWF multimeric sizes because of the increased fluid shear stress generated in the circulation. This reflected increased proteolytic activity of ADAMTS13, which correlates with increased fluid shear stress in *in-vivo*.

Factor VIII (FVIII) has also been shown to enhance the proteolytic activity of ADAMTS13 under high shear stress. Although the mechanism in which this is achieved is not yet clear, it has been suggested that binding of FVIII to the D'D3 domain of VWF promotes conformational changes of the VWF multimers (Zheng, 2013; Shankaran and Neelamegham, 2004). FVIII may pull the VWF D'D3 domain away from the neighbouring A1 and A2 domains under shear, increasing the peak tensile force exerted on the A2 domain, enhancing its unfolding, which exposes the VWF A2 domain for cleavage by ADAMTS13 (Cao *et al.* 2008; Skipwith *et al.* 2010). However, the ability of FVIII to enhance cleavage of VWF by ADAMTS13 can be reversed by adding thrombin, which has been shown to inactivate ADAMTS13 (Zheng, 2013). The factors that enhance the proteolytic activity of ADAMTS13 are summarised in **Figure 2.9**.

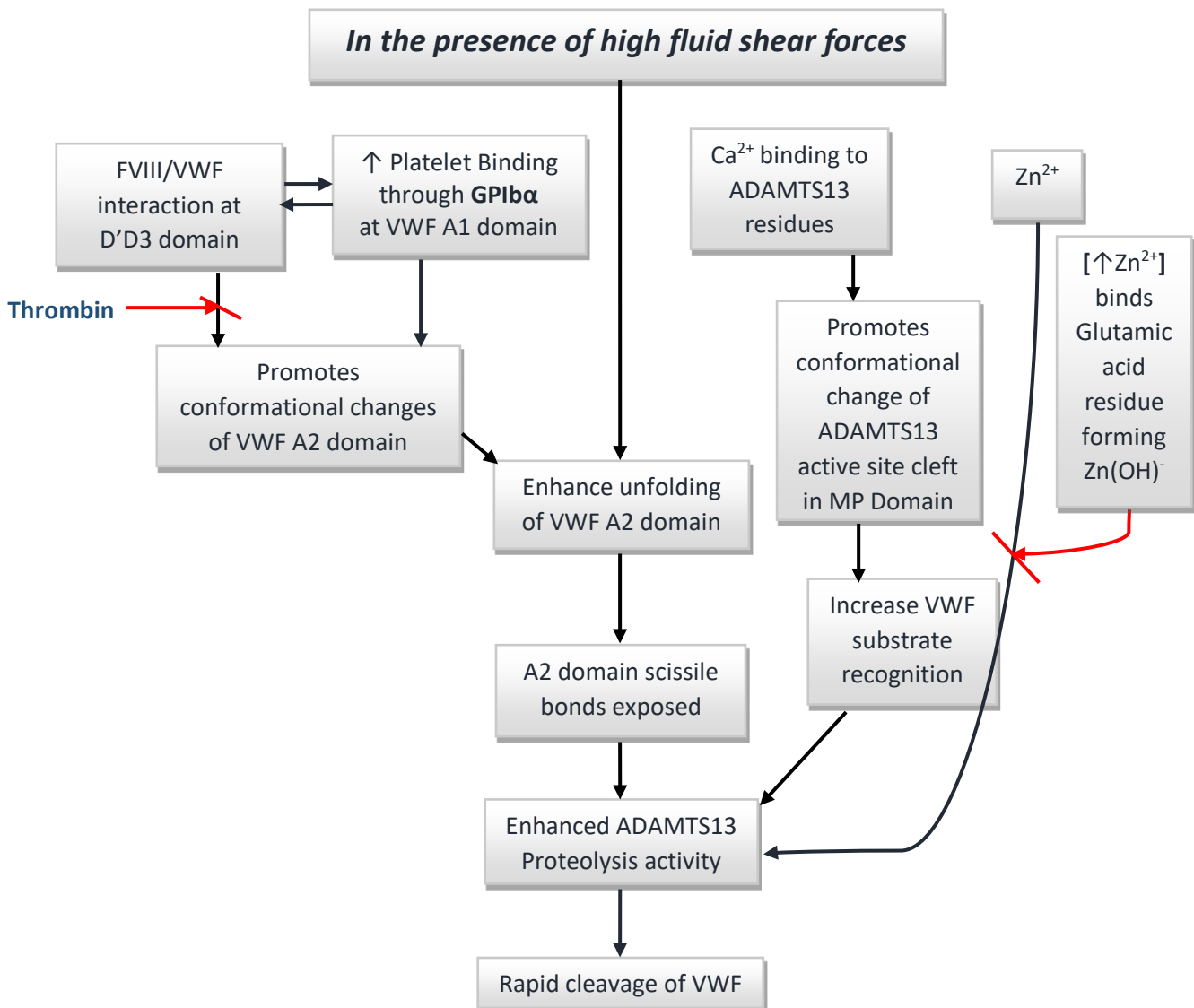


Figure 2.9: Summary of factors enhancing the proteolytic activity of ADAMTS13.

The factors that regulate the proteolytic activity of ADAMTS13 at substrate level include factors on the surfaces of endothelial cells, where the constitutively secreted VWF are anchored, and in the microcirculation under high shear forces. Both FVIII and GPIIb binding on the VWF domains have synergic effects that enhance VWF proteolysis by ADAMTS13 under flow. Thrombin has an inhibitory influence. Calcium (Ca²⁺) and zinc (Zn²⁺) binding to ADAMTS13 also enhance the rate of proteolysis of VWF by ADAMTS13, while too high concentration of Zn²⁺ inhibit the proteolytic activity of ADAMTS13.

Interaction of GPIIb with the A1 domain of VWF also increases the proteolytic activity of ADAMTS13 towards the VWF substrate under static or flow conditions (Skipwith *et al.* 2010; Chen *et al.* 2012; Shim *et al.* 2007). This interaction increases the ADAMTS13 access to the VWF A2 domain. Binding of platelets on each side of the VWF A2 domain scissile bond enhances the unfolding of the A2 domain and enhances proteolysis by ADAMTS13 in a fashion similar to the action of FVIII (Nishio *et al.* 2004; Shankaran and Neelamegham, 2004). Without bound platelets, the A1 domain of VWF has

an inhibitory effect on cleavage by ADAMTS13 by stabilizing the native conformation of the A2 domain and impairing the binding of ADAMTS13. However, when the A1 domain binds to GPIIb α on the platelets, the digestion of VWF by ADAMTS13 is enhanced. Both FVIII and GPIIb α binding to the VWF domains act synergically to enhance VWF proteolysis by ADAMTS13 under flow conditions (Skipwith *et al.* 2010).

Metal ions such as calcium (Ca²⁺) and zinc (Zn²⁺) also enhance ADAMTS13 proteolysis of VWF. Studies have demonstrated that these metal ions cooperatively modulate the interaction between VWF and ADAMTS13 (Furlan *et al.* 1996; Tsai 1996; Tsai and Lian, 1998; Tsai *et al.* 1997). Even low concentrations (<3 nM) of Ca²⁺ and Zn²⁺ enhanced the proteolytic activity of ADAMTS13 by approximately ≈ 3 and ≈ 2 fold respectively and ≈ 6 fold in combination, suggesting a cooperative activation action. However, other studies showed that too high concentrations (>3 nM) of Zn²⁺ can inhibit the proteolytic activity of ADAMTS13 due to the formation of Zn(OH)⁺ that binds the catalytic Glu residue within its active site. Calcium, on the other hand, binds directly to residues in the MP domain to stimulate ADAMTS13 activity. The strong binding of Ca²⁺ to ADAMTS13 modulates the shape of the functional loop of ADAMTS13 (Gardner *et al.* 2009). When the Ca²⁺ ions are bound to the MP domain, conformational changes of the active site cleft take place to increase substrate recognition necessary for efficient proteolysis by ADAMTS13. Cleavage of VWF is therefore also dependent on conformational changes that require calcium binding on the ADAMTS13. Thus, the ability of ADAMTS13 to recognise and cleave VWF substrate is also dependent on the presence of its structural features (Tsai, 1996; Anderson *et al.* 2006).

2.4.2. Factors that inhibit the proteolytic activity of ADAMTS13

ADAMTS13 proteolytic activity is regulated by local coagulation proteinases namely; thrombin, FXa and plasmin at the site of vascular injury (Crawley *et al.* 2005). The factors that inhibit proteolysis activity of ADAMTS13 at the site of vascular injury are summarised in **Figure 2.10**.

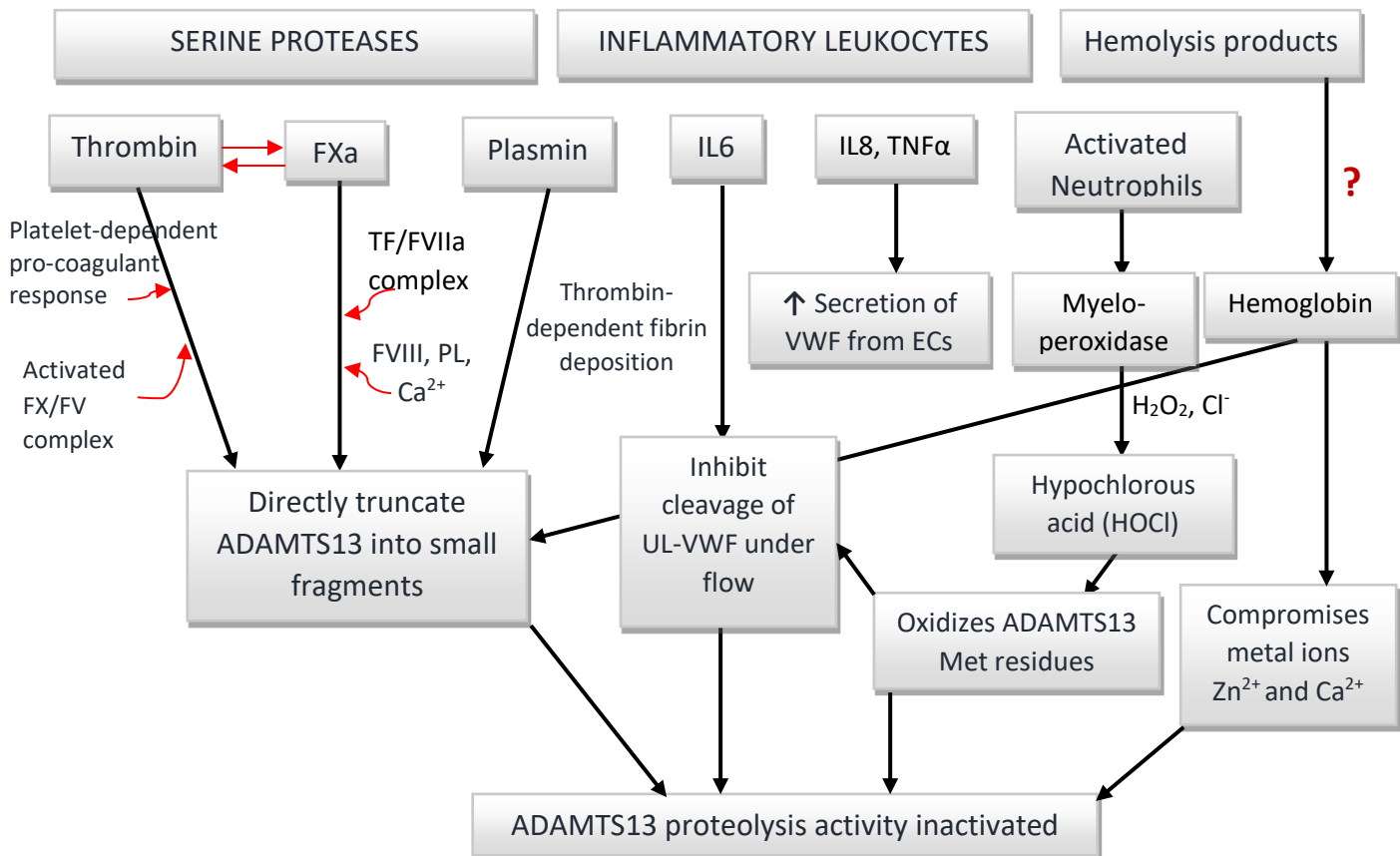


Figure 2.10: Summary of factors inhibiting the proteolytic activity of ADAMTS13.

Thrombin, FXa and plasmin inactivate the proteolytic activity of ADAMTS13 by digesting it into small non-functional fragments. Interleukin-6 (IL-6), interleukin-8 (IL-8) and tissue necrosis factor α (TNF α) secreted during an inflammatory response inhibit cleavage of UL-VWF multimers under flow, while increasing secretion of VWF from endothelial cells (ECs), which has the potential to overwhelm the available ADAMTS13 in the circulation. Activated neutrophils oxidizes the Met residues of ADAMTS13 resulting in inactivation of the proteolytic activity of ADAMTS13. Haemoglobin released from lysed erythrocytes trapped in platelet-rich thrombi in the circulation is also reported to inhibit ADAMTS13 proteolytic activity by compromising Ca^{2+} and Zn^{2+} metal ions binding to ADAMTS13.

During primary haemostasis, a break in the vascular wall initiates binding of VWF to the sub-endothelial matrix (collagen) under flow. Once VWF is immobilized, unfolding of VWF is promoted by flow shear stress to expose an increased number of platelet/matrix binding sites. When platelets bind to VWF, they become activated and initiates glycoprotein IIa/IIIb receptor complex mediated platelet aggregation. Activated platelets also secrete phospholipids (phosphatidylserine) necessary for initiating a pro-coagulant response that leads to thrombin generation. At the same time, an injured vessel wall also brings plasma into contact with tissue factor (TF). Activated Factor VII (FVIIa) in the circulation binds to TF and forms TF-FVIIa complexes, which in turn activates Factor X (FX). Factor X (FX) in turn activates thrombin in the presence of factor V (FV). Thus, both the activated FX and FV form a complex that initiate thrombin generation. Thrombin further increases platelet

activation via the protease-activated receptor mechanism, resulting in the formation of a platelet plug, which enhances efficient thrombin generation. Plasmin is activated following initiation of the coagulation cascade and mediates fibrinolysis (Crawley *et al.* 2005; Collen, 1999). In short, thrombin released from the surfaces of platelets and TF-bearing cells triggers fibrin generation, since it cleaves fibrinogen at fibrino-peptides A and B, which assemble to eventually form a fibrin gel (Hantgan and Hermans, 1979; Weisel, 1986). This is followed by the release of plasminogen activators (tPA) embedded within fibrin, which in turn activates plasminogen to plasmin to effect fibrinolysis of the fibrin clots.

During the initial stages of thrombin generation, platelet rich thrombi are composed entirely of plasma VWF on the outer surface with an inner core of platelet-derived thrombin, which acts as a core adhesive ligand (Matsui *et al.* 2002). The proteolytic action of the proteases, thrombin and FXa, inactivate the proteolytic activity of ADAMTS13 during clot formation at the site of vascular damage (Crawley *et al.* 2005). However, the rate at which FXa proteolyzes ADAMTS13 is slower when compared to thrombin's effect, which cleaves ADAMTS13 in a time- and concentration-dependent manner (Crawley *et al.* 2005). The ADAMTS13 fragments of different sizes were generated as detected by Western blotting, when recombinant ADAMTS13 was incubated with varying concentrations of human thrombin for different periods of time (Crawley *et al.* 2005). This finding suggests that thrombin directly interacts with ADAMTS13 at different sites, including at thrombin exosite I, for cleavage. Once ADAMTS13 is cleaved by thrombin, it loses its ability to cleave VWF. Interestingly, cofactors of thrombin, such as thrombomodulin and heparin, markedly inhibited the proteolysis of ADAMTS13 by thrombin (Crawley *et al.* 2005).

Crawley *et al.* (2005) also demonstrated that plasmin cleaves ADAMTS13 at different sites, but the ADAMTS13 fragments generated by thrombin, FXa and plasmin were all similar in sizes, but not identical. This data suggests that these coagulation proteases cleave ADAMTS13 at different sites. However, ADAMTS13 digested by plasmin had the same proteolytic action on VWF as ADAMTS13 fragments generated by thrombin. Plasmin is probably important in the modulation of ADAMTS13 activity at sites of haemostatic plug formation, especially during tissue repair of a vessel as VWF plays an important role in tissue repair (Yau *et al.* 2015).

The activity of ADAMTS13 is therefore closely regulated by the proteolytic action of thrombin, FXa and plasmin to allow effective thrombus formation at the site of injury. During haemostasis, the action of thrombin regulates ADAMTS13 activity prominently in platelet/VWF rich thrombi. Plasmin effects partial proteolysis of ADAMTS13, as it is activated slowly by a thrombin-dependent pathway to effect fibrinolysis of platelet-derived fibrinogen. Furthermore, plasmin cleaves and thereby

inactivates ADAMTS13 at lower concentrations compared to thrombin, which controls the extent and integrity of clot in an effort to maintain haemostasis (Feys *et al.* 2010).

Other factors that can influence the interaction between ADAMTS13 and UL-VWF multimers include inflammatory leukocytes (Bernado *et al.* 2004) and products of haemolysis (Studt *et al.* 2004). Endothelial cells and leukocytes secrete pro-inflammatory cytokines, such as interleukin-6 (IL-6), interleukin-8 (IL-8) and tissue necrosis factor α (TNF α) during an inflammatory response (Wolff *et al.* 1998; Tousoulis *et al.* 2003; Esmon 2000; Hillyer *et al.* 2003; Lowe *et al.* 2003; Pudil *et al.* 2001; Ueda 1999). An *in-vitro* experimental study by Bernado *et al.* (2004), showed that only IL-8 and TNF α stimulate the release of new UL-VWF multimers from endothelial cells in a concentration-dependent manner under flow. Interleukin 6 (IL-6) was shown to directly inhibit the proteolytic activity of ADAMTS13 on UL-VWF multimers under flow and under static condition, no cleavage of UL-VWF multimers was detected (Bernado *et al.* 2004). The exact mechanism by which IL-6 interacts with ADAMTS13 is still unknown but a study by Dong *et al.* (2003) suggested that IL-6 may impair docking of ADAMTS13 to the UL-VWF string under flow conditions.

Neutrophils have also been shown to regulate the proteolytic activity of ADAMTS13 during inflammation (Wang *et al.* 2015). Activated neutrophils generate hypochlorous acid (HOCl), a potent oxidant, produced from hydrogen peroxide and chloride ions in a reaction catalysed by the heme-containing enzyme myeloperoxidase (MPO). Hypochlorous acid (HOCl) oxidate key methionine residues to methionine sulfoxide in functional domains of ADAMTS13, thereby inhibiting its function (Fu *et al.* 2001; Wang *et al.* 2007; Taggart *et al.* 2000; Chen *et al.* 2010; Glaser *et al.* 1992). The Met residues at position 249 of ADAMTS13 is probably the most important in the proteolytic activity of ADAMTS13 as its function is to maintain the hydrophobic environment of the catalytic site (Bode *et al.* 1999). Chen *et al.* (2010) showed that HOCl also oxidizes VWF at Met1606, which is at the cleavage site of ADAMTS13, making the VWF substrate resistant to proteolytic ADAMTS13. In addition, it was also found that VWF became more adhesive as a result of oxidation of its methionine residues.

A study by Ono *et al.* (2006) also showed that leukocyte elastase can inactivate ADAMTS13 by cleaving it into truncated forms and further demonstrated that these enzymes can hydrolyse UL-VWF multimers at the ADAMTS13 cleaving site. These results indicate that inflammatory leukocytes contribute to prothrombic tendencies associated with reduced ADAMTS13 activity and increased VWF concentrations. Interleukin 8 (IL-8) and TNF α stimulate an increased secretion of UL-VWF multimers from endothelial cells, and IL-6 rapidly inhibit cleavage of new VWF by ADAMTS13

(Bernado *et al.* 2004), which can result in exhausting the ADAMTS13 capacity, which occurs in some cases of TTP such as HIV-associated TTP (Schwameis *et al.* 2015).

High concentrations of haemoglobin have also been reported to inhibit ADAMTS13 activity under static conditions in congenital forms of TTP (Studt *et al.* 2004). Haemoglobin in plasma of patients with TTP originate from lysed erythrocytes trapped in platelet-rich thrombi in the circulation. Studt *et al.* (2004) showed that haemoglobin inactivation of ADAMTS13 is temperature-, time- and concentration dependent. The extent of the effect and pathophysiological role of free haemoglobin in TTP is not clear, but studies indicate that metal ions Ca^{2+} and Zn^{2+} , which are needed for ADAMTS13 activity, may become compromised by free haemoglobin, resulting in inhibition of ADAMTS13 activity (Furlan *et al.* 1996; Tsai, 1996). Inhibition of ADAMTS13 related to free haemoglobin has been demonstrated in patients with intravascular haemolysis, haemolytic anaemias and incompatible erythrocyte transfusion (Pimstone, 1972).

2.4.3. Endothelial dysfunction

An intact vascular endothelium is crucial in maintaining the haemostatic balance. Endothelium is a dynamic system able to shift its anticoagulant/antithrombotic state to a procoagulant/prothrombotic state to promote healing mechanisms when necessary. The presence of perturbative factors such as, oxidative stress and infectious agents, such as HIV infection can cause impairment of the endothelium. Resulting in loss of thrombo-protection due to changes including increased expression of adhesive molecules on the endothelial surface.

Activated endothelial cells (ECs) express phosphatidylserine on their cell membranes, which generated FVIIa-tissue factor (TF) complexes capable of generating thrombin thereby shifting the haemostatic balance to a pro-coagulant state. Thrombin activates more pro-coagulant factors such as platelets. The injured endothelium also secretes VWF and P-selectin molecules, which could potentially overwhelm the ADAMTS13 proteolytic capacity (Jackson, 2011).

An inflamed endothelium also expresses other surface adhesion molecules such as inflammatory cytokines (TNF α , IL-1b), endothelial leukocyte adhesion molecules (ELAMs), integrins, cell adhesion molecules (CAMs), and fibrinogen $\alpha_v\beta^3$ complexes (Furie and Furie, 2004; Albelda and Buck, 1990). Rolling and adhesion of platelets and inflammatory cells result in the accumulation of these cells at the site of injury with detachment of ECs and platelet deposition and microvascular thrombosis (Jackson, 2011). Inflammatory cytokines can therefore play a pathogenic role in TTP by effecting

secretion of UL-VWF multimers from endothelial cells and inhibiting the activity of ADAMTS13 (Bernado *et al.* 2004).

2.4.4. Microparticles (MPs) and ADAMTS13

Microparticles (MPs) are cell fragments that are shed from activated cells in stressful conditions, such as cell injury, inflammation or apoptosis. Studies have shown that MPs down-regulate ADAMTS13 activity and promote microvascular thrombosis in TTP (Jimenez *et al.* 2005; Jimenez *et al.* 2001; Ahn *et al.* 1996). Activation of ECs and platelets occur in TTP due to thrombotic and inflammatory processes with subsequent release of MPs from platelets and ECs. Endothelial microparticles (EMPs) and platelets microparticles (PMP) can interact with platelets and leukocytes to further promote thrombotic events.

Endothelial cell (EC) injury is implicated in the pathogenesis of acquired TTP and EMP levels are therefore elevated in TTP patients (Jimenez *et al.* 2005; Jimenez *et al.* 2003). The EMP and PMP with their leukocytes conjugates can be detected by flow cytometry using a combination of fluorescent-labeled antibodies (Chirinos *et al.* 2005). The formation of EMPs is stimulated by TNF- α , inflammatory cytokines, thrombin, lipopolysaccharides and low shear stress (Leopold, 2013). During EC activation, released EMPs express many of the receptors of the parent cell including TF, which may trigger pro-thrombotic events as it is the main trigger of thrombin generation via the TF/FVIIa pathway. Furthermore, EMPs contain phosphatidylserines translocated from the inner to the outer leaflet of the EC membrane, which can support coagulation response by providing a catalytic surface for assembly of prothrombinase complexes (Ovanesov *et al.* 2005; Majumder *et al.* 2011).

The EMPs interact with UL-VWF and promote VWF-dependent thrombosis in TTP (Jy *et al.* 2005). The EMPs containing VWF thus greatly induce platelets aggregates. They are capable of adsorbing additional VWF from plasma by providing extra binding sites for platelets. The EMP subsets also carry UL-VWF multimers, which down-regulate ADAMTS13 activity and enhance formation of platelet aggregates (Jimenez *et al.* 2005). In addition, the EMPs isolated from TTP plasma added to normal plasma inactivated ADAMTS13 in the plasma (Jimenez *et al.* 2005).

EMP's and PMP's also interact with monocytes during inflammation to induce TF-dependent pro-coagulant activity (Sabatier *et al.* 2002b). The PMP that shed off from aggregating platelets can in turn, cause platelet and EC activation through the transcellular delivery of arachidonic acid (Barry *et al.* 1998). Platelet microparticles (PMP's) also provide a catalytic phospholipid surface for assembly of prothrombinase complexes (Sims *et al.* 2001). In addition, PMP's can bind and activate

neutrophils and monocytes *in vitro* (Jy *et al.* 2002b). A strong correlation between aCD11b expression in leukocytes and platelet-leukocyte conjugates has been found in venous thromboembolism (Chirinos *et al.* 2005). Thus platelet adhesion to leukocytes upregulates leukocyte activation and is a pathogenic link between thrombosis to inflammation *in vivo* (Sabatier *et al.* 2002b; Jy *et al.* 2002b). The release of EMPs, PMP's and their interactions with leukocytes can therefore amplify thrombotic events, although further research in this regard is needed.

2.5. Deficiency of ADAMTS13

Severe deficiency of ADAMTS13 activity and increased UL-VWF in plasma are risk factors for the development of TTP due to the accumulation of UL-VWF multimers in plasma with the formation of disseminated platelet-rich microvascular thrombi (Zheng *et al.* 2015). Clinically, TTP is characterized by the presence of microangiopathic haemolytic anaemia, thrombocytopenia, fluctuating neurological abnormalities, renal dysfunction, and fever with or without end organ damage (Cruccu *et al.* 1994). TTP can either relate to (1) congenital ADAMTS13 deficiency, or (2) acquired ADAMTS13 deficiency of <10%.

2.5.1. Congenital ADAMTS13 deficiency (cTTP)

To date, over 150 mutations have been identified in the variable regions of ADAMTS13 domains in congenital TTP (cTTP) patients, **Figure 2.11** (Joly *et al.* 2017; Lancellotti *et al.* 2013; Levy *et al.* 2011). These mutations are spread throughout the ADAMTS13 gene, resulting in frameshifts or deletions, missense and nonsense mutations. Disease causing mutations can result in secretion of a dysfunctional ADAMTS13 protein or proteolytic inactive ADAMTS13, or reduced secretion of ADAMTS13 (Kokame *et al.* 2002; Studt *et al.* 2004; Veyradier *et al.* 2004). Congenital TTP (cTTP) causes severe deficiency of ADAMTS13, which is present without any ADAMTS13 autoantibodies.

Experimental studies have indicated that mutations in the non-catalytic domains (DTCS) or even complete absence of these domains can greatly affect the proteolytic activity of ADAMTS13 and substrate recognition (De Groot *et al.* 2009; Gao *et al.* 2008; Ai *et al.* 2005). While, mutations in the TSP1 repeats and CUB domains have shown to affect the proteolytic activity of ADAMTS13 towards VWF under flow conditions (Apte, 2009; Turner *et al.* 2009; Ai *et al.* 2005; Vomund and Majerus, 2009). Mutations in the CUB domains alone were shown to inhibit the proteolytic activity of ADAMTS13 under flow and not static conditions (Tao *et al.* 2005; de Maeyer *et al.* 2010; Jin *et al.* 2009).

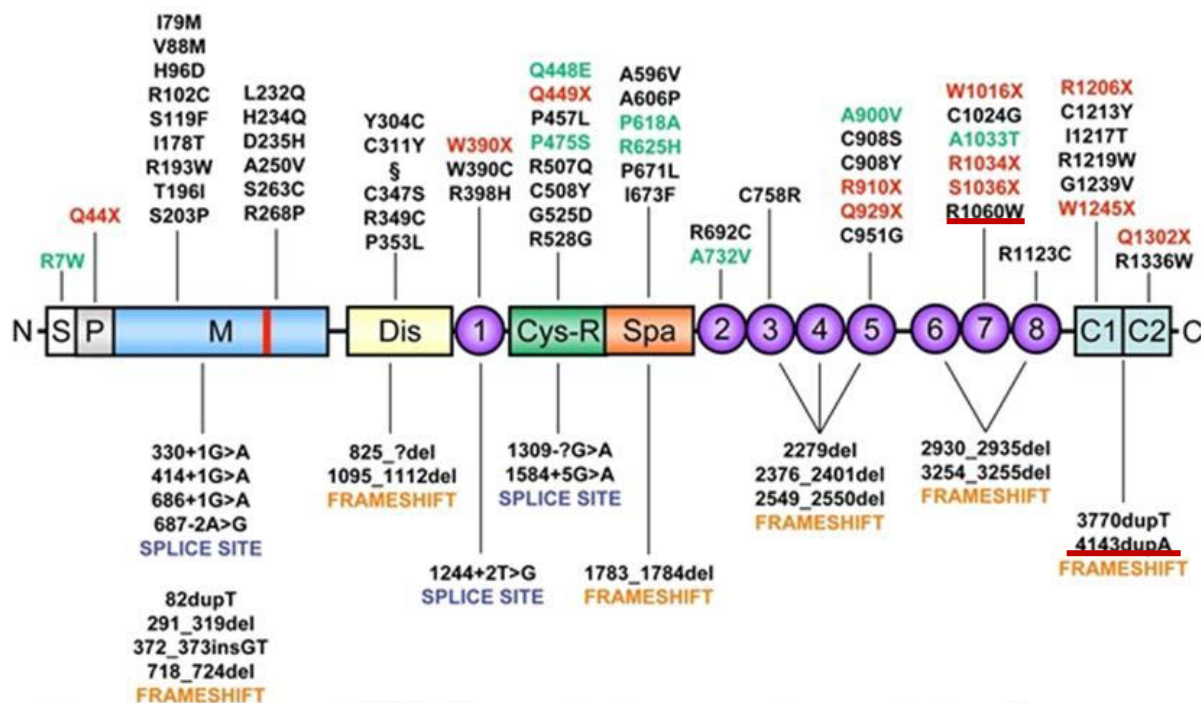


Figure 2.11: Locations of mutations in variable regions of ADAMTS13 gene in patients with c TTP (Lancellotti *et al.* 2013). The nonsense mutations are highlighted in red, and SNP's in green. Below the domain structure of ADAMTS13 are splice mutations of ADAMTS13 mRNA and frameshift mutations. The two most common mutations (R1060W and 4143dupA) are underlined in red.

Although cTTP-causing mutations can present from early childhood, most female patients with cTTP causing mutations present during pregnancy (Alwan *et al.* 2019; Scully *et al.* 2014). Recently, two recurring mutations have been identified as significant for their characteristic presentation in cTTP. The first being a missense mutation (rs142572218) at exon 24 R1060W, which manifests in female patients during pregnancy (Camilleri *et al.* 2008; Scully *et al.* 2014). The second mutation is located at exon 29 c.4143dupA and results in a frameshift mutation (rs387906343). This mutation has been shown to be more prevalent in the central European and Norway population (von Krogh *et al.* 2016; Schneppenheim *et al.* 2006).

In a recent observational study by Alwan *et al.* (2019), 73 confirmed cTTP cases from the UK-registry were collected over 15 years and retrospectively analysed. Seventy percent (70%) of cTTP patients were females and had underlying missense mutation associated with late disease onset, usually during pregnancy. Approximately 64% had heterozygous mutations and 34% were affected by homozygous mutations. Alwan *et al.* (2019) reported that patients with cTTP due to mutations of the ADAMTS13 gene just before the Spacer domain (pre-Spacer mutations) had earlier presentations and more severe form of TTP compared to patients with mutation after the Spacer domain (post-Spacer mutations). Additional studies of site-directed mutagenesis and phenotypic expression are however indicated.

Patients with cTTP with either homozygous or double heterozygous mutations of the ADAMTS13 gene present with severe deficiency of ADAMTS13 (Scully *et al.* 2014). About 90% of homozygous individuals present with TTP phenotype and heterozygous individuals usually have ADAMTS13 activity levels ranging from 40% -70% of normal and may not have phenotypic expression of TTP.

2.5.2. Acquired ADAMTS13 deficiency

Acquired ADAMTS13 deficiency is often associated with a severe ADAMTS13 activity level of $\leq 10\%$ and the presence of antibodies to ADAMTS13 in more than 90% of cases (Scully *et al.* 2008; Rieger *et al.* 2005; Tsai and Lian, 1998). Severe deficiency of ADAMTS13 occurs mostly in patients with idiopathic TTP and the pathogenesis relates to ADAMTS13 autoantibodies, which are inhibitory in upto 95% of the cases (Sadler *et al.* 2008; Klaus *et al.* 2004; Soejima *et al.* 2003; Coppo *et al.* 2004; Tsai and Lian 1998; Tsai *et al.* 2001; Zheng *et al.* 2004).

Most pathogenic autoantibodies to ADAMTS13 in acquired TTP are of the IgG class and, less frequently, of the IgM/IgA class (Tsai and Lian, 1998; Scheiflinger *et al.* 2003; Ferrari *et al.* 2007). Two main mechanisms of autoantibody-mediated ADAMTS13 deficiency have been identified in acquired TTP. ADAMTS13 autoantibodies inhibiting (neutralizing) ADAMTS13's activity towards VWF and non-inhibitory autoantibodies which promote increased clearance of ADAMTS13 in the circulation by forming immune complexes (Thomas *et al.* 2015; Scheiflinger *et al.* 2003; Rieger *et al.* 2005). Since most of acquired idiopathic TTP patients present with decreased ADAMTS13 antigen levels. It is possible that autoantibody-mediated ADAMTS13 depletion is the dominant pathogenic mechanism underlying severe acquired ADAMTS13 deficiency and both inhibitory and non-inhibitory autoantibodies can result in ADAMTS13 depletion or clearance (Shelat *et al.* 2006). Not all acquired TTP patients have inhibitory autoantibodies to ADAMTS13 as 30-50% of acquired TTP patients present with non-inhibitory autoantibodies (Ludwig *et al.* 2017; Thomas *et al.* 2015; Scheiflinger *et al.* 2003).

As mentioned above, the majority of acquired TTP patients have IgG autoantibodies to ADAMTS13 with/without associated IgM and IgA autoantibodies (Rieger *et al.* 2005; Ferrari *et al.* 2007; Scheiflinger *et al.* 2003). The biological function of the IgG/IgA/IgM antibodies is determined by their specificity, affinity and subclass distribution, which results in different immunologic effects. The different immunoglobulin classes are associated with different pathogenic mechanisms. All IgG subclasses (IgG1, IgG2, IgG3, and IgG4) have been detected in patients with acquired TTP, and probably inhibiting ADAMTS13 activity. The IgG4 is the most prevalent subclass and is detected in 90% of patients with acquired TTP patients, followed by IgG1 in 52%, IgG2 in 50% and IgG3 in 33%

(Ferrari *et al.* 2009; McDonald *et al.* 2009; Ferrari *et al.* 2007). The pathogenicity of IgG4 autoantibody is associated with blocking ADAMTS13 enzymatic activity leading to VWF accumulation and microvascular thrombosis (Sinkovits *et al.* 2018).

High levels of free circulating IgG4 autoantibodies is associated with relapses in acquired TTP patients (Ferrari *et al.* 2007). It has been suggested that IgG subclasses and IgM autoantibodies increase complement activation, which promotes clearance of ADAMTS13 protein from the circulation (Scheiflinger *et al.* 2003; Schaller *et al.* 2014). The prognostic value of IgA autoantibodies has not been delineated but are always detected in combination with IgG/IgM autoantibodies. High levels of IgA autoantibodies in combination with other immunoglobulins was described in 3 patients with acute idiopathic TTP (Ferrari *et al.* 2007). (Ferrari *et al.* 2007).

Monitoring ADAMTS13 autoantibody titres may also be of clinical importance in acquired TTP as levels may correlate with the severity of the disease. Ferrari *et al.* (2007) monitored levels of inhibitory ADAMTS13 autoantibody in 32 patients presenting with relapsing-remitting acute idiopathic TTP and found that eighty-nine (89%) percent of these patients presented with inhibitory ADAMTS13 autoantibodies, while 94% presented with high ADAMTS13 IgG/IgM/IgA autoantibodies titres. High titers of inhibitory ADAMTS13 autoantibodies with undetectable ADAMTS13 levels persisted in patients who relapsed. High autoantibody titres have also been associated with delayed response to plasma exchange therapy and early death, suggesting the presence of refractory autoantibodies (Coppo *et al.* 2010; Ferrari *et al.* 2007; Tsai, 2000). These results were consistent with findings of similar studies (Igari *et al.* 2012; Page *et al.* 2017; Tsai and Li, 2001). These results also indicate that ADAMTS13 autoantibody detection is therefore a potentially useful tool in monitoring the risk TTP relapse in patients with acquired TTP.

Studies using animal models have investigated the significance of inhibitory autoantibodies to ADAMTS13. Feys *et al.* (2010) were able to induce early stage TTP in a baboon model by injecting healthy animals with murine monoclonal antibody against the metalloprotease, which resulted in severe ADAMTS13 deficiency of < 5%. Inhibitory antibodies against the TSP1-2 domain administered in healthy control animals had no effect on ADAMTS13 activity. Another study explored the pathogenicity of single chain variable fragments (scFv) derived from IgG ADAMTS13 autoantibody cloned from a TTP patient to induce acquired TTP in mice (Ostertag *et al.* 2016). In their results, mice that received naked DNA encoding human anti-ADAMTS13 scFv developed sustained full inhibition of ADAMTS13 activity and increased UL-VWF multimer concentrations. These animal studies highlighted the significant contribution of ADAMTS13 autoantibodies to the pathogenesis of acquired TTP.

2.5.2.1. Loss of immune tolerance in acquired TTP

Under normal conditions, the immune system is able to recognise antigens expressed by invading pathogens, while ignoring self-antigens through the mechanisms of immune tolerance, which is the ability of the immune system to become unresponsive to autoreactive lymphocytes thus preventing damage to host cell tissues (Janeway *et al.* 2001). In other words the immune system is able to identify and eliminate lymphocytes that are autoreactive and preserves those that will respond to invading foreign pathogens. Failure of immunologic tolerance of self because of genetic and environmental factors can result in autoimmunity. Autoimmune responses arise from recognition of self-antigens by low affinity autoreactive T-cells that have escaped negative selection in the thymus as well as medium/low affinity autoreactive B cells that enter the peripheral circulation. The activation of autoreactive B-cells to self-antigens in the periphery is dependent on T-cell activation (discussed in the sub-sections **2.5.2.1.1** and **2.5.2.1.2** below).

2.5.2.1.1. T-cell tolerance

The T-lymphocytes originate in the bone marrow and mature in the thymus and express T-cell receptors (TCRs) which are antigen specific. In the thymus, T-cells rearrange their TCR genes to express a vast variety of TCRs with wide antigen specificity. The fate of developing immature T-cells depends on their interactions with self-antigen peptides presented on major histocompatibility complex (MHC) class II molecules of dendritic cells. Dendritic cells are the most important antigen-presenting cells during T-cell priming (Yewdall *et al.* 2010) and provide co-stimulatory signals that complete the immune activation process. Autoreactive immature T-cells that bind with strong affinity to self-antigens are selected for programmed cell death (apoptosis). Autoreactive immature T-cells that bind self-antigen on MHC II with low affinity undergo a positive selection and can escape into the periphery. In the peripheral tolerance system, the escaped autoreactive T-cell either undergo apoptosis (peripheral clonal deletion) or survive but remain inactivated if the necessary signals for activation are not present (anergy).

Mechanisms that lead to loss of immune tolerance to ADAMTS13 in acquired TTP have been suggested in the literature (Kremer Hovinga *et al.* 2018). Activation of ADAMTS13-specific CD4⁺ T-cells requires recognition of ADAMTS13 peptides bound to HLA molecules of antigen presenting cells. Human leukocyte antigen (HLA) molecules encoded in MHC class II are important for recognition and presentation of peptides to T-cells. As such, HLA molecules have been implicated as predisposing factors to the development of autoimmune diseases including immune mediated TTP (Studt *et al.* 2004; Joseph *et al.* 1994). There is an increased frequency of HLA-DRB1*11, HLA-

DQB1*03 and HLA-DQB1*0503 genotypes in Caucasian patients with acquired TTP (Scully *et al.* 2010; Coppo *et al.* 2010; Mancini *et al.* 2016). Mancini *et al.* (2016) also documented the presence of a single nucleotide polymorphism (rs6903608) located in the HLA-DRB9 locus immunochip analysis and suggested that it predisposes to occurrence of acquired TTP. The presence of HLA-DRB4 is thought to be protective against acquired TTP (Scully *et al.* 2010; Coppo *et al.* 2010). Another potential mechanism for the development of autoimmunity relates to differences in the stability of HLA-DQ proteins with instability predisposing to the escape of potentially autoreactive T-cells from negative selection in the thymus (Miyadera *et al.* 2015).

2.5.2.1.2. B-cell tolerance

B-cell tolerance, which screen against autoreactive B-cells, begins in the bone marrow with the elimination of developing B-lymphocytes that display strong binding affinities to self-antigens. B-cells are capable of re-arranging their immunoglobulin genes termed receptor editing (Yewdall *et al.* 2010). During this process, B-cells with high affinity binding to self-antigens generate an intracellular signal, which results in rearrangement of light chain immunoglobulin genes and the self-reactive light chain sequence is deleted and then replaced by a new one. The B-cell matures if the new light chain sequence is non-reactive. If the new light chain is still reactive, further light chain re-arrangement will be attempted until no new combinations are available but the B-cell undergoes programmed cell death (apoptosis) or anergy (permanent state of unresponsiveness to antigen) if a suitably non-reactive sequence is not achieved. Anergic B-cells can enter the circulation where they survive for few days and then undergo apoptosis. Autoreactive B-cells that have low or medium binding affinity to self-antigen may survive in the circulation (Tiller *et al.* 2007; Wardemann *et al.* 2003). Low affinity binding autoantibodies are poly-reactive and can recognise self-antigens as well as pathogen derived antigens (Wardemann *et al.* 2003).

Not all autoantibodies are pathogenic and polyclonal IgM and IgG autoantibodies can sometimes protect against autoimmunity (Mannoor *et al.* 2013; Nimmerjahn *et al.* 2008). Studies suggest that pathogenicity of autoantibodies depends on the extent of glycosylation/sialylation patterns of the Fc region since it affects immunoglobulin-effector cell binding but the control of these processes is poorly understood (Strait *et al.* 2015; Böhm *et al.* 2014; Goulabchand *et al.* 2014). Polyclonal IgG can exhibit anti-inflammatory or pro-inflammatory mechanisms determined by the degree of glycosylation/sialylation of the Fc region (Anthony and Ravetch, 2010). IgG Fc receptors that mediate activating signals include FcγRI (CD64), FcγRIIIA (CD16a) and FcγRIIB (CD16b), and inhibitory Fc receptors include FcγRIIA and FcγRIIB (CD32). Hess *et al.* (2013), demonstrated that

poorly sialylated IgGs that were generated in a T-cell dependent process in mice were pro-inflammatory compared to IgG derived in a T-independent immune reaction that were highly sialylated. Furthermore, the degree of antibody sialylation was also regulated by interactions of B-cells with CD4⁺T-cells (McHeyzer-Williams *et al.* 2009).

Antigen presentation by B-cells promotes expansion of activated T-cell clones with effector functions (Crawford *et al.* 2006; Barr *et al.* 2010; Barr *et al.* 2012). In turn, T-cells alter the type of antibody produced to a different isotype, which suggests that B- and T-cell interactions play a crucial role in modulating glycosylation patterns as well as autoantibody pathogenicity. Ludwig *et al.* (2017) argues that, once autoantibodies production has started, it is maintained by ongoing activation of autoreactive B-cells and, ultimately plasma cells, with ongoing autoantibody production.

2.5.2.2. ADAMTS13 antigen presentation to CD4⁺ T-cell

Antigen presentation by dendritic cells to CD4⁺ T-cells occurs in the lymphoid tissues and peripheral organs. ADAMTS13 is endocytosed by dendritic cells via the macrophage mannose receptor and peptide antigens are presented on the HLA molecules of MHC class II of these cells (Sorvillo *et al.* 2012). The MHC class II/ADAMTS13 peptide complexes on dendritic cells recognise and bind low affinity autoreactive CD4⁺T-cell receptors. In turn, the recognition receptors CD80/CD40 and CD40/CD40L are triggered to promote proliferation and differentiation of autoimmune lymphocytes through co-stimulatory binding signals. The activated autoreactive CD4⁺ T cells will then secrete cytokines to stimulate autoreactive B cells activation, resulting in the production of ADAMTS13-specific autoantibodies.

Hrdinová *et al.* (2018), described these events in **Figure 2:12**, as well as the recently identified ADAMTS13 peptide sequences, which preferentially bind to risk-associated HLA alleles of MHC class II and results in acquired TTP (Sorvillo *et al.* 2012; Verbij *et al.* 2016). The ADAMTS13 peptide sequence FINVAPHAR preferentially bind MHC class II of healthy individuals and TTP patients who are positive for the HLA-DRB1*11 allele. While healthy individuals and TTP patients who are positive for the HLA-DQB1*03 allele had preferential binding properties to peptide sequence ASYLIRDTHSLR. Both these peptide sequences are derived from the C-terminal CUB2 domain of ADAMTS13. These investigations suggest that autoreactive T-cell receptors that recognise and binds CUB2 domain peptides may potentially be involved in the pathophysiology of acquired TTP.

In a separate study, Hrdinová *et al.* (2018) also identified additional ADAMTS13 peptide sequences from the Metalloprotease domain, TSP1 repeats and Cysteine-rich/Spacer domains with

preferential binding to HLA-DQ and HLA-DR alleles using mass spectrometry analysis. The four novel ADAMTS13 peptide sequences identified on the HLA-DQ alleles belonged to the Cysteine-rich domain (WGAAVPHSQ and LDGTRCMPS), TSP1-2 (NYSCLDQARKELVETVQCQ) and CUB1 domain (QADCAVAIGRPLG). The ADAMTS13/CUB1 peptide sequence was also identified in both HLA-DR and HLA-DQ alleles. Studies to determine whether the novel peptides identified on HLA-DQ may potentially trigger the events that leads to the initial onset of acquired TTP are still to follow.

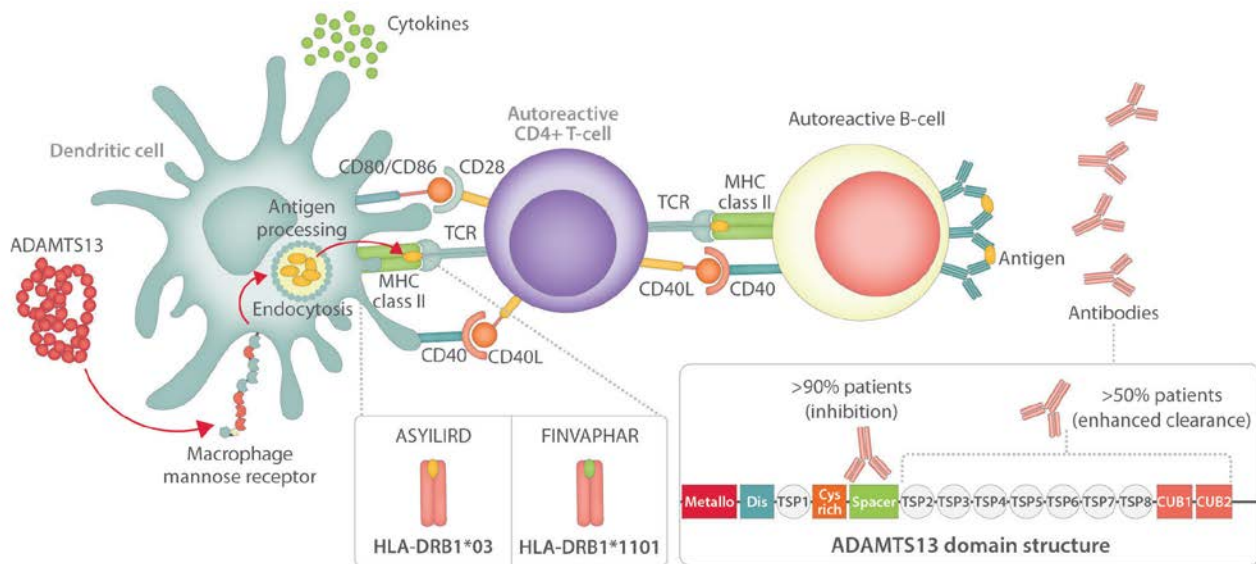


Figure 2:12. Schematic presentation of the onset of immune-mediated TTP (Hrdinová *et al.* 2018).

Dendritic cell endocytose ADAMTS13, process it to peptides, which are presented on MHC class II. ADAMTS13-derived peptides ASYLIRD and FINVAPHAR are presented on HLA-DRB1*03 and HLA-DRB1*1101 respectively. In the presence of specific autoreactive CD4⁺ T-cells, the complex MHC-II/peptide will be recognised by TCR, which will cause activation of the CD4⁺ T-cell, which interacts with autoreactive B-cell facilitating the production of ADAMTS13-specific autoantibodies.

2.5.2.3. ADAMTS13-antibody Immune complexes

Binding of autoantibodies to ADAMTS13 results in the formation of immune complexes, which are proinflammatory, promoting tissue damage and autoimmune disease processes (Toong *et al.* 2011; Weissmann *et al.* 2009). The prevalence of circulating autoantibody/ADAMTS13 immune complexes has been detected in patients with acquired TTP and their persistence over time (Ferri *et al.* 2014; Lotta *et al.* 2014). However, the role of these circulating immune complexes in the pathophysiology of TTP has not been conclusively determined.

In a large cohort of 68 patients presenting with acute TTP, Ferrari *et al.* (2014), detected ADAMTS13-specific immune complexes in 97% of patients using immunoprecipitation and these persisted in

93% of patients during remission of TTP despite normal ADAMTS13 antigen levels and activity. Immunoglobulin G4 (IgG4) was the most prevalent ADAMTS13/antibody immune complexes detected in both situations. The presence of free circulating IgG4 ADAMTS13 autoantibodies was associated with relapses but the utility of IgG4/ADAMTS13 immune complexes to predict relapses has not been established.

Another study by Lotta *et al.* (2014), also measured the prevalence of circulating ADAMTS13 immune complexes in 55 patients presenting with acute TTP with a novel ELISA. Circulating ADAMTS13-specific immune complexes was detected in 47% of patients with severe ADAMTS13 antigen and activity levels, presenting with ADAMTS13 autoantibodies compared to 37% of patients with no ADAMTS13 autoantibodies. The authors also found that patients with increasing levels of circulating ADAMTS13-specific immune complexes required a higher number of plasma exchange procedures to attain remission. This observation justifies the need to determine the prognostic relevance of these immune complexes and their role in the pathophysiology of TTP.

2.5.2.4. Epitope mapping studies

The autoantibody response in acquired TTP is polyclonal with varying sizes of target epitopes on the ADAMTS13 domains. Epitope mapping is a process of identifying the antigenic peptide sequences responsible for eliciting an immune response by antibodies (Onoue *et al.* 1965). Epitope identification requires a systematic screening of the whole antigen, using serologic screening techniques. A number of serological approaches have been used for epitope mapping studies, which include Western blot (Chou *et al.* 2005), phage display (Böttger and Böttger, 2009), microarrays (Fritzen *et al.* 2018), immunofluorescence (Kong *et al.* 2016), radioimmunoassay and ELISA (Reineke, 2009) techniques. Identifying antigenic determinants can assist in profiling changing humoral immune responses of individual patients during disease progression and/ or monitor therapeutic interventions. Epitope mapping can also provide important information for targeted therapy development.

Limited epitope mapping studies have revealed autoantibody binding to different ADAMTS13 domains using different techniques, **Table 2.1**. The ADAMTS13 Spacer domain has epitopic residues to ADAMTS13 IgG autoantibodies in 90-100% of acquired TTP cases (Luken *et al.* 2005; Klaus *et al.* 2004; Soejima *et al.* 2003; Zheng *et al.* 2010). The IgG autoantibodies cloned from plasma of patients with acquired TTP were shown to exert an inhibitory effect on recombinant ADAMTS13 Cysteine-rich and Spacer domain fragments in *in-vitro* studies (Luken *et al.* 2005; Klaus *et al.* 2004; Soejima *et al.* 2003). Another study utilised single chain variable fragments (ScFv's) derived from inhibitory

IgG cloned from a patient with acquired TTP on remission (Ostertag *et al.* 2016). Epitope mapping revealed that the Cysteine-rich/Spacer fragments were constantly inhibited by these autoantibodies. The remaining ADAMTS13 fragments did not react with the inhibitory IgG ScFv's. However, other non-inhibitory subsets of 23 IgG ScFv with different genetic background reacted with ADAMTS13 fragments including the Cysteine-rich/Spacer domain fragment, which indicates that not all IgG autoantibodies reacting with Cysteine-rich/Spacer domains are inhibitory.

Luken *et al.* (2006) further showed that purified inhibitory ADAMTS13 autoantibodies target specific epitopic residues at position 572-579 and 657-666 of the Spacer domain. Another study detected additional antigenic residues in the Spacer domain at position 636, 637, 639 and 640 to a human monoclonal antibody fragment isolated from a TTP patient (Casina *et al.* 2015). Subsequent studies demonstrated that residues at position 568 and 592, 658-665 as well 662 and 687 of the ADAMTS13-Spacer domain are targeted by purified mAb and pAb IgG cloned from patients with acquired TTP and influenced recognition, binding and cleavage efficiency of ADAMTS13 to substrate VWF (Yamaguchi *et al.* 2011; Pos *et al.* 2011). Considering the important role of the Spacer domain in providing high-affinity binding of ADAMTS13 at positions 658-666 to VWF substrate at position 1660-1668. The major antigenic determinants identified in the Spacer domain may contribute to acquired decreased ADAMTS13 activity.

Thomas *et al.* (2015) showed that not all IgG autoantibodies detected in acquired TTP patients are inhibitory against the ADAMTS13 domains. The non-inhibitory antibodies directed against the Spacer domains were cloned from patients with acquired TTP and their activity analysed using recombinant ADAMTS13 fragments purified from mammalian cells with Fluorescence Resonance Energy Transfer (FRETs) assay. The results indicated a decreased ADAMTS13 activity, suggesting that the presence of non-neutralizing autoantibodies also affected the activity of ADAMTS13 in the circulation *in vivo*. These findings supported the results of Scheiflinger *et al.* (2003), that demonstrated that non-neutralizing autoantibodies influenced the half-life of ADAMTS13 leading to decreased ADAMTS13 activity. Both studies suggest that non-neutralizing autoantibodies may be the primary pathogenic autoantibodies in most acquired TTP cases.

Patients with acquired TTP may also have autoantibodies, which bind to additional domains of ADAMTS13. One study found that 56% of patients with acquired TTP had IgG autoantibodies which reacted to the Met – TSP1-1 domains and 64% reacted with the CUB domains (Klaus *et al.* (2004). They also detected autoantibody binding to the propeptide residues in 20% of acquired TTP patients using western blotting. In another study by Luken *et al.* (2005), IgG autoantibodies derived from acquired TTP patients did not bind to the propeptide fragment in all test plasmas. The propeptide

functions solely to transport ADAMTS13 protein in the circulation and autoantibodies binding to the propeptide region may not be pathogenic (Majerus *et al.* 2003).

Autoantibodies binding to the Met/Dis/TSP1-1 domains may interfere with the catalytic activity of ADAMTS13, although further investigations are required. The TSP1-1 is reported as the most antigenic domain following the Cysteine-rich/Spacer and CUB domains (Luken *et al.* 2005; Klaus *et al.* 2004; Soejima *et al.* 2003). Autoantibodies binding to TSP1-1 may interfere with ADAMTS13-endothelial cell surface interactions via CD36 as well with VWF. The remaining TSP1 2-8 repeats of ADAMTS13 have been shown to be less reactive to autoantibodies (Zheng *et al.* 2010; Klaus *et al.* 2004; Pos *et al.* 2011).

The C-terminal TSP1 5-8 and CUB domains mediate protein-to-protein interactions and bind ADAMTS13 to VWF (Feys *et al.* 2009). In addition, the CUB domains have a regulatory role towards the activity of ADAMTS13 by interacting with the Spacer domain in the circulation (Apte, 2009). Thus, autoantibodies binding to the CUB domains might interfere with the ability of ADAMTS13 to bind to VWF thus compromising its proteolytic activity. Although the CUB domains are considered dispensable under flow conditions, the significance of the presence of autoantibodies binding to these domains is yet to be determined. It is however, suggested that autoantibodies targeting the C-terminal domains could promote the formation of immune complexes that lead to clearance of ADAMTS13 in the circulation (Ostertag *et al.* 2016). Whether the deposition of these immune complexes on tissues also contribute to the pathophysiology of acquired TTP, remains to be determined.

It is interesting to note that Grillberger *et al.* (2014) found that about 5% of healthy individuals had IgG autoantibodies to ADAMTS13, which shared linear epitopes with those found in acquired TTP patients. However, these autoantibodies were non-inhibitory and had low affinity binding to the ADAMTS13. Whether or not non-pathogenic anti-ADAMTS13 antibodies predispose to the development of acquired TTP and the circumstances leading to pathogenic transformation are not clear.

The results of epitope mapping studies of full length ADAMTS13 and individual ADAMTS13 domain fragments with autoantibodies cloned from patients with acquired TTP using different methods are summarised in **Table 2.1**. Although there are discrepancies in autoantibody binding to other ADAMTS13 domains, the Spacer domain has constantly been identified as being the most antigenic domain and, is also critical in ADAMTS13-VWF proteolytic activity.

Table 2.1: A summary of IgG autoantibody-ADAMTS13 epitope mapping studies.

| Study | No. of acquired TTP patients Ig cloned | Source of ADAMTS13 protein expression | Epitope mapping Method | ADAMTS13 domains analysed | Results of autoantibody Reactivity |
|------------------------------|--|---------------------------------------|---|--|--|
| Soejima <i>et al.</i> 2003 | 3 acquired TTP patients | Mammalian HeLa cell line. | Purified Inhibitory IgG autoantibodies. Western blotting. | C/S | 3/3 |
| Klaus <i>et al.</i> 2004 | 25 acute idiopathic TTP patients | <i>E.coli</i> phage display library | IgG clones. Western blotting. | Propeptide M/D/T1 TSP1-1 C/S T2-8 CUB1-2 | 5/25 14/25 14/25 25/25 7/25 16/25 |
| Luken <i>et al.</i> 2006 | 1 acquired TTP patient on remission | High five Insect cells | V-gene phage display libraries of B cell clone IgG mAb. Immunoprecipitation. | D/T S | 1 mAB 3 mAb |
| Zheng <i>et al.</i> 2010 | 67 idiopathic TTP patients. | Mammalian HEK 293 cells | Cloned IgG autoantibodies. Immunoprecipitation and Western blotting. | M/D/T1 M/D/T/C/S T 2-8 T 2-8/CUB1-2 | 8/67 65/67 24/67 31/67 |
| Yamaguchi <i>et al.</i> 2011 | 13 acquired TTP patients, 2 patients failed. | <i>E.coli</i> phage display library | Immobilized IgG autoantibodies and ADAMTS13 phage library in solution. | Signal/Propetide M D T1 C S T2-8 C1-2 | 2/11 5/11 2/11 1/11 2/11 7/11 7/11 1/11 |
| Thomas <i>et al.</i> 2015 | 92 acquired TTP patients | Mammalian HEK293 cells | Purified IgG autoantibodies. ELISA-based assays. | M/D/T/C/S TSP1 2-8 CUB1-2 | 89/92 26/92 28/92 |
| Ostertag <i>et al.</i> 2016 | 4 acquired TTP patient. | Mammalian HEK 293 cells | Inhibitory soluble 23-scFv mAb IgG clones. Immunoprecipitation, and Western blotting, | M/D/T1 M/D/T/C/S T 2-8 T 2-8/CUB1-2 | 1/23 15/23 3/23 9/23 |

The ADAMTS13 domains targeted by autoantibodies in HIV related and other causes of secondary TTP have also not been determined. HIV-associated TTP in patients with low CD4⁺ T-cell counts of <200 mm³ and high viral loads is associated with increased incidence of autoantibody, which contribute to the pathophysiology of TTP in HIV-infected patients. The current study aims to determine whether the Spacer domain is particularly immunogenic in patients with HIV-associated TTP and whether there is linearity of epitopes between idiopathic and HIV-associated TTP patients.

The binding of antibodies to an antigen is referred to as B cell mapping. B-cell epitopes are classified as either conformational (discontinuous) or non-conformational (linear). Non-conformational B-cell

epitopes typically comprise on average 15-20 residues derived from discontinuous segments of the antigen through folding to produce a linear, contiguous surface that is recognised by an antibody (Kringelum *et al.* 2013; Van Regenmortel, 2009). The characteristics of epitope areas have been described in previous studies. According to Kringelum *et al.* (2013), an average epitope size is ~10 - 25 amino acid residues long with a linear stretch of 5 or more residues constituting more than half of the epitope size in 85% of epitopes. Epitopes are also more surface exposed, suggesting they protrude from the antigen surface than the remaining antigen (Andersen *et al.* 2006; Rubinstein *et al.* 2008).

Peptide libraries have successfully been used to identify epitopes in antigen-antibody interactions (Böttger and Böttger A. 2009; Sloodstra *et al.* 1996; Blake and Litzi-Davis, 1992). Synthetic soluble overlapping peptide libraries are used for identifying antibody epitopes by scanning the entire sequence of a protein in its primary structure (Reineke, 2009; Pinilla *et al.* 1994; Houghten *et al.* 1991). Peptide library is a systematic combination of a large number of different peptides that display multiple short (10 – 30 amino acids), linear peptide fragments in parallel to deduce specific epitopes (Liu *et al.* 2003). A series of short overlapping peptide fragments synthesized from an antigen usually detects for linear epitopes (Heuzenroeder, 2009). Peptide library also provide a rapid and cost-effective solution for a variety of applications in proteomics, including epitope-mapping studies. Peptide libraries can be efficiently synthesized, producing many peptide sequences that can be used for binding assays. Antigenic peptides can be screened following the addition of specific test antibody, of which binding can be monitored using both qualitative and quantitative methods, such as in Enzyme-linked immunosorbent assay (ELISA) (Heuzenroeder, 2009).

2.5.3. Subtypes of TTP

Acquired TTP is more common than inherited TTP (Scully *et al.* 2017) occurring more frequently in females between the ages of 30 - 40 years (Terrell *et al.* 2010). According to the UK- and USA TTP-HUS registry data, the black (African) population is more affected than other races (Reese *et al.* 2013; Terrell *et al.* 2010; Scully *et al.* 2008). The majority of acquired TTP cases are idiopathic but secondary causes include pregnancy, infections with for example HIV, drug exposure, malignancy, cell or tissue transplantation, and, the recently observed, pancreatic-associated TTP (Scully *et al.* 2014).

Pregnancy-associated TTP accounts for 12-31% of all secondary TTP cases and ~90% of women with congenital and ~40% with previous acquired TTP will relapse during pregnancy which relates to the

decreased ADAMTS13 activity associated with pregnancy (Scully *et al.* 2012; Vesely *et al.* 2004; Alwan *et al.* 2019). Proteins found in the placental circulation serve as antigens that can trigger maternal antibody production against ADAMTS13 (Fyfe-Brown *et al.* 2013).

Drug induced TTP accounts for ~15% of acquired TTP cases (Scully *et al.* 2008) and agents such as cyclosporine, quinine, ticlopidine, clopidogrel, mitomycin and oestrogen-containing medication have been identified as potential triggers of immune mediated TTP (Medina *et al.* 2001) and generally have poor outcomes with high mortality rates (Dlott *et al.* 2004). The predictive value of ADAMTS13 deficiency in drug induced TTP is controversial, as moderate to severe ADAMTS13 activity levels have been reported in patients with drug induced TTP (Vesely *et al.* 2003; Tsai *et al.* 2000). Drug discontinuation or dose reduction and plasma exchange therapy can be effective (Medina *et al.* 2001; Trimarchi *et al.* 2001).

Thrombotic thrombocytopenic purpura (TTP) related to malignancy are either precipitated by chemotherapy or the disease process itself. The most common cancer associated with TTP is adenocarcinomas (Scully *et al.* 2012), bone marrow metastasis and secondary myelofibrosis (Morton and George, 2016; Chang and Naqvi, 2003). The prognosis of TTP in cancer is poor and treatment should target the underlying malignancy causing TTP (Regierer *et al.* 2011; Farhat *et al.* 2009) with plasma exchange therapy having minimal efficacy (Farhat *et al.* 2009; Chang and Naqvi, 2003). Severe ADAMTS13 deficiency is not always detected in these patients (Fontana *et al.* 2001) and enable regular administration of chemotherapy (Regierer *et al.* 2011; Farhat *et al.* 2009).

Pancreatic-associated TTP cases have recently been reported in which TTP affects the pancreas with thrombotic occlusions of the pancreatic microvasculature and the resultant tissue ischaemia manifesting as acute pancreatitis (Bergmann *et al.* 2008; Hosler *et al.* 2003; Swisher *et al.* 2007; Ali *et al.* 2014; McDonald *et al.* 2009). In turn, pancreatitis can result in TTP, which is related to endothelial injury mediated by inflammatory cytokines with increased release of UL-VWF multimers and inhibition of ADAMTS13 proteolytic activity (Bergmann *et al.* 2008). Combined plasma exchange with corticosteroid therapy has led to favourable outcomes in these patients although ADAMTS13 is only moderately reduced (McDonald *et al.* 2009).

2.5.3.1. HIV-associated TTP

The acquired form of TTP associated with HIV infection is still the most common TTP observed in the South African population (Masoet *et al.* 2019). TTP in HIV infected patients, first reported in 1987, has a 15 – 40 higher incidence as compared to non-infected individuals (Jokela *et al.* 1987;

Becker *et al.* 2004; Visagie and Louw, 2010; Gunther *et al.* 2007). South Africa has the highest HIV infection in the world (Statistics SA, 2019), and current reports indicate that about 80% of TTP cases are related to HIV infection (Masoet *et al.* 2019; Louw *et al.* 2018). The incidences of HIV-associated TTP are also higher in the sub-Saharan Africa higher compared to the rest of the world (Gunther *et al.* 2006; Visagie and Louw, 2010).

International TTP registries have also reported on the prevalence of HIV infection among patients diagnosed with TTP (Benjamin *et al.* 2009; Blombery *et al.* 2016; Mariotte *et al.* 2016; George *et al.* 2012; Jang *et al.* 2011; Fujimura and Matsumoto, 2010; Scully *et al.* 2008). The incidences of HIV-associated TTP are predicted to increase over time in countries with high prevalence of HIV infection especially amongst black female patients (George *et al.* 2012; Louw *et al.* 2018; Reese *et al.* 2013; Hart *et al.* 2011; Terrell *et al.* 2010). Relapses are also more common, occurring in ~60% of patients, with a higher mortality rates vs. TTP in HIV uninfected patients (Hart *et al.* 2011; Terrell *et al.* 2010)

The incidence of HIV-associated TTP was expected to decline with widespread access to anti-retroviral therapy (ART) (Becker *et al.* 2004) but currently remains significant (Masoet *et al.* 2019; Louw *et al.* 2018). Thrombotic thrombocytopenic purpura (TTP) is most commonly observed in advanced HIV disease in ART naïve patients with high viral loads and low CD4⁺ T-cell counts of <200 /mm³ (Hart *et al.* 2011; Benjamin *et al.* 2009; Gunther *et al.* 2007). Thrombotic thrombocytopenic purpura (TTP) has even recently been described in HIV infected patients with viral loads below detectable limit on ART (Louw *et al.* 2018; Novitsky *et al.* 2005). Inflammation associated with immune reconstitution in response to ART is suggested as a potential trigger in these patients (Mounzer *et al.* 2007). The presence of the HIV viral antigen p24 on endothelial cells suggest a mechanistic link between HIV infection and TTP (del Arco *et al.* 1993).

The diagnosis of TTP is based on clinical findings of microangiopathic haemolytic anaemia (MAHA) with excessive schistocytes (>1%) on morphological examination of the peripheral blood smear and significant thrombocytopenia of <30 x 10⁹/l, in the absence of another cause of MAHA such as disseminated intravascular coagulation (DIC). A negative Coombs test excludes autoimmune haemolytic anaemia (George, 2010; Meiring *et al.* 2012). HIV testing is included in the initial TTP investigations due to high incidences of TTP associated with HIV infection in South Africa. Common clinical symptoms include neurological abnormalities, haemorrhage and less frequently renal failure is observed (Swart *et al.* 2019).

Severe ADAMTS13 activity of <10% is key to the diagnosis of TTP and this parameter is often used to differentiate TTP from other TMA's (George *et al.* 2012; Moake, 2002, Reese *et al.* 2013; Scully *et al.* 2008; Peyvandi *et al.* 2008, Thomas *et al.* 2015; Scully *et al.* 2007). However, ADAMTS13 testing

is not routinely available and the diagnosis of TTP often relies on clinical parameters and morphologic analysis of peripheral blood smear. The TTP PLASMIC scoring system is a validated algorithm to estimate the probability of severe ADAMTS13 deficiency based on clinical and routine laboratory parameters but the utility in HIV associated TTP is low due to heterogeneity of the disorder (Li *et al.* 2018; Bentley *et al.* 2013).

The pathogenesis of HIV-associated TTP is still speculative and the initial precipitating factor(s) require further elucidation. The disorder is regarded to develop due to heterogeneous mechanisms related to the viral infection. HIV endothelial dysfunction is considered to play a role in the pathogenesis (Cruccu *et al.* 1994; Gunther *et al.* 2006; Fujimura and Matsumoto 2010; Pos *et al.* 2011). Although other investigators suggest endothelial dysfunction may not be the primary cause of TTP but the end result of the MAHA process (de Wit *et al.* 2003). Inflammation or opportunistic infections associated with HIV have been suggested to contribute to acute TTP in HIV infected patients (George *et al.* 2012). Many studies have shown synergy between inflammatory cytokines and viral proteins implicated in endothelial dysfunction in HIV infection (Marincowitz *et al.* 2019; Zhang *et al.* 2008; Hunt, 2012). High viral loads may initiate an acute inflammatory response with resultant endothelial damage and loss of its natural anticoagulant properties.

Increased secretion of inflammatory cytokines (IL-6, IL-8, TNF α) can trigger an increased secretion of plasma UL-VWF multimers from endothelial cells while simultaneously inhibiting the activity of ADAMTS13 (Bernado *et al.* 2004). The increased secretion of UL-VWF may be sufficient to overwhelm the capacity of ADAMTS13 (Schwameis *et al.* 2015; Bernado *et al.* 2004). In addition, FXa, plasmin and thrombin also further inactivate ADAMTS13 by proteolysis (Crawley *et al.* 2005). These events may precipitate an acute episode of TTP in HIV infection, even with normal levels of ADAMTS13. Von Willebrand factor (VWF) levels are markedly elevated in HIV infected patients with high viral loads (Aukrust *et al.* 2000). Meiring *et al.* (2012) also detected increased levels of tissue factor in HIV positive ART naïve patients, which contributes to the thrombotic potential and might contribute to the onset of HIV-associated TTP. Elevated levels of D-dimers have also been detected in HIV-related TTP, which is likely to reflect the formation of microthrombi in response to increased VWF release. The hyaline thrombi that form further enhance thrombin generation and production of plasmin further decreasing ADAMTS13 activity through proteolysis. Impaired cleavage of UL-VWF multimers eventually overwhelms the ADAMTS 13 proteolytic capacity resulting in TTP (Gunther *et al.* 2006).

Furthermore, other factors suggested to contribute to ADAMTS 13 deficiency in patients with HIV-associated TTP are viral infection in megakaryocytes, immune-mediated destruction and toxic drug

side effects. (Cruccu *et al.* 1994). Micronutrient deficiencies of i.e. zinc and calcium together with autoantibodies and aberrant T-cell responses to ADAMTS13 are further potential triggers of HIV-associated TTP (Meiring *et al.* 2012; Boro *et al.* 2011; Massabki *et al.* 1997).

ADAMTS13 autoantibodies are considered the most important cause of severe ADAMTS13 deficiency in patients with acquired TTP (Klaus *et al.* 2004; Soejima *et al.* 2003; Coppo *et al.* 2004; Tsai and Lian, 1998; Tsai *et al.* 2001; Zheng *et al.* 2004). Patients with HIV-associated TTP and low CD4⁺ T-cell counts of < 200 cells/mm³ and high viral loads have increased incidence of autoantibodies (Chen *et al.* 2002). Some patients with HIV-associated TTP do not have detectable ADAMTS 13 neutralising autoantibodies (Zheng *et al.* 2004; Scully *et al.* 2005; Gunther *et al.* 2007). Non-neutralizing antibodies could increase clearance of or inhibit ADAMTS13 binding to the endothelium without directly interfering with its activity (Scheiflinger *et al.* 2003; Thomas *et al.* 2015). It is possible that mechanisms independent of severe ADAMTS13 deficiency could be operational in HIV-associated TTP.

The pathogenesis of HIV-associated TTP is probably therefore heterogeneous and the existing literature consists largely of observational case series in small cohorts with limited data regarding ADAMTS13 activity and the presence of ADAMTS13 autoantibodies. Larger international studies on acquired TTP either do not include, or specifically exclude HIV-positive patients (Vesely *et al.* 2003; Payvandi *et al.* 2004; Zheng *et al.* 2004) and the exact role of autoantibodies to ADAMTS13 in HIV-associated TTP remains to be investigated.

Two previous South African studies have detected autoantibodies to ADAMTS13 in 50% of patients with HIV-associated TTP (Gunther *et al.* 2007; Meiring *et al.* 2012). Gunther *et al.* (2007) defined these autoantibodies as inhibitory in 38% of patients through mixing studies. Both these local studies also reconfirmed increased VWF antigen levels in HIV-associated TTP patients but the ADAMTS13 level were variable ranging from very severe ADAMTS13 deficiency of <5% up to normal levels (Hart *et al.* 2011). These differences could possibly be explained by unsuitable ADAMTS13 assays that were employed. Furthermore, Meiring *et al.* (2012) also documented the presence of autoantibodies to ADAMTS13. The authors only detected these antibodies in 50% of HIV-positive patients with TTP on ART and in ~80% of HIV-positive ART-naive patients without TTP.

Inhibitory antibodies are absent in hereditary TTP (Furlan *et al.* 1998). However, inhibitory autoantibodies are not present in all cases of acquired TTP such as in HIV-associated TTP. Instead, non-neutralizing ADAMTS13 IgG/IgM/IgA autoantibodies may be present (Scheiflinger *et al.* 2003). Non-neutralizing antibodies are thought to reduce the amount of circulating ADAMTS13 through

antibody-mediated clearance or block proteolytic cleaving of VWF and further investigations, with epitope mapping techniques, will shed light on the pathophysiology of HIV-associated TTP.

It is interesting to note that the frequency of ADAMTS13 autoantibodies in HIV positive patients without TTP was higher than the HIV-associated TTP group in a study by Meiring *et al.* (2012). The pathogenicity of these autoantibodies should be investigated. Inflammation related to chronic infections such as HIV can alter antibody glycosylation patterns and alter antibody auto-reactivity (Lu *et al.* 2016; Akerman *et al.* 2013; Moore *et al.* 2005; Alter *et al.* 2018; Jennewein and Alter *et al.* 2017 Goulabchand *et al.* 2014). High levels of agalactosylated antibodies, which induce chronic antibody-mediated inflammation, have been observed in HIV infected patients and also in patients with autoimmune diseases (Moore *et al.* 2005; Alter *et al.* 2018). Chronic infection may result in loss of galactosylated, anti-inflammatory IgG antibodies and high viral loads with associated inflammation may be associated with converting non-pathogenic anti-ADAMTS13 antibodies into pathogenic autoantibodies resulting in TTP.

Certain human leukocyte antigen (HLA) molecules (section 2.5.2.2) predispose to acquired TTP (Coppo *et al.* 2010). HIV-infection may be a triggering factor in these individuals with these genetic backgrounds. The frequency of these predisposing HLA genotypes have not been investigated in local South African cohorts and further studies are indicated in this regard.

The mechanisms of autoantibody formation in HIV infection are still not completely clear but cross-reactivity between viral and self-antigens is suggested (Susal *et al.* 1992; Golding *et al.* 1989). Studies that quantified HIV RNA in tissues demonstrated that 90% of all HIV virions are attached to the surface of follicular dendritic cells in the lymphoid tissues (Chen *et al.* 2002). These cells are the major initiators of immune response and do not always process antigen, but display it in its native form which could potentially stimulate B cells to produce antibodies directed against other native self-antigens (Tan *et al.* 1988). HIV bearing activated dendritic cells specifically targets helper CD4⁺ T-cells. The memory helper T-cells are rapidly infected and destroyed, leading to decreased activation and survival of cytotoxic T- and B-cells that can destroy virally infected cells. The rapid loss of memory helper T-cells leads to immune dysregulation and associated immunodeficiency and tolerance of auto-reactive B-cells (Yewdall *et al.* 2010).

The relationship between ADAMTS13 autoantibodies and HIV-associated TTP is not yet clear. Fewer HIV-associated TTP cases present with ADAMTS 13 autoantibodies compared to idiopathic acquired TTP cases (Gunther *et al.* 2007; Meiring *et al.* 2012; Coppo *et al.* 2004), which suggests that the contribution of ADAMTS13 autoantibodies to the deficiency of ADAMTS13 in HIV-associated TTP

may be different to idiopathic acquired TTP. Autoantibodies to ADAMTS13 in acquired TTP are also considered reliable prognostic biomarkers that can predict patient outcomes (Coppo *et al.* 2010; Ferrari *et al.* 2007; Tsai and Lia, 2001). Monitoring ADAMTS13 autoantibody titres as a predictive tool to predict recurrence/relapse may be of clinical importance in HIV-associated TTP patients with ADAMTS13 autoantibodies. The pathogenic ADAMTS13 autoantibodies must therefore be identified and their contribution to the TTP disease process should be investigated.

The multiple pathogenic factors contributing to HIV-associated TTP are depicted in **Figure 2.13**.

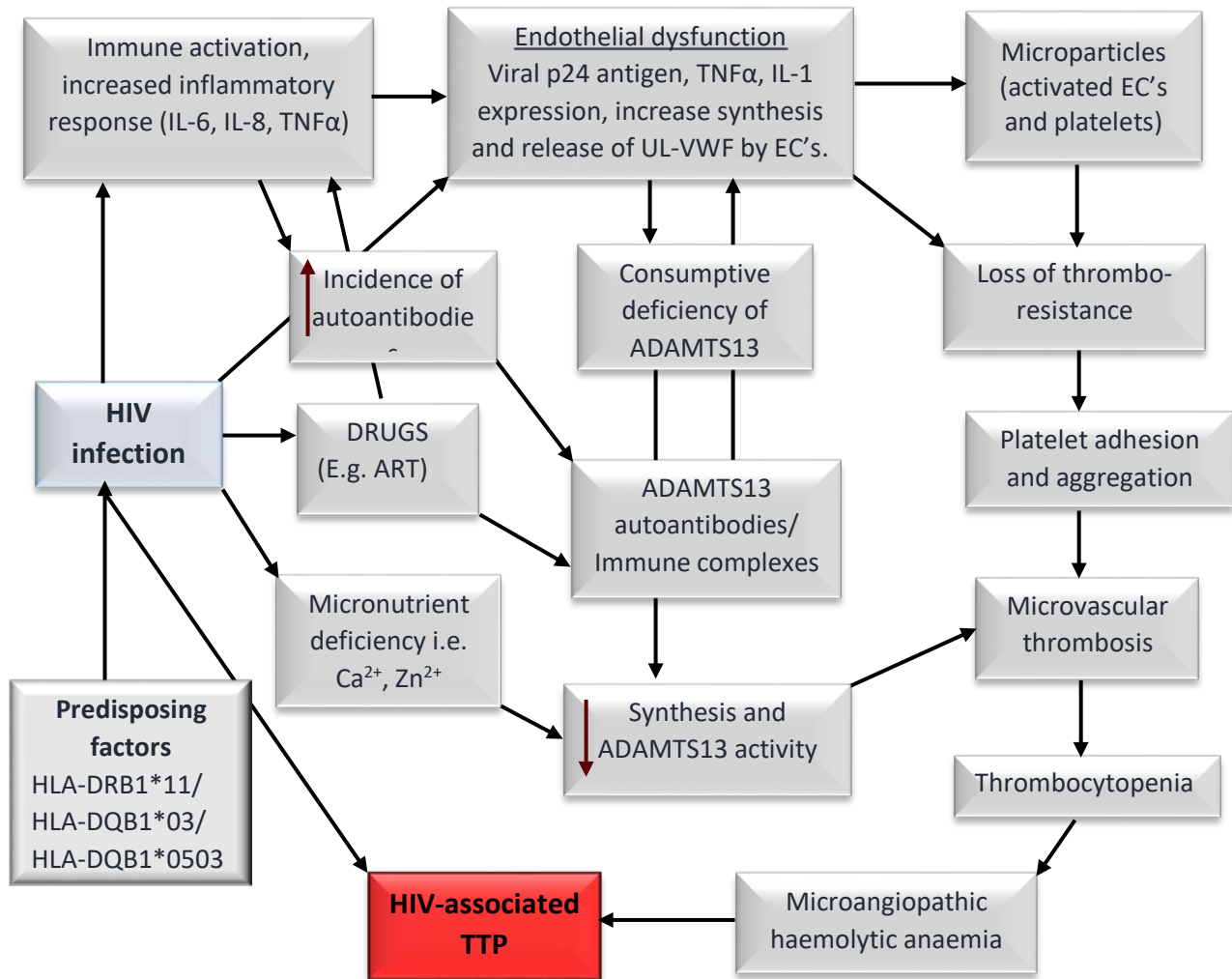


Figure 2:13. Contributing factors in HIV-associated TTP development.

2.6. HIV-associated thrombotic microangiopathies (TMA's)

The thrombotic microangiopathies (TMAs) are a group of diseases characterized by microangiopathic haemolytic anaemia and thrombocytopenia with microvascular thrombosis (Moake, 2002). The incidence of TMAs is increased in HIV infected people often occurring in more advanced end stage disease (Ripamonti *et al.* 1996; Becker *et al.* 2004; George *et al.* 2012). The

TMAAs can however also be the presenting disease process of underlying HIV infection (Sood *et al.* 1996; Blazes *et al.* 2004). The TMAAs include TTP and haemolytic uremic syndrome (HUS) (**Table 2.2**). TTP and HUS have been reported in HIV infected patients (George *et al.* 2004). The presenting features of TMAAs (del Arco *et al.* 1993) in HIV infected patients are similar to that in HIV uninfected people and the same diagnostic criteria can be applied (Bachmeyer *et al.* 1995). Overlapping clinical features between the different TMAAs can lead to diagnostic uncertainty (Moake, 2002).

Endothelial injury commonly occurs in HIV infection and results in endothelial dysfunction which could possibly be the pivotal pathogenic event in TMAAs (Bell *et al.* 1997; Hymes and Karpatkin, 1997). Severe ADAMTS13 deficiency (activity <10%) with/without the presence of ADAMTS13 autoantibodies and neurological dysfunction favours a diagnosis of acquired TTP (Coppo *et al.* 2004; Vesely *et al.* 2003). Nevertheless, ADAMTS 13 activity levels of up to 20% has been reported in patients with HIV-associated TTP (Park *et al.* 2009; Gunther *et al.* 2007; Meiring *et al.* 2012).

Haemolytic uremic syndrome (HUS) is a disorder of complement dysregulation and results in a TMA, which primarily affects the kidneys (Nester *et al.* 2015). Mutations or lowered levels of complement inhibitors can result in inappropriate complement activation with formation of terminal membrane attack complexes (MACs) effecting cellular damage and development of a TMA (Carson and Johnson, 1990; Ikeda *et al.* 1997; Tedesco *et al.* 1997). Diagnostic tests for HUS include assays that assess the presence of mutations of or antibodies against the complement regulatory proteins but these assays are not available in routine laboratories (Cataland *et al.* 2014). Studies have found a possible link between complement activation, severe ADAMTS13 deficiency and acquired TTP (Reti *et al.* 2012; Wu *et al.* 2006).

Treatment of TMAAs often involve plasma exchange therapy (PEX) with or without immunosuppressive therapy. Poor response to PEX is characterized by a lack of hematologic response and a worsening end-organ injury (Cataland and Wu, 2013) which can be managed with intensifying immunosuppressive therapy to suppress ADAMTS13 autoantibodies but an alternative diagnosis for the clinical and laboratory features should also be considered.

2.6.1. Other systemic conditions

Systemic conditions that present with TMAAs (**Table 2.2**) including systemic lupus erythematosus (SLE), Disseminated Intravascular Coagulation (DIC), and pregnancy-associated syndromes (preeclampsia and haemolysis, elevated liver function tests and low platelets (HELLP)) may mimic the clinical features of acquired TTP (Ahmed *et al.* 2002). However, these conditions do not cause a

severe deficiency of ADAMTS 13 activity of <10% which is observed in acquired TTP patients in whom it constitutes a laboratory diagnostic feature but reduced ADAMTS13 activities of between 10% - 50% may still be observed in these conditions (Pourrat *et al.* 2015).

Table 2.2: Systemic conditions presenting with MAHA and thrombocytopenia.

DIC-disseminated intravascular coagulation; SLE-systemic lupus erythematosus; HELLP-haemolysis, elevated liver function tests and low platelets.

| Syndrome | Clinical presentation | Laboratory data |
|--|---|---|
| DIC (Disseminated intravascular coagulation) | Caused by infection, malignancy, or vascular abnormality such as Kasabach-Merrit syndrome. | Prolonged PT/PTT, thrombocytopenia, decreased fibrinogen, elevated D-dimers. |
| SLE (Systemic lupus erythematosus) | May be associated with hypertension, renal insufficiency and autoimmune cytopenias. | Autoantibodies characteristic of SLE such as anti-Double stranded DNA. Prolonged PTT. |
| Pre-eclampsia and HELLP (pregnancy-related syndromes) | Severe hypertension and liver involvement in pregnant patient. Abnormalities resolve with delivery. | Elevated hepatic transaminases. |
| Hematopoietic or solid organ transplant | Maybe associated with exposure to cytotoxic chemotherapy, radiation, systemic infection or calcineurin inhibitor. | No specific findings |

The presenting features of a DIC are very similar to that of TTP and making the correct diagnosis can be difficult (Wada *et al.* 2018). The TMAs are also often associated with DIC, and vice versa. The pathogenic mechanism of DIC includes increase activation and consumption of the coagulation factors and platelets with the generation of fibrin (Wada, 2004). TTP on the other hand is characterized by MAHA and a severe ADAMTS13 deficiency and hence the different diagnostic criteria for a DIC (**Table 2.2**). The recommended treatment in patients with TTP (viz. PEX) and DIC (viz. treatment of the precipitating condition) is also different (Rock *et al.* 1991; Wada *et al.* 2013).

Systemic lupus erythematosus (SLE) can present with features, which are similar to those in TTP patients including thrombocytopenia, haemolytic anaemia, neurological abnormalities and fever. Patients with SLE can also present with low levels of ADAMTS13, which may suggest common

pathophysiologic pathways (Mannuci *et al.* 2003; Perez *et al.* 2011). In addition, the renal biopsy in SLE may show pathologic features of TMA, further complicating the differentiation between SLE and TTP. The presence of numerous schistocytes favours the diagnosis of TTP (Porta *et al.* 1993). Thrombocytopenic thrombotic purpura (TTP) can also occur in patients with SLE although this is not common but if present, results in increased mortality (George *et al.* 2008). PEX and immunosuppression treatment can be successful.

The haemolysis elevated liver enzymes and low platelet count (HELLP) syndrome is a complication of pregnancy that can lead to multiple organ failure (Weinstein, 1982). The diagnosis of pre-eclampsia complicated by HELLP can present a diagnostic challenge (Pourrat *et al.* 2015; Ben *et al.* 2010) as HELLP syndrome closely mimics other TMAs such as TTP and HUS presenting with thrombocytopenia, haemolysis, elevated liver enzymes and renal damage. A differential diagnosis of TTP should be considered in patients with HELLP syndrome who has neurologic abnormalities and HUS must be considered when renal impairment present (Pourrat *et al.* 2015). The ADAMTS13 levels are mildly decreased in HELLP syndrome patients at levels of 12% - 43% which is different from that in patients with TTP who have levels of <10% (Lattuada *et al.* 2003). If ADAMTS13 testing is not immediately available, correct diagnosis relies on the significant elevation in liver transaminases in HELLP syndrome patients (Keiser *et al.* 2012). Plasma exchange (PEX) therapy may have therapeutic benefit in patients with HELLP syndrome who have low ADAMTS13 activity levels.

The challenges relating to distinguishing between TTP and other TMAs highlights the need for identifying sensitive and specific biomarkers to ensure timely and appropriate therapy.

2.7. ADAMTS13 assays for acquired TTP diagnosis

There are a number of laboratory assays available for measuring ADAMTS13 levels and inhibitory autoantibodies, which can assist in the diagnosis of acquired TTP. Several immunoassays, such as the ELISAs are available for the detection and quantification of ADAMTS13 antigen levels in human plasma (Technoclone[®], Austria; American Diagnostica[®], USA; Bethyl laboratories[®], USA). However, the quantification of ADAMTS13 antigen alone is of limited diagnostic value as it is unable to discriminate between full length ADAMTS13 and truncated/mutated ADAMTS13 (Feys *et al.* 2006; Reiger *et al.* 2006). It is also unclear how the assays are affected by the presence of antibody-bound ADAMTS13 complexes, which could result in false normal levels of ADAMTS13 antigen (Reiger *et al.* 2006). Hence, the utility of functional ADAMTS13 activity assays which should be included in the TTP investigation panel (Shelat *et al.* 2006; Zheng *et al.* 2004; Coppo *et al.* 2006; Rieger *et al.* 2006).

Several ADAMTS13 activity assays are available which measure VWF cleavage products by direct and indirect methods. The VWF multimer analysis for example provide evidence of the proteolytic activity of ADAMTS13. The SDS Agarose gel electrophoresis and SDS-PAGE assays are direct tests of ADAMTS13 activity that, when combined with western blotting, allows for visualization of the degraded VWF fragments. However, these methods are time-consuming and are performed with potentially dangerous denaturing agents. The recently developed Fluorescence Resonance Energy Transfer (FRETs-VWF73) assay is a more rapid assay for measuring ADAMTS13 activity in a single step procedure (Kokame *et al.* 2005). In the FRETs-VWF73 assay, a synthetic 73 amino acid peptide VWF fragment that contains the ADAMTS13 cleavage site at the A2 domain is labelled with fluorescence markers that release fluorescence when cleaved by ADAMTS13. Fluorescence increases over time when FRETs-VWF73 is incubated with a normal citrate plasma sample containing ADAMTS13, while ADAMTS13 deficient plasma does not result in the release of fluorescence.

The indirect ADAMTS13 activity assays include the residual collagen binding (CB) assay, ristocetin-induced aggregation and functional ELISA assays. Both the residual CB and ristocetin assays rely on purified VWF or normal plasma incubated with test plasma in the presence of a denaturing agent to promote VWF multimer cleavage by ADAMTS13. In the CB assay, the residual VWF is measured by detecting binding to collagen type III with subsequent ELISA quantification utilising a conjugated anti-VWF antibody. With the ristocetin assay, residual VWF is measured by ristocetin-induced platelet aggregation using a platelet aggregometer. Functional ELISAs makes use of recombinant VWF73 fragments with ADAMTS13 cleavage sites which are immobilized on an ELISA plate together with an antibody conjugated with an enzyme. The amount of residual VWF73 fragments are measured after ADAMTS13 is added to the plate, using a second antibody that recognizes only the cleaved VWF fragments. The ADAMTS13 activity in the test plasma is therefore inversely proportional to the residual concentration VWF.

Several limitations may interfere with the clinical utility of activity assay results. Firstly, these assays measure ADAMTS13 in static conditions and do not reflect the *in vivo* physiological flow conditions. This may be important for the conformational changes that allow optimal ADAMTS13 enzymatic activity. Secondly, ADAMTS13 activity assays make use of denaturing agents that expose the cleavage site in the VWF substrate enhance its susceptibility to cleavage by ADAMTS13. These agents could also affect ADAMTS13 activity measurements and inhibit ADAMTS13-antibody interactions. Furthermore, the presence of other proteases in plasma could interfere with VWF cleavage or degrade ADAMTS13 itself. Factors such as hyperlipemia, elevated haemoglobin levels and hyperbilirubinemia could influence ADAMTS13 activity results (Studt *et al.* 2005; Meyer *et al.*

2007; Eckmann *et al.* 2007; Raife *et al.* 2009; Lam *et al.* 2007). Some of these assays, such as the multimer assays, are not available for routine diagnostic tests but may be suitable for specialised laboratories.

Mixing studies are also performed to detect the presence of inhibitory ADAMTS13 autoantibodies in acquired TTP patients. Almost 90 % of acquired TTP cases are associated with reduced ADAMTS13 activity of <10% together with inhibitory autoantibodies. Bethesda assay similar to those used to measure inhibitory FVIII antibodies are utilised to detect inhibitory ADAMTS13 antibodies (Vendramin *et al.* 2018; Alwan *et al.* 2017; Scully *et al.* 2008). These autoantibodies can be titrated by mixing studies and heat inactivated in patient and normal plasma samples (Peyvandi *et al.* 2004; Tsai and Lian *et al.* 1998). Bethesda assays however generally lack sensitivity.

In cases where the inhibitor is not detected or the inhibitor titer is too low to be detected, Western blotting assay or ELISA assays can be used to detect non-neutralizing antibodies (Zheng *et al.* 2009). The assumption is that non-inhibitory autoantibodies will reduce ADAMTS13 antigen levels by increasing its clearance in vivo rather than blocking ADAMTS13 enzymatic activity. The Western blotting assay is reported to be more sensitive than the quantitative ELISAs but plasma dilutions and the structure of ADAMTS13 molecules that are coated onto the plates can result in inter-assay discrepancies, which can affect assay sensitivity and positive cut-off values. It is also not clear whether clinically irrelevant autoantibodies may be detected as a result of antigen presentation (Peyvandi *et al.* 2010). Most of the detected inhibitory antibodies have been shown to target the Cysteine-rich and Spacer domains of the ADAMTS13 protein using western blotting. However, autoantibodies in TTP cases occurring secondarily to an existing condition, such as in HIV, have not yet been detected or identified. Furthermore, the activity of these autoantibodies still needs to be determined under flow conditions to help predict their pathogenicity in acquired TTP in general.

Flow-based assays have been developed for the detection and characterization of ADAMTS13 autoantibodies (Grillberger *et al.* 2014; Rieger *et al.* 2005; Tsai *et al.* 2006; Li *et al.* 2011). The objective of flow-based assays is to assess any discrepancies between inhibitor assays in order to predict inhibitor activity under flow. In a recent study by Grillburg *et al.* (2014), a novel flow-based assay was developed to compare the activity of inhibitory antibodies under static and flow conditions. Their results indicated that ADAMTS13 autoantibodies may show inhibitory activity in vivo that are not consistent with the inhibitor levels determined in routine static assays such as the FRETS-VWF17 assay. The assumption is that some epitopes exposed under shear stress may not be exposed in a static environment.

The ADAMTS13 assays have proved important in differentiating between the TMAs and can assist with prognostication and predicting treatment outcomes (Grillberger *et al.* 2014; Kokame *et al.* 2005; Zheng *et al.* 2004). Severely reduced ADAMTS13 activity of <10% together with inhibitory autoantibodies may indicate the need for intensification and prolongation of PEX and early introduction of immunosuppressive therapy. There is no absolute antibody titre that indicates a worse prognosis, but titres can be used in combination with other clinical information, such as high creatinine and troponin T levels to predict disease outcomes. Available ADAMTS13 assays can however not measure the potency of antibodies (Hughes *et al.* 2009).

2.8. Treatment of TTP

TTP is a medical emergency, with the mortality rate exceeding 90% if appropriate treatment is not timeously applied (Moake, 2002). The mainstay of current treatment for patients with HIV-associated TTP is plasma exchange (PEX) or infusion together with ART which results in recovery of the CD4⁺ T-cell levels while normalizing the ADAMTS13 antigen levels. PEX replaces defective ADAMTS13, while at the same time removing ADAMTS13 autoantibodies (Rock *et al.* 1991; Boro *et al.* 2011). Infusion of frozen plasma on the other hand replaces the ADAMTS13 enzyme in the patient's plasma to normal levels. Immunosuppressant therapy suppresses the production of ADAMTS13 autoantibodies in patients with acquired TTP. PEX therapy is more effective than plasma infusion in the treatment of acquired TTP (Rock *et al.* 1991). Plasma infusion is the treatment of choice in congenital TTP cases. A study by Novitsky *et al.* (2005) demonstrated that HIV positive patients with TTP respond well to plasma infusion alone and PEX therapy was reserved for relapsed and resistant TTP cases (Novitsky *et al.* 2005; Scully *et al.* 2012). These findings support suggestions that HIV-associated TTP may have a different pathophysiology to acquired idiopathic TTP.

Steroids are also widely used in combination with PEX in the initial treatment of acute TTP. Which have shown favourable outcomes with up to 91% remissions (Scully *et al.* 2010; de Fante, 2006; Ferrari *et al.* 2007). However, there is currently no consensus on whether the combination approach is superior to PEX alone.

Additional immunosuppressants such as cyclosporine (CSA) is indicated in refractory and relapsed patients with acquired TTP in an attempt to decrease autoantibody production (Pasquale *et al.* 1998). Cyclosporine regulates T-cell via its action on the cytokine interleukin 2 (IL-2) and reduces T-helper cell activity. Improved clinical and haematological picture has been observed early in the administration of the CSA therapy (Cataland *et al.* 2007). However, when CSA is administered in high

doses, it can also precipitate the MAHA, which is observed in TTP patients. The CSA therapy in combination with PEX results in a remission rate of 89% (Cataland and Wu, 2013).

Plasma exchange (PEX) therapy with normal levels of ADAMTS13 can also be combined with Rituximab in resistant HIV-associated TTP to prevent recurrent episodes of TTP (Garvey, 2008). Rituximab is an anti-CD20 monoclonal antibody that specifically depletes B-cells responsible for eliciting autoimmune responses. It targets the premature and mature B-cells in blood, lymph nodes and the bone marrow. A CD20 is expressed at high levels on B-cells causing a dense monoclonal antibody accumulation on the cell membrane resulting in complement dependent cytotoxicity. A CD20 is a very resistant marker with a prolonged cell surface half-life. Rituximab is also used as second line therapy in idiopathic TTP with ADAMTS13 autoantibodies and has been shown to normalize ADAMTS13 activity while achieving and maintaining remission in acute TTP and reduces relapses (Scully *et al.* 2007; Fakhouri *et al.* 2005; Herbei and Venugopal, 2006).

Several studies have evaluated different treatment combinations. Combined treatment with steroids and PEX was compared to CSA and PEX in acute TTP patients and concluded that CSA therapy achieves higher remission rate (89%) compared to steroids (83%) with fewer PEX sessions needed to achieve remission and fewer subsequent relapses (Cataland *et al.* 2007). Rituximab has demonstrated success in acquired TTP patients with high ADAMTS13 autoantibody titers and infections complications related to immunosuppression has not been observed (Sculley *et al.* 2007). Additional randomised control studies are still needed to further determine the effectiveness of immunosuppressive therapies in acquired TTP.

Protease inhibitors, such as Bortezomib, that can suppress plasma cells may have therapeutic efficacy in relapsed and resistant patients with acquired TTP (Ludwig *et al.* 2017; Alexander *et al.* 2015; Patriquin *et al.* 2016). Furthermore, clinical investigations have shown that the combination of both Rituximab and Bortezomib can result in depletion of both autoreactive B-cells as well as long lasting refractory autoantibodies (Hofmann *et al.* 2018; Khodadadi *et al.* 2015; Taddeo *et al.* 2015). However, the use of Bortezomib remains a therapeutic challenge due to its side effects.

Other drug interventions for TTP include Caplacizumab (Peyvandi *et al.* 2016) and recombinant ADAMTS13, which is still in clinical trials (Scully *et al.* 2007). Caplacizumab is an anti-von Willebrand factor nanobody, which inhibits interactions between UL-VWF multimers and platelets. Recombinant ADAMTS13 (i.e. BAX930) may provide alternative replacement therapy for patients with ADAMTS13 deficiency. Once successful, these drugs may be used for treatment and prevention of TTP, including congenital, acquired idiopathic and secondary forms of TTP, such as HIV-associated TTP.

2.9. Relapses

Relapse is defined as an acute TTP episode at least 30 days after remission from the index TTP episode (Scully, 2010). About 20% - 50% acquired TTP patients with severe ADAMTS13 deficiency and ADAMTS13 autoantibodies experience TTP relapses (Peyvandi *et al.* 2008; Del Fante *et al.* 2006; Scully *et al.* 2008). Autoantibody titres alone cannot be used as a predictive tool for relapses, but can be used to monitor therapeutic response. Patients with a low ADAMTS13 activity of <10% with the presence of inhibitory ADAMTS13 autoantibodies have shown to have a 3 times higher risk of relapse during the first year (Sculley *et al.* 2007; Ferarri *et al.* 2007). Gender was not found to be a risk factor for relapse of acquired TTP (Peyvandi *et al.* 2008).

Plasma exchange (PEX) can reduce TTP associated mortality rate by up to 20% and ART after the initial episode of TTP can assist in preventing relapses which relates reconstitution of the immune system. However, relapses may be more common in HIV-associated TTP patients with severe ADAMTS13 deficiency and ADAMTS13 autoantibodies, and mortality is also greater compared to other patients with acquired TTP (Scully *et al.* 2012; Boro *et al.* 2011; Moake, 2002).

2.10. Rationale of the study

HIV-associated TTP is an acquired form of TTP often associated with severe deficiency of ADAMTS13 activity of <10% (Moake, 2002). HIV infection increases the risk of autoimmunity since it depletes CD4⁺ lymphocytes to counts of less than 200/mm³ and high viral loads is associated with an increased incidence of autoantibodies which can be directed against ADAMTS13. However, the relationship between anti-ADAMTS13 antibodies and the pathogenesis of HIV-associated TTP is not clear, as the autoantibody status in these patients has not yet been determined. Determining ADAMTS13 antigenic peptides in HIV-associated TTP can shed light on the contribution of these autoantibodies to the function and clearance of ADAMTS13, and assist in profiling potential humoral immune responses in HIV-associated TTP. Furthermore, the detection, quantification and characterization of ADAMTS13 autoantibodies may be potentially valuable in patients with HIV-associated TTP translating to improved clinical outcomes. The results of this study will contribute to a better understanding of HIV-associated TTP.

2.11. Aim and Objectives

The aim of this study was to determine the ADAMTS13 autoantibody status in HIV-associated TTP patients and provide novel insight into the specific antigenic regions (epitopes) on ADAMTS13 domains that are affected by these autoantibodies.

With the following objectives:

1. To measure ADAMTS13 (antigen levels, activity, and ADAMTS13 autoantibodies) and VWF (antigen levels, propeptide levels and UL-VWF multimeric patterns) in HIV-associated TTP and HIV positive non-TTP patient plasma samples.
2. To identify inhibitory ADAMTS13 autoantibodies in HIV-associated TTP patient plasma samples using mixing studies.
3. To characterize different classes of antibodies to ADAMTS13, which are present in HIV-associated TTP and HIV positive non-TTP patient plasma samples.
4. To extract, purify and quantify IgG autoantibodies to ADAMTS13 present in HIV-associated TTP and HIV positive non-TTP patient plasma samples.
5. To use a synthetic ADAMTS13 peptide library designed by GenScript® (USA) for epitope mapping studies using purified IgG autoantibodies to ADAMTS13 isolated from HIV-associated TTP and HIV positive non-TTP patient plasma samples.

CHAPTER 3: METHODOLOGY

3.1. Ethics

Ethics approval for this study was obtained from the Health Sciences Research Ethics committee of the University of the Free State (UFS-HSD2019/0027/3007), with permission to conduct the research from the Free State Department of Health Provincial Research Committee and to use the blood samples from the National Health Laboratory Service (FS_201903_005).

3.2. Study design

This study was an observational, case-control study.

3.3. Study participants

3.3.1. HIV-associated TTP patients

The current study is based on the analysis of fifty-nine (59) frozen, anonymized citrate plasma samples from patients diagnosed with HIV-associated TTP collected from 2017 to 2019 as part of a larger study on the pathogenesis of HIV associated TTP (Ethics approval: HSREC 90/2017).

The plasma samples originated from all areas of South Africa and were sent to the Specialised Haemostasis laboratory of the National Health Laboratory Service (NHLS) at the University of the Free State, Bloemfontein, as part of the diagnostic work-up of patients suffering from HIV associated TTP. The NHLS Specialised Haemostasis laboratory in Bloemfontein serves as a national referral centre for ADAMTS13 testing. Pathologists requested ADAMTS13 tests on these samples to confirm the diagnosis of TTP. The Specialised Haemostasis laboratory stores samples at -80°C for at least one year to perform additional requested tests.

3.3.2. HIV positive non-TTP control patients

Hundred (100) HIV positive plasma samples from HIV infected patients without TTP were included as a control cohort with permission from the NHLS. The NHLS Universitas Academic Laboratories receive 30 000 - 35 000 plasma samples per month for routine HIV viral load testing on HIV infected, community-integrated patients who attend ARV-clinics in Bloemfontein and surrounding areas

including the Northern Cape. The residual plasma samples are made available for research after approval from the respective ethics committee, which in this instance was the University of the Free State Health Sciences Research Ethics Committee.

3.4. Inclusion criteria

3.4.1. HIV-associated TTP plasma samples

The diagnostic criteria for HIV-associated TTP were laboratory findings of infection with HIV, severe ADAMTS13 deficiency (<10%), thrombocytopenia (platelet count <100x10⁹/L), microangiopathic haemolytic anaemia (reduced haemoglobin and increased red cell fragments (schistocytes) as confirmed by a haematopathologist) with an elevated serum lactate dehydrogenase (LDH) level which is frequently > 800 U/L. The presence of ADAMTS13 autoantibodies and the absence of additional causes of a microangiopathic haemolytic anaemia such as disseminated intravascular coagulation (DIC) i.e. normal haemostasis parameters, further strengthened the diagnosis of HIV associated TTP. Creatinine test was also included to assess renal function and renal impairment was considered to be present when creatinine levels were > 90.0 µg/L.

The above diagnostic criteria for HIV associated TTP have previously been employed by multiple published studies (Moake, 2002, Reese *et al.* 2013; Scully *et al.* 2008; Peyvandi *et al.* 2008, Thomas *et al.* 2015; Scully *et al.* 2007). The laboratory inclusion criteria used for HIV-associated TTP diagnosis are summarised in **Table 3.1**.

Table 3.1 Laboratory inclusion criteria for HIV-associated TTP diagnosis.

| Laboratory Test (units) | Laboratory findings | |
|--|------------------------|------------------------------------|
| | Normal values / ranges | HIV-TTP patients |
| Full Blood Count: | | |
| • Schistocytes on morphological examination of slide | Absent | Present |
| • Platelet count ($10^9/L$) | 150 – 450 | <100 |
| • Haemoglobin (g/dL) | 12.1 – 17.2 | < 12.1 |
| Lactate dehydrogenase (LDH) (U/L) | 100 – 190 | Elevated and frequently > 800 |
| Creatinine ($\mu\text{g/L}$) | 49 – 90 | >90 |
| Coombs test | Negative | Negative |
| ADAMTS13 antigen levels (%) | 50-150 | Usually < 5 |
| ADAMTS13 activity (%) | 50-150 | Usually <10 |
| ADAMTS13 autoantibodies | Negative | Positive |
| HIV status | Negative | Positive |
| Anti-retroviral therapy (ART) at presentation | N/A | Either ART naïve or on ART therapy |

Patients with suspected acquired TTP are always screened for HIV infection as this disorder is a known complication of HIV infection, especially in patients with very low CD4⁺ counts (Louw *et al.* 2018; Swart *et al.* 2019; Ripamonti *et al.* 1996). All patient plasma samples included in the current study were confirmed to be HIV positive by enzyme-linked immunosorbent assay (XpressBio[®], USA).

The presence of other HIV-associated thrombotic microangiopathies (TMAs) or HIV-associated malignancies and infections were excluded as far as possible based on clinical parameters, serological test results, radiological imaging and microbiological or histological assessments where appropriate (Gunther *et al.* 2007). This was an observational study and patients were treated at the discretion of a treating physician. Plasma samples were collected before the start of plasma therapy, either exchange or infusion, which was commenced after study sample collection and according to local treatment protocols. Laboratory data pertinent to each TTP sample, including ADAMTS13 antigen levels and ADAMTS13 activity results, are reflected and summarized in **Appendix B**.

3.4.2. HIV positive control plasma samples

The HIV-positive status of the study samples was confirmed via the unique NHLS sample identification number. The CD4⁺ T cell count and viral load for each sample were also extracted from the laboratory information system (LIS). All plasma samples collected were confirmed to be HIV positive by enzyme-linked immunosorbent assay (XpressBio[®], USA). Laboratory data (CD4⁺ T cell count, viral load and details of ART treatment) for the HIV positive patients are summarized in **Appendix C**. The NHLS unique identification number was further utilized to exclude the presence of laboratory features of TTP on the HIV infected control cohort without TTP.

3.4.3. De-identification of samples

All samples used in this study were de-identified. The NHLS samples all have a specific laboratory number that can be traced back to the patient identification details. A double-blind method was used to de-identify all samples, i.e. HIV-associated TTP patients and HIV positive control cohorts without TTP and random unique study numbers were assigned to the samples. A unique study number was allocated to each sample to ensure confidentiality. A data collection sheet comprising of unique study numbers was generated. The results obtained from the study were kept confidential and were only accessible by the researchers.

3.4.4. Specimen collection, processing, and storage

All study plasma samples were collected in 3.2% (0.109 M) tri-sodium Citrate BD Vacutainers[®] (BD, USA) and transported frozen on dry ice to the Specialized Haemostasis laboratory. Plasma samples were processed and stored according to the approved guidelines published in the CLSI document H21-A5 (ISO/TC 212 standards, 2008) for coagulation testing. In short, nine (9) parts of blood sample was collected by venepuncture in 1 part of 3.2% (0.109 M) tri-sodium citrated anticoagulant solution tube (BD Vacutainer[®], BD, USA). The blood was then centrifuged at 2000g for 15 minutes to obtain platelet poor plasma, which was divided into 0.5mL aliquots and stored at -70°C at the Specialized Haemostasis laboratory. Plasma samples are stable when frozen at -70°C for at least 18 months (Woodhams *et al.* 2001). Before testing, frozen plasma samples were thawed at 37°C and assayed within 4 hours. All tests were performed on original aliquots that had not been previously thawed.

3.4.5. Pooled normal plasma

Lyophilized human Pooled Normal Plasma (PNP) was obtained from STAGO® (Stago Diagnostica®, France), and included in experimental assays as normal control (i.e. VWF analysis, autoantibody measurements, Peptide ELISA assays). Plasma collected from 20 normal human volunteers is pooled during the manufacturing of the STAGO® PNP and is free of viral agents such as HIV, HCV and Hepatitis B. For this study, PNP was confirmed to be HIV negative by enzyme-linked immunosorbent assay (XpressBio®, USA). The lyophilized commercial PNP was stored at 2-8°C and reconstituted with distilled water and allowed to stand at room temperature (18-25 °C) for 30 minutes before use.

3.5. Materials and methods

3.5.1. The HIV status of collected patient plasma samples

The HIV status of all patient plasma samples was determined using Human Immunodeficiency Viruses antigen and antibody ELISA kit from XpressBio Life Sciences®, USA. This kit is a two-step incubation sandwich ELISA-based assay, which uses polystyrene microwell strips pre-coated with recombinant HIV antigens (recombinant HIV-1 gp41, gp120 and recombinant HIV-2 gp36) and horseradish peroxidase (HRP)-conjugated-anti-HIV (p24) antibodies. The assay was performed according to the manufacturer's instructions. In short, frozen plasma samples were rapidly thawed in a 37°C water bath (WNB 45, Memmert®, Germany) before performing the assay.

For the assay, 20µL biotinylated anti-HIV (p24) antibodies together with 100µL patient's plasma samples were added to the wells, except for the blank wells. Positive and negative controls, as well as a blank, were included with each run. The plate was covered and incubated for 1 hour at 37°C. After the incubation step, the plate was washed 5 times with a diluted wash buffer. This was followed by adding 100µL/well of the HRP-conjugate, except the blank wells. The plate was incubated for another 30 minutes at 37°C and again washed 5 times. Then 100µL of the chromogenic substrate (50µL chromogen A and 50µL chromogen B) was added to each well including the blank. The plate was covered and incubated at 37°C for 30 minutes in the dark. The reaction was stopped with the addition of 50µL of stop-solution to each well and absorbance measured at 450 nm with a reference wavelength at 630 nm using the ELISA plate reader (BioTek Instruments Inc.®, USA). The cut-off value was calculated from the mean absorbance value for three negative controls. Samples with optical density (OD) at 450 nm values above the negative cut-off value were considered positive and samples with OD₄₅₀ values less than the negative cut-off value were considered negative.

3.5.2. Measurement of ADAMTS13 antigen and ADAMTS13 activity levels

The Specialised Haemostasis laboratory previously determined the ADAMTS13 antigen and activity levels of the HIV-associated TTP patient plasma samples as part of the TTP diagnostic work-up of patients and the results were included in the study. Therefore, this section included the determination of ADAMTS13 antigen and ADAMTS13 activity levels in HIV positive plasma samples.

A Technozyme® ADAMTS13 activity/antigen fluorogenic ELISA kit (Technoclone®, Austria) was used to perform these assays. This kit assay has previously been validated clinically useful in the diagnosis of TTP (Crist and Rodgers, 2009).

The ELISA assay and reagent preparations were performed according to the manufacturer's instructions (Technoclone®, Austria). Before assaying, frozen plasma samples were rapidly thawed in a 37°C water bath (WNB 45, Memmert®, Germany).

The kit test strips are provided already coated with a monoclonal human anti-ADAMTS13 antibody, directed against the CUB domains. The steps involved in this assay are shown in **Figure 3.1**. In short, 50µL of calibrators, controls, and plasma samples were added in duplicate to test wells. The test strips were sealed and incubated for 2 hours at room temperature. After every incubation step, the test strips were washed 3 times with PBS/1% Tween-20 (pH 7.3) using a microplate washer (VACUTECH®, RSA). The activity of ADAMTS13 was determined first by adding 50µL/well of the reconstituted activity substrate to the test strip. The fluorescence was subsequently measured immediately for a duration of 15 minutes with one-minute intervals at an excitation wavelength of 325 nm and an emission wavelength of 410 nm using a fluorescent ELISA plate reader (Synergy HT spectrophotometer, Biotek®, USA). The ADAMTS13 activity of the samples was calculated from the reference curve extrapolated from the standard used.

Once the reading was completed, ADAMTS13 antigen levels of the samples were determined as follows: the same test strips were washed three times, and the conjugate working solution (anti-ADAMTS13 POX, 50µ/well) was added to the test strips to detect bound ADAMTS13 antigen. The test strips were incubated for 1 hour at room temperature and after that, 50µL of the antigen substrate solution was added to each test well and the test strips incubated again for another 15 minutes in a 36°C incubator (B6 incubator, Heraeus instruments, Hanau®, Germany). Finally, 50µL of the stop solution was added to the test wells to stop the reaction and the fluorescence measured at the same wavelengths as for the ADAMTS13 activity measurement. A standard curve was

generated and the ADAMTS13 concentration of the samples calculated from the curve. The ADAMTS13 antigen concentration and activity levels were reported in % of normality. Normal ranges using this assay kit are between 50% - 150% for ADAMTS13 antigen and activity levels.

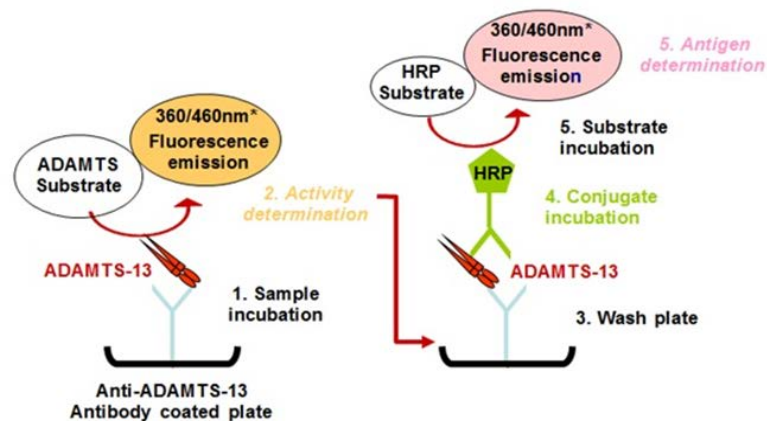


Figure 3.1: Schematic presentation of the steps involved in the determination of the ADAMTS13 antigen and activity levels using the Technoclone[®] assay. (Downloaded from www.technoclone.com).

3.5.3. Measurement of Autoantibodies to ADAMTS13

3.5.3.1. Anti-ADAMTS13 IgG antibodies

Plasma samples from the HIV-associated TTP group and HIV positive control group were screened for the presence of IgG antibody to ADAMTS13. Samples from HIV-associated TTP patients with ADAMTS13 activity of <10% were selected for the determination of antibodies to ADAMTS13 as per other studies in literature (Thomas *et al.* 2015; Scully *et al.* 2007; Alwan *et al.* 2017; George, 2015).

A Technozyme anti-ADAMTS13 autoantibody ELISA-based kit (Technoclone[®], Austria) used for the detection of ADAMTS13-IgG autoantibodies by the Specialised Haemostasis lab was also used in the current study. This is a standardized chromogenic assay designed to detect ADAMTS13-IgG autoantibodies in human plasma. The ELISA assay and reagent preparations were performed according to the manufacturer's instructions (Technoclone[®], Austria). The kit contains a 96-well plate that is coated with full-length recombinant ADAMTS13 protein.

In short, standard plasma, control plasma, and study plasma samples were prepared according to the manufacture's instruction. Then 100µL of each diluted plasma/standard/control sample was added in duplicate into designated test wells coated with recombinant ADAMTS13 and incubated for 60 minutes at room temperature. This incubation step allowed for the IgG antibodies in the sample to bind the ADAMTS13 protein-coated wells. After each incubation step, PBS/1% Tween-20, pH 7.3 was used to wash the test wells using ELISA microplate washer (VACUTEC[®], RSA). A 100µL

enzyme-labelled anti-human IgG (anti-human IgG POX) antibody was added to each test well for antibody detection and the test wells were incubated for another 60 minutes. After a washing step, 100µL of 3,3',5,5'-Tetramethylbenzidine (TMB) substrate solution was added to react with the enzyme conjugate. The test strips were incubated for another 10 minutes at room temperature and the reaction was stopped by adding 30µL/well of sulphuric acid (4M H₂SO₄) at room temperature. The OD was read at 450 nm using an ELISA microplate reader (Synergy HT, BioTek Instruments Inc.®, USA). A standard curve was generated and the IgG levels of the samples extrapolated from the standard curve. Results were interpreted as negative when the ADAMTS13 autoantibody titer is less than 12 U/mL, borderline when titer is between 12 and 15 U/mL and positive when titer is 15 U/mL and more.

3.5.3.1.1. Mixing studies

Mixing studies were performed as described by Vendramin *et al.* (2018), Alwan *et al.* (2017), and Scully *et al.* (2008) with slight modifications. Mixing studies were done to determine the presence of neutralizing IgG inhibitors to ADAMTS13 in HIV-associated TTP plasma samples and HIV positive plasma samples with ADAMTS13 activity levels less than 10%.

The test plasma samples were mixed with PNP in a 50:50 mixing study, and the ADAMTS13 activity measured with the Technozyme® ADAMTS13 activity assay, as described in **3.5.2**. The presence of a strong inhibitor was defined as persisting ADAMTS13 activity of less than 10% after attempts at correction with 50:50 mixing studies. The PNP was confirmed to have normal ADAMTS13 activity levels of 50-150%. Therefore, in the absence of an inhibitor, the addition of a PNP should correct the ADAMTS13 activity by more than 50% towards normal. However, a mixing test result of less than <50% ADAMTS13 activity indicated no correction, therefore the presence of an inhibitor.

Thereafter, a modified Bethesda method similar to the one commonly used to evaluate the presence of coagulation FVIII inhibitors was used to analyse the strength of neutralizing anti-ADAMTS13 antibodies (Kasper *et al.* 1975; Vendramin *et al.* 2018; Ferrari *et al.* 2007). One Bethesda unit is defined as the concentration of inhibitor in a plasma sample that reduce ADAMTS13 activity to 50% in pooled normal plasma in a 50:50 mix. The presence of an inhibitor is indicated by a residual ADAMTS13 activity of 25% - 75% in the mixed sample i.e. 50:50 mix of a test sample and PNP (Vendramin *et al.* 2018). Test samples with residual activity of more than 75% were reported as <0.5 BU/mL, which equates to the absence of a clinically significant inhibitor.

Patient plasma samples were incubated in a water bath at 56°C for 60 minutes to eliminate endogenous ADAMTS13 activity and centrifuged for 5 minutes at 1500g. A test plasma with strong inhibitors present (indicated by persisting ADAMTS13 activity <10% after attempts at correction with mixing studies) was then serially diluted 1:2, 1:4, 1:8 and 1:16 with saline compared to the samples with weaker inhibitors that were diluted 1:2. All samples were then further diluted 1:1 with PNP and incubated at 25°C for 2 hours. Pooled normal plasma diluted 1:1 with saline was used as a negative control. After that, the ADAMTS13 activity of all the dilutions was determined with the Technozyme® ADAMTS13 activity assay.

The residual ADAMTS13 activity was calculated using the formula as described by Vendramin *et al.* (2018) with slight modifications.

$$\text{The \% ADAMTS13 residual activity} = \left[\frac{\text{ADAMTS13 activity value of the test sample}}{\text{ADAMTS13 activity value of the control sample}} \right] \times 100\%$$

The ADAMTS13 inhibitor level (Bethesda Unit (BU)) is calculated from the residual ADAMTS13 activity measured after mixing studies by the formula:

$$\text{ADAMTS13 inhibitor (BU)} = \left[\frac{2 - \log(\text{residual ADAMTS13 activity})}{0.30103} \right] \times \text{dilution factor of sample,}$$

and expressed as inhibitor unit per millilitre (BU/mL). Samples with an inhibitor titer of more than 0.5 BU/mL were classified as having inhibitors.

3.5.3.2. IgM and IgA antibodies

Samples with a positive titer of anti-ADAMTS13 IgG antibodies were screened for the presence of IgM and IgA antibodies.

3.5.3.2.1. Total IgM and IgA antibodies in plasma

Total plasma immunoglobulin (IgM and IgA) levels were determined in HIV-associated TTP and HIV positive plasma samples using commercial human IgM and IgA ELISA kits from Bethyl Laboratories® (USA). The ELISA assays, reagents and standards preparations were performed according to the manufacturer's instructions (Bethyl Laboratories, Inc®, USA).

In two separate experiments, a sandwich ELISA was used to screen for human IgM or IgA present in test samples. The microtiter surface plates were received pre-coated with either anti-human IgM or anti-human IgA antibodies. For each standard curve, the standard sample was diluted to 250, 83.3, 27.8, 9.26, 3.09, 1.03 and 0 ng/mL, and the test plasma samples diluted 1:10 000 in dilution buffer. Then 100µL of standard and sample was added to designated wells in duplicate. The plates were covered and incubated at room temperature for 1 hour. The plates were washed with wash buffer 4 times using the microplate washer after each incubation step. Hundred (100) µL of anti-human IgM/ IgA detection antibody was added to each well and the plate was covered and incubated at room temperature for another hour. This was followed by the addition of 100µL of HRP solution and another incubation for 30 minutes. Then 100µL/well of TMB substrate solution was added and the plates incubated in the dark for 30 minutes at room temperature. Finally, the reaction was stopped by adding 100µL/well of the stop solution and absorbance read at 450 nm using a microplate reader. The concentration of the IgM and IgA in the samples was calculated from the extrapolated standard curve. Thereafter, the final IgM/IgA concentrations in the original undiluted sample were determined by multiplying the measured concentrations by the dilution factor. According to the manufacturer, normal reference ranges for healthy adults for IgA is 1.1-2.6 mg/mL and for IgM is 0.23-1.4 mg/mL in sodium citrate plasma.

3.5.3.2.2. Anti-ADAMTS13 IgM and IgA antibodies

Antibodies (IgM and IgA) to ADAMTS13 in HIV-associated TTP plasma and HIV positive control samples were determined using an ELISA-based method. The ELISA assay was performed according to the methodologies of Scheiflinger *et al.* (2003), Rieger *et al.* (2005) and Ferrari *et al.* (2007) with slight modifications.

In two separate ELISA experiments, a 96-well plate pre-coated with full-length recombinant ADAMTS13 (Technoclone[®], Austria) was used. Patient plasma samples were diluted 1:100 in PBS/1% Tween-20, and 100µL per well was added to the plate and incubated for 60 minutes at 37°C temperature. The plate was washed 4 times with PBS/1% Tween-20 using a microplate washer (VACUTEC[®], RSA) after each incubation step. Bound anti-IgM and IgA antibodies to ADAMTS13 were detected using HRP-conjugated monoclonal anti-human IgM antibody (Abcam[®], USA) specific to the human µ-chain and HRP-conjugated Anti-Human IgA antibody (Abcam[®], USA) specific to the human α-chain. The detection antibodies used in these experiments were specific for their immunoglobulin isotype to prevent any cross-reaction. The plates were incubated at room temperature for 60 minutes. Bound antibodies were detected using a substrate solution of Ortho-phenylenediamine

(OPD, 5% in 0.1M Citric acid and 0.2M Na_2HPO_4 with 0.012% H_2O_2) and the reaction stopped using 30 μL /well of sulphuric acid (4M H_2SO_4). After that, absorbance was measured at 490 nm with a reference wavelength of 630 nm that was subtracted from each OD_{490} value obtained.

Pooled normal human plasma (PNP) was included as a control and the cut-off value for a positive IgM/IgA titer was calculated as the average of the PNP OD_{490} value plus 2 standard deviations (2SD) calculated from several lots of PNP samples (Kumar and Rao, 1991). Patient plasma samples with values above the cut-off value were identified as positive for autoantibodies to the ADAMTS13 protein. The cut-off OD_{490} value for anti-ADAMTS13 IgM obtained was 0.139 and for anti-ADAMTS13 IgA was 0.114, (calculations included in **Supplementary data 1**). The results were interpreted as either positive (+) for the presence or negative (-) for the absence of anti-ADAMTS13 IgM and IgA antibodies.

Intra-assay and inter-assay precision of these two assays were determined by evaluating a single PNP sample and a reference TTP plasma samples positive for IgM/IgA autoantibodies to ADAMTS13 in 20 consecutive assay runs for IgM and IgA detection respectively (intra-assay), and on 5 different days as well (inter-assay). The results were expressed as the percent coefficient of variation (%CV) according to the standard formula: $\% \text{CV} = \text{SD}/\text{mean} \times 100\%$. The acceptable %CV for immunoassays was expected to be less than 20% (Findlay *et al.* 2000).

3.5.4. VWF analysis

Quantitative analysis of VWF antigen (VWF:Ag) and VWF propeptide (VWFpp) levels were determined with standard ELISA-based assays. Plasma levels of VWF:Ag and VWFpp levels reflect endothelial damage associated with TTP (Stufano *et al.* 2012; Haberichter *et al.* 2006; Ito-Habe *et al.* 2011; Lotta *et al.* 2011; van Mourik *et al.* 1999). A quantitative assessment of the VWF multimers size distribution was also performed with a quantitative immunoblotting assay. VWF analysis was performed on plasma samples from the HIV-associated TTP group (n=59) and the HIV-positive control group (n=100). Pooled normal human plasma (PNP) was included as a control.

3.5.4.1. VWF antigen (VWF:Ag) levels

The VWF:Ag ELISA-based assay was performed using the reference method detailed in the standard operating procedure (SOP) for the determination of VWF:Ag (SHL1-v5) currently used by the NHLS Special Haemostasis laboratory.

In short, high binding ELISA plates (Nunc[®], Denmark) were coated with 100µL/well rabbit anti-human VWF antibody (2µL; P0226, Dako, Denmark) diluted in 12 mL phosphate-buffered saline (PBS, pH 7.4) per plate, and incubated overnight at 4°C in a humid container. After the incubation period, the plate was washed once with PBS/0.1% Tween-20 (Merck[®], USA) to remove the unbound antibody, using a microplate washer (VACUTECH[®], RSA). The World Health Organisation (WHO) 6th international standard plasma for VWF (NIBSC[®], UK) was used as a calibrator and added in the following concentrations: 100%, 50%, 25%, 12.5%, 6.25%. Normal (N) and abnormal (P) controls (Siemens, USA) were also included to ensure the accuracy and reproducibility of our results. The patient's plasma samples and controls were double diluted 1:50 and 1:100 in PBS (pH 7.4) 0.1% Tween-20. The PBS/Tween-20 acts as a blocking solution to cover all the remaining binding surfaces of the plate that are not occupied by the coated protein. Then, 100µL/well of the standard, the study samples and control samples were added in duplicate to the coated plate, covered with parafilm (Lasec[®], USA), and incubated for 2 hours at 36°C (B6 incubator, Heraeus instruments[®], Germany). After 2 hours, the plates were washed 4 times with PBS/ 0.1% Tween-20. Then 100µL/well of a detection polyclonal rabbit anti-human VWF conjugated to horseradish peroxidase (1.5µL; P0226, Dako[®], Glostrup, Denmark) diluted in 12mL PBS/Tween-20 was added and the plate incubated at room temperature for a further 1 hour. After another wash step, 90µL/well of OPD substrate solution was added and the plate incubated for 3 minutes. Finally, the reaction was stopped by adding 30µL/well of stop solution consisting of sulphuric acid (4M H₂SO₄). The absorbance was measured at 490 minus 630nm (490-630nm) using the microplate reader (BioTek Synergy HT reader[®], USA). The VWF results of test plasma samples were read off from the reference curve.

The VWF:Ag levels were calculated using the GraphPad Prism software 6 (GraphPad Software[®], USA) and reported in percentage (%) of normality. Normal ranges for VWF antigen levels are 50% - 150%.

3.5.4.2. VWF propeptide (VWFpp) levels

The VWF propeptide (VWFpp) levels were determined with reference to the methodologies described by Nossent *et al.* (2006), Haberichter, 2015, and Eikenboom *et al.* (2013) using mouse anti-human VWFpp antibody pair (MW1639, Cell science[®], Newburyport, Massachusetts) by ELISA based assay.

A high binding ELISA plate (Nunc MaxiSorp[®], ThermoFisher Scientific[®], USA) was coated with 100µL/well of coating antibody (120µL CS-M193902-A; clone CLB-Pro 35) diluted in 12mL coating buffer (0.1 M carbonate/bicarbonate buffer, pH 9.6), covered with adhesive seal and incubated

overnight at 4°C. After the incubation period, the plate was washed 5 times with wash buffer (PBS/ 0.1% Tween-20) and incubated for 2 hours at 37 °C with 200µL/well of dilution buffer with 1% bovine serum albumin (PBS/ 0.1% Tween-20/ 1% BSA, Sigma[®], USA) to prevent non-specific binding. A standard plasma (WHO 6th international standard plasma) was serially diluted 1:10, 1:20, 1:40, 1:80, 1:160, 1:320, 1:640, 1:1280 and test samples were diluted 1:100 in dilution buffer (PBS/ 0.1% Tween-20/ 1% BSA). After the 2-hour incubation step, the plate was washed five times again with wash buffer, and 100µL/well of the prepared standards and samples added in duplicates. A dilution buffer was included as a blank. The plate was covered and incubated again for 2 hours at 37°C. Following another washing step 5x, 100µL/well of the HRP conjugated detection antibody (120µL CS-M193902-A; clone CLB-Pro 14.3), diluted in 12mL dilution buffer was added and the plate covered and incubated for another 2 hours at 37°C. The plate was washed again, and 100µL/well of the OPD-substrate solution added and the plate incubated in the dark for 15 minutes. Finally, the reaction was stopped by adding 100µL/well of stop solution - sulphuric acid (4M H₂SO₄) and absorbance read at 490-630 nm within 30 minutes using an ELISA reader (BioTek Synergy HT reader[®], USA).

The results of test plasma samples were read off from the reference curve. The VWFpp levels were calculated using the GraphPad Prism software (GraphPad Software[®], USA) and reported in percentage (%). The normal reference range of plasma VWFpp is between 60% - 140%.

3.5.4.3. VWF multimer analysis

The VWF multimer analysis was performed with reference to the methodologies of Furlan *et al.* (1997) and the currently used NHLS SOPs (SHL5v3) for VWF Multimer analysis in the Special Haemostasis laboratory. VWF multimer analysis was performed on both HIV-associated TTP and HIV-positive control plasma samples. A PNP sample was included as normal control.

VWF multimer analysis was performed using gel electrophoresis on sodium dodecyl sulphate (SDS 0.7%) agarose gel. The SDS sample buffer allows for the separation of proteins to become fully denatured and dissociate from each other (Laemmli, 1970). The patient's plasma samples were diluted in sample buffer (0.01 M Na₂HPO₄, 37mM Iodoacetate, 1% SDS, dissolved in distilled water; pH 7). The normal control sample with normal VWF:Ag levels (50-150%) was diluted 1:40, and samples with VWF:Ag levels above (>143%) were diluted 1:80, and with VWF:Ag (<41%) were diluted 1:20 in sample buffer (pH 7.0). After sample preparation, diluted samples were incubated at 37°C for 1 hour to inactivate any proteases present in the samples that may produce a breakdown of

products, giving rise to spurious banding. After that, 10 μ L bromophenol blue (BPB, Abcam[®], UK) was added to 90 μ L of each diluted plasma sample and centrifuged at 14000 rpm for 1 minute. Bromophenol blue was used as a tracking dye during gel electrophoresis, allowing the progress of molecules moving through the gel to be monitored. After that, 10 μ L of plasma sample (in duplicates) was pipetted onto each lane of the agarose gel for electrophoresis and allowed to run for \pm 3 hours.

Following electrophoresis, the separated protein bands were electro-blotted onto a nitrocellulose membrane (Biorad[®], USA) assembled in a Western Blot sandwich for visualization. The electrophoretic transfer conditions were maintained at a current limit of 0.300 A (300 mA) and 15 Volts for 1 hour and 5 minutes in a Trans-Blot semi-dry electrophoretic transfer system (BioRad[®], USA) at 4°C. After electro-blotting, the membrane was blocked with 5% skimmed milk (Difco[™], BD Biosciences[®], USA) diluted in 200mL Tris-buffered Saline with Tween-20 (TBS-T; 0.05M Tris, 0.1M NaCl, 0.1% Tween-20, dissolved in distilled water; pH 7.4) for 1 hour and 15 minutes to prevent non-specific binding. This was followed by several washing steps with TBS-T. After that, the separated VWF multimers were detected using a rabbit anti-human VWF antibody conjugated to HRP (P0226, Dako[®]) diluted 1: 2666 in TBS-Tween and incubated for another hour and 15 minutes at room temperature. A western blot chemiluminescence HRP-detection reagent (Takara Bio Inc. [®], Japan) was then added and the illuminating membrane exposed to an X-ray film for visualization using Gene tools analysis software (Syngene[®], USA).

3.5.5. Extraction of IgG autoantibodies

3.5.5.1. Antibody IgG extraction

Total IgG was isolated from the plasma samples of the HIV- associated TTP group (n=53) and HIV positive control group (n=18) using NAb[™] Protein G spin columns according to the manufacturer's instruction (gravity-flow purification protocol, ThermoFisher Scientific[®], USA). Plasma samples with positive anti-ADAMTS13 IgG antibody titers were used in this part of the analysis.

In short, the columns and buffers were allowed to equilibrate to room temperature for 15 minutes. The columns were placed in a 15mL falcon tube (Greiner bio-one[®], USA) to allow the storage solution to drain. To equilibrate a column, 5mL of binding buffer (PBS (NaCl 8g, Na₂HPO₄ 1.44g, NaH₂PO₄ 0.24g, 1L dH₂O) pH 7.2 with HCl) was added to the column and allowed to drain through. In the meantime, 1mL patient plasma sample containing IgG was diluted 1:1 with a binding buffer and then added to the equilibrated column for the IgG antibodies to bind to the column. After that, the column was washed with 15mL of binding buffer again to remove all unwanted substances. After

the last wash, 5mL of the elution buffer that contained 0.1M glycine-HCl buffer, pH 2.3) was added to the column and the IgG antibodies were eluted from the column in 5 x 1mL fractions in eppendorf tubes (Eppendorf Tubes[®], Germany) each containing 100µL neutralizing buffer (1M Tris-HCl, pH 8.0). The eluted fractions were stored at 4°C for further analysis. Each column was regenerated by adding 8mL of the elution buffer, which was allowed to flow through. Followed by adding 3mL of a storage solution (0.02% sodium azide in PBS) to the column and stored at 4°C for later use.

3.5.5.2. Quantification of purified IgG

The protein concentration of the eluted IgG fractions was determined with a BioDrop[®] spectrophotometer (BioDrop µlite, SERVA[®], Germany). The spectrophotometer was calibrated and blanked with elution buffer before analyzing the protein sample. The protein concentration of the sample was calculated by measuring absorbance at 280 nm. The instrument calculated the final concentration of the protein in mg/mL. To assess the purity of the isolated protein sample, fractions with an absorbance ratio of 260 divided by 280 (260/280) smaller than 0.6 indicated the absence of nucleic acid contamination and were then pooled (Wilfinger *et al.* 1997).

3.5.5.3. The SDS-PAGE analysis of purified IgG

Purified IgG antibodies were analysed by electrophoresis on 10% SDS polyacrylamide gel electrophoresis (PAGE) within a vertical slab gel apparatus (Bio-Rad[®], USA) at 100 Volts (PowerPac[™] HC, Bio-Rad[®], USA). A control human monoclonal IgG antibody (Abcam[®], USA) was included. The SDS PAGE was performed at the NHLS Bloemfontein department of Virology, following the standardized operating procedure (SOP). The IgG antibody was denatured in sodium dodecyl sulphate (SDS) sample buffer under reducing and non-reducing conditions. The reducing sample buffer (5x) contains 0.3M Tris-HCl pH 6.8, 50% glycerol, 5% SDS, 0.01% Bromophenol blue, 100 nM dithiothreitol (DTT) and distilled water. The DTT was omitted in the non-reducing sample buffer. These buffers were prepared according to the methods of Laemmli (1970).

For the gel electrophoresis, the separating gel mixture was prepared first, pipetted into the gel cast to a height of 1 cm, and allowed to solidify for 60 minutes at room temperature. The stacking gel was then prepared, and the mixture pipetted on top of the separating gel to fill the cast and to allowed to solidify for 60 minutes. The 8% separating gel contained 2.67 mL of 30% Bis-acrylamide, 2.75 mL of 1.5 M Tris-HCL, 100µL of 10% SDS, 2 mL of 50% glycerol, 75µL of 10% Ammonium persulphate, 10µL of TEMED and 2.395 mL deionized water. The 4% stacking gel contained 0.667

mL of 30% Bis-acrylamide, 1.375 mL of 1.5 M Tris-HCL, 50 μ L of 10% SDS, 1 mL of 50% glycerol, 37.5 μ L of 10% Ammonium persulphate, 10 μ L of TEMED and 1.861 mL deionized water. The IgG samples were diluted to a final concentration of 150 μ g/mL in 75 μ L in PBS, pH 7.4. After that, the protein sample was diluted 4:1 in respective sample buffers. Samples were incubated for 5 minutes at 90°C and then centrifuged at 13000 rpm for 60 seconds. ThermoFisher Scientific protein ladder (PageRuler™ Prestained 10-180kDa Ladder, ThermoFisher Scientific®, USA) was used to estimate the separated protein in the samples. Six (6) μ L of the ladder was pipetted into the first well of each gel, followed by the addition of 30 μ L of the prepared samples into respective wells. The gel electrophoresis was run at 140 V for 60 minutes in a tank filled with running buffer (30g Tris, 144g glycine and 10g SDS in 1L dH₂O).

Once electrophoresis was completed, the gels were placed in Coomassie Blue staining (0.1% Coomassie blue, 40% ethanol, 10% acetic acid) for 1 hour at room temperature. The gels were rinsed with water and placed in a destaining solution (10% ethanol, 7.5% acetic acid) at room temperature on an orbital shaker until the desired background was achieved. Molecular weight size for the IgG antibody is estimated to be 150 KD, while the molecular weight of a heavy chain is 50 KD and a light chain is 30 KD.

3.5.5.4. Dialysis of purified IgG protein

Antibody purities were dialyzed to remove unwanted low molecular weight substances/salt contamination. Two hundred microliter (200 μ L) of the antibody solution was transferred to pre-wet dialysis cups (10K MWCO Slide-A-Lyzer Mini Dialysis devices, ThermoFisher Scientific®, USA). The filled dialysis cups were capped and placed in mini dialysis floating devices, which were transferred into a suitably sized beaker containing 3L PBS dialysis buffer (NaCl 11.68g, Na₂HPO₄ 9.44g, NaH₂PO₄ 5.28g in 2L dH₂O, pH 7.4) as shown in **Figure 3.2**. Antibodies were dialyzed at 4°C for 24 hours against 3L volumes of PBS buffer while stirring using a magnetic stirrer. The buffer was changed every 6-8 hours. Once dialysis was completed, the dialyzed IgG protein concentration was determined using a spectrophotometer at 280 nm again. The eluted pure IgG protein as determined by the 260/280 absorbance ratio were pooled and aliquoted into 1.5mL eppendorf tubes (Eppendorf Tubes®, Germany) and stored at 4°C until use.

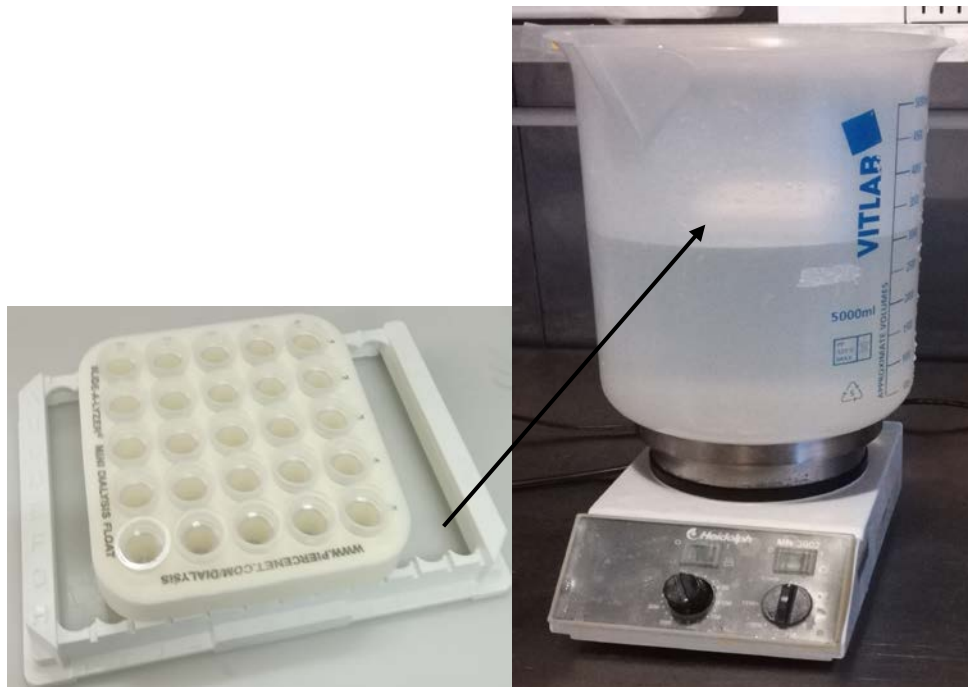


Figure 3.2: A Mini floating device with 2mL dialysis cups fitted and placed into a suitable sized beaker.

3.5.6. Epitope mapping studies of anti-ADAMTS13 IgG antibodies in HIV-associated TTP.

3.5.6.1. Synthetic peptides

An overlapping peptide library derived from the ADAMTS13 protein (GenBank accession: NM_139026.4; **Appendix A**) was designed and then synthesized by GenScript® (USA). The peptide library consisted of 105 biotinylated peptides which were used to screen for regions containing linear B-cell epitopes using an ELISA-based method. Synthetic peptides were biotinylated at the N-terminus (GenScript®, USA). Peptide libraries for large proteins, such as ADAMTS13, are available but extremely expensive. Therefore, to minimize costs, we selected domains that significantly contribute to the function of ADAMTS13 and the binding of VWF under static conditions, according to published literature (see **section 2.1**). Our synthetic peptide library consisted of peptides from the metalloprotease domain, the disintegrin-like domains, the Cysteine-rich domain and the Spacer domains. The grouping of the synthesized peptide library is shown in **Table 3.2**.

Table 3.2: The ADAMTS13 domain groupings selected for designing a peptide library.

| Domain grouping | Position in ADAMTS13 amino acid sequence | Structure-Function |
|--|--|--|
| Metalloprotease – Disintegrin domains (highlighted red and yellow) | 75 - 383 | Catalytic domains. |
| Cysteine-rich - Spacer domains (highlighted grey and magenta) | 440 - 680 | Critical role in substrate recognition and binding, promoting proteolysis of VWF by ADAMTS13 |

A peptide length of 20 amino acids that allowed a complete coverage of the domains was selected while minimizing the costs of the library production. The designed peptides were designed in a 20-mer/15-mer overlapping format with an offset of 5 amino acids, as shown in **Figure 3.3**.

```
AAGGILHLELLVAVGPDVFQ
  LHLELLVAVGPDVFQAHQED
    LVAVGPDVFQAHQEDTERYV
      PDVFQAHQEDTERYVLTNLN
        AHQEDTERYVLTNLNIGAE
          TERYVLTNLNIGAELLRDPS
            LTNLNIGAELLRDPSLGAQF
              IGAELLRDPSLGAQFRVHLV
                LRDPSLGAQFRVHLVKMVIL
                  LGAQFRVHLVKMVLTEPEG
                    RVHLVKMVLTEPEGAPNIT
                      KMVILTEPEGAPNITANLTS
```

Figure 3.3. Overlapping linear peptide sequences from the Metalloprotease domain 75-150.

The designed peptides are 20 amino acids long with 15 overlapping amino acids and an offset of 5 amino acids.

Peptides were obtained as a lyophilised powder (1 mg) with a purity of more than 75% in individually labeled vials. Each biotinylated peptide was reconstituted to 1 mg/mL in distilled water and/ or with DMSO (Dimethyl sulfoxide, Merck®, USA) as recommended by GenScript® (USA). The reconstituted peptides were aliquoted to 100µL and stored at -20°C until use. A list of linear overlapping peptides derived from the selected ADAMTS13 domains is presented in **Tables 3.3** and **3.4** respectively. Each peptide is 20 amino acids long, with 15 overlapping amino acids and an offset of 5 amino acids. Peptide name is derived from the relevant domain name and the relevant amino acid position is relative to the coding region of full-length ADAMTS13 protein.

Table 3.3: List of peptide sequences of the ADAMTS13 Metalloprotease to disintegrin-like domains (75-384).

| No.: | Domain | Position | aa sequence | Length |
|---------------------------|-----------------------------|-----------------|----------------------|---------------|
| MP1 | Metalloprotease | 75 – 94 | AAGGILHLELLVAVGPDVFQ | 20 |
| MP2 | Metalloprotease | 80 – 99 | LHLELLVAVGPDVFQAHQED | 20 |
| MP3 | Metalloprotease | 85 – 104 | LVAVGPDVFQAHQEDTERYV | 20 |
| MP4 | Metalloprotease | 90 – 109 | PDVFQAHQEDTERYVLTNLN | 20 |
| MP5 | Metalloprotease | 95 – 114 | AHQEDTERYVLTNLNIGAEI | 20 |
| MP6 | Metalloprotease | 100 – 119 | TERYVLTNLNIGAEELLRDP | 20 |
| MP7 | Metalloprotease | 105 – 124 | LTNLNIGAEELLRDP | 20 |
| MP8 | Metalloprotease | 110 – 129 | IGAEELLRDP | 20 |
| MP9 | Metalloprotease | 115 – 134 | LRDP | 20 |
| MP10 | Metalloprotease | 120 – 139 | LGAQFRVHLV | 20 |
| MP11 | Metalloprotease | 125 – 144 | RVHLV | 20 |
| MP12 | Metalloprotease | 130 – 149 | KMVILTEPEG | 20 |
| MP13 | Metalloprotease | 135 – 154 | TEPEG | 20 |
| MP14 | Metalloprotease | 140 – 159 | APNITANLT | 20 |
| MP15 | Metalloprotease | 145 – 164 | ANLT | 20 |
| MP16 | Metalloprotease | 150 – 169 | SLLS | 20 |
| MP17 | Metalloprotease | 155 – 174 | CGWSQTIN | 20 |
| MP18 | Metalloprotease | 160 – 179 | TINPEDD | 20 |
| MP19 | Metalloprotease | 165 – 184 | DDTDPGHADL | 20 |
| MP20 | Metalloprotease | 170 – 189 | GHADLVLYIT | 20 |
| MP21 | Metalloprotease | 175 – 194 | VLYIT | 20 |
| MP22 | Metalloprotease | 180 – 199 | RFDLE | 20 |
| MP23 | Metalloprotease | 185 – 204 | LPDGNRQVRG | 20 |
| MP24 | Metalloprotease | 190 – 209 | RQVRGVTQLG | 20 |
| MP25 | Metalloprotease | 195 – 214 | VTQLGGACSPT | 20 |
| MP26 | Metalloprotease | 200 – 219 | GACSPTWSCLIT | 20 |
| MP27 | Metalloprotease | 205 – 224 | TWSCLIT | 20 |
| MP28 | Metalloprotease | 210 – 229 | ITEDTGFDL | 20 |
| MP29 | Metalloprotease | 215 – 234 | GFDL | 20 |
| MP30 | Metalloprotease | 220 – 239 | VTIAHEIGHS | 20 |
| MP31 | Metalloprotease | 225 – 244 | EIGHS | 20 |
| MP32 | Metalloprotease | 230 – 249 | FGLEHDGAP | 20 |
| MP33 | Metalloprotease | 235 – 254 | DGAP | 20 |
| MP34 | Metalloprotease | 240 – 259 | SGCGPSGHV | 20 |
| MP35 | Metalloprotease | 245 – 264 | SGHVMASDGA | 20 |
| MP36 | Metalloprotease | 250 – 269 | ASDGA | 20 |
| MP37 | Metalloprotease | 255 – 274 | APRAGLAW | 20 |
| MP38 | Metalloprotease | 260 – 279 | LAWSPC | 20 |
| MP39 | Metalloprotease | 265 – 284 | CSRRQLLS | 20 |
| MP/Dis40 | Metalloprotease/Disintegrin | 270 – 289 | LLSLSAGRARC | 20 |
| MP/Dis41 | Metalloprotease/Disintegrin | 275 – 294 | SAGRARC | 20 |
| MP/Dis42 | Metalloprotease/Disintegrin | 280 – 299 | RCVWD | 20 |
| Table continues... | | | | |

| Table continues... | | | | |
|--------------------|-----------------------------|-----------|-----------------------|--------|
| No.: | Domain | Position | aa sequence | Length |
| MP/Dis43 | Metalloprotease/Disintegrin | 285 – 304 | PPRPQPGSAGHPPDAQPGLY | 20 |
| Dis44 | Disintegrin | 290 – 309 | PGSAGHPPDAQPGLYYSANE | 20 |
| Dis45 | Disintegrin | 295 – 314 | HPPDAQPGLYYSANEQCRVA | 20 |
| Dis46 | Disintegrin | 300 – 319 | QPGLYYSANEQCRVAFGPKA | 20 |
| Dis47 | Disintegrin | 305 – 324 | YSANEQCRVAFGPKAVACTF | 20 |
| Dis48 | Disintegrin | 310 – 329 | QCRVAFGPKAVACTFAREHL | 20 |
| Dis49 | Disintegrin | 315 – 334 | FGPKAVACTFAREHLMCQA | 20 |
| Dis50 | Disintegrin | 320 – 339 | VACTFAREHLMCQALSCHT | 20 |
| Dis51 | Disintegrin | 325 – 345 | AREHLMCQALSCHTDPLDQ | 20 |
| Dis52 | Disintegrin | 330 – 349 | DMCQALSCHTDPLDQSSCSR | 20 |
| Dis53 | Disintegrin | 335 – 354 | LSCHTDPLDQSSCSRLLVPL | 20 |
| Dis54 | Disintegrin | 340 – 359 | DPLDQSSCSRLLVPLLDGTEC | 20 |
| Dis55 | Disintegrin | 345 – 364 | SSCSRLLVPLLDGTECGVEK | 20 |
| Dis56 | Disintegrin | 350 – 369 | LLVPLLDGTECGVEKWCSKG | 20 |
| Dis57 | Disintegrin | 355 – 374 | LDGTECGVEKWCSKGRCRSL | 20 |
| Dis58 | Disintegrin | 360 – 379 | CGVEKWCSKGRCRSLVELTP | 20 |
| Dis/TSP1 59 | Disintegrin/TSP1-1 | 365 - 383 | WCSKGRCRSLVELTPIAAVH | 20 |

Table 3.4: List of peptide sequences from the ADAMTS13 Cysteine-rich to Spacer domains (440-684).

| No.: | Domain | Position | aa sequence | Length |
|-----------|----------------------|-----------|------------------------|--------|
| Cys1 | Cysteine-rich | 440 – 459 | KTQLEFMSQQCARTDGQPLR | 20 |
| Cys2 | Cysteine-rich | 445 – 464 | FMSQQCARTDGQPLRSPGG | 20 |
| Cys3 | Cysteine-rich | 450 – 469 | CARTDGQPLRSPGGASFYH | 20 |
| Cys4 | Cysteine-rich | 455 – 474 | GQPLRSPGGASFYHWGAAV | 20 |
| Cys5 | Cysteine-rich | 460 – 479 | SSPGGASFYHWGAAVPHSQG | 20 |
| Cys6 | Cysteine-rich | 465 – 484 | ASFYHWGAAVPHSQGDALCR | 20 |
| Cys7 | Cysteine-rich | 470 – 489 | WGAAVPHSQGDALCRHMCRA | 20 |
| Cys8 | Cysteine-rich | 475 – 494 | PHSQGDALCRHMCRAI GESF | 20 |
| Cys9 | Cysteine-rich | 480 – 499 | DALCRHMCRAIGESFIMKRG | 20 |
| Cys10 | Cysteine-rich | 485 – 504 | HMCRAIGESFIMKRGDSFLD | 20 |
| Cys11 | Cysteine-rich | 490 – 509 | IGESFIMKRGDSFLDGTRCM | 20 |
| Cys12 | Cysteine-rich | 495 – 514 | IMKRGDSFLDGTRCMPSPGPR | 20 |
| Cys13 | Cysteine-rich | 500 – 519 | DSFLDGTRCMPSPGREDGTL | 20 |
| Cys14 | Cysteine-rich | 505 – 524 | GTRCMPSPGREDGTLSLCVS | 20 |
| Cys15 | Cysteine-rich | 510 – 529 | PSGPREDGTLSLCVSGSCRT | 20 |
| Cys16 | Cysteine-rich | 515 – 534 | EDGTLSLCVSGSCRTFGCDG | 20 |
| Cys17 | Cysteine-rich | 520 – 539 | SLCVSGSCRTFGCDGRMDSQ | 20 |
| Cys18 | Cysteine-rich | 525 – 544 | GSCRTFGCDGRMDSQQVWDR | 20 |
| Cys19 | Cysteine-rich | 530 – 549 | FGCDGRMDSQQVWDRQCVCVCG | 20 |
| Cys/Spa20 | Cysteine-rich/Spacer | 535 – 554 | RMDSQQVWDRQCVCVGGDNST | 20 |
| Cys/Spa21 | Cysteine-rich/Spacer | 540 – 559 | QVWDRQCVCVGGDNSTCSPRK | 20 |

Table continues...

| Table continues... | | | | |
|--------------------|----------------------|-----------|-----------------------|--------|
| No.: | Domain | Position | aa sequence | Length |
| Cys/Spa22 | Cysteine-rich/Spacer | 545 – 564 | CQVCG DNSTCSPRKGSFTA | 20 |
| Cys/Spa23 | Cysteine-rich/Spacer | 550 – 569 | GDNSTCSPRKGSFTAGRARE | 20 |
| Spa24 | Spacer | 555 – 574 | CSPRKGSFTAGRAREYVTFLL | 20 |
| Spa25 | Spacer | 560 – 579 | GSFTAGRAREYVTFLLVTPN | 20 |
| Spa26 | Spacer | 565 – 584 | GRAREYVTFLLVTPNLTSVY | 20 |
| Spa27 | Spacer | 570 – 589 | YVTFLLVTPNLTSVYIANHR | 20 |
| Spa28 | Spacer | 575 – 594 | TVTPNLTSVYIANHRPLFTH | 20 |
| Spa29 | Spacer | 580 – 599 | LTSVYIANHRPLFTHLAVRI | 20 |
| Spa30 | Spacer | 585 – 604 | IANHRPLFTHLAVRIGGRYV | 20 |
| Spa31 | Spacer | 590 – 609 | PLFTHLAVRIGGRYVVAGKM | 20 |
| Spa32 | Spacer | 595 – 614 | LAVRIGGRYVVAGKMSISPN | 20 |
| Spa33 | Spacer | 600 – 619 | GGRYVVAGKMSISPNTTYP | 20 |
| Spa34 | Spacer | 605 – 624 | VAGKMSISPNTTYPSSLLEDG | 20 |
| Spa35 | Spacer | 610 – 629 | SISPNTTYPSSLLEDGRVEYR | 20 |
| Spa36 | Spacer | 615 – 634 | TTYPSSLLEDGRVEYRVALTE | 20 |
| Spa37 | Spacer | 620 – 639 | LLEDGRVEYRVALTEDRLPR | 20 |
| Spa38 | Spacer | 625 – 644 | RVEYRVALTEDRLPRLEEIR | 20 |
| Spa39 | Spacer | 630 – 649 | VALTEDRLPRLEEIRIWGPL | 20 |
| Spa40 | Spacer | 635 – 654 | DRLPRLEEIRIWGPLQEDAD | 20 |
| Spa41 | Spacer | 640 – 659 | LEEIRIWGPLQEDADIQVYR | 20 |
| Spa42 | Spacer | 645 – 664 | IWGPLQEDADIQVYRRYGEE | 20 |
| Spa43 | Spacer | 650 – 669 | QEDADIQVYRRYGEEYGNLT | 20 |
| Spa44 | Spacer | 655 – 674 | IQVYRRYGEEYGNLTRPDIT | 20 |
| Spa45 | Spacer | 660 – 679 | RYGEEYGNLTRPDITFTYFQ | 20 |
| Spa/TSP1 46 | Spacer/TSP1-2 | 665 – 684 | YGNLTRPDITFTYFQPKPRQ | 20 |

3.5.6.2. Development of a Peptide ELISA

A Peptide ELISA was developed using the synthetic peptides from our peptide library (GenScript®, USA) as antigens and an HRP conjugated monoclonal anti-Human IgG antibody specific for the Fc-region (Abcam®, United Kingdom) as a detection antibody. The schematic presentation of the peptide ELISA principle is shown in **Figure 3.4**.

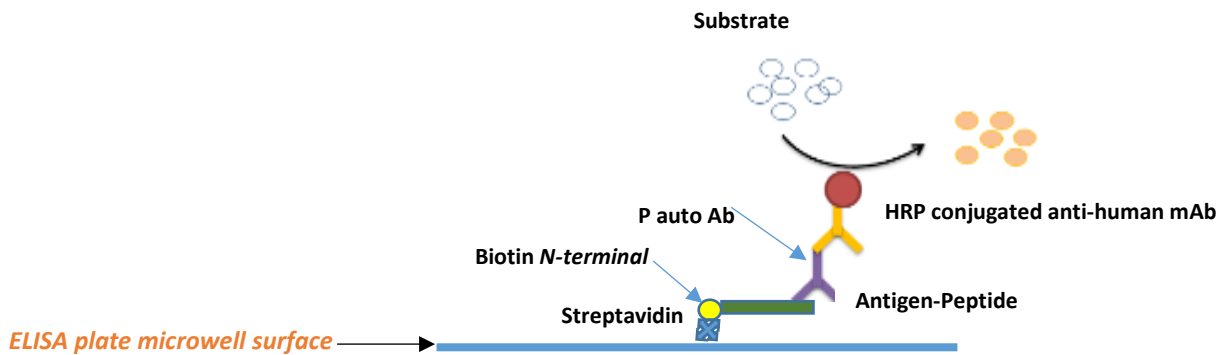


Figure 3.4. A schematic presentation of a Peptide ELISA.

Biotinylated peptides are immobilized to a streptavidin-coated microwell. Binding events are observed from incubating a primary antibody (isolated IgG's form patient's plasma) and an HRP-linked secondary antibody. The addition of a substrate elicits a chromogenic signal.

Purified ADAMTS13 IgG autoantibodies extracted from 53 individual HIV-associated TTP plasma samples and 18 HIV positive control plasma samples were used to identify peptides with potential epitope sites. To develop the peptide ELISA, we first had to determine the viability of the streptavidin surface of the plate by doing a plate viability assay.

3.5.6.3. Plate viability assay

The viability of the streptavidin (SA) surface coated plate to biotin-binding capacity was determined using methodologies published by Sigma-Aldrich® (USA) with slight modifications to the protocol. Lyophilized streptavidin (5mg) purchased from GenScript® (USA) was diluted in 5mL distilled water to produce a final stock concentration of 1mg/mL and stored in aliquots of 1mL at -20°C. In order to coat the ELISA plate (Nunc®), the 1mg/mL streptavidin stock was diluted to a final concentration of 200ng/mL in PBS (pH 7.4). The 200 ng/mL concentration is recommended to be the optimal concentration for SA coating ELISA plates that can bind biotin (GenScript®, USA).

For the assay, 100µL of the diluted SA solution (200 ng/mL) was added to wells of the ELISA plate. The plate was sealed and incubated at 4°C overnight. The following day, the plate was washed 4 times with 300µL/well of PBS/0.05% Tween-20 using a microplate washer. A biotinylated horseradish peroxidase antibody (1 mg/mL; P09568, Sigma-Aldrich®, USA) was diluted 1:10000, 1:20000, 1:30000, 1:40000 and 1:50000 in PBS/0.05% Tween-20 and 50µL was added per well. These dilutions are further referred to as dilution 1, 2, 3, 4, and 5. A negative control (streptavidin-peroxidase (S5512, Sigma-Aldrich®, USA) of the same dilutions was also added to a set of wells in duplicate. A blank (50µL/well of PBS/0.05% Tween-20) was further added in duplicate. The wells

were incubated at room temperature for 30 minutes and washed four times again with PBS/0.05% Tween-20. After the final wash, 50µL/well of OPD substrate was added and incubated for 15 minutes at room temperature. The reaction was stopped with 25µL/well sulphuric acid (4M H₂SO₄) and absorbance measured at 490-360 nm. The mean OD₄₉₀ value of the blank was subtracted from each mean OD₄₉₀ value of the sample. A curve with good linearity indicates biotin binding.

3.5.6.4. Peptide ELISA

To develop the Peptide ELISA, the purified IgG of a plasma sample that tested positive for IgG autoantibodies to ADAMTS13 was used as positive control and an IgG depleted PNP was used as a negative control. The negative control sample was depleted of IgG antibodies using Protein G affinity chromatography described in **3.5.4.1**. In short, PNP was added to the equilibrated column at room temperature and allowed to drain through. The IgG-free plasma was collected into a 1.5 mL Eppendorf tube (Eppendorf Tubes[®], Germany).

The biotinylated peptides served as antigens in this ELISA and were first pooled together in pools of ten peptides each. A peptide pool with good antigenicity was selected for the development of the peptide ELISA method.

Checkboard titrations (CBT) were performed to determine the optimal concentrations for coating of biotinylated peptides, antibody concentration for optimal binding, and the concentration of the commercial HRP-conjugated anti-human IgG antibody. This is a very important part of setting up an ELISA, which allows testing with an optimal concentration of coated peptides that is able to successfully bind antibodies, which can be detected with an optimal amount of conjugated anti-human antibody at a low background.

First, titrations of the biotinylated peptides include the following: 16, 8, 4, 2, 1, and 0.5 µg/mL each in a pool containing multiple peptides. A purified IgG antibody that was known to bind positively to ADAMTS13 was diluted to 1, 4, 8, 12, 16, 20, and 24 µg/mL. The negative control sample was diluted 1:50, 1:100, 1:200, 1:400, 1:800, 1:1600 and 1:3200. The commercial HRP conjugated monoclonal anti-human IgG antibody (Abcam) was diluted to the recommended dilution of 1:1000 according to the manufacturer. The peptides, control samples and the HRP-conjugated anti-human IgG antibody were diluted in PBS/ 0.05% Tween-20 (11.68g NaCl, 9.44g Na₂HPO₄, 5.38g NaH₂PO₄ and 1mL, Tween-20 dissolved in 2L dH₂O).

For the titration assay, the plates were pre-coated with 200ng/mL streptavidin incubated overnight at 4°C and washed before use. The plates were washed 4x with 300µL/well of PBS/ 0.05% Tween-

20 (pH 7.4) using microplate washer (VACUTEC[®], RSA) between incubation steps. After that, different dilutions of diluted peptides were added (100µL/well) from column 1 to column 6, while the blank was added in column 7. The plate was incubated for 2 hours at 37°C, and then washed 4 times again. A hundred µL of each dilution of the control sample was added from row A to row G, while the blank was added to row H. One of the columns, column 7 did not contain diluted peptides but contained a dilution range of the control sample. Row H however, contained a dilution range of the peptide but no control sample. These rows served as background controls to measure non-specific background binding. The negative control sample was added in the same way as the positive control sample on a separate ELISA plate. The plates were incubated again at 37°C for 1 hour. Then, 100µL/well of diluted HRP conjugated anti-human IgG detection antibody diluted 1:1000 was added to the plate and incubated for 1 hour at room temperature. This was followed by another wash step and 100µL/well of the OPD substrate was added to both the plates. The plates were incubated for 10 minutes until a visible colour change was observed. Then 30µL/well of sulphuric acid (4M H₂SO₄) was added to the plate to stop the reaction, and absorbance measured at 490-630 nm. The titrations of the peptides and controls for the Peptide ELISA assay are shown in **Figure 3.5**.

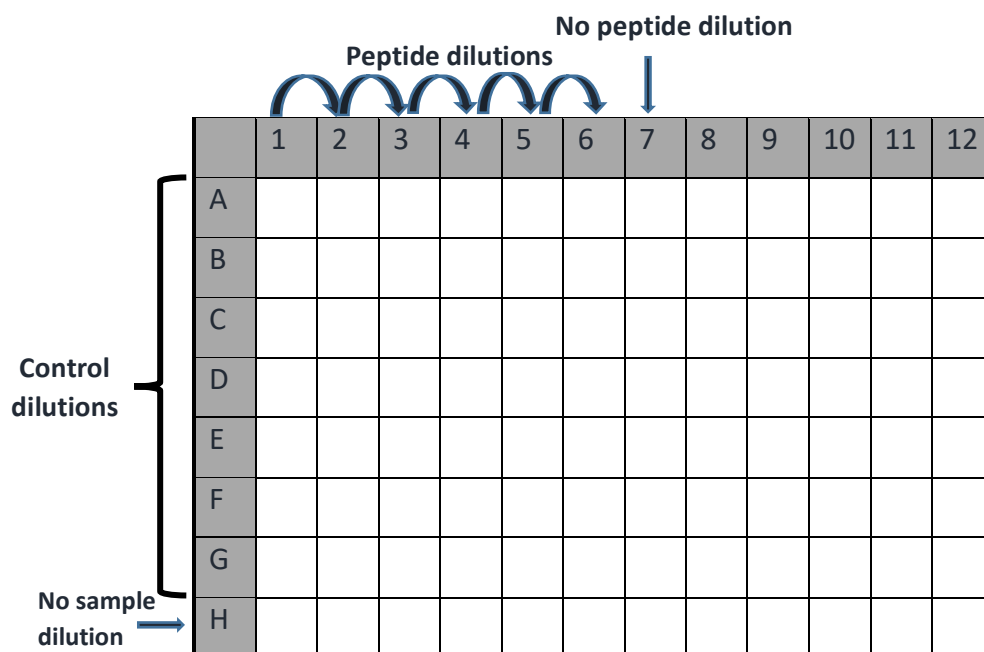


Figure 3.5: Checkerboard titration of peptide antigen and control samples.

Columns 1 to 6 contained a dilution range of peptides and rows A to G contains a dilution range of control samples. Row 7 contains no peptides but contains a dilution range of the control sample and row H contains a dilution range of the peptides, but no control sample.

To determine the appropriate conjugate dilution that allows a strong signal to be produced while minimizing background interference, the HRP conjugated monoclonal anti-human IgG antibody was diluted from 1:500, 1:1000, 1:2000, 1:4000, 1:8000, 1:16000 to 1:32000.

The ELISA procedure was followed the same way as in the initial titration assay for peptides and the IgG antibodies. In short, a streptavidin-coated ELISA plate was washed 4 times, coated with a pre-determined optimal concentration of pooled peptides, and incubated for 2 hours at 37°C. Following another wash step 4x, 100µL/well of the optimum dilution of the negative control sample was added to the plate in duplicate in columns 1 and 2, and of positive control in columns 3 and 4. A blank was added to columns 5 and 6. The plate was incubated at 37°C for 1 hour. Then 100µL/well of dilution range of HRP conjugated detection antibody was added from row A to G in duplicate. The plate was incubated for 1 hour at room temperature and washed again. Lastly, 100µL/well of OPD substrate was added to the plate and the reaction stopped with sulphuric acid after 10 minutes. Then absorbance was measured at 490-630nm. The titrations of the HRP-conjugated anti-human detection antibody are shown in **Figure 3.6**.

| | | Control samples | | | | Blank | | | | | | | |
|---|-----------------------|-----------------|---|---|---|-------|----|---|---|---|----|----|----|
| | | 1 | 2 | 3 | 4 | 5 | 6 | 7 | 8 | 9 | 10 | 11 | 12 |
| HRP-conjugated detection antibody | Conjugate dilution | A | B | C | D | E | F | G | H | | | | |
| | 1:500 | N | N | P | P | BL | BL | | | | | | |
| | 1:1000 | | | | | | | | | | | | |
| | 1:2000 | | | | | | | | | | | | |
| | 1:4000 | | | | | | | | | | | | |
| | 1:8000 | | | | | | | | | | | | |
| | 1:16000 | | | | | | | | | | | | |
| | 1:32000 | | | | | | | | | | | | |

Figure 3.6: Checkerboard titration of HRP conjugated detection antibody.

Dilution of the peptide coat and the control samples (N-negative, P- positive) was constant for the whole plate. The conjugate detection antibody diluted from 1:500 to 1:32000 was added from row A to G. BL=blank.

To minimize the non-specific binding, blocking conditions were optimized following the methodologies of Waritani *et al.* (2017), with slight modifications. Different blocking solutions were prepared using the BSA protein (Bovine serum albumin, Sigma, USA) at different concentrations (0.5%, 1%, and 2%), diluted in PBS/ 0.05% Tween-20 solution. To measure non-specific binding, a blank was included with each dilution on the plate. The plate was blocked at 37°C for 2 hours.

The same ELISA procedure was followed to assess blocking conditions. The streptavidin-coated ELISA plate was washed once and blocked with 200 μ L/well of different concentrations of blocking buffer. After blocking, the plate was washed 4x with PBS/0.05% Tween-20. The plate was coated with an optimal concentration of pooled peptides from columns 1 to 6 and incubated for another 2 hours at 37°C. Columns 7 to 12 contained no peptide coating. Following another wash step, the plate was blocked again with 200 μ L/well of different dilutions of blocking buffer. Then incubated for another 2 hours at 37°C and washed again. A 100 μ L/well of the optimal concentration of the positive and negative control samples was added to the plate and incubated at 37°C for 1 hour. Followed by the addition of 100 μ L/well of HRP conjugated detection antibody diluted to optimal concentration. PBS/0.05% Tween-20 was included as a blank on the plate. Lastly, 100 μ L/well of OPD substrate was added to the plate and the reaction stopped with sulphuric acid after 10 minutes. The absorbance was measured at 490-630 nm. The titrations of the blocking buffer are shown in **Figure 3.7**.

| BSA dilution | | Peptide coated wells | | | | | | Peptide non-coated wells | | | | | |
|--------------|---|----------------------|---|---|---|----|----|--------------------------|---|---|----|----|----|
| | | 1 | 2 | 3 | 4 | 5 | 6 | 7 | 8 | 9 | 10 | 11 | 12 |
| 0.5% BSA | A | P | P | N | N | BL | BL | P | P | N | N | BL | BL |
| | B | | | | | | | | | | | | |
| 1% BSA | C | P | P | N | N | BL | BL | P | P | N | N | BL | BL |
| | D | | | | | | | | | | | | |
| 2% BSA | E | P | P | N | N | BL | BL | P | P | N | N | BL | BL |
| | F | | | | | | | | | | | | |
| | G | | | | | | | | | | | | |
| | H | | | | | | | | | | | | |

Figure 3.7: Checkerboard titration of blocking conditions.

Different blocking dilutions were used in peptide coated and peptide non-coated wells. Samples (N-negative; P-positive) were prepared the same way for both antigen-coated and non-coated wells to determine background noise for all the wells. BL-blank.

Once the Peptide ELISA was optimized, assay precision was determined using separate ELISA assays. A positive control (a purified sample containing IgG antibody against ADAMTS13) and a negative control sample were assayed 20 times in a single ELISA plate. The developed Peptide ELISA plate procedure was followed as previously described.

Intra-assay and inter-assay precision of the developed Peptide ELISA was determined by using a purified anti-ADAMTS13 IgG sample and a negative control sample. The samples were assayed 20 times on one plate (intra-assay) and on 5 different days (inter-assay) to validate the developed peptide ELISA. The results were expressed as the percentage coefficient of variation (%CV) according to the standard formula: $\% CV = SD/mean \times 100\%$.

The positive cut-off value for the Peptide ELISA system was determined using the mean absorbance of a negative control plus 2 standard deviations (Kumar and Rao, 1991). Samples with OD value at 490-630 nm that were higher than the cut-off value was considered as positive and samples with the OD value at 490-630 nm that was less than the cut-off value were considered as negative. The mean OD₄₉₀ of two blank wells was subtracted from each OD₄₉₀ value of the sample wells.

3.5.6.5. Monitoring binding of purified IgG antibodies to linear overlapping peptides of ADAMTS13 using Peptide ELISA.

Epitope mapping studies involved the screening of our peptide library consisting of 105 overlapping biotinylated peptides to monitor binding events for each patient's purified IgG sample using the Peptide ELISA. All our synthetic peptides had a purity of more than 75% and for the assay, peptides were tested individually and not in a pool.

We first pre-coated a 96-well microtiter plate (Nunc) with 100µL/well of streptavidin (200ng/mL, GenScript[®], USA) diluted in PBS buffer (pH 7.2) and incubated it overnight at 4°C. The following day, the plates were washed 4x with 300µL/well of PBS/ 0.05% Tween-20 (pH 7.4) using the microplate washer (VACUTEC[®], RSA) and blocked with 200µL/well of blocking buffer for 2 hours at 37°C. The plates were washed again 4x after incubation, and 100µL/well of each diluted peptide was added to a pre-coated microtiter plate and incubated at 37°C for 2 hours. This was followed by another washing step (4x). The plates were blocked again with 200µL/well of blocking buffer for 2 hours at 37°C. Following another wash step (4x), 100µL/well of the purified IgG antibody from each patient diluted in PBS/ 0.05% Tween-20 was added in duplicate to each plate. A blank and a negative control sample (IgG depleted plasma sample) were included in duplicate in each plate. The plates were incubated for 1 hour at 37°C and then washed again 4x. We then added 100µL/well of an HRP-conjugated monoclonal anti-human IgG antibody (Abcam[®]) for detection. The plates were incubated for one hour at room temperature, followed by another wash 4x. Lastly, 100µL/well of the OPD substrate was added to the plates and the plates incubated for 10 minutes at room

temperature. To stop the reaction, 30µL/well of sulphuric acid (4M H₂SO₄) was added to the plate, and the absorbance measured at 490-630 nm.

The mean OD₄₉₀ value of the two blanks was subtracted from all other OD₄₉₀ values. Each plate contained a negative control. Samples with OD₄₉₀ values greater than the cut-off value (mean absorbance of the negative control plus 2 standard deviations) were considered as having positive binding to the respective peptide and samples with OD₄₉₀ values of less than the cut-off value were considered as having no binding to the respective peptide.

3.6. Statistical analysis

Results were summarized by frequencies, percentages (categorical variables) and means, standard deviations or percentiles (numerical variables). Groups were compared using the Student's T-test and a *p*-value of < 0.05 was considered as statistically significant. GraphPad Prism software 6 (GraphPad Software Inc[®], CA, USA) was used for all the statistical analyses.

Chapter 4: Results

Study samples were confirmed to be from HIV positive patients by HIV (1+2) Antigen/Antibody ELISA analyses (Xpress bio[®], USA) (Table 4, *Supplementary data 2*).

4.1. ADAMTS13 antigen and activity levels

The results of ADAMTS13 antigen and activity levels for both groups (HIV positive patients with and without TTP) are presented in Table 4.1 (*Supplementary data 3*). The ADAMTS13 parameters of HIV-associated TTP and HIV positive patient samples were compared, and assessed for statistically significant differences.

We found statistically significant differences between the two groups ($p < 0.05$). The HIV-associated TTP group presented with severely reduced to undetectable ADAMTS13 antigen and activity levels. The HIV positive control group in contrast had slightly reduced ADAMTS13 antigen and activity levels (Figure 4.1).

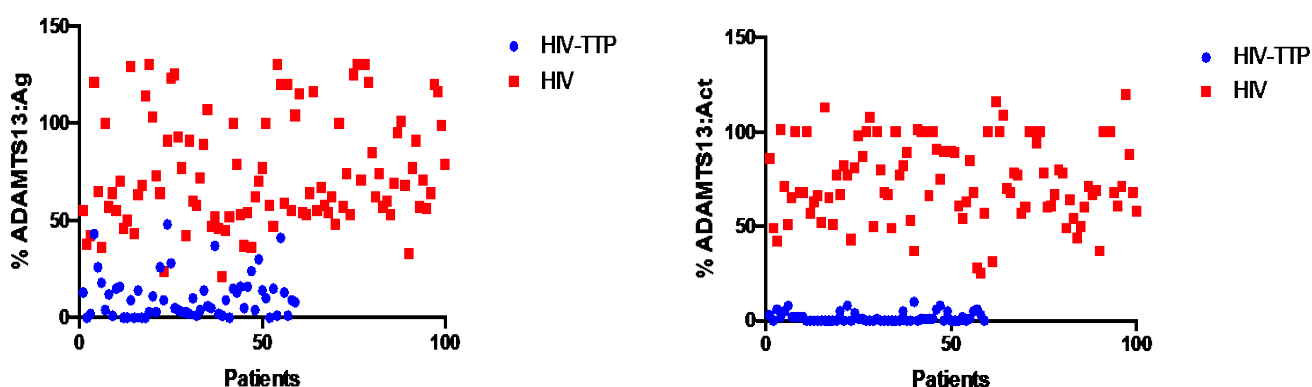


Figure 4.1: ADAMTS13 antigen and activity levels of plasma samples from patients with HIV-associated TTP (blue circles) and the HIV positive patients without TTP plasma group (red squares).

Fifty-nine (59) plasma samples from patients confirmed to suffer from HIV-associated TTP with severely reduced ADAMTS13 activity of less than 10% were selected, including 30 plasma samples with undetectable ADAMTS13 activity. The ADAMTS13 antigen levels of HIV-associated TTP patient plasma samples ranged from 0% – 48%, including 8 samples having undetectable ADAMTS13 antigen levels of 0%.

Hundred (100) control plasma samples from HIV positive patients without TTP had ADAMTS13 antigen levels ranging from 36% - 130% with ~85% in the normal range of 50% - 160% and 15% with

slightly low levels of 36% - 50%. The ADAMTS13 activity levels detected in this control group of patients with HIV infection but without TTP ranged from 25% - 116%, with 11% being below 50% (25-49%), and 89% in the normal range (50-150%). The ADAMTS13 antigen and ADAMTS13 activity levels of the HIV-associated TTP group and the HIV positive control group are compared in **Table 4.1.1**. Statistical significance was indicated when there was a p -value of <0.05 .

Table 4.1.1: ADAMTS13 antigen and ADAMTS13 activity levels of HIV-associated TTP and HIV positive without TTP patient plasma samples.

| Parameter | HIV-associated TTP group (n=59) | HIV positive group (n=100) | Significance (p -value) |
|---|--|---|-------------------------------|
| <ul style="list-style-type: none"> Median ADAMTS13 antigen levels (range) Mean \pmSD | <ul style="list-style-type: none"> 9 (0-48) % 10.88\pm11.58 | <ul style="list-style-type: none"> 66 (36-130) % 72.24\pm29.73 | <0.05 |
| <ul style="list-style-type: none"> Median ADAMTS13 activity (range) Mean \pmSD | <ul style="list-style-type: none"> 0 (0-10) % 1.81\pm2.12 | <ul style="list-style-type: none"> 71 (25-116) % 74.12\pm21.14 | <0.05 |

n, number of samples.

The 2 groups differed significantly with the HIV-associated TTP patients group having reduced ADAMTS13 antigen and significantly reduced activity levels.

4.2. Autoantibodies to ADAMTS13

4.2.1. Anti-ADAMTS13 IgG antibodies

Fifty-three, 53 (90%) of the 59 plasma samples from HIV-associated TTP patients had anti-ADAMTS13 IgG autoantibodies compared to 18 from the 100 HIV-positive patient samples without TTP (18%), which was a statistically significant difference ($p < 0.05$) (**Table 4.2, Supplementary data 4**).

The HIV-associated TTP patient plasma samples had anti-ADAMTS13 IgG antibody titers ranging from 2-223 μ g/mL with 53 (90%) samples with titers >15 μ g/mL (positive), 7% with clinically insignificant titers of < 12 (negative) and 3% with a borderline result of 12-15 μ g/mL.

Seven (7) HIV-associated TTP patient samples (samples TTP-7, -35, -37, -43, -51, and -53) had significantly reduced ADAMTS13 antigen and activity levels but insignificant anti-ADAMTS13 IgG antibody titers pointing towards possible congenital TTP or an alternative pathophysiological mechanism of the TTP disease.

The HIV positive control cohort plasma samples had anti-ADAMTS13 IgG antibody titers ranging from 1-87 $\mu\text{g}/\text{mL}$ with 18% of samples with titers $> 15 \mu\text{g}/\text{mL}$ (positive), 74% with titers of < 12 (negative) and 8% with a borderline result of 12-15 $\mu\text{g}/\text{mL}$ (**Figure 4.2**).

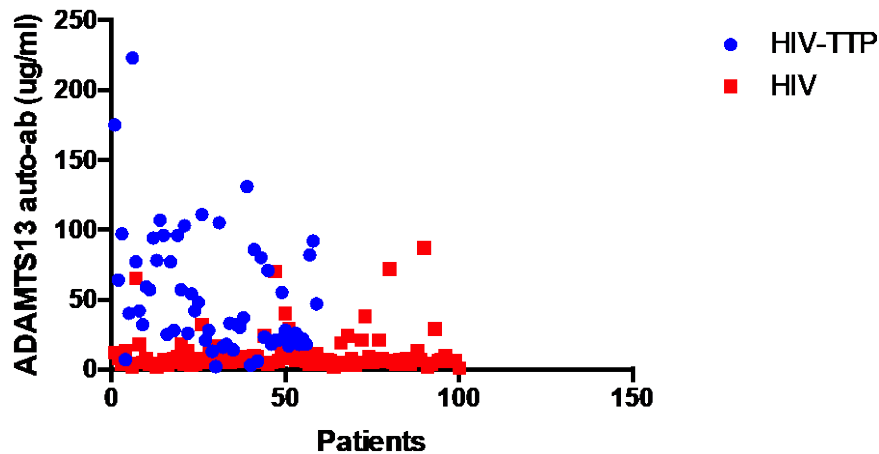


Figure 4.2: Anti-ADAMTS13 IgG antibody results of the HIV-associated TTP (blue circles) and the HIV positive (red squares) patient plasma samples.

The anti-ADAMTS13 IgG autoantibody titers between the HIV-associated TTP group and the HIV positive group are compared in **Table 4.2.1** (Statistical significance, p -value < 0.05).

Table 4.2.1: Anti-ADAMTS13 IgG autoantibodies in HIV-associated TTP and HIV positive control cohorts.

| Parameter | HIV-associated TTP group (n=59) | HIV positive group (n=100) | Statistics (p-value) |
|--|---|---|-------------------------|
| <ul style="list-style-type: none"> Median Anti-ADAMTS13 IgG antibody titer (ranges) | <ul style="list-style-type: none"> 42 (2 – 223) $\mu\text{g}/\text{mL}$ | <ul style="list-style-type: none"> 7 (1 – 87) $\mu\text{g}/\text{mL}$ | $p < 0.05$ |
| <ul style="list-style-type: none"> Mean \pm SD | <ul style="list-style-type: none"> 54.88 \pm 43.26 | <ul style="list-style-type: none"> 11.76 \pm 14.78 | |

n, number of samples.

The ADAMTS13 levels were compared to the anti-ADAMTS13 IgG antibody titer in both groups. There was no correlation between the ADAMTS13 antigen levels and the antibody titres in the HIV-associated TTP cohort (**Figure 4.3**). However, patient plasma samples with high anti-ADAMTS13 IgG antibody titers had low median ADAMTS13 antigen levels of 4.5%, which was lower compared to those with low anti-ADAMTS13 IgG titers and a high median ADAMTS13 antigen levels of 12.5%. The statistics of the ADAMTS13 antigen levels and the anti-ADAMTS13 IgG titers in HIV-associated TTP with high and low autoantibody titers are shown in **Table 4.2.2**.

Table 4.2.2: ADAMTS13 antigen levels and anti-ADAMTS13 IgG antibody titer results of HIV-associated TTP patient plasma samples.

| Parameter | High anti-ADAMTS13 IgG antibody titer (n=24) | Low anti-ADAMTS13 IgG antibody titer (n=29) |
|--|---|---|
| <ul style="list-style-type: none"> Median Anti-ADAMTS13 IgG antibody titer (ranges) Mean \pm SD | <ul style="list-style-type: none"> 89 (54 – 223) μg/mL 94\pm38.72 | <ul style="list-style-type: none"> 26 (16 – 48) μg/mL 27\pm9.34 |
| <ul style="list-style-type: none"> Median ADAMTS13 antigen levels (ranges) Mean \pm SD | <ul style="list-style-type: none"> 4.5 (0 – 30) % 7.08\pm7.55 | <ul style="list-style-type: none"> 12.5 (0 – 48) % 14\pm13.06 |

n, number of samples.

There was no correlation between ADAMTS13 levels and anti-ADAMTS13 IgG titer in the HIV positive control cohort samples: 17 of the 18 patient samples with positive anti-ADAMTS13 IgG antibody titers had normal ADAMTS13 antigen and activity levels. However, 1 HIV positive plasma sample (sample HIV-60) had a high anti-ADAMTS13 IgG titer (87 μ g/mL) and a slightly low ADAMTS13 antigen level (37%) and activity (33%).

4.2.1.1. Mixing studies

Mixing studies were performed on HIV-associated TTP patient samples with an ADAMTS13 activity of less than 10% together with a positive anti-ADAMTS13 IgG antibody titer. The results of the mixing studies and the inhibitory Bethesda units for individual HIV-associated TTP patient plasma samples are presented in **Table 4.3 (Supplementary data 5)**.

Thirty-six, 36 (68%) plasma samples from 53 HIV-associated TTP patients had inhibitory anti-ADAMTS13 IgG antibodies, while non-inhibitory anti-ADAMTS13 IgG antibodies were detected in 17 (32%) plasma samples using mixing studies. Samples detected with inhibitory (neutralizing) anti-ADAMTS13 IgG antibodies is interpreted as “No correction”, while the presence of non-neutralizing anti-ADAMTS13 IgG antibodies is interpreted as “Correction” in **Table 4.3**.

Sixteen (16) of the 36 HIV-associated TTP patient plasma samples with inhibitory anti-ADAMTS13 IgG antibodies had strong inhibitors indicated by a persisting ADAMTS13 activity of <10% in 50:50 mixing studies. Twenty (20) samples had a positive antibody titer but low inhibition, as shown by the Bethesda assay, suggesting the presence of weak inhibitors. Interestingly, samples TTP-9 and -20 had high titers of anti-ADAMTS13 IgG antibodies (223 and 77 μ g/mL respectively), but corrected with the mixing test, indicating the absence of inhibitory autoantibodies. This may suggest an

antibody-mediated clearance of ADAMTS13 in these samples. Statistics of the anti-ADAMTS13 IgG antibody titer results and Bethesda assay results for HIV-associated TTP plasma samples are presented in **Table 4.3.1**.

Table 4.3.1: Anti-ADAMTS13 IgG antibody concentrations and Bethesda Inhibitory (BU) results in HIV-associated TTP patient plasma samples.

| Anti-ADAMTS13 IgG antibodies | Number of samples | Median Anti-ADAMTS13 IgG antibody titer (ranges) | Median Bethesda Units (BU/mL) (ranges) |
|------------------------------|-------------------|--|--|
| Non inhibitory | 17/53 | 26 (17 - 223) µg/mL | <0.5 |
| Low inhibition <5BU | 17/53 | 42 (18 - 86) µg/mL | 1.85 (0.64 – 4.54) BU |
| Strong inhibition >5BU | 19/53 | 96 (32 – 175) µg/mL | 9.74 (5.10–17.92) BU |

4.2.2. IgM and IgA antibodies

4.2.2.1. Total IgM and IgA antibodies in patient plasma

Patient plasma samples with HIV-associated TTP as well as HIV infected control cohort without TTP with positive anti-ADAMTS13 IgG titers were screened for total plasma IgM and IgA antibodies (**Table 4.4, Supplementary data 6**).

Plasma concentrations of IgM and IgA antibodies from individual HIV-associated TTP patient samples were slightly increased compared to those from the HIV infection without TTP (the control cohort), with a statistically significant difference ($p < 0.05$).

The IgM levels were increased in 38 of the 53 (72%) HIV-associated TTP patient samples compared to 2 of the 18 (11%) HIV positive control cohort patient samples and IgA levels were increased in 21 of the 53 (40%) HIV-associated TTP patient samples and were normal in the HIV positive control cohort samples (**Table 4.4.1**).

Table 4.4.1: The mean concentrations of IgM and IgA in HIV-associated TTP and HIV positive groups.

| Parameter | HIV-associated TTP group (n=53) | HIV positive group (n=18) | Significance (p-value) |
|--|---|--|---------------------------|
| <ul style="list-style-type: none"> • Median IgM level (ranges) • Mean ± SD | <ul style="list-style-type: none"> • 1.6 (1.05 – 2.35) mg/mL • 1.59 ± 0.27 | <ul style="list-style-type: none"> • 0.61 (0.2 – 2) mg/mL • 0.82 ± 0.46 | <i>p</i> < 0.05 |
| <ul style="list-style-type: none"> • Median IgA level (ranges) • Mean ± SD | <ul style="list-style-type: none"> • 1.85 (1.06 - 2.98) mg/mL • 2.10 ± 0.60 | <ul style="list-style-type: none"> • 1.6 (1.41 – 1.92) mg/mL • 1.66 ± 0.15 | <i>P</i> < 0.05 |

n, number of samples.

4.2.2.2. Anti-ADAMTS13 IgM and IgA antibodies

Qualitative determination of anti-ADAMTS13 IgM and IgA antibodies were performed. The results of the IgM and IgA autoantibodies to ADAMTS13 detected in individual HIV-associated TTP and HIV positive control plasma samples are presented in **Table 4.5A (Supplementary data 1)**.

Anti-ADAMTS13 IgM antibodies were present in 16 (30%) and absent in 37 (70%) of the 53 HIV-associated TTP patient plasma samples. Anti-ADAMTS13 IgA antibodies were present in 34 (64%) and absent in 19 (36%) of the HIV-associated TTP patient plasma samples. Both anti-ADAMTS13 IgM and IgA autoantibodies were detected in only 15 (28%) of the 53 HIV-associated TTP patient plasma samples (**Figure 4.3**).

Five, 5 (28%) of the 18 plasma samples from the control cohort had anti-ADAMTS13 IgM antibodies and 4 (22%) had anti-ADAMTS13 IgA antibodies. Both anti-ADAMTS13 IgM and IgA antibodies were detected in 4 (22%) of these 18 plasma samples (**Figure 4.3**).

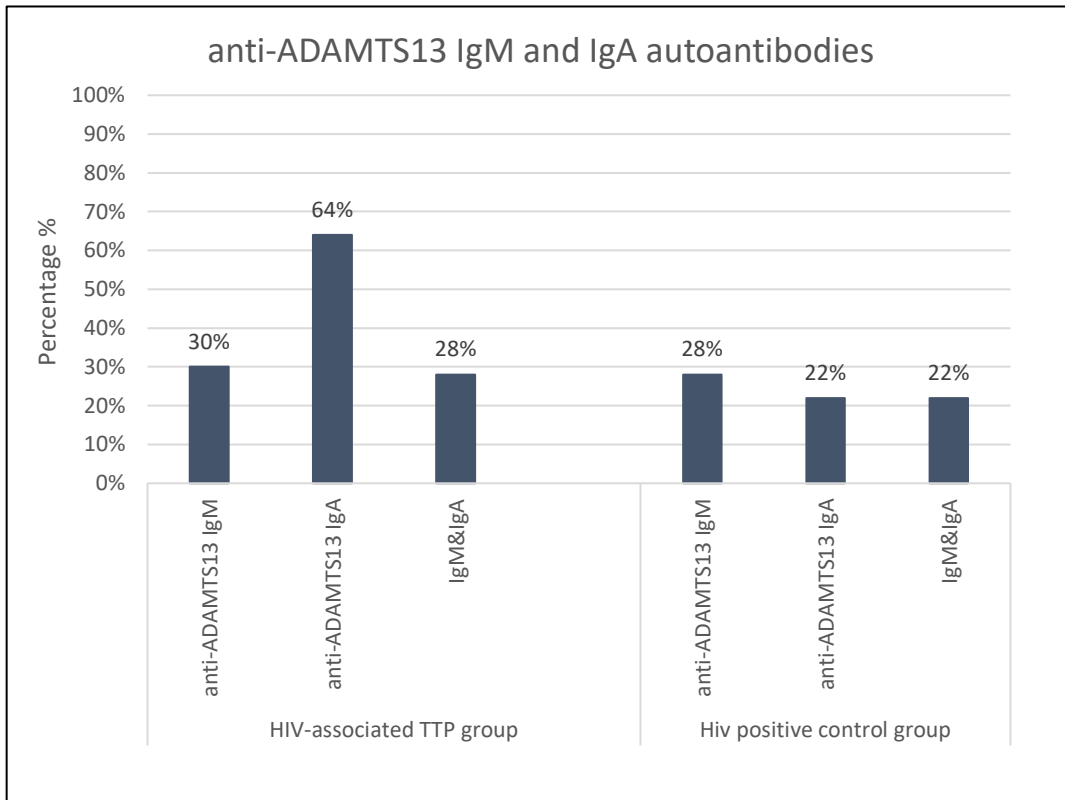


Figure 4.3: Anti-ADAMTS13 IgM and IgA autoantibody results in HIV-associated TTP and HIV positive control cohort patient plasma samples.

The validation results of the anti-ADAMTS13 IgM and IgG antibody assay are presented in **Table 4.5.1** and **Table 4.5.2**, respectively. Both anti-ADAMTS13 IgM and IgA ELISA assays showed good reproducibility of results with an inter-assay coefficient of variation (CV) of 5.74% and 6.54% respectively with calculations included in **Table 4.5B (Supplementary data 6)**.

Table 4.5.1: Precision results for anti-ADAMTS13 IgM antibody ELISA assay.

| Statistic(s) | Intra-assay precision results | |
|--|-------------------------------|--------------------------|
| | Samples Positive for IgM | Samples Negative for IgM |
| Mean OD (M) | 0.41 | 0.10 |
| Standard deviation (SD) | 0.02 | 0.01 |
| Coefficient of variation (CV) = (SD/M)*100% | 4.09% | 7.36% |
| Inter-assay CV = (CV of Positive + CV of Negative)/2 | 5.74% | |

Table 4.5.2: Precision results for anti-ADAMTS13 IgA antibody ELISA assay

| Statistic(s) | Intra-assay precision results | |
|--|-------------------------------|--------------------------|
| | Samples Positive for IgA | Samples Negative for IgA |
| Mean (M) | 0.26 | 0.09 |
| Standard deviation (SD) | 0.02 | 0.01 |
| Coefficient of variation (CV) = (SD/M)*100% | 6.13% | 6.94 |
| Inter-assay CV = (CV of Positive + CV of Negative)/2 | 6.54% | |

4.3. VWF analysis

The HIV-associated TTP patient plasma samples (n=59) with severe ADAMTS13 activity of <10% and the control cohort samples (n=100) were analyzed for VWF levels and statistically significant differences were calculated.

4.3.1. VWF antigen (VWF:Ag) levels

Eighteen, 18 (14%) of the HIV-associated TTP patient samples had normal VWF:Ag levels (50 - 150%) and 49 (86%) had VWF:Ag levels above the normal range i.e. >150% of which 29 (51%) had significantly raised VWF:Ag of more than 200%. In the HIV positive control cohort, 31% of the samples had VWF:Ag levels within the normal range of 50-150%, while 69% had increased levels of >150%, of which 24 (24%) were significantly raised at >200% (**Table 4.6 of Supplementary data 7**).

In summary, the VWF:Ag levels in both the HIV-associated TTP group and the HIV positive control group were normal to significantly increased 70-700% and 61-538% respectively. No statistically significant difference was observed between the 2 groups (*p-value* = 0.15, thus >0.05) (**Table 4.6.1**).

Table 4.6.1: von Willebrand factor antigen levels in HIV-associated TTP and HIV positive plasma samples.

| Statistic(s) | HIV-associated TTP group (n=59) | HIV positive group (n=100) |
|---|---------------------------------|----------------------------|
| Median VWF:Ag level (range) | 201 (70 - 700) % | 190 (61-538) % |
| Mean ± SD | 230 ± 120 % | 206 ± 88 % |
| Statistical significance (<i>p-value</i>) | <i>p</i> =0.15 | |

n-number of samples.

The VWF:Ag levels in the patient plasma samples of both groups were compared in respect of ADAMTS13 levels. Plasma samples with abnormally high VWF:Ag levels (>150%) had severely reduced ADAMTS13 levels (**Table 4.6.2**). HIV-associated TTP patient samples had a high median VWF:Ag level of 217% with low median ADAMTS13 antigen and activity levels (median antigen 9% and activity of 1%) suggesting that severe ADAMTS13 deficiency results in accumulation of VWF in HIV-associated TTP patient. The HIV positive control cohort also had high median VWF:Ag levels with normal ADAMTS13 levels (median ADAMTS13 antigen of 68% and activity of 73%) and no causative link was therefore apparent between VWF:Ag and ADAMTS13 levels in this group.

Table 4.6.2: The VWF:Ag levels and ADAMTS13 levels in HIV-associated TTP group and HIV positive control group.

| Parameters | HIV-associated TTP group (n=49) | HIV positive group (n=69) |
|---|--|---|
| <ul style="list-style-type: none"> • Median VWF:Ag levels (ranges) • Mean ± SD | <ul style="list-style-type: none"> • 217 (152 – 700) % • 249 ± 118 | <ul style="list-style-type: none"> • 220 (155 – 538) % • 243 ± 80 |
| <ul style="list-style-type: none"> • Median ADAMTS13 antigen levels (ranges) • Mean ± SD | <ul style="list-style-type: none"> • 9 (0-48) % • 12 ± 12 | <ul style="list-style-type: none"> • 68 (33 – 130) % • 74 ± 28 |
| <ul style="list-style-type: none"> • Median ADAMTS13 activity levels (ranges) • Mean ± SD | <ul style="list-style-type: none"> • 1 (0-10) % • 2 ± 3 | <ul style="list-style-type: none"> • 73 (31 – 100) % • 75 ± 19 |

n, number of samples.

4.3.2. VWF propeptide (VWFpp) levels

The results of VWF propeptide levels from individual plasma samples from the HIV-associated TTP and HIV positive control groups are presented in **Table 4.7** of **Supplementary data 8**.

Increased VWFpp levels were detected in 48 (81%) of the 59 HIV-associated TTP patient plasma samples and in 94 (94%) of the 100 HIV positive control cohort plasma samples respectively. However, 11 (19%) of the 59 HIV-associated TTP patient plasma samples and 6 (6%) of the 100 HIV positive cohort plasma samples had normal VWFpp levels. No significant difference in VWFpp levels was observed between plasma samples of the 2 groups. Also, no statistically significant difference was observed between the VWFpp level and VWFpp/VWF:Ag ratios (p 0.701 and 0.287) respectively (**Table 4.7.1**).

Increased VWFpp to VWF:Ag ratios of >3 were observed in 8 (14%) of the 59 HIV-associated TTP patient plasma samples and in 18 (18%) of the HIV positive control cohort plasma samples (**Table 4.7.1**).

Table 4.7.1: VWFpp levels for the HIV-associated TTP and HIV positive plasma samples.

| Parameters | HIV-associated TTP group (n=59) | HIV positive group (n=100) | Statistical significance (p value) |
|--|---|---|---------------------------------------|
| <ul style="list-style-type: none"> • Median VWFpp levels (ranges) • Mean ± SD | <ul style="list-style-type: none"> • 294 (30 – 1275) % • 371 ± 262 | <ul style="list-style-type: none"> • 311 (83- 1331) % • 387 ± 249 | P = 0.701 |
| <ul style="list-style-type: none"> • Median VWFpp/ VWF:Ag ratio (ranges) • Mean ± SD | <ul style="list-style-type: none"> • 1.35 (0.24 – 5.88) • 1.76 ± 1.30 | <ul style="list-style-type: none"> • 1.76 (0.45 – 5.05) • 1.97 ± 1.00 | P = 0.287 |

n, number of samples.

4.3.3. VWF multimers analysis

Samples with distinctive multimeric patterns from the HIV-associated TTP patients and HIV positive control cohort samples are shown in **Figure 4.4** with PNP sample multimer pattern also shown as comparison. Each lane shows the VWF multimeric patterns of an individual plasma sample from the HIV-associated TTP patients, HIV positive control group and PNP. VWF multimer patterns obtained from all the HIV-associated TTP and HIV positive individual plasma samples are shown in **Figure 4.4.1** in the **Supplementary data 9** set. VWF multimer structures were examined using gel electrophoresis on a 0.7% SDS agarose gel.

Normal VWF multimer patterns, as compared to patterns in PNP, were observed in 49 (86%) of the 59 HIV-associated TTP patient plasma samples and 70% of HIV positive cohort samples. The dense (dark) multimer patterns observed correlated with the extremely high VWF:Ag levels detected in these plasma samples. Samples TTP (-11, -13, -18, -59, -60, and -65) and HIV (-1, -184, and -192) represent these multimer patterns in **Figure 4.4**.

Normal multimeric patterns similar to that of PNP were observed in 14% of the HIV-associated TTP patient plasma samples with normal VWF:Ag levels (50% - 150%). Samples TTP (-34, -61, and -33) and HIV (-25, -185) represent these multimer patterns in **Figure 4.4**.

The plasma samples with a high VWFpp/VWF:Ag ratio, demonstrated loss of the largest VWF multimers, suggesting clearance of large VWF multimers in the circulation. This clearance of the

large VWF multimers may be due to the trapping of these multimers in the vasculature. The loss of the largest VWF multimers was seen in 14% (8) of the 59 HIV-associated TTP patient samples (TTP-10, -12, -6, -8, -16, -17, -24, and -52) and 18% (18) of the 100 control cohort samples (HIV-195, -32, -36, -120, -133, -134, -135, -142, -149, -154, -162, -163, -174, -177, -99, -106, -43, and -14). These multimer patterns are represented by samples TTP6, TTP10 and HIV32 in **Figure 4.4**.

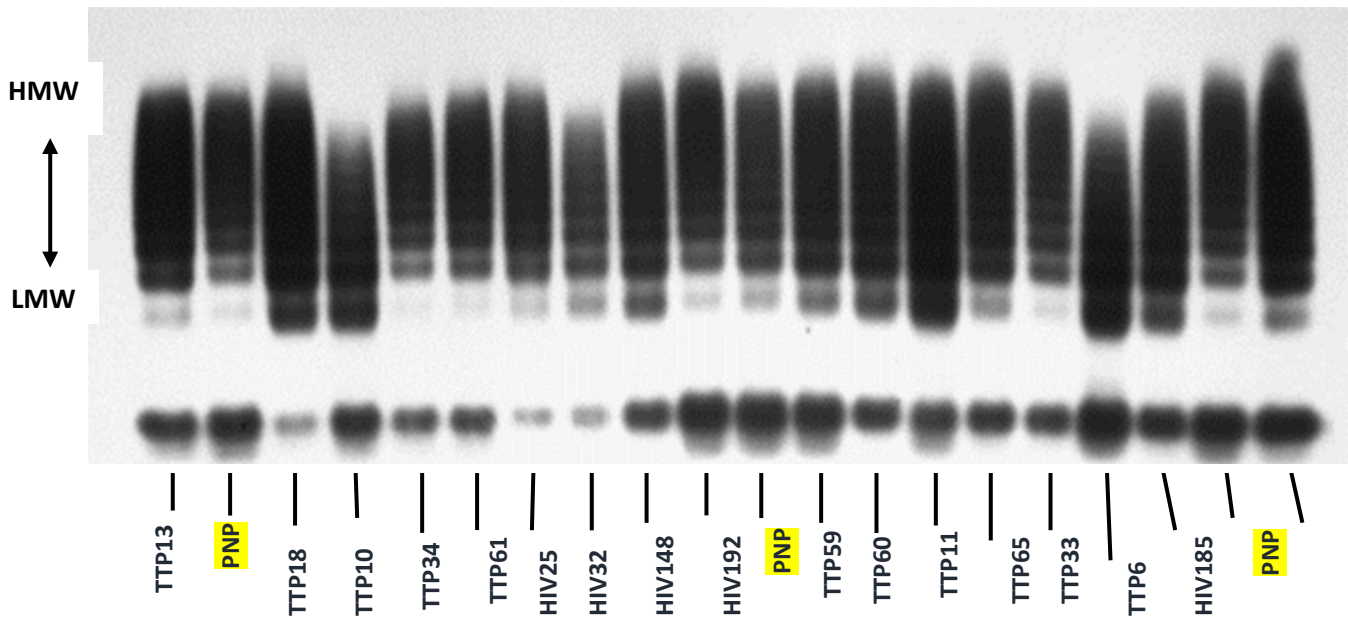


Figure 4.4: Plasma VWF multimer patterns.

Multimer patterns on 0.7% SDS agarose gel electrophoresis for the individual HIV-associated TTP patient and HIV positive control patient plasma samples. Human pooled normal plasma (PNP, highlighted yellow) samples were analyzed in parallel for comparison. TTP samples (TTP-11, -13, -18, -59, -60 and -65) and HIV control samples (HIV-1, -184, -192) showed the presence of large VWF with increased density. TTP samples (TTP-34, -61 and -33) and HIV control samples (HIV-25 and -185) showed normal multimer patterns compared to PNP; samples TTP-6, -10 and -32 showed a loss of the largest multimers.

HMW, high molecular weight; LMW, molecular weight.

4.4. Extraction of IgG autoantibodies

Immunoglobulin G (IgG) autoantibodies from HIV-associated TTP patient samples and control HIV positive control plasma samples were isolated and quantified.

4.4.1. Quantification of purified IgG antibodies

Extraction efficiencies ranged from 1-15 mg/mL of IgG antibody per individual plasma sample using NAb™ Protein G spin columns. Concentrations obtained from purified IgG antibodies isolated from individual HIV-associated TTP plasma samples and HIV positive plasma samples are presented in **Table 4.8** of **Supplementary data 10**. Only protein fractions with the desired absorbance 260/280 ratio of <0.6 were deemed as nucleic acid-free and were pooled. The statistics of the purified IgG

antibody concentrations obtained from plasma samples of the HIV-associated TTP and the HIV positive control groups are summarized in **Table 4.8.1**.

Table 4.8.1: Obtained concentrations of Purified IgG antibody from plasma samples.

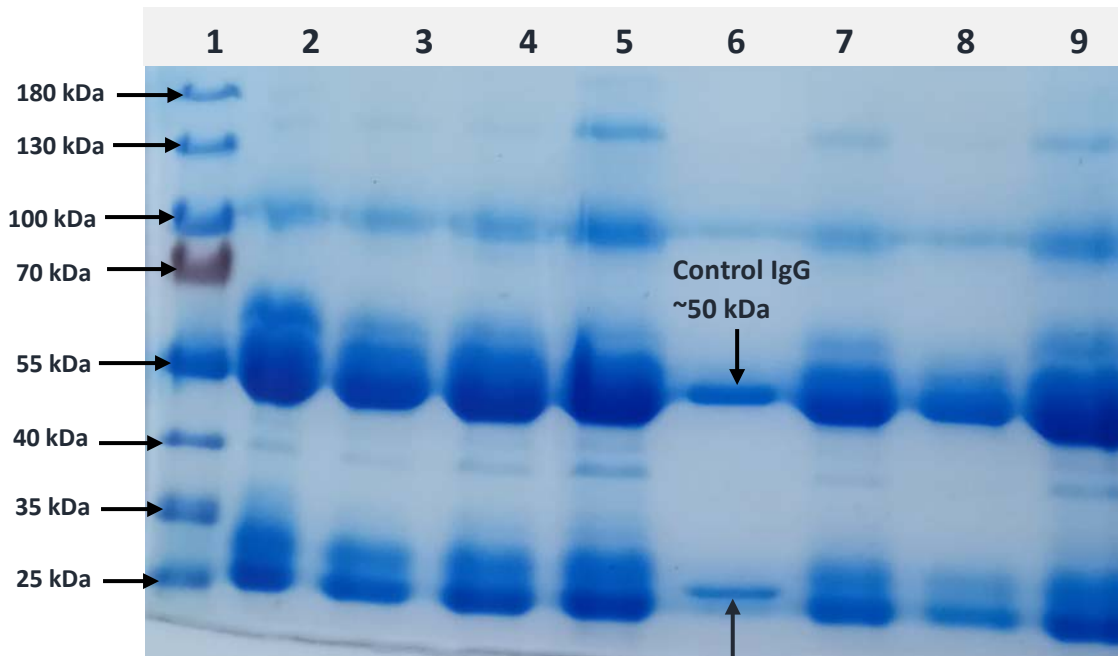
| Statistic(s) | HIV-associated TTP group n=53 | HIV positive group n=18 |
|---|---|--|
| <ul style="list-style-type: none"> • Median IgG antibody concentrations (ranges) • Mean \pm SD | <ul style="list-style-type: none"> • 5.68 (1.32 – 14.26) mg/mL • 6.63 \pm 3.63 | <ul style="list-style-type: none"> • 3.07 (1.3 – 6.8) mg/mL • 3.31 \pm 2.09 |
| <ul style="list-style-type: none"> • Median Absorbance 260/280 ratio (ranges) • Mean \pm SD | <ul style="list-style-type: none"> • 0.54 (0.51 – 0.598) • 0.54 \pm 0.05 | <ul style="list-style-type: none"> • 0.55 (0.51 – 0.59) • 0.56 \pm 0.03 |

n, number of samples.

4.4.2. The SDS-PAGE analysis of purified IgG

Purified IgG antibodies were obtained from 53 HIV-associated patient plasma and 18 HIV positive control plasma samples. The IgG samples were separated under reducing and non-reducing conditions on a 10% SDS-PAGE to confirm the presence of purified IgG antibody. Under reducing conditions, a band at a molecular weight size of ~50 kDa correlate with IgG heavy chain and a band at ~25 kDa with the light chain. The molecular weight for the intact IgG antibody is ~150 kDa, and a band around this position is observed under non-reducing conditions. A ThermoFisher Scientific® PageRuler™ Pre-stained Protein Ladder is shown in **Figure 4.5**. lane 1 and a control human monoclonal IgG antibody (Abcam®, USA) in lane 3 and 6 under reducing and non-reducing conditions respectively.

A. Reducing SDS-PAGE



B. Reducing and Non-Reducing SDS-PAGE

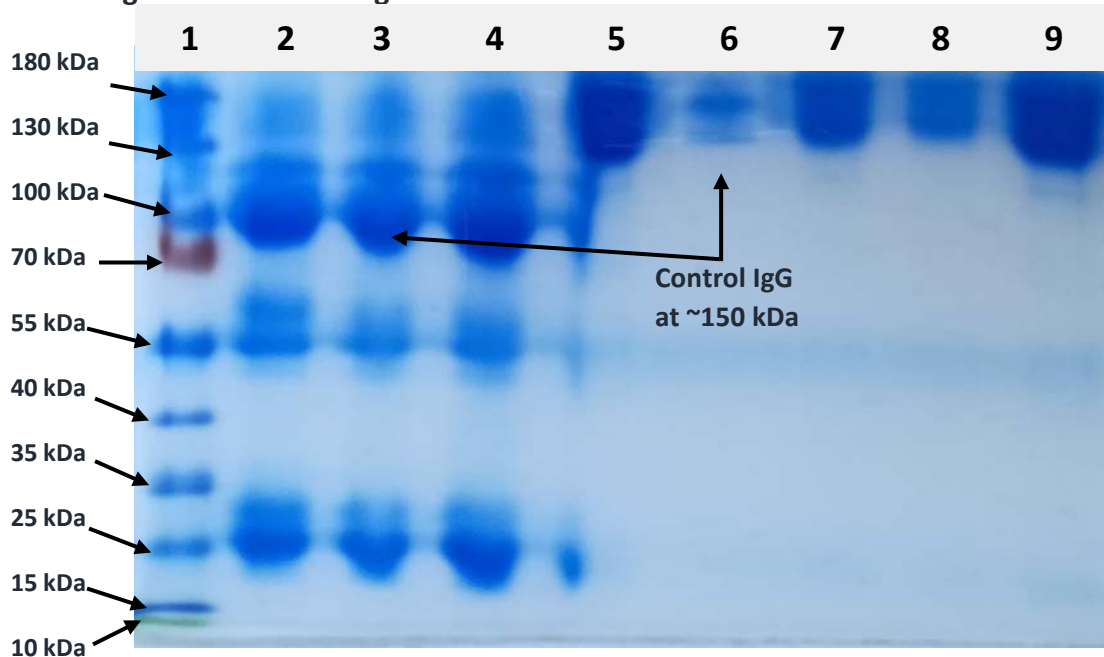


Figure 4.5. SDS-PAGE of purified IgG antibodies.

A. Reducing SDS-PAGE of purified IgG antibodies: Protein ladder (ThermoFisher Scientific™) in lane 1, sample in lanes 2-5 and 7-9 and a control in lane 6, all with 2 bands at ~50 kDa and ~25 kDa molecular weight.

B. Reducing and non-reducing SDS-PAGE of purified IgG antibody: Protein ladder in lane 1, samples in lanes 2 and 4, control in lane 3. Antibody fragments at ~75 kDa molecular weight band represent the presence of both the heavy and a light chain, and a band at ~50 kDa and ~25 kDa represent the presence of a heavy chain and light chain respectively. Lanes 6-9: non-reducing condition with the control in lane 6 and patient IgG in lanes 7 to 9, indicating a band at ~150 kDa (130-180 kDa) for intact IgG antibody.

4.5. Epitope mapping studies of anti-ADAMTS13 IgG antibodies in HIV-associated TTP patient samples.

4.5.1. Peptide library

A peptide library consisting of 105 linear overlapping peptides from the proximal domains of ADAMTS13 were screened for possible epitope regions for the purified anti-ADAMTS13 IgG isolated from 53 HIV-associated TTP patient and 18 HIV positive control cohort plasma samples. A Peptide ELISA assay was used to screen for the possible epitope regions. The Peptide ELISA was optimized before continuing with epitope mapping studies.

4.5.2. Development of a Peptide ELISA

4.5.2.1. Plate viability assay

The results of the plate viability assay confirmed that the multi-well plates used in the Peptide ELISA were properly coated with streptavidin. The standard curve of different streptavidin concentrations indicated acceptable linearity (**Figure 4.6**), suggesting that streptavidin is able to bind biotin even at the lowest dilution. The maximum OD₄₉₀ value of at least 1.5 observed at the highest dilution showed that the coated streptavidin did bind strongly to biotin in an ELISA assay.

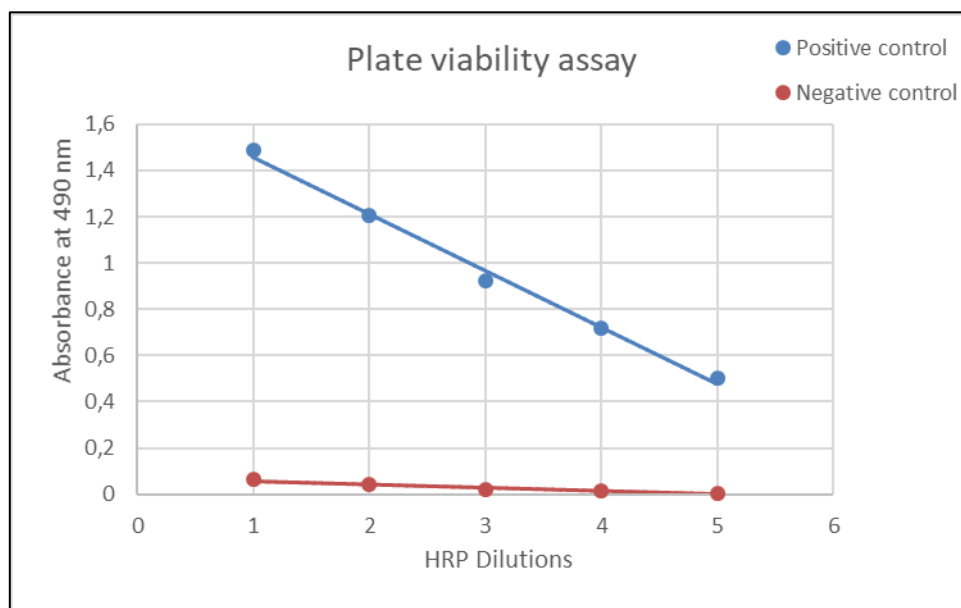


Figure 4.6: Standard curve for streptavidin-biotin binding.

4.5.2.2. Peptide ELISA

The Peptide ELISA was optimized using the checkerboard titration (CBT) method. The optimization results are presented in **Figure 4.7 A** to **Figure 4.7 E**. The raw data for the optimization results is included in **Supplementary data 11**.

The optimal coating concentration for the peptides was determined to be 4 μ g/mL (**Figure 4.7 A**). Peptide dilution of 4 μ g/mL indicated that sufficient antigen is available to bind antibodies optimally. An antibody concentration of 12 μ g/mL produced a low background level of interference and was chosen as the optimal concentration for the study (**Figure 4.7 B**) and, at a dilution of 1:4 yielded a good color development related to antibody binding. A negative control dilution of 1:200 produced a low background level of interference and was chosen as the optimal dilution for the study experiments (**Figure 4.7 C**). The optimal dilution for the HRP-conjugated anti-human IgG antibody was chosen to be 1:2000 since it produced low background binding (**Figure 4.7 D**). The blocking conditions were optimized at 37°C incubation for 2 hours with PBS/1% BSA/0.05% Tween-20 at pH 7.4 to prevent non-specific binding and minimize background interference. Blocking with BSA protein reduced background noise while still allowing antibodies to bind. Thus, a 1% BSA concentration was chosen to prepare a blocking buffer (**Figure 4.7 E**).

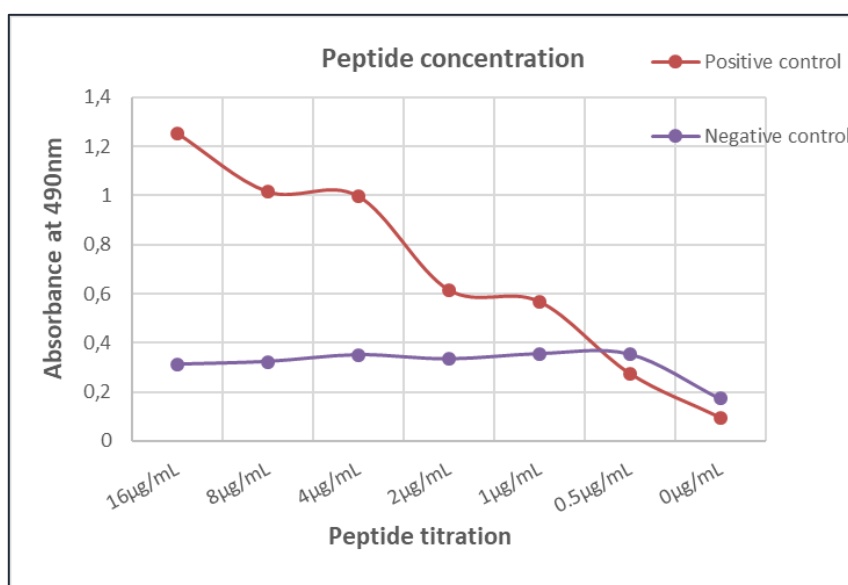


Figure 4.7 A: Optimization of the Peptide ELISA working conditions.

Absorbance results obtained at 490 nm for the positive and negative control samples plotted on the Y-axis against different peptide antigen titrations plotted on the X-axis. Peptide dilution of 4 μ g/mL was sufficient for binding antibodies maximally.

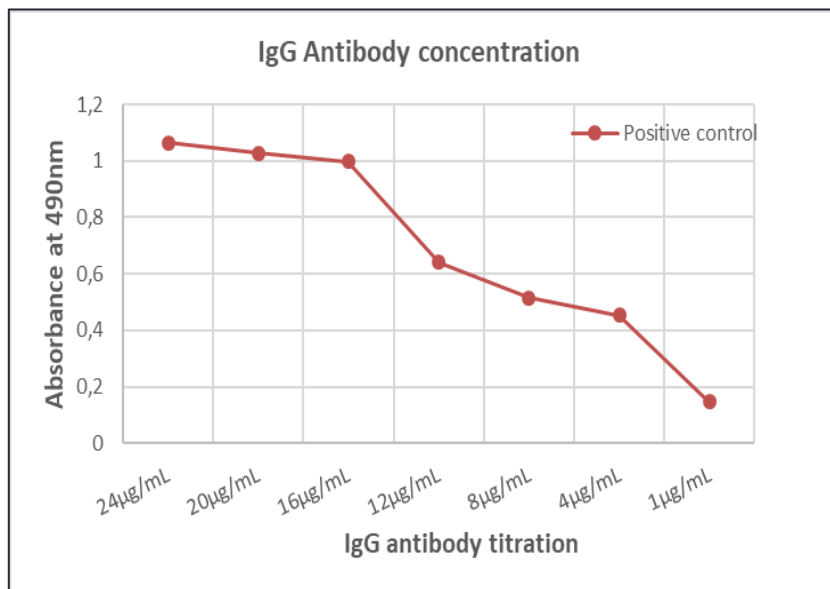


Figure 4.7 B: Optimization of the Peptide ELISA working conditions.

Absorbance results obtained at 490 nm for the positive control plotted on the Y-axis against different IgG antibody titrations plotted on the X-axis. The antibody concentration of 12µg/mL produced a low background and was chosen as the optimal concentration.

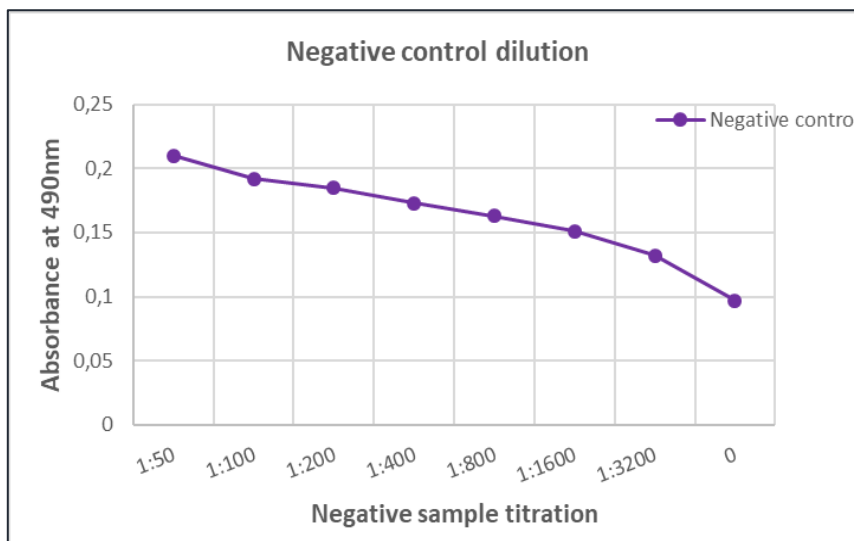


Figure 4.7 C: Optimization of the Peptide ELISA working conditions.

Absorbance results obtained at 490 nm for the negative control plotted on the Y-axis against different dilutions of the negative control sample plotted on the X-axis. The negative control dilution of 1:200 produced low background and was chosen as the optimal dilution.

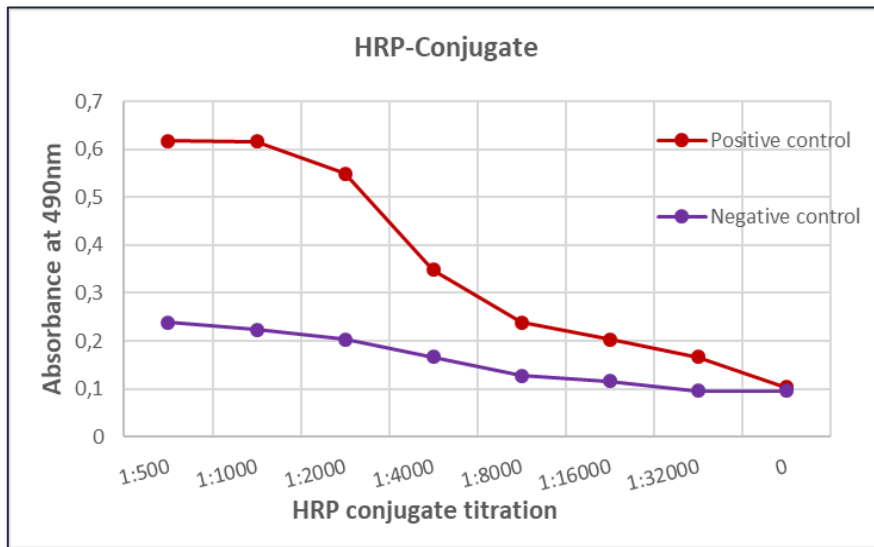


Figure 4.7 D: Optimization of the Peptide ELISA working conditions.

Absorbance results obtained at 490 nm for the positive and the negative control samples plotted on the Y-axis against different HRP-conjugated detection antibody titrations plotted on the X-axis. The optimal dilution for the HRP-conjugated anti-human IgG antibody was chosen to be 1:2000 since it produced low background binding.

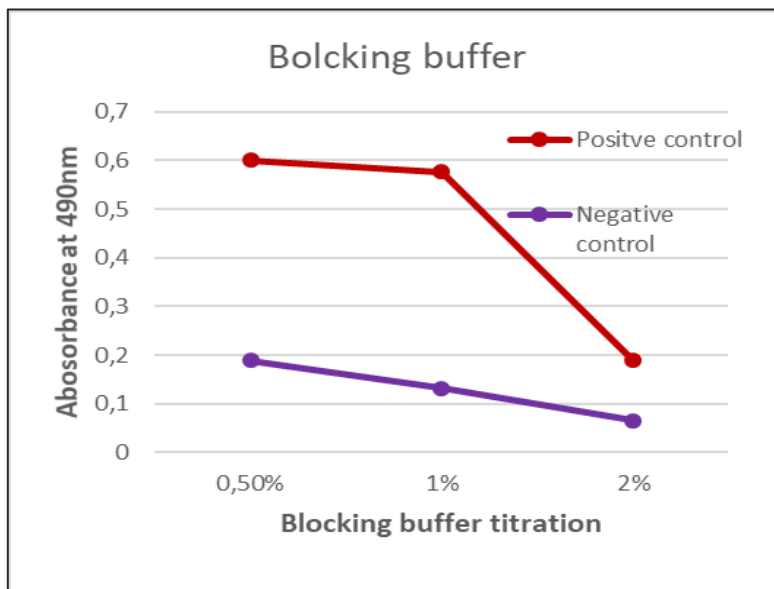


Figure 4.7 E: Optimization of the Peptide ELISA working conditions.

Absorbance results obtained at 490 nm for the positive and negative control samples plotted on the Y-axis against different blocking buffer titrations plotted on the X-axis. Blocking with 1% BSA protein reduced background noise while still allowing antibodies to bind. Thus, a 1% BSA concentration was chosen for preparing a blocking buffer.

Peptide ELISA assay validation: The intra-assay and inter-assay precision calculations for the developed Peptide ELISA assay are presented in **Table 4.9**, calculations included in **Supplementary data 11**. The developed Peptide ELISA assay showed reproducibility and consistency for the positive control and negative control. The inter-assay coefficient of variation of 5.93% indicated that our assay is validated to be used in epitope mapping studies.

Table 4.9: Shows the precision results for anti-ADAMTS13 IgG antibody in Peptide ELISA assay

| Statistic(s) | Intra-assay precision results | |
|---|-------------------------------|-----------------|
| | Positive sample | Negative sample |
| Mean (M) | 0.521 | 0.139 |
| Standard deviation (SD) | 0.03 | 0.01 |
| % Coefficient of variation (CV) = (SD/M)*100% | 5.77% | 6.09% |
| <i>Inter-assay CV = (Positive CV + Negative CV)/2</i> | 5.93% | |

Cut- off value determined from the OD₄₉₀ values of the negative control: The cut-off value for the ELISA system was determined with the mean absorbance of a negative control plus 2 standard deviations (SDs), as described by Kumar & Rao (1991). Calculations are included in **Supplementary data 11**. Samples with OD value at 490 nm higher than the cut-off value of 0.21 were considered as positive and samples with the OD value at 490 nm less than the cut-off value were considered as negative.

The calculation was as follow:

$$\text{Mean value plus 2 (SDs) = } 0.15 + 0.057 = 0.21.$$

Epitope-mapping studies were performed on an ADAMTS13 peptide library consisting of 105 overlapping biotinylated peptides from the proximal domains of ADAMTS13, and the results are presented in the next section.

4.5.2.3. Binding of purified IgG antibodies to linear overlapping peptides of ADAMTS13 using Peptide ELISA


The mean OD₄₉₀ of two blank wells was subtracted from each OD₄₉₀ value of each sample. Samples with OD₄₉₀ value more than the cut-off value were considered as positive and samples with the

OD₄₉₀ value less than the cut-off value were considered as negative. The cut-off value was calculated from the mean plus 2 standard deviations of the negative control sample. There was minor reactivity observed from some samples with bound IgG autoantibodies to peptides producing significantly low OD values and these binding interactions were considered non-specific. A summary of ADAMTS13 domains that reacted with IgG autoantibodies isolated from individual HIV-associated TTP and HIV positive patient plasma samples is presented in **Table 4.10.1**. The details of reactive peptides from all 4 ADAMTS13 domains selected and OD values obtained for each patient sample are presented in **Table 4.10** of *Supplementary data 12*.

Ninety-four (94%) of HIV-associated TTP patient plasma samples had IgG autoantibodies that bind to linear peptides of all 4 selected ADAMTS13 proximal domains. Forty-two (42%) of the plasma samples had IgG autoantibodies binding with the linear peptides of the ADAMTS13 Metalloprotease domain and 58% to both the Metalloprotease and the Disintegrin-like domains. None of the HIV-associated TTP patient samples had IgG autoantibodies that only reacted with the Disintegrin-like domain. However, 98% of HIV-associated TTP patient samples showed reactivity towards linear peptides from both the Cysteine-rich and Spacer domains. Only one sample showed IgG autoantibody reactivity towards the linear peptides of the Spacer domain and not the Cysteine-rich domain. Finally, 94% of HIV-associated TTP patient samples had IgG autoantibodies that bind to linear peptides of all 4 proximal domains of ADAMTS13 that were investigated (**Table 4.10.1**).

None of the 18 HIV positive control cohort samples had IgG autoantibodies against linear peptide of all 4 domains of ADAMTS13. The IgG autoantibodies with reactivity towards the Metalloprotease domain alone was present in 17% of these samples, and 83% of the samples contained IgG autoantibodies that reacted to both the Metalloprotease domain and the Disintegrin-like domains. No HIV positive control cohort sample had IgG autoantibodies that reacted to the Disintegrin-like domain alone. Thirty-nine (39%) of the HIV positive control cohort samples did not have IgG autoantibodies that bind to linear peptides of the Cysteine-rich and Spacer domains. Twenty-eight (28%) of the HIV positive control samples had IgG autoantibodies that bind the Cysteine-rich domain only, and 33% showed reactivity towards linear peptides of the Spacer domain only. Only one HIV positive sample (HIV-68) had IgG autoantibodies that showed reactivity towards linear peptides of all 4 ADAMTS13 proximal domains investigated (**Table 4.10.1**).

Table 4.10.1: ADAMTS13 domains with reactivity towards IgG antibodies of individual HIV-associated TTP and HIV positive control patient plasma samples.

| ADAMTS13 domains | HIV-associated TTP group <i>n</i> =53 | HIV-positive group <i>n</i> =18 |
|--|--|------------------------------------|
| Metalloprotease domain only | 22/53 (42%) | 3/18 (17%) |
| Disintegrin-like domain only | 0/53 (0%) | 0/18 (0%) |
| Both Metalloprotease and Disintegrin-like domains together | 31/53 (58%) | 15/18 (83%) |
| Cysteine-rich domain only | 0/53 (0%) | 5/18 (28%) |
| Spacer domain only | 1/53 (2%) | 6/18 (33%) |
| Both Cysteine-rich and Spacer domains together | 52/53 (98%) | 0/18 (0%) |
| All four ADAMTS13 domains  | 31/53 (78%) | 1/18 (6%) |

n, number of samples.

The results from the epitope mapping studies will be presented in 2 sections namely: results for the Metalloprotease domain and Disintegrin-like domain in section 1 and the results of the Cysteine-rich and Spacer domain in section 2.

Section 1. Metalloprotease and Disintegrin-like domains binding events:

The IgG autoantibodies isolated from 53 HIV-associated TTP patient plasma samples and 18 HIV positive control plasma samples showed binding to various epitope regions of the Metalloprotease and the Disintegrin domains and, in some areas, even shared linear epitopes.

The IgG autoantibodies from both HIV-associated TTP patient and HIV-positive control cohort samples showed binding to linear peptides MP1, MP9 – MP10, and MP18 – MP21 of the Metalloprotease domain. Ninety-six (96%) of HIV-associated TTP patient samples had IgG autoantibodies binding to linear peptides MP37 to MP40 and only 1 HIV positive control cohort sample (HIV-60) had IgG autoantibodies that showed similar binding events. Both groups had IgG autoantibodies binding to various linear peptides of the Disintegrin-like domain of ADAMTS13. Forty-two (42%) of HIV-associated TTP patient samples and 17% of HIV positive control cohort samples had IgG autoantibodies which reacted to linear peptides of the Metalloprotease domain

only and not to the Disintegrin-like domain. Neither group had IgG autoantibodies that reacted only to linear peptides of the Disintegrin-like domain.

Five (5) different binding patterns of the IgG autoantibodies in HIV-associated TTP patient plasma samples were observed (represented by samples: TTP -1, -6, -9, -18, and -33 in **Figure 4.8**) and 3 different binding patterns of IgG autoantibodies in the HIV-positive control cohort samples were observed (represented by samples: HIV -32, -98 and -60 in **Figure 4.9**). The absorbance readings at 490 nm obtained from IgG autoantibody binding to individual linear peptides are indicated on the Y-axes and individual linear peptides on the X-axes of the **Figures**. The peptide number in the **Figures** is representative of the peptide sequence on the full ADAMTS13 peptide library (**Appendix A**).

The IgG autoantibody-binding patterns in the HIV-associated TTP patient samples are presented in **Figure 4.8 A-E**.

A.

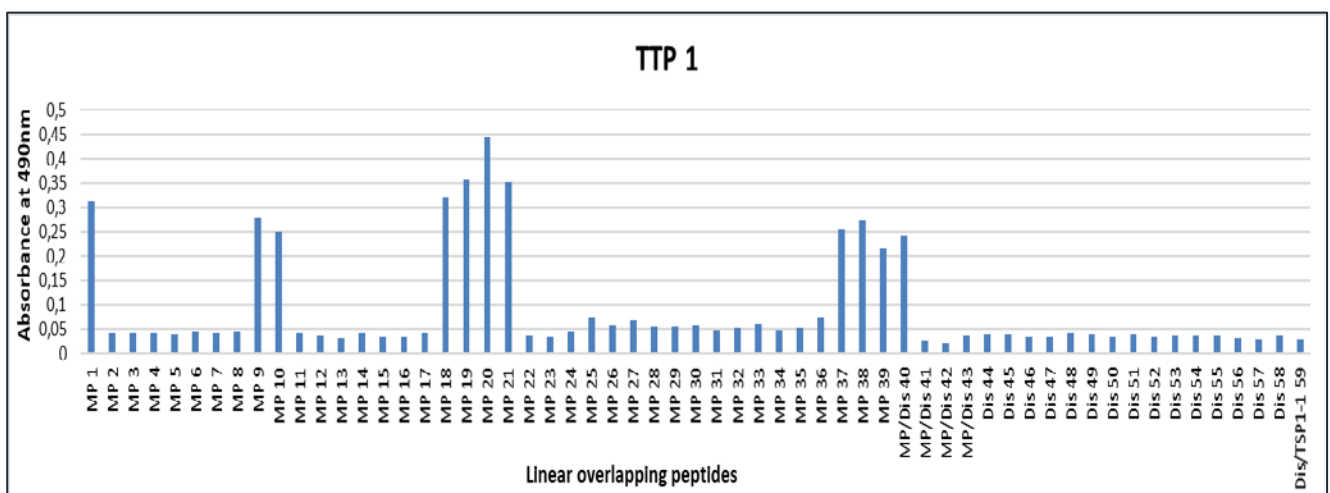


Figure 4.8 A: IgG autoantibody-binding patterns observed in individual HIV-associated TTP patient samples.

The Y-axis represents absorbance measured at 490 nm and the X-axis the individual linear peptides. The IgG autoantibodies from TTP patient samples 1 (TTP1) bound only to the Metalloprotease (MP) domain on linear peptide MP1, MP 9-10, MP18-21 and MP37-40. No IgG antibody binding was observed on linear peptides of the Disintegrin-like (Dis) domain. A similar binding pattern was observed from IgG autoantibodies of samples TTP-5, -8, -10, -11, -12, -14, -15, -16, -19, -22, -24, -25, -27, -29, -34, -38, -42, -48 and -72.

B.

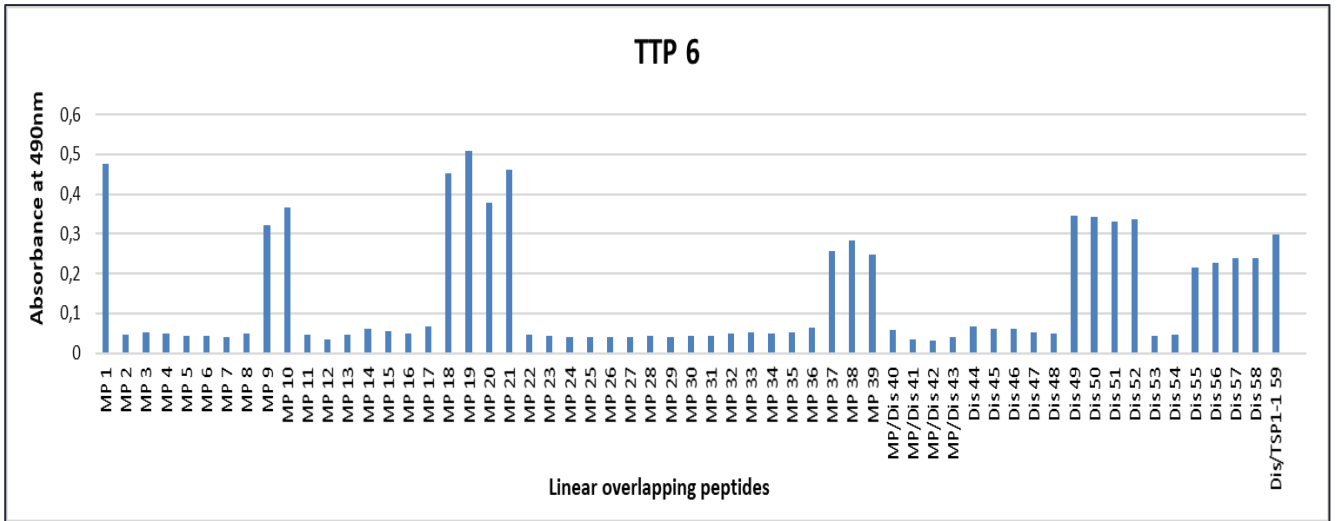


Figure 4.8 B: IgG autoantibody-binding patterns observed in individual HIV-associated TTP patient samples.

The Y-axis shows absorbance measured at 490 nm and the X-axis the individual linear peptides. The IgG autoantibodies from sample TTP-6 bound to linear peptides of both the MP and the Dis domains. The IgG autoantibodies had reactivity towards the same linear epitopes as observed in **Figure 4.8 A**. However, the IgG autoantibodies also recognized linear peptides towards the distal part of the Dis domain. A similar binding pattern was observed from IgG autoantibodies of samples TTP-13, -21, -28, -39, -40, -45, -55, -57, -58, -59, -64, -66 and -69.

C.

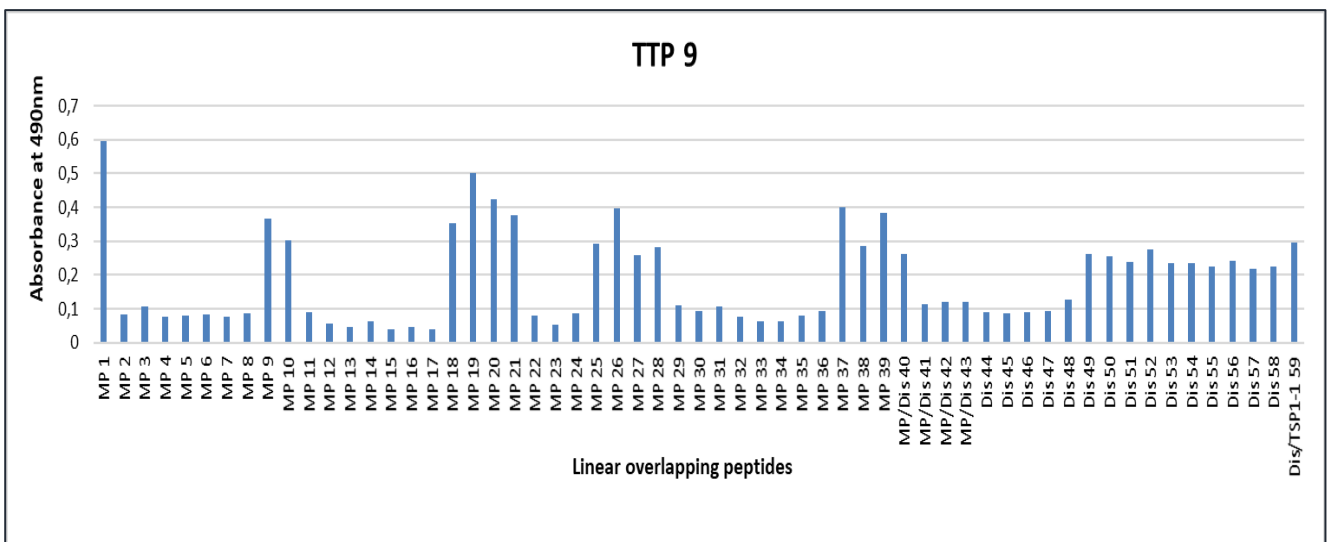


Figure 4.8 C: IgG autoantibody-binding patterns observed from individual HIV-associated TTP patient samples.

The Y-axis shows absorbance measured at 490 nm and the X-axis the individual linear peptides. The IgG autoantibodies from sample TTP-9 showed reactivity to various linear peptides of both the MP and the Dis domains suggesting the presence of multiple epitopes. Similar binding patterns were found in samples: TTP-20, -23, -49 and -71.

D.

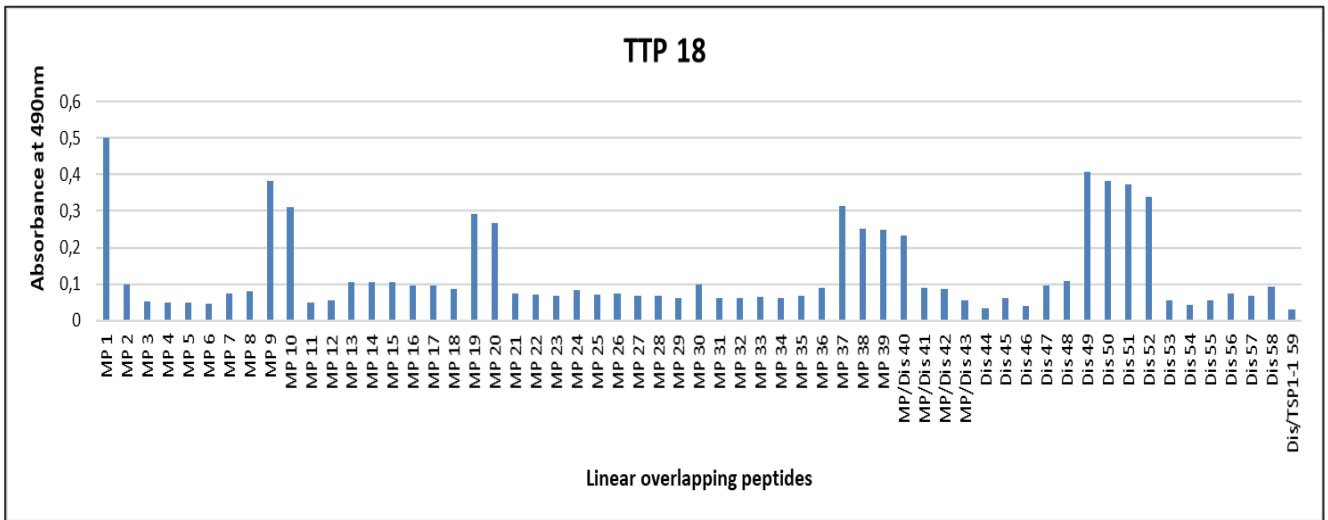


Figure 4.8 D: IgG autoantibody-binding patterns observed from individual HIV-associated TTP patient samples.

The Y-axis shows absorbance measured at 490 nm and the X-axis the individual linear peptides. The HIV associated TTP sample TTP-18 showed multiple binding sites to the MP and the Dis domains, but a different binding pattern to the one observed from sample TTP-9. HIV-associated TTP samples TTP-28 and TTP-39 had IgG autoantibodies with similar binding patterns to linear peptides of the MP and the Dis domains.

E.

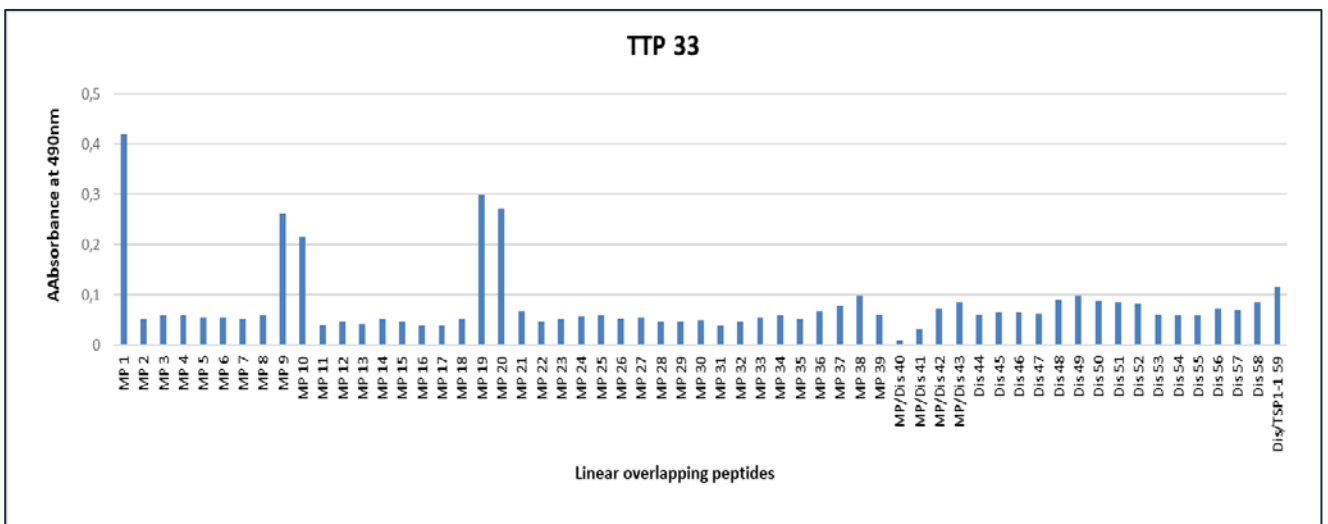


Figure 4.8 E: IgG autoantibody-binding patterns observed from individual HIV-associated TTP samples.

The Y-axis shows absorbance measured at 490 nm and the X-axis the individual linear peptides. HIV-associated TTP samples TTP-33 and -50 had IgG autoantibodies reacting with linear peptides of the MP domain only (MP1, MP9-10 and MP19-20). The IgG of these samples had fewer epitope reactions on the MP-domain vs. other IgG antibodies from other HIV-associated TTP patients. No antibody binding was observed on linear peptides of the Dis domain.

The IgG autoantibody-binding patterns of individual HIV positive control cohort samples are presented in **Figure 4.10 A-C**.

A.

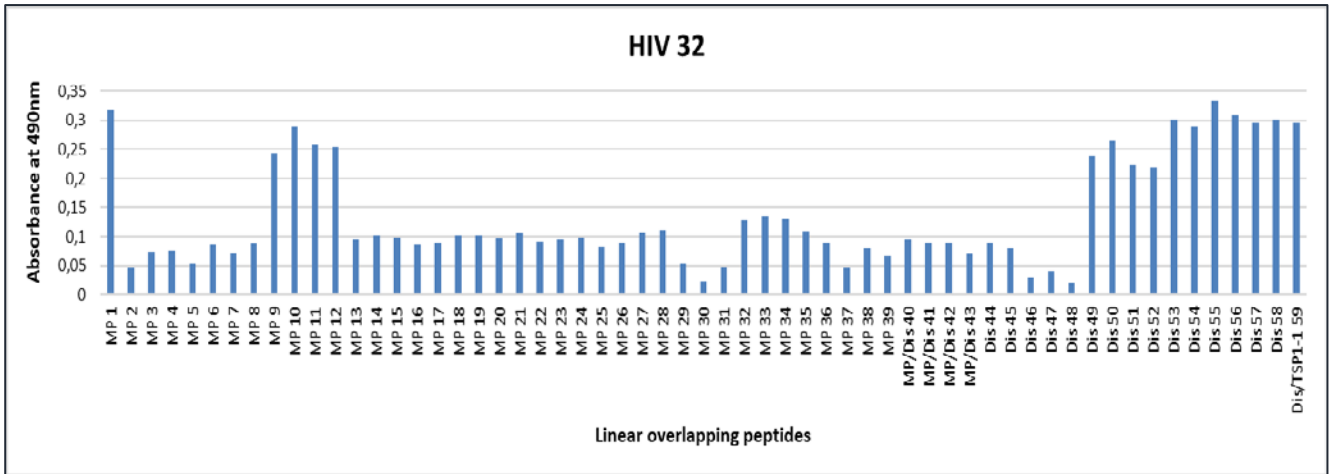


Figure 4.9 A: IgG autoantibody-binding patterns from individual HIV positive control cohort samples.

The Y-axis shows absorbance measured at 490 nm and the X-axis the individual linear peptides. The IgG autoantibodies from sample HIV-32 showed binding to the proximal part of the MP domain (linear peptide MP1 and MP9-10) and the distal part of the Dis domain (Dis49-Dis/TSP1-1 59). The IgG autoantibodies from samples HIV-3, -130, -156, -161, -108, -43 showed a similar binding pattern.

B.

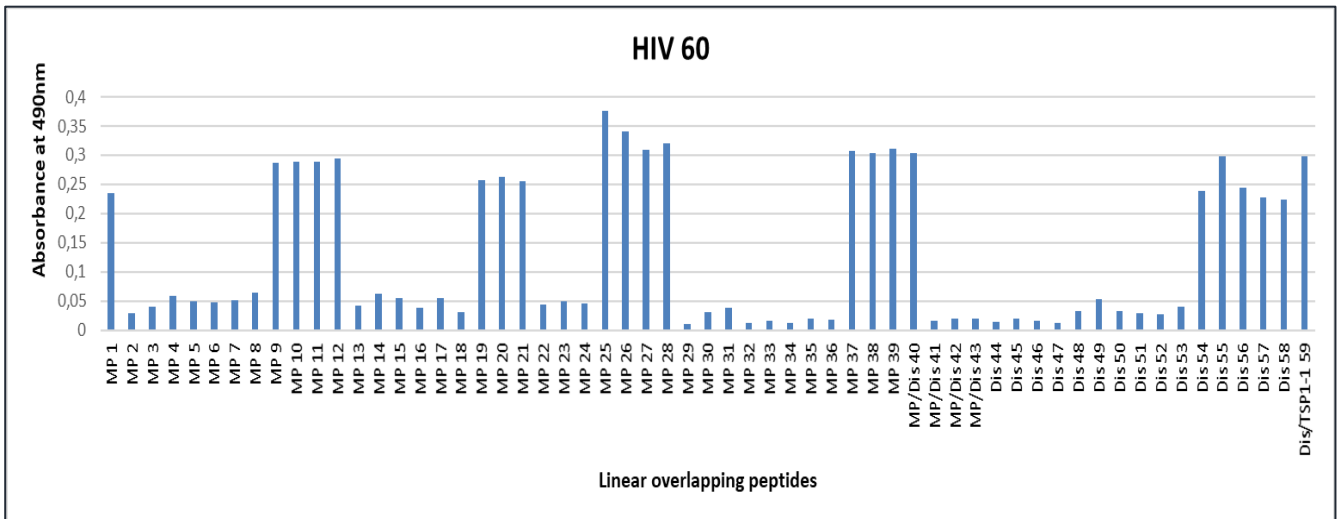


Figure 4.9 B: IgG autoantibody-binding patterns from individual HIV positive control cohort samples.

The Y-axis shows absorbance measured at 490 nm and the X-axis the individual linear peptides. IgG autoantibodies from sample HIV-60 showed binding to various linear peptides of the MP domain and the Dis domain. IgG autoantibodies isolated from the HIV-control sample 60 had almost similar binding patterns to the IgG autoantibodies from the HIV-associated TTP patient samples (**Figure 4.9 C**). The IgG autoantibodies from sample HIV-137, -164, -46, -163, -94, -106 and -68 also showed a similar binding pattern.

C.

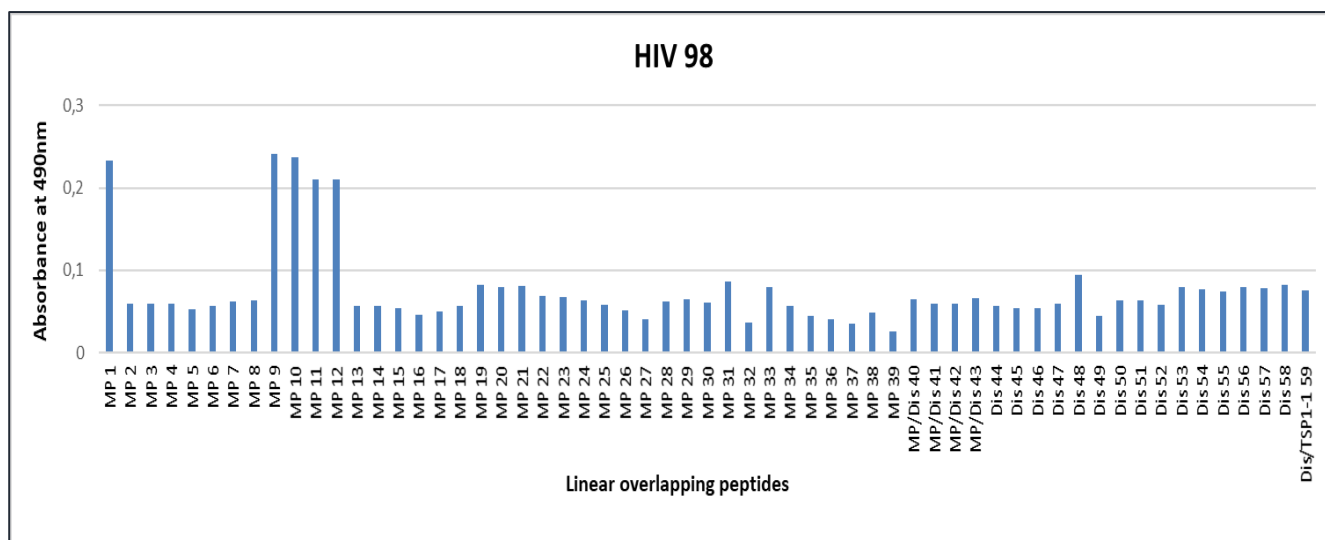


Figure 4.9 C: IgG autoantibody-binding patterns from individual HIV positive control cohort samples.

The Y-axis shows absorbance measured at 490 nm and the X-axis the individual linear peptides. The IgG autoantibodies from sample HIV-98 showed positive binding to linear peptides from only the proximal part of the MP domain and no IgG binding was detected to the Dis domain. The IgG autoantibodies from samples HIV-122 and -165 showed a similar binding pattern.

Prediction of potential antibody epitopes

Different IgG autoantibody-binding patterns were observed and potential epitope regions were identified using mapping analysis with overlapping linear peptides of the ADAMTS13 MP and Dis domains. A list of linear peptides from these domains with potential antigenic regions identified by mapping studies is presented in **Table 4.11** with raw data in **Supplementary data 13**.

Table 4.11: Linear peptides with potential antigenic regions in the Metalloprotease (MP) and Disintegrin (Dis)-like domains.

| Peptide | Peptide sequence | Position | HIV-associated TTP patient group (n=53) | HIV positive control cohort (n=18) |
|-------------------|---|-----------|---|------------------------------------|
| MP1 | AAGGILHLELLVAVGPDVFQ | 75 – 94 | 53/53(100%) | 18/18(100%) |
| MP1-MP8 | LHLELLVAVGPDVFQAHQEDTERYVLTNLNIGAE LLR DPSLGAQFRVHLV | 80 - 129 | 0/53 | 2/18(11%) |
| MP9-MP10 | LRDPSLGAQFRVHLV KM VILTEPEG | 115 – 139 | 53/53(100%) | 15/18(83%) |
| MP9-MP12 | LRDPSLGAQFRVHLV KM VILTEPEGAPNITANLTS | 125 – 149 | 0/53 | 3/18(17%) |
| MP18-MP21 | TINPED DTDP GHADLVLYITRF DLELPDGN RQVRG | 160 – 194 | 15/53(28%) | 0/18 |
| MP19-MP20 | DDTDP GHADLVLYITRF DLELPDGN | 165 – 189 | 37/53(70%) | 0/18 |
| MP19-MP21 | DDTDP GHADLVLYITRF DLELPDGNRQVRG | 165 – 194 | 4/53(8%) | 5/18(28%) |
| MP25-MP28 | VTQLGGACSP TWSCLIT EDTGFDLGGVTIAHEIGHS | 195 – 229 | 10/53(19%) | 10/18(56%) |
| MP29-MP34 | GFDLGV TIAHEIGHSF GLEHDGAPGSGCGPSGHV MAS DGAAPRAG | 215 – 249 | 0/53 | 2/18(11%) |
| MP33-MP36 | DGAPGSGCGPSGHV MASDGA APRAGLAWSPCSR RQ | 235 – 269 | 3/53(6%) | 2/18(11%) |
| MP37-MP39 | APRAGLAWSPCSR RQLLS LLSAGRARCVWD | 255 – 284 | 26/53(49%) | 0/18 |
| MP37-MP/Dis40 | APRAGLAWSPCSR RQLLS LLSAGRARCVWDPPRPQ | 255 – 289 | 25/53(47%) | 1/18(6%) |
| MP40-MP/Dis44 | LLSLLSAGRARCVWDPPRPQGSAGHPPDAQ PGLY YSANE | 270 – 304 | 0/53 | 1/18(6%) |
| MP/Dis41-Dis44 | SAGRARCVWDPPRPQGSAGHPPDAQ PGLY YSANE | 275 – 309 | 0/53 | 1/18(6%) |
| MP/Dis43-Dis46 | PPRPQGSAGHPPDAQ PGLY YSANEQCRVAFGPKA | 285 – 319 | 1/53(2%) | 0/18 |
| Dis44-Dis47 | PGSAGHPPDAQ PGLY YSANEQCRVAFGPKAVACTF | 290 – 324 | 2/53(4%) | 0/18 |
| Dis45-Dis48 | HPPDAQ PGLY YSANEQCRVAFGPKAVACTFAREHL | 295 - 334 | 1/53(2%) | 0/18 |
| Dis49-Dis52 | FGPKAVACTFAREH LDMCQALSCHTD PLDQSSCSR | 315 – 349 | 4/53(7%) | 0/18 |
| Dis49-Dis/TSP1 59 | FGPKAVACTFAREH LDMCQALSCHTD PLDQSSCSR LLVPLDGT ECCGVEK WCSKGR CRSLVELT PIAAVH | 315 - 383 | 5/53(9%) | 6/18(33%) |
| Dis53-Dis58 | LSCHTDPLDQSSCSRLLVPLDGT ECCGVEK WCSKGR CRSLVELT RCRSLVELTP | 335 – 379 | 5/53(9%) | 1/18(6%) |
| Dis53-Dis/TSP1 59 | LSCHTDPLDQSSCSRLLVPLDGT ECCGVEK WCSKGR CRSLVELT RCRSLVELTPIAAVH | 335 – 383 | 5/53(9%) | 3/18(17%) |
| Dis55-Dis/TSP1 59 | S SCSR LLVPLDGT ECCGVEK WCSKGR CRSLVELT IAAVH | 345 – 383 | 2/53(4%) | 1/18(6%) |
| Dis56-Dis/TSP1 59 | LLVPLDGT ECCGVEK WCSKGR CRSLVELT PIAAVH | 350 - 383 | 2/53(4%) | 0/18 |
| Dis57-Dis/TSP1 59 | LDGT ECCGVEK WCSKGR CRSLVELT PIAAVH | 355 – 383 | 1/53(2%) | 0/18 |
| Dis58-Dis/TSP1 59 | CGVEK WCSKGR CRSLVELTPIAAVH | 360 – 383 | 2/53(4%) | 0/18 |
| Dis/TSP1 59 | WCSKGR CRSLVELT PIAAVH | 365 - 383 | 11/53(21%) | 0/18 |

Amino acid residues in the overlapping regions of antigenic peptides in red. Peptide names are derived from the relevant domain names and amino acid position relative to the coding region of full-length ADAMTS13 protein. n, number of samples.

Section 2: Binding events to the Cysteine-rich domain and the Spacer domain:

The IgG autoantibodies from samples of both HIV-associated TTP patients and HIV-positive control cohort samples showed similar binding patterns towards the linear peptides of the Cysteine-rich and the Spacer domains.

HIV-associated TTP plasma samples had IgG autoantibodies that reacted to specific peptides of the Cysteine-rich and the Spacer domains. Eighty-seven (87%) of samples from the HIV-associated TTP patients had IgG autoantibodies that bind linear peptides Cys1-10, and 79% of samples had IgG autoantibodies that bind to Cys13-20 of the Cysteine-rich domain. Furthermore, 77% of all plasma samples had IgG autoantibodies that bind to linear peptides Spa24 to Spa40 of the Spacer domain.

All (100%) HIV-associated TTP patient plasma samples had IgG autoantibodies binding linear peptides Spa42-Spa/TSP1-2 46 of the Spacer domain, while only 11% of HIV positive control cohort samples had IgG autoantibodies with similar binding patterns.

The IgG autoantibodies from sample TTP-72 (representing 2% of the HIV-TTP patient samples), and 22% of the HIV positive control cohort samples (HIV-46, -60, -163, -164, -165, and -98) reacted with linear peptides from the Spacer domain only.

Twenty-eight percent (28%) of the samples in the HIV positive control cohort (HIV-32, -122, -137, -106 and -68) had IgG autoantibodies that showed binding to linear peptides Cys1-10 from the Cysteine-rich domain only.

Thirty-nine (39%) of the HIV positive control cohort samples (HIV-33, -130, -156, -161, -94, -108 and -43) did not have IgG autoantibodies binding to linear peptides from the Cysteine-rich or Spacer domains.

The 4 IgG autoantibody-binding patterns from the HIV-associated TTP patient group were detected and are represented by samples TTP-66, -16, -14 and -72 with only 1 IgG autoantibody binding pattern in the HIV control cohort detected in sample HIV- 32 (**Figure 4.10 A – E**).

A.

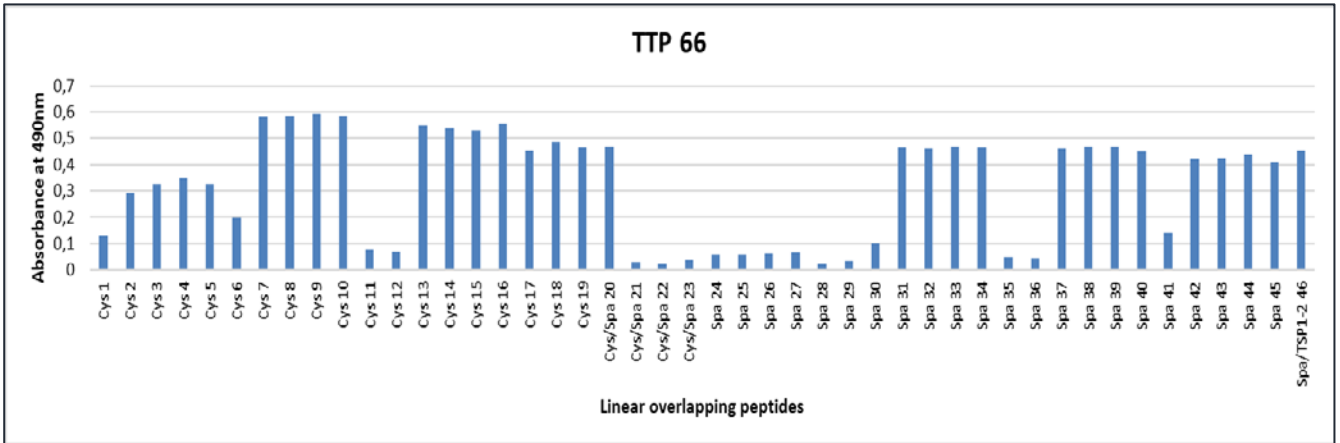


Figure 4.10 A: IgG autoantibody-binding patterns from individual HIV-associated TTP patient samples.

The Y-axis shows absorbance measured at 490 nm and the X-axis the individual linear peptides. The IgG autoantibodies from sample TTP-66 reacted with various linear overlapping peptides of the Cys and the Spacer domains suggesting the presence of multiple epitopes. Sample TTP-9, -20, -31, -49, -55, -57, -64, -67, -69 and -71 also showed similar binding pattern.

B.

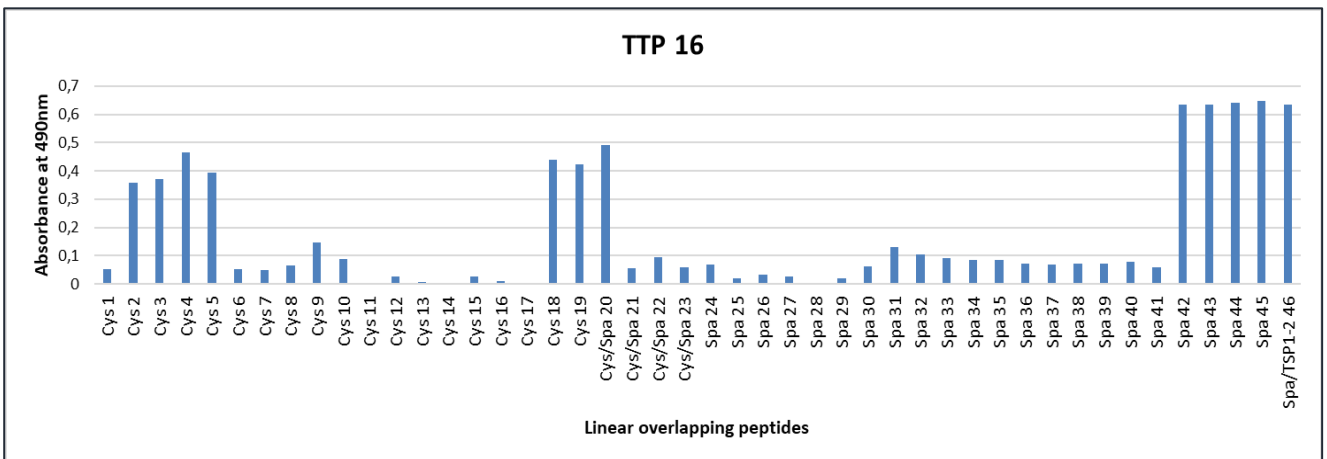


Figure 4.10 B: IgG autoantibody-binding patterns from individual HIV-associated TTP patient samples.

The Y-axis shows absorbance measured at 490 nm and the X-axis the individual linear peptides. The IgG autoantibodies from sample TTP-16 showed strong binding to linear peptides Spa42-46 at the distal part of the Spacer domain. The linear peptides Cys2-5 and Cys18-Cys/Spa20 also showed reactivity to IgG autoantibodies. Samples TTP-17 and _19, showed similar binding patterns.

C.

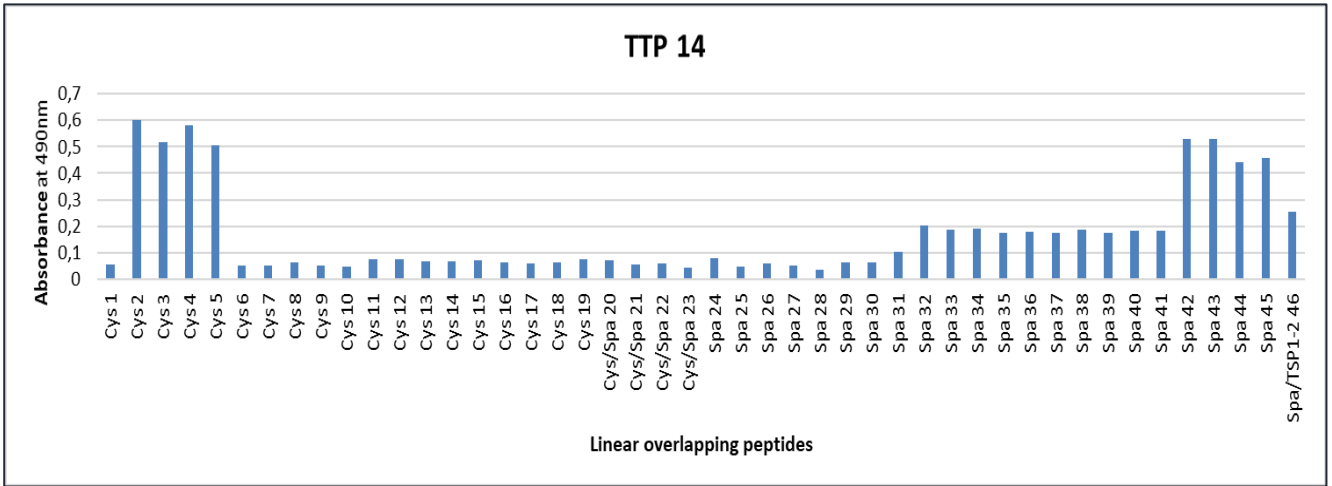


Figure 4.10 C: IgG autoantibody-binding patterns from individual HIV-associated TTP patient samples.

The Y-axis shows absorbance measured at 490 nm and the X-axis the individual linear peptides. The IgG autoantibodies from sample TTP-14 showed reactivity to linear peptides at the proximal part of the Cys domain and linear peptides at the distal part of the Spacer domain. There was minor reactivity observed with some peptides of the Spacer domain with bound IgG autoantibodies to peptides producing low OD values, which were considered to be non-specific. HIV-associated TTP samples TTP-1, -6, -13, -15, -21 and -22 had similar antibody-binding patterns.

D.

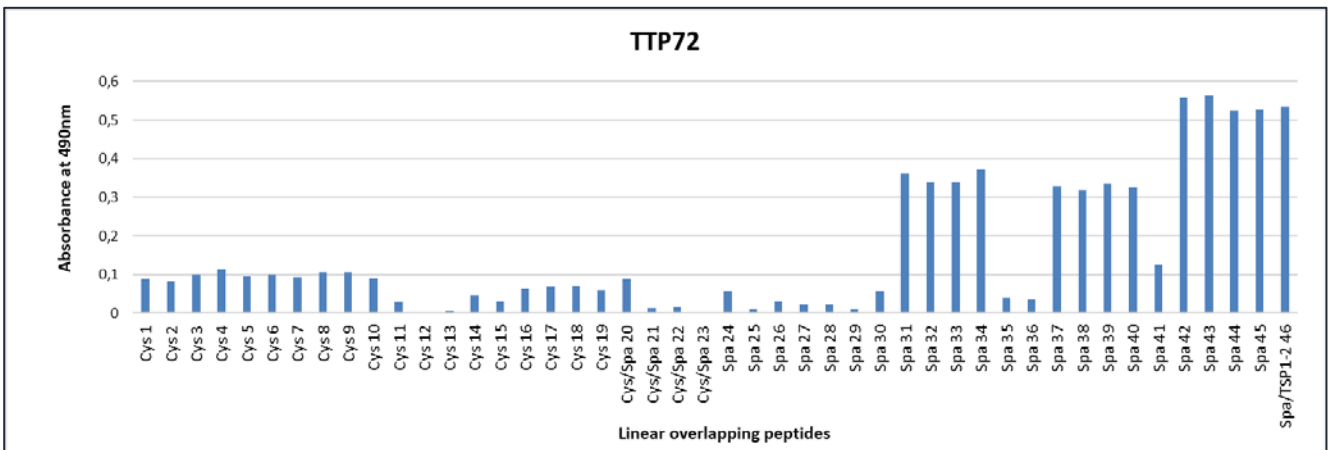


Figure 4.10 D: IgG autoantibody-binding patterns from individual HIV-associated TTP patient samples.

The Y-axis shows absorbance measured at 490 nm and the X-axis the individual linear peptides. Sample TTP-72 had IgG autoantibodies reacting to linear peptides of the Spacer domain only. No IgG autoantibody reactivity was observed with linear peptides of the Cys domain. HIV positive samples HIV-46, -60, -163, -164, -165 and -94 showed similar binding patterns.

E.

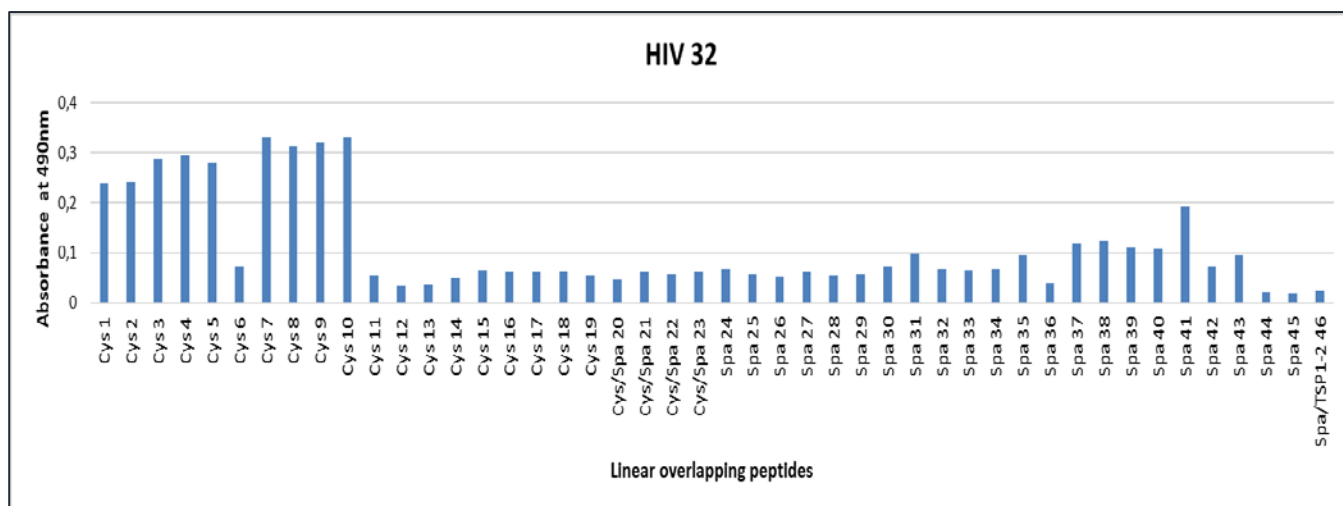


Figure 4.10 E: IgG autoantibody-binding patterns from individual HIV positive control cohort samples.

The Y-axis shows absorbance measured at 490 nm and the X-axis the individual linear peptides. IgG autoantibodies from HIV-32 had a positive reaction to linear peptides of the Cys domain only. No IgG autoantibody binding to the Spacer domain was detected. HIV positive control cohort samples HIV-122, -137, -106 and -68 showed a similar binding pattern.

Predicting potential antibody epitopes

Potential epitope regions were identified using mapping analysis after different IgG autoantibody binding patterns were observed in both groups. Overlapping linear peptides of the ADAMTS13 Cysteine-rich and Spacer domains that bind IgG autoantibodies were used to map potential antigenic amino acid residues. A list of linear peptides from these domains with potential antigenic regions identified by the Peptide ELISA assay is presented in **Table 4.12**. The raw data of mapping studies for potential epitope residues determined from reactive peptide amino acid sequences are presented in **Supplementary data 13**.

Table 4.12: Linear peptides with potential antigenic regions detected from the Cysteine-rich (Cys) and Spacer (Spa) domains.

| Peptide Name | Peptide sequence | Position | HIV-associated TTP group n=53 | HIV positive group n=18 |
|-------------------|--|-----------|-------------------------------|-------------------------|
| Cys1 - Cys4 | KTQLEFMSQQCARTDGQPLRSSPGGASFYHWGAAV | 440 - 474 | 2/53 (4%) | 0/18 |
| Cys3 - Cys6 | CARTDGQPLRSSPGGASFYHWGAAVPHSQGGDALCR | 450 - 484 | 8/53 (15%) | 0/18 |
| Cys2 - Cys5 | FMSQQCARTDGQPLRSSPGGASFYHWGAAVPHSQG | 445 - 479 | 23/53 (43%) | 0/18 |
| Cys3 - Cys5 | CARTDGQPLRSSPGGASFYHWGAAVPHSQG | 450 - 479 | 6/53 (11%) | 0/18 |
| Cys3 - Cys10 | CARTDGQPLRSSPGGASFYHWGAAVPHSQGDALCR HMCRAIGESFIMKRGHMCRAIGESFIMKRGDSFLD | 450 - 504 | 4/53 (8%) | 1/18 (6%) |
| Cys7 - Cys10 | WGAAVPHSQGDALCRHMCRAIGESFDALCRHMCR AIGESFIMKRGDSFLD | 470 - 504 | 11/53 (21%) | 4/18 (22%) |
| Cys13 - Cys16 | DSFLDGTTRCMPSPREDGTLSLCVSGSCRTFGCDG | 500 – 534 | 7/53 (13%) | 0/18 |
| Cys17 - Cys/Spa20 | SLCVSGSCRTFGCDGRMDSQQVWDRFCQVCGGGDNST | 520 – 554 | 29/53 (55%) | 0/18 |
| Cys18 - Cys/Spa20 | GSCRTFGCDGRMDSQQVWDRFCVCGGGDNST | 525 – 554 | 1/53 (2%) | 0/18 |
| Cys13 - Cys/Spa20 | DSFLDGTTRCMPSPREDGTLSLCVSGSCRTFGCDG RMDSQQVWDRFCVCGGGDNST | 500 - 554 | 5/53 (9%) | 0/18 |
| Spa24 - Spa 28 | CSPRKSFTAGRAREYVTLTVPNLTSVYIANHRPLFTH | 555 – 594 | 1/53 (2%) | 0/18 |
| Spa31 - Spa 34 | PLFTHLAVRIGGRYVAGKMSISPNTTYPSSLLEDG | 590 – 624 | 40/53 (75%) | 1/18 (6%) |
| Spa31 - Spa39 | PLFTHLAVRIGGRYVAGKMSISPNTTYPSSLLEDGRVEYR VALTEDRLPRLEEIRIWGPL | 590 – 649 | 2/53 (4%) | 0/18 |
| Spa37 - Spa40 | LLEDGRVEYRVALTEDRLPRLEEIRIWGPLQEDAD | 620 – 654 | 27/53 (51%) | 4/18 (22%) |
| Spa42-Spa/TSP2 46 | IWGPLQEDADIQVYRRYGEYGNLTRPDITFTYFQPKPRQ | 645 – 684 | 53/53(100%) | 2/18(22%) |

Amino acid residues in the overlapping regions of antigenic peptides are highlighted in red. Peptide names are derived from the relevant domain names and the relevant amino acid position relative to the coding region of full-length ADAMTS13 protein.

n, number of samples.

Summary of epitope mapping results

The ADAMTS13 Metalloprotease, Disintegrin-likes, Cysteine-rich and Spacer domains were the primary targets for antibody binding in HIV-associated TTP patient samples, while the Metalloprotease and Disintegrin-like domains the primary targets for antibody binding in the HIV positive control cohort plasma samples. Immunoglobulin IgG autoantibody binding results and the shared and non-shared linear ADAMTS13 peptide epitopes for each domain in both the HIV-associated TTP patient and the HIV positive control cohorts are summarized in **Figure 4.11** and **Table 4.13** respectively.

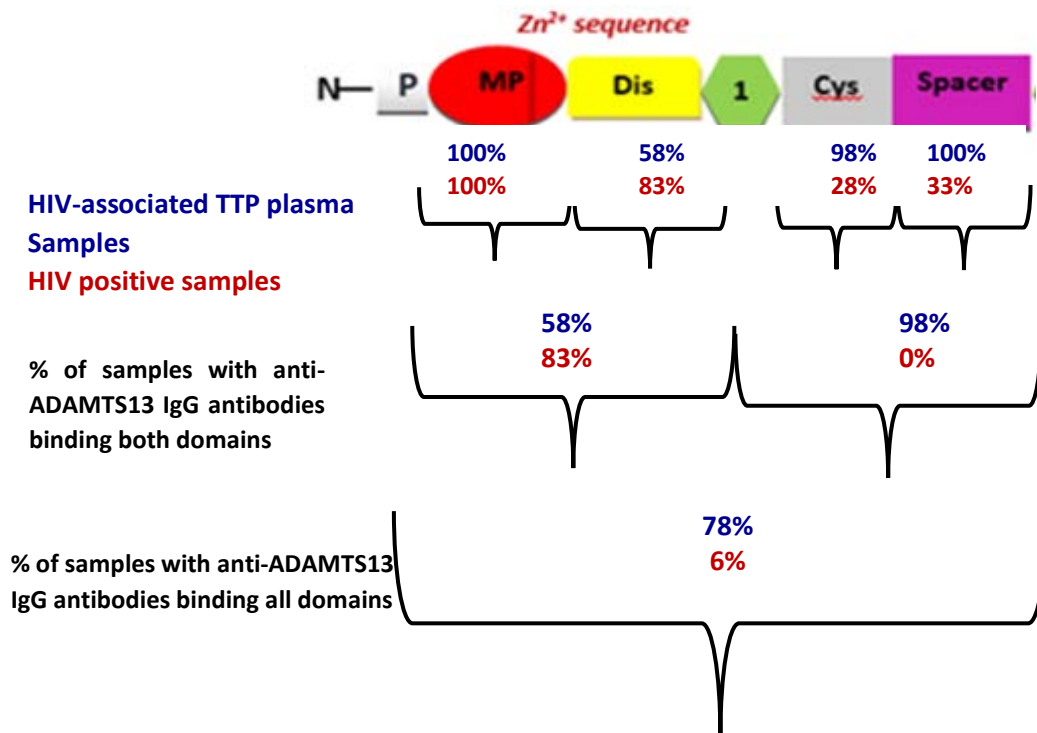


Figure 4.11: Anti-ADAMTS13 IgG antibody proximal domain binding sites.

The number of samples with antibodies binding each domain is shown in **blue** for the HIV-associated TTP patient group and in **red** for the HIV positive control cohort. This study found that the ADAMTS13 Metalloprotease, Disintegrin-like Cysteine-rich and Spacer domains were the primary targets for antibody binding in HIV-associated TTP patient plasma samples, while the Metalloprotease and Disintegrin-like domains were the primary targets for antibody binding in HIV positive control cohort samples.

N, N-terminal side; P, propeptide; MP, Metalloprotease domain; Dis, Disintegrin-like domain; TSP1-1, Thrombospondin motif 1; Cys, Cysteine-rich domain; Spacer, Spacer domain.

Table 4.13: Shared and non-shared linear ADAMTS13 peptide epitope regions binding IgG autoantibodies isolated from HIV-associated TTP patient and HIV positive control cohort samples.

| Binding domains | Metalloprotease domain aa epitope regions | Disintegrin-like domain aa epitope regions | Cysteine-rich domain aa epitope regions | Spacer domain aa epitope regions |
|----------------------------|---|--|---|----------------------------------|
| Shared epitope regions | 75 – 80 | 169 – 189 | 445 – 479 | 595 – 619 |
| | 125 – 139 | 320 – 345 | 455 – 469 | 625 – 649 |
| | 200 – 224 | 350 – 379 | 475 - 504 | 650 - 669 |
| | 260 – 284 | 340 - 379 | | |
| Non-shared epitope regions | 80 – 124 | 275 – 304 | 505 – 529 | 560 - 586 |
| | 220 – 244 | 290 – 324 | 540 – 564 | |
| | 240 – 264 | 355 – 376 | | |
| | | 365 – 374 | | |

aa, amino acids.

Chapter 5: Discussion

Thrombotic thrombocytopenic purpura (TTP) that occurs secondary to HIV infection is currently the form of TTP observed most in the Sub-Saharan African population (Swart *et al.* 2019). ADAMTS13 protein plays a central role in the pathogenesis of acquired TTP and autoantibodies targeting this enzyme may be the primary cause of severe ADAMTS13 deficiency in HIV-associated TTP. Furthermore, several studies have confirmed the importance of measuring autoantibodies to ADAMTS13 during the management of patients with TTP (Alwan *et al.* 2017; Thomas *et al.* 2015; Scheiflinger *et al.* 2003; Tsai *et al.* 2000; Zheng *et al.* 2001; Furlan *et al.* 1997). However, the ADAMTS13 autoantibody status in HIV-associated TTP patients has not yet been fully investigated.

The objectives of this study were to investigate ADAMTS13 autoantibody status in HIV-associated TTP patients by comparing the immunological properties as well as isotype distribution of these auto-reactive immunoglobulins in plasma samples of HIV infected patients with TTP prior to the initiation of plasma therapy. The primary objective of this study was to utilise epitope-mapping analysis to elucidate the specific antigenic regions (epitopes) on ADAMTS13 domains targeted by anti-ADAMTS13 IgG autoantibodies in patients with HIV-associated TTP. A secondary objective of the study was to determine the binding specificities of ADAMTS13 IgG autoantibodies in HIV infected patients without TTP.

Fifty-nine (59) HIV-associated TTP patient plasma samples with severe ADAMTS13 activity of less than 10% were included in the study sample analysis. A finding of severe ADAMTS13 activity (<10%) is a laboratory parameter that differentiates TTP from other TMAs (Reese *et al.* 2013; Scully *et al.* 2008; Peyvandi *et al.* 2008). The plasma samples were collected before the start of plasma therapy in patients presenting with the first episode of acute HIV-associated TTP. A hundred (100) HIV positive plasma samples were included as a control group.

ADAMTS13 antigen and activity levels in the HIV-associated TTP patient samples as well as in the HIV positive patient control cohort without TTP were measured with the validated commercially available Technozyme® ADAMTS13 ELISA kit (Technoclone®, Austria). This assay has utility in the diagnosis of TTP since it offers precision at low ADAMTS13 activity levels and it uses fluorescence detection (Crist and Rodgers, 2009). Important to note is that this ELISA kit detects free as well as antibody-bound ADAMTS13 and measures both ADAMTS13 antigen and the activity levels. The comparison between ADAMTS13 antigen and activity levels may provide insight into the inhibitory effects on ADAMTS13 autoantibodies.

A statistically significant difference ($p < 0.05$) was observed between the ADAMTS13 antigen and activity levels in HIV-associated TTP patient samples and HIV positive control cohort samples. The HIV-associated TTP patient samples had significantly reduced ADAMTS13 antigen and especially activity levels compared to the HIV positive control group. The ADAMTS13 antigen and activity levels observed in the HIV-associated TTP patient group also correlated with those documented in previous studies by Meiring *et al.* (2012) and Gunther *et al.* (2007). Multiple contributing pathophysiological factors are suggested for the reduced ADAMTS13 antigen and activity levels in HIV-associated TTP patients (**Figure 2.14**), including autoantibodies to ADAMTS13. However, not all patients with HIV-associated TTP present with a severe deficiency of ADAMTS13 activity (Gunther *et al.* 2007). Previous studies have demonstrated that patients with severe decreased ADAMTS13 antigen and activity levels have a higher risk of TTP relapses (Peyvandi *et al.* 2008; Ferrari *et al.* 2007). ADAMTS13 antigen and activity levels thus have utility in predicting relapses of HIV-associated TTP.

Fifteen, 15 (15%) of the 100 HIV positive cohort plasma samples had slightly reduced ADAMTS13 levels ranging from 25 to 50% (normal range is from 50-150%). It is suggested that the synthesis of metalloproteases, such as ADAMTS13 protein, is decreased in HIV positive patients (Kaiser *et al.* 2006). HIV infection causes micronutrient deficiencies (Irlam *et al.* 2013; Semba and Tang, 1999) of Zinc (Zn^{2+}) and Calcium (Ca^{2+}) which are essential micronutrients for ADAMTS13 enzymatic function (Crawley *et al.* 2011; Semba and Tang, 1999; Irlam *et al.* 2013). Therefore, slightly reduced ADAMTS13 activities are expected in HIV positive patients, as previously reported by Gunther *et al.* (2007) and Meiring *et al.* (2012). Reduced ADAMTS13 antigen and activity levels have pathophysiological relevance in acquired TTP (Rieger *et al.* 2006).

ADAMTS13 antibody-mediated inhibition, predominantly of the IgG isotype, has been reported in the majority of HIV-associated TTP patients with severe deficiencies of this protease (Alwan *et al.* 2017; Thomas *et al.* 2015; Scheiflinger *et al.* 2003; Tsai *et al.* 2000; Reese *et al.* 2013; Scully *et al.* 2008; Peyvandi *et al.* 2008). Autoantibody responses in HIV-associated TTP patients were assessed by measuring the concentration and inhibitory potential of anti-ADAMTS13 IgG antibodies. The IgM and IgA isotype distribution in HIV-associated patient and control cohort were also determined.

The anti-ADAMTS13 IgG concentration was measured in 59 patients with HIV-associated TTP and in 100 HIV infected control patients without TTP and found that 90% (53/59) of the HIV-associated TTP patient plasma samples had positive anti-ADAMTS13 IgG antibodies. Our findings correlate with reports in the literature regarding the frequency of autoantibodies in acquired TTP patients (Rieger *et al.* 2005; Tsai *et al.* 2006) suggesting that an immune-mediated activity against ADAMTS13 is

present in almost all patients presenting with HIV-associated TTP. A previous study by Alwan *et al.* (2017) also indicated that increased anti-ADAMTS13 IgG antibody titers are associated with poor prognosis in TTP patients. However, the frequency of anti-ADAMTS13 IgG antibodies detected in HIV-associated TTP patient samples differed from the results of Meiring *et al.* (2012) and Gunther *et al.* (2007), which detected autoantibodies in 50% of HIV-associated TTP patients. Interestingly, only 18% of the HIV positive patients without TTP and on antiretroviral therapy (ART) in the current study had anti-ADAMTS13 IgG antibodies, which again was different from the findings of Meiring *et al.* (2012) reporting anti-ADAMTS13 IgG antibodies in 50% of HIV positive patients without TTP in patients on ART.

We also compared ADAMTS13 levels with anti-ADAMTS13 autoantibody titers in both groups and found a negative correlation between the ADAMTS13 antigen levels and autoantibody titers in the HIV-associated TTP group. Patient plasma samples with high anti-ADAMTS13 IgG antibody titers had a low median antigen level of 4.5%, while those with low anti-ADAMTS13 IgG titers had a higher median ADAMTS13 antigen level of 12.5%. Previous studies by Alwan *et al.* (2019) and Thomas *et al.* (2015), also found that patients with markedly elevated anti-ADAMTS13 IgG antibody titers presented with significantly low ADAMTS13 antigen levels and it is suggested that patients with significantly reduced antigen levels might contain non-neutralizing (non-inhibitory) antibodies. It is further postulated that the inhibitory anti-ADAMTS13 IgG antibodies may not be the primary factor affecting ADAMTS13 activity in these patients and that autoantibodies may increase clearance of ADAMTS13 (Thomas *et al.* 2015). Our findings also confirm that non-neutralizing anti-ADAMTS13 IgGs are present in HIV-associated TTP patient plasma samples. Published studies support the suggestions that ADAMTS13 antigen depletion is another antibody-mediated mechanism involve in the pathogenesis of TTP *in vivo* (Scheiflinger *et al.* 2003 and Thomas *et al.* 2015). Studies by Hughes *et al.* (2009), Rieger *et al.* (2005), and Tsai *et al.* (2006) also showed that deficient ADAMTS13 antigen levels and high autoantibody titers in patients with acute TTP are associated with poor outcomes relating to cardiac and neurological events with resultant mortality.

Autoantibodies in HIV positive individuals might be due to the dysregulated immune system (Meiring *et al.* 2012). HIV infection increases autoimmunity, which results in compromised self-antigen recognition (Massabki *et al.* 1997). All the HIV-infected patients in the control arm of the current study was on ART and the current study could therefore not confirm this hypothesis. Also, no correlation was present between ADAMTS13 levels and anti-ADAMTS13 IgG titers in 17 of the 18 HIV positive cohort samples except in 1 sample (HIV-60) which contained slightly lower ADAMTS13 levels (~30%) together with a high anti-ADAMTS13 IgG antibody titer of 87 µg/ml. These results may

suggest that the presence of a high titer of anti-ADAMTS13 IgG antibodies might potentially be a contributing factor to reduced ADAMTS13 levels.

Although the ELISA based method is a more sensitive assay for the detection of total anti-ADAMTS13 IgG antibodies present in plasma, the Technozyme® ADAMTS13 IgG ELISA screens for the presence of both inhibitory and non-inhibitory antibodies indiscriminately and mixing studies were therefore performed to confirm the presence of inhibitory anti-ADAMTS13 IgG antibodies in HIV-associated TTP patients with ADAMTS13 activity <10%. Mixing studies are useful to screen for inhibitors without being as specific as the Bethesda assay. The Bethesda method has been utilised in studies to detect functional anti-ADAMTS13 IgG antibodies (Vendramin *et al.* 2018). Therefore, HIV-associated TTP plasma samples with inhibitors during 50:50 mixing studies were analysed using the Bethesda method with ADAMTS13 activity determination using the Technozyme® ELISA assay.

Several factors were taken into consideration when performing the Bethesda assay as detailed in studies by Mancini *et al.* 2012 who found that a pre-incubation temperature of 37°C seemed to influence the enzyme stability when a fluorescence detection based method is used. Therefore, it was suggested that mixed patient and pooled normal plasma (PNP) should be incubated at a temperature of 25°C for optimal for ADAMTS13 recovery. Another factor to take into consideration is the justification for the 2-hour incubation of patient and PNP mix, which is followed in most published Bethesda assay protocols. A study by Vendramin *et al.* 2018, showed that a 2-hour incubation time allows maximum interaction between the antibody and the enzyme. We thus incubated our test plasma samples and PNP mix for 2 hours at 25°C. Another factor that is suggested for consideration during the Bethesda assay is restoring the stability of ADAMTS13 in plasma collected in citrated tubes by adding calcium (Ca²⁺) before incubating the plasma mix (Vendramin *et al.* 2018) since citrate chelates calcium and zinc ions and thus influences ADAMTS13 activity. The ADAMTS13 Metalloprotease domain contains zinc and calcium-binding sites necessary for the proteolytic activity (Zheng, 2013). However, a study by Vendramin *et al.* (2018) reported only a slight difference in ADAMTS13 activity with and without the addition of Calcium. Therefore, in this study, the standardized Technozym® ELISA based-assay was performed without the addition of Calcium.

We detected positive anti-ADAMTS13 IgG antibody titers in 64% (34 of the 53) HIV-associated TTP patient samples, which did not correct with 50:50 mixing studies, suggesting the presence of inhibitory anti-ADAMTS13 IgG antibodies. Sixteen of these plasma samples (47%) had a significantly raised inhibitor by Bethesda assay, indicating the presence of strong inhibitors since the ADAMTS13 activity stayed less than <10% after 50:50 mixing studies. The other 18 (53%) HIV-associated TTP patient plasma samples had weak inhibitors using the Bethesda assay. Two interesting samples (TTP-

9 and -20) had very high anti-ADAMTS13 antibody titers, but no inhibitory anti-ADAMTS13 antibodies in 50:50 mixing studies. This supports the hypothesis that inhibitory antibodies are not the only mechanism for ADAMTS13 depletion in acquired TTP patients. A previous study by (Vendramin *et al.* 2018) also reported two TTP patients with high anti-ADAMTS13 IgG antibody titers without detectable inhibitory ADAMTS13 antibodies.

This study also investigated the laboratory evidence of autoimmunity in HIV-associated TTP plasma samples by also measuring IgM and IgA titers to emphasize the relationship between the disease and the immunological parameters. Normal ranges of IgM and IgA antibody levels were observed in plasma samples from the HIV positive control group with CD4⁺ lymphocyte count of more than 200mm³. However, the HIV-associated TTP plasma samples were detected with slightly increased plasma IgM and IgA antibodies and had a CD4⁺ count of less than 200mm³. A relationship between autoantibodies and CD4⁺ T-lymphocyte count has previously been documented (Chen *et al.* 2002; Susal *et al.* 1992; McHeyzer *et al.* 2009). It is reported that autoantibodies can trigger T-cell apoptosis by crosslinking Ig-related T-cell membrane molecules and gp120, a glycoprotein on the HIV envelope, resulting in CD4⁺ T-cell depletion with loss of integrity of the immune system (Kopelman and Zola-Pazner, 1988; Gentric *et al.* 1991). HIV infection therefore predisposes patients to autoimmune responses. Autoantibodies have prognostic significance in infectious diseases such as infections with HIV and have diagnostic value in HIV-associated TTP.

We further investigated IgM and IgA autoantibodies directed towards the ADAMTS13 protease in HIV-associated TTP patient plasma samples and this is, to our knowledge, the first study to screen for these additional autoantibody isotypes in HIV-associated TTP patients. The presence of other immunoglobulin isotype anti-ADAMTS13 autoantibodies possibly supports the pathogenic role of immunologic mechanisms in TTP-associated phenotypic expression. Although anti-ADAMTS13 IgG autoantibodies predominated in the HIV-associated TTP samples, 30% of these patient samples had anti-ADAMTS13 IgM and 64% had anti-ADAMTS13 IgA antibodies. These findings were similar to previous studies in HIV negative patients with acquired TTP (Ferrari *et al.* 2009; Rieger *et al.* 2005; Scheiflinger *et al.* 2003).

An interesting observation was that more HIV-associated TTP patient samples presented with anti-ADAMTS13 IgA autoantibodies (64%) compared to IgM subtype (30%) which is different from previous studies in which IgM were detected more frequently vs. IgA autoantibodies in acquired TTP patients (Rieger *et al.* 2005; Scheiflinger *et al.* 2003). IgM antibodies are involved in primary immune response, and IgA antibodies are produced in the secondary immune response. It is possible that the diagnosis of HIV-associated TTP is delayed due to diagnostic uncertainty.

IgM autoantibodies might influence the half-life of ADAMTS13 by virtue of its ability to activate the complement system. Moderately elevated complement activation has been reported in acute TTP episodes (Reti *et al.* 2012; Cataland *et al.* 2014). Another possible mechanism is that IgM autoantibodies might bind to the endothelial surface and mediate cellular uptake of the IgM-conjugated antigen thus compromising ADAMTS13 activity *in vivo* (Scheiflinger *et al.* 2003). IgA autoantibody effector functions might also influence the half-life of ADAMTS13 in plasma (Roos *et al.* 2001). The exact clinical significance of IgM and IgA autoantibodies in HIV-associated TTP patients is not clear but may play a role in the reduced ADAMTS13 levels as has been observed in other autoimmune diseases. Eighteen HIV positive control cohort samples had anti-ADAMTS13 IgG antibodies and 22% of these 18 samples also contained IgM and IgA autoantibodies but their clinical significance remains unclear.

The primary function of ADAMTS13 is to regulate VWF multimers size. VWF analysis therefore has utility in HIV-associated TTP diagnosis and prognostication as a marker of endothelial activation. The ratio between VWF propeptide (VWFpp) and VWF:Ag levels in plasma can be used to evaluate endothelial cell activation and clearance rates of VWF under pathologic conditions such as TTP (van Mourik *et al.* 1999; Haberichter *et al.* 2015; Romani *et al.* 2003). With this study, we investigated the VWF parameters in 59 HIV-associated TTP patient plasma samples with severe ADAMTS13 activity of <10% and in 100 HIV positive control plasma samples.

Elevated VWF:Ag and VWFpp levels were found in 80% of HIV-associated TTP patient samples. This is in agreement with previous studies (Lotta *et al.* 2011; Ito-Habe *et al.* 2011). It is suggested that elevated VWF:Ag and VWFpp levels are biomarkers of acute endothelial cell activation (Stufano *et al.* 2011) and thrombosis risk (Nossent *et al.* 2006). We found a high median VWF:Ag level with a low median ADAMTS13 level in the HIV-associated TTP patient samples. Increased VWFpp reflects increased VWF synthesis, which could lead to platelet and endothelial cell activation (Banno *et al.* 2006).

No difference was however detected between the VWF:Ag levels of the HIV-associated TTP patients and the HIV positive control group. The presence of high VWF levels has also been correlated with the progression of HIV and HIV-related diseases (Aukrust *et al.* 2000). This study confirms that the presence of HIV infection promotes persistent endothelial cell activation, even during ART, and may have an essential role in the pathophysiology of HIV-associated TTP. However, no correlation was detected between ADAMTS13 levels and the presence of UL-VWF multimers in the HIV positive control samples.

The VWFpp/ VWF:Ag ratio was significantly increased in only 14% of the HIV-associated TTP patient samples and 18% of HIV positive cohort samples. Increased VWFpp/VWF:Ag ratio indicates increased clearance or removal of UL-VWF multimers from the circulation and an increased risk of bleeding (Haberichter *et al.* 2006). Our findings differed from those of previous studies (Stufano *et al.* 2011; Lotta *et al.* 2011) which documented higher VWFpp/VWF:Ag ratios in the majority of patients with significantly low ADAMTS13 activity levels of <10%. However, another study argued that this correlation between the VWFpp/VWF:Ag ratio and ADAMTS13 activity does not necessarily exist (Andersson *et al.* 2012) and the current study supports this argument. Instead, high VWF:Ag and VWFpp levels may reflect disease severity. The current study highlights the value of VWF analysis in the diagnosis of HIV-associated TTP, which can be used to indicate the severity of the condition in these patients.

The VWF multimeric patterns in HIV-associated TTP patient samples were compared with the multimeric pattern in HIV positive control cohort and human pooled normal plasma (PNP). Multimer analysis is a qualitative assessment of the size distribution of VWF multimers (small, intermediate, large, or very large), as well as their migration pattern (Ledford-Kraemer, 2010) which provides evidence of decreased or impaired ADAMTS13 proteolytic activity in TTP (Furlan *et al.* 1997).

The VWF multimer analysis was performed using the SHL5v3: VWF multimer analysis method in routine use in the Special Haemostasis laboratory for sub-typing of von Willebrand disease (VWD). The assay detects the presence or absence of very large VWF multimers, which can have utility in the diagnosis of TTP (Banno *et al.* 2006; Furlan *et al.* 1997; Pos *et al.* 2010). The limitation of this assay is the long turnaround time of 3 days although it is easy to perform.

The presence of ULVWF multimers detected in most of the plasma samples with very high VWF:Ag levels confirm a deficient ADAMTS13 proteolytic activity in the plasma of patients with TTP. A previous study also showed that a deficient ADAMTS13 alone is sufficient to cause the accumulation of large VWF multimers in plasma, leading to a prothrombotic state in mice (Banno *et al.* 2006) and additional studies in TTP patients (Schwameis *et al.* 2015; Furlan *et al.*, 1999).

The loss of large multimers detected in 14% of the HIV-associated TTP patient samples, and in 18% of the HIV-positive cohort samples suggest clearance of large VWF multimers from the circulation as trapping occurs in the micro-vasculature. However, this finding has also been observed in TTP patients during remission (Stufano *et al.* 2012) and may reflect the background prothrombotic state in patients with persistent endothelial activation and release of VWF (Banno *et al.* 2006).

The current study confirmed that HIV-associated TTP patients had the same VWF multimeric characteristics with accumulation of ultra large VWF multimers as patients with other forms of acquired TTP. A study by Aukrust *et al.* (2000) indicated that the presence of HIV infection triggers endothelial activation that results in increased VWF release and a relative ADAMTS13 deficiency might trigger the onset of TTP in HIV infected patients (Cruccu *et al.* 1994; Gunther *et al.* 2006; Fujimura and Matsumoto 2010; Pos *et al.* 2011).

The primary objective of this study was to provide novel insights into potential epitopic regions on the ADAMTS13 protein for autoantibodies interaction. The IgG antibodies are primarily involved in the pathogenesis of other acquired forms of TTP by effecting decreased ADAMTS13 protein in plasma (Luken *et al.* 2006) but these antibodies have not been characterized in acquired HIV-associated TTP. The results of the current study show that all IgG antibodies isolated from 53 HIV-associated TTP patient plasma samples had multiple binding sites on the four functional domains of ADAMTS13 investigated. Anti-ADAMTS13 IgG antibodies were also detected in HIV positive control cohort samples and had similar binding specificities as the autoantibodies in HIV-associated TTP patients.

A Peptide ELISA approach was used to evaluate IgG antibodies binding to synthetic linear overlapping peptides of the ADAMTS13 protein. Peptide libraries are expensive for large proteins, such as ADAMTS13 protein. Therefore, to minimize costs, we selected domains that contributed significantly to the function of ADAMTS13 and towards the substrate VWF according to published literature (**Section 2.1**). The selected ADAMTS13 proximal domains include the Metalloprotease, Disintegrin-like, Cysteine-rich and Spacer domains. These domains interact with unravelled VWF substrate and are necessary for the proteolytic activity of ADAMTS13. Furthermore, their activity towards VWF fragments under static conditions has been evaluated demonstrating individual influences on ADAMTS13 activity (Thomas *et al.* 2015).

The advantage of a Peptide ELISA approach is that it provides an overview of all peptide residue regions that could possibly be affected by autoantibodies and allows immunological active regions to be identified. Another advantage of the Peptide ELISA is that it allows the detection of linear continuous epitopes that interact with paratopes based on their primary structure. Previous reports indicate that epitopes are more exposed on the surface than the remaining antigen, suggesting that they protrude from the antigen surface (Andersen *et al.* 2006; Thornton *et al.* 1986). Furthermore, it is also indicated that an average epitope residue size is ~10 - 25 amino acids with a linear stretch of 5 or more residues. These linear parts constitute more than half of the epitope size in most (85%)

epitopes (Kringelum *et al.* 2013). The main limitation of a Peptide ELISA is that it does not reveal which antibodies are inhibitory and which are non-inhibitory towards the ADAMTS13 antigen.

For this study, 105 linear overlapping synthetic peptides were designed and manufactured by GenScript® (USA) for use in a Peptide ELISA assay. A peptide length that allowed complete coverage of the ADAMTS13 domains was selected still affording the minimization of costs. The advantage of using synthetic peptides is the fact that large quantities of defined peptides can be synthesized at low cost while avoiding the need for biochemical purification and expression of native immunogens that are labour intensive and requires expertise (Bustin *et al.* 2003). Synthetic peptides are also protected against proteolysis and degradation *in vitro* (Seebach and Gardiner, 2008). The advantage of using overlapping peptides is that every possible epitope within a protein is covered. Furthermore, peptides were biotinylated on the N-terminal side to maximally expose the epitope of the peptide.

Purified intact antibodies are needed when performing epitope-mapping studies (Luken *et al.* 2005). IgG antibodies were isolated using a protein G affinity purification method which is the preferred method to obtain human IgG antibodies from a mixture of immunoglobulins of different isotypes (Huse *et al.* 2002). This method proved to be efficient as sufficient quantities of the antibody were obtained with the commercially available protein G spin columns. The method is also not time-consuming and is the least expensive method available for purifying antibodies. Protein G also allowed the intact structure of the IgG (both the heavy chain and the light chain) to bind through the Fc portion of the antibody, as indicated by the results of the SDS PAGE. SDS PAGE is the most widely used method to detect and visualize a purified protein within a gel matrix (Nasiri *et al.* 2017; Osborne and Brooks, 2006).

The purity of the isolated antibody was assessed using spectrophotometer analysis. Contamination-free purity extracts were obtained as indicated by the 260/280 ratio readings of less than <0.6 observed for each sample (**Supplementary Data 9**). A protein in a solution absorbs ultraviolet light at 280nm and nucleic acid contaminants at 260nm, which contributes to the total absorbance of the sample. A 260/280 nm absorbance ratio of more than 0.6 indicates DNA contamination, while a 260/280 nm ratio of less than 0.6 indicates that the protein is free from nucleic acid contaminants (Wilfinger *et al.* 1997). A dialysis step was also included to reduce salt contamination from antibody solutions. This step is required, especially when glycine has been used to elute the antibodies, since glycine can facilitate buffer salt crystallization causing pH shifts and potentially affecting stability of the protein (Pikal-Cleland *et al.* 2002).

Our epitope-mapping studies indicated that anti-ADAMTS13 IgG antibodies identified similar immuno-dominant epitopes in the HIV-associated TTP group and the HIV positive control cohort but additional binding sites were also identified in the two groups. We also observed that the Cysteine-rich and spacer domains harbour major binding sites in the HIV-associated TTP patients but not in the HIV positive control cohort.

The first immune-dominant epitope region was identified in the Metalloprotease domain. All the HIV-associated TTP samples and the HIV positive control cohort samples showed reactivity to the first peptide of the Metalloprotease domain. The potential epitope region was identified and comprised of amino acids "AAGGI" at position 74-80 in the full ADAMTS13 nucleotide sequence. These amino acid residues are located on the C-terminal part of the propeptide domain on the ADAMTS13 protein. The propeptide domain is reported to function as a molecular chaperone of ADAMTS13 and does not affect the enzymatic action of the protein or its expression levels (Majerus *et al.* 2003). Therefore, it is unclear what effect autoantibodies binding to the propeptide domain will have on the function of ADAMTS13. A previous study also detected IgG antibodies binding the propeptide domain in 20% of acquired TTP patient plasma samples (Klaus *et al.* 2004).

Another immune-dominant epitope for all the IgG antibodies from the HIV-associated TTP patient plasma samples was identified at position 125-139, a potential epitopic region with the amino acid sequence "RVHLVKMVLTEPEG" in the region coding the Metalloprotease domain. Other potential epitope regions were identified at amino acid residues 169-189, 200-224, 220-244 and 260-284 on the Metalloprotease domain. These regions contain the ADAMTS13 catalytic sequence as well as ADAMTS13 sub-sites, which are important for ADAMTS13 interaction with VWF (Xiang *et al.* 2011). Autoantibodies that bind to these regions may affect the interaction of ADAMTS13 with the VWF substrate. All plasma samples from the HIV-associated TTP patient group and 55% of the HIV positive control cohort samples had IgG antibodies binding to these regions. The effect of these IgG antibodies on ADAMTS13 activity needs to be investigated in future studies.

The current study also demonstrated that 58% of the IgG autoantibodies from HIV-associated TTP patient samples and 83% from the HIV positive control cohort samples interacted with various linear peptides from the Disintegrin-like domain. This domain has been reported to significantly increase the cleavage efficiency and specificity of ADAMTS13 (Ai *et al.* 2005; De Groot *et al.* 2009; Xiang *et al.* 2011; Crawley *et al.* 2011). The Disintegrin-like domain contains exocites at Arg349 and Leu350 residues that form weaker interactions with the unravelled VWF A2 domain residues at Asp1614 and Ala1612 close to the cleavage site. Thus, antibodies that bind to both the Metalloprotease domain and the Disintegrin-like domain may affect the ability of the ADAMTS13 protease to interact

with the VWF substrate. Furthermore, the Metalloprotease domain was identified as the most antigenic region when compared to the Disintegrin-like domain in both groups.

Previous studies on epitope-mapping in acquired TTP patients have identified antibodies that bind to the Metalloprotease and Disintegrin-like domains of ADAMTS13 (Klaus *et al.* 2004; Zheng *et al.* 2010). However, the frequency of antibodies binding to these domains in other studies was different to the findings in the current study. Klaus *et al.* (2004) detected antibodies binding the ADAMTS13 catalytic domains in 56% of patients with acquired TTP using immunoblotting. While Zheng *et al.* (2010) detected IgG antibodies from 96% of the plasma samples of acquired TTP patients that bind to the ADAMTS13 catalytic domains by using immunoprecipitation and western blotting. In the study, we found that all 100% of the HIV-associated TTP patient samples had anti-ADAMTS13 IgG antibodies that bind to specific regions on the ADAMTS13 Metalloprotease and Disintegrin-like domains and that 83% of the HIV positive control cohort had similar anti-ADAMTS13 IgG autoantibodies.

We also found that 98% of HIV-associated TTP patient samples had IgG autoantibodies that bind to both the Cysteine-rich as well as the Spacer domains. All of these samples contained autoantibodies that bind to the Spacer domain alone which is in agreement with previous studies that showed that both the Cysteine-rich and Spacer domains are constantly involved in antibody binding in patients with acquired TTP (Zheng *et al.* 2010; Soejima *et al.* 2003; Klaus *et al.* 2004; Luken *et al.* 2005). The Cysteine-rich and Spacer domain have been found valuable for efficient *in vivo* VWF ADAMTS13 proteolysis (De Groot *et al.* 2015; Jin *et al.* 2010; Gao *et al.* 2008; Gao, 2006; Majerus *et al.* 2005; Akiyama *et al.* 2009) and thus, IgG autoantibodies that bind to these domains may interfere with ADAMTS13 activity.

The current study observed two immune-dominant epitopes on the Cysteine-rich domain and all the HIV-associated TTP patient IgG autoantibodies interacted with these epitopes. Potential epitope regions were identified on linear overlapping peptides with residues at position 445-504 and 505-564 of the Cysteine-rich domain to which 28% of the HIV positive control samples had autoantibodies. This domain has been shown to promote conformational changes in the Spacer domain, thus allowing the Spacer domain to interact with the VWF (De Groot *et al.* 2011). Therefore, antibodies binding to the Cysteine-rich may also affect ADAMTS13-VWF interactions.

An interesting finding was that all plasma samples from the HIV-associated TTP patient group showed IgG autoantibody binding to amino acid residues 645-684 from the Spacer domain. A potential epitopic region with the amino acid sequence “QEDADIQVRRYGEYGNLTRPDITFTYFQ” located at position 650-669 on the full ADAMTS13 nucleotide sequence was then identified.

However, several other regions also contributed to the antigenicity of the Spacer domain. About 79% of the TTP patient samples had IgG autoantibody binding at linear overlapping peptides at position 590-624 and 51% at position 625-649 of the ADAMTS13 Spacer domain. Only one HIV-associated TTP patient plasma sample had IgG autoantibody binding at amino acid residues 560-586 of the Spacer domain. The observed differences in epitope specificity suggest that at least three binding patterns of antibodies to the Spacer domain are present in patients with HIV-associated TTP.

The Spacer domain is essential for proteolysis of full-length VWF under flow conditions (Jin *et al.* 2010). A previous study by Luken *et al.* (2006) also identified potential epitope regions 572-579 and 657-666 in the Spacer domain in all acquired TTP patient samples analysed. Another study by Pos *et al.* (2010) also identified autoantibodies binding residues 660, 661 and 665 as pathogenic antibodies resulting in TTP. These residues were also shown to interact with the VWF A2 domain, suggesting that antibodies binding to these residues affect binding exosite of the ADAMTS13 protein. In this study, we also found that the potential epitope regions identified harbours these specific residues. Indicating that IgG autoantibodies in HIV-associated TTP patients may have similar anti-ADAMTS13 antibody binding patterns to the Spacer domains, similar to other forms of acquired TTP, considering the important role of the spacer domain in providing high-affinity binding of ADAMTS13 at positions 658-666 to VWF substrate at position 1660-1668 (**section 2.1**). The major antigenic determinants identified in the spacer domain may contribute to a compromised ADAMTS13 activity and induce acquired ADAMTS13 deficiency. Furthermore, the inhibitory and non-inhibitory autoantibodies in HIV-associated TTP patients did not necessarily exhibit distinct binding patterns, because the Fc-mediated antibody effector function of these autoantibodies might be different.

Another interesting finding is that 39% of IgG autoantibodies detected in the HIV positive control group did not show any binding to the Cysteine-rich and Spacer domains of ADAMTS13 suggesting evolution of autoantibodies as the TTP disease progress. This is often referred to as epitope spreading. Although purified IgG autoantibodies from the HIV positive control samples shared some linear epitopes with HIV-associated TTP patients, they were not inhibitory towards ADAMTS13. The difference may be due to different antibody binding affinity. It has previously been demonstrated that HIV positive individuals present with high levels of galactosylated antibodies, which induce chronic antibody-mediated inflammation in autoimmunity (Moore *et al.* 2005; Alter *et al.* 2018) and it is therefore postulated that chronic inflammation related to high viral loads may be associated with the altering the pathogenicity of anti-ADAMTS13 autoantibodies.

The results of this study showed that the ADAMTS13 proximal domains contain various epitope regions for anti-ADAMTS13 IgG autoantibody interaction in HIV-associated TTP patients. Therefore, it is evident that a polyclonal mixture of anti-ADAMTS13 IgG antibodies is present in HIV-associated TTP patients with similar binding patterns interacting with specific epitopes in the ADAMTS13 proximal domains. These include amino acid residues 125-139, 169-189, 200-224, 220-244 and 260-284 in the Metalloprotease domain, 445-504 and 505-564 in the Cysteine-rich domain, and 650-669, 590-624 and 625-649 in the Spacer domain. We also showed that HIV positive individuals without TTP had anti-ADAMTS13 IgG autoantibodies that share linear epitopes with anti-ADAMTS13 IgG antibodies detected in HIV-associated TTP patients.

Chapter 6: Conclusion

In conclusion, this study has shown that most HIV-associated TTP patients with significantly reduced ADAMTS13 activity of <10% had anti-ADAMTS13 IgG autoantibodies. Patients with a high anti-ADAMTS13 IgG antibody titer were deficient in ADAMTS13 antigen levels indicating that autoantibodies have functions beyond the inhibition of ADAMTS13 activity and may effect antibody-mediated clearance of ADAMTS13. It is also likely that ADAMTS13 activity is impaired by antibody binding to ADAMTS13 and block its substrate-cleaving activity. The presence of anti-ADAMTS13 IgM and IgA autoantibodies and the absence of inhibiting IgG autoantibodies in some patients with HIV-associated TTP further support suggestions that ADAMTS13 antibody-mediated depletion may contribute to the reduction of ADAMTS13 activity. Therefore, ADAMTS13 replacement therapy in HIV-associated TTP patients could possibly be beneficial. Interestingly, HIV infection and associated inflammation may contribute to compromised ADAMTS13 activity levels.

From our observations, both ADAMTS13, including autoantibody titers, and VWF parameters should be included in the diagnostic panel for HIV-associated TTP patients as these parameters have diagnostic and prognostic value.

Importantly, the epitope-mapping analysis revealed that anti-ADAMTS13 IgG antibodies detected in HIV-associated TTP patients bind to various antigenic regions on the Metalloprotease, Cysteine-rich, and Spacer domains while IgG antibodies in HIV negative individuals with TTP target mostly the Cysteine and Spacer domains. In this study we identified immunodominant epitopes in HIV-associated TTP patients, suggesting that these IgG autoantibodies have dominant immune responses to specific antigenic regions of ADAMTS13 potentially affecting the proteolytic activity of this enzyme.

This is the first study to report on the epitopes affected by anti-ADAMTS13 IgG antibodies in both HIV-associated TTP and HIV positive patient plasma samples. Some IgG antibodies of HIV positive patients shared linear epitope regions identified by anti-ADAMTS13 IgG antibodies from HIV-associated TTP patients. However, the Cysteine-rich and Spacer domains were not constantly involved in binding anti-ADAMTS13 IgG antibodies in the control cohort without TTP, unlike the HIV-associated TTP patients. Furthermore, a large percentage (68%) of anti-ADAMTS13 IgG autoantibodies detected in HIV-associated TTP patients were inhibitory, while the anti-ADAMTS13 IgG autoantibodies detected in HIV positive controls were not inhibitory. Whether or not the autoantibodies in HIV serve as the basis for the emergence of high affinity, pathogenic autoantibodies remains unclear and further studies are indicated. The current study suggests that

anti-ADAMTS13 antibodies may correlate with clinical outcomes and should be included in the routine clinical diagnostics for improving TTP disease management outcomes in South Africa. Monitoring ADAMTS13 autoantibody titers to ascertain the risk of relapse may be of clinical importance in HIV-associated TTP patients.

This study has improved our understanding of the immunological response potentially involved in HIV-associated TTP. This study also recommends screening for inhibitory anti-ADAMTS13 IgG autoantibodies to characterize the pathophysiology of HIV-associated TTP.

Limitations and Future studies

The first limitation which impacted on the study timelines was access to samples from patients with confirmed HIV-associated TTP which is a relatively rare disorder and the diagnosis of TTP remains challenging.

Secondly, we did not screen the whole ADAMTS13 protein for potential epitopic regions, due to the costs involved in obtaining a peptide library of the full-length ADAMTS13 protein. Thus, only the ADAMTS13 proximal domains were selected, based on their structure-function properties. Future studies might include screening the remaining ADAMTS13 distal domains for potential epitope regions. It will also be interesting to determine the epitope regions recognized by anti-ADAMTS13 IgM and IgA autoantibodies to understand the antibody-mediated mechanisms involved. It will also be of value to determine whether the presence of anti-ADAMTS13 IgG antibodies in HIV positive individuals precedes the clinical disease onset of TTP potentially identifying at risk HIV infected subgroups. Our study therefore has laid a foundation for future studies that aim to investigate the significance, isotypes and titres of ADAMTS13 autoantibodies in HIV-associated patients with and without TTP.

Furthermore, it has previously been indicated that individuals with specific human leukocyte antigens (HLA) may be at risk for developing acquired TTP (Coppo *et al.* 2010). HIV-infection may be a triggering factor for individuals with these genetic backgrounds. Therefore, studies are needed to screen for the risk associated HLA molecules in our population, both in HIV infected and HIV-associated TTP patients in order to increase our understanding of HIV-associated TTP. It will thus be interesting to determine whether HIV positive individuals with high anti-ADAMTS13 IgG titers also have the risk associated HLA molecules.

Screening assays such as the detection of ADAMTS13 autoantibodies using lateral flow assays might be developed for point-of-care testing to monitor therapeutic interventions and to determine the

different stages of the disease. Future studies may also include the design of epitope-based vaccines that can reduce the amount of ineffective antibodies in infected individuals. It may also be of benefit to develop functional ADAMTS13 variants with reduced antigenicity to such antibodies for the treatment of patients with autoantibodies to ADAMTS13.

Impact of the study

This study has provided a novel insight into epitope-specific binding of anti-ADAMTS13 IgG autoantibodies in HIV-associated TTP and HIV infected patients without TTP and has highlighted the contribution of ADAMTS13 autoantibodies to the function and clearance of ADAMTS13 in HIV-associated TTP. Humoral immune responses play an important role in the pathogenesis of HIV-associated TTP and increased understanding is needed for better management of TTP in HIV-infected individuals. Characterizing autoantibodies present in HIV-associated TTP patients may be of clinical importance in predicting relapses and monitoring efficiency of therapeutic interventions. Therefore, our study has laid a foundation for future studies that aim to investigate the prognostic significance of autoantibodies (antibody classes, subclasses and concentration) to ADAMTS13 in patients with initial presentations of HIV-associated TTP. This study has therefore improved our understanding of HIV-associated TTP.

REFERENCES

- Ackerman** ME, Crispin M, Yu X, Baruah K, Boesch AW, Harvey DJ, Dugast AS, Heizen EL, Ercan A, Choi I, Streeck H, Nigrovic PA, Bailey-Kellogg C, Scanlan C, Alter G. 2013. Natural variation in Fc glycosylation of HIV-specific antibodies impacts antiviral activity. *The Journal of Clinical Investigation*, 123(5): 2183-92. DOI: 10.1172/JCI65708.
- Ahmed** S, Siddiqui RK, Siddiqui AK, Zaidi SA, Cervia J. 2002. HIV associated thrombotic microangiopathy – A Review. *Postgraduate Medical Journal*, 78: 520–525. <https://pmj.bmj.com/content/postgradmedj/78/923/520.full.pdf>.
- Ahn** YS, Jy W, Kolodny L, Horstman LL, Mao WW, Valant PA, Duncan RC. 1996. Activated platelet aggregates in thrombotic thrombocytopenic purpura: decrease with plasma infusions and normalization in remission. *British Journal of Haematology*, 95: 408-415.
- Ai** J, Smith P, Wang S, Zhang P, Zheng XL. 2005. The proximal carboxyl-terminal domain of ADAMTS13 determine substrate specificity and are all required for cleavage of von Willebrand factor. *Journal of Biological Chemistry*, 280: 29428-29434. [PubMed: 15975930]
- Akiyama** M, Takeda S, Kokame K, Takagi J, Miyata T. 2009. Crystal structures of the noncatalytic domains of ADAMTS13 reveal multiple discontinuous exocites for von Willebrand factor. *Proceedings of the National Academy of Sciences of the United States of America*, 106(46): 19274-19279.
- Albelda** SM and Buck CA. 1990. Integrins and other cell adhesion molecules. Review. *The Federation of American Society for Experimental Biology Journal*, 4(11): 2868-2880.
- Alexander** T, Sarfert R, Klotsche J, Kühl AA, Rubbert-Roth A, Lorenz HM, Rech J, Hoyer BF, Cheng Q, Waka A, Taddeo A, Wiesener M, Schett G, Burmester GR, Radbruch A, Hiepe F, Voll RE. 2015. The proteasome inhibitor bortezomib depletes plasma cells and ameliorates clinical manifestations of refractory systemic lupus erythematosus. *Annals of the Rheumatic Diseases* 74(7): 1474-1478. DOI: 10.1136/annrheumdis-2014-206016.
- Ali** MA, Shaheen JSS, Khan MA. 2014. Acute pancreatitis induced thrombotic thrombocytopenic purpura. *Indian Journal of Critical Care Medicine*, 18(2): 107–109. DOI: 10.4103/0972-5229.126084
- Alter** G, Ottenhoff THM, Joosten SA. 2018. Antibody glycosylation in inflammation, disease and vaccination. *Seminars in Immunology*, 39: 102-110. <https://doi.org/10.1016/j.smim.2018.05.003>.
- Alwan** F, Vendramin C, Liesner R, Clark A, Lester W, Dutt T, Thomas W, Gooding R, Biss T, Watson HG, Cooper N, Rayment R, Cranfield T, van Veen JJ, Hill QA, Davis S, Motwani J, Bhatnagar N, Priddee N, David M, Crowley MP, Alamelu J, Lyall H, Westwood JP, Thomas M, Scully M. 2019. Characterization and treatment of congenital thrombotic thrombocytopenic purpura. *Journal of Blood*, 133(5): 1644-1665. DOI: 10.1182/blood-2018-11-884700.
- Alwan** F, Vendramin C, Vanhoorelbeke K, Langley K, McDonald V, Austin S, Clark A, Lester W, Gooding R, Biss T, Dutt T, Cooper N, Chapman O, Cranfield T, Douglas K, Watson HG, van Veen JJ, Sibson K, Thomas W, Manson L, Hill QA, Benjamin S, Ellis D, Westwood JP, Thomas M, Scully M. 2017. Presenting ADAMTS13 antibody and antigen levels predict prognosis in immune-mediated thrombotic thrombocytopenic purpura. *Blood*, 130(4): 466-471. DOI: 10.1182/blood-2016-12-758656.
- Andersen** PH, Nielsen M, Lund O. 2006. Prediction of residues in discontinuous B-cell epitopes using protein 3D structures. *Protein Science*, 15: 2558–2567.

- Anderson** PJ, Kokame K, Sadler JE. 2006. Zinc and calcium ions cooperatively modulate ADAMTS13 activity. *Journal of Biological Chemistry*, 281(2): 850-857. DOI: 10.1074/jbc.M504540200.
- Andersson** HM, Siegerink B, Luken BM, Crawley JT, Algra A, Lane DA, Rosendaal FR. 2012. High VWF, low ADAMTS13 and oral contraceptives increase the risk of ischemic stroke and myocardial infarction in young women. *Blood*, 119: 1555–1560. <https://doi.org/10.1182/blood-2011-09-380618>
- Anthony** RM, Ravetch JV. 2010. A novel role for the IgG Fc glycan: the anti-inflammatory activity of sialylated IgG Fcs. *Journal of Clinical Immunology*, 30 (*Supplementary 1*): S9–S14.
- Apte** SS. 2009. A disintegrin-like and metalloprotease (reprolysin-type) with thrombospondin type 1 motif (ADAMTS) superfamily: functions and mechanisms. *Journal of Biological Chemistry*, 284: 31493-31497. [PubMed: 19734141].
- Aukrust** P1, Bjørnsen S, Lunden B, Otterdal K, Ng EC, Ameln W, Ueland T, Müller F, Solum NO, Brosstad F, Frøland SS. 2000. Persistently elevated levels of von Willebrand factor antigen in HIV infection. Downregulation during highly active antiretroviral therapy. *Thrombosis and Haemostasis*, 84(2): 183-187.
- Bachmeyer** C, Blanche P, Séréní D, Salmon D, Gâteau G, Dreyfus F, Sicard D. 1995. Thrombotic thrombocytopenic purpura and hemolytic uremic syndrome in HIV-infected patients. *The Journal of Acquired Immune Deficiency Syndromes*, 9: 532–543.
- Banno** F, Kokame K, Okuda T, Honda S, Miyata S, Kato H, Tomiyama Y, Miyata T. 2006. Complete deficiency in ADAMTS13 is prothrombotic, but it alone is not sufficient to cause thrombotic thrombocytopenic purpura. *Blood*, 107: 3161-3166.
- Bao** J, Xiao J, Mao Y and X. Long Zheng. 2014. Carboxyl-terminus of ADAMTS13 directly inhibits platelet aggregation and ultra large VWF string formation under flow in a free thiol-dependent manner. *Arteriosclerosis, Thrombosis, and Vascular Biology Journal*, 34(2): 397–407.
- Barr** TA, Brown S, Mastroeni P, Gray D. 2010. TLR and B cell receptor signals to B cells differentially program primary and memory Th1 responses to *Salmonella enterica*. *Journal of Immunology*, 185: 2783-2789.
- Barr** TA, Gray M, Gray D. 2012. B cells: programmers of CD4 T cell responses. *Infectious Disorders - Drug Targets*, 12: 222–231.
- Barry** OP, Praticò D, Savani RC, FitzGerald GA. 1998. Modulation of monocyte-endothelial cell interactions by platelet microparticles. *Journal of Clinical Investigation*, 102(1):136-144. DOI: 10.1172/JCI2592.
- Becker** S, Fusco G, Fusco J, Balu R, Gangjee S, Brennan C, Feinberg J, Collaborations in HIV Outcomes Research/US Cohort. 2004. HIV-associated thrombotic microangiopathy in the era of highly active antiretroviral therapy: an observational study. *Clinical Infectious Diseases* 1, 39(*Supplementary 5*): S267-S275.
- Bell** WR, Chulay JD, Feinberg JE. 1997. Manifestations resembling thrombotic microangiopathy in patients with advanced human immunodeficiency virus (HIV) disease in a cytomegalovirus prophylaxis trial (ACTG 204). *Medicine*, 76: 369–380.
- Ben** S, Rodríguez F, Severo C, Debat N. 2010. A Case of HELLP Syndrome in a Patient with Immune thrombocytopenic Purpura. *Obstetrics and Gynecology International*, 692163: 1-4. <http://dx.doi.org/10.1155/2010/692163>
- Benjamin** M, Terrell DR, Vesely SK, Voskuhl GW, Dezube BJ, Kremer Hovinga JA, Lämmle B, George JN. 2009. Frequency and significance of HIV infection among patients diagnosed with thrombotic thrombocytopenic purpura. *Clinical Infectious Disease*, 48(8):1129–1137.

- Bergmann** IP, Kremer Hovinga JA, Lammle B, Peter HJ, Schiemann U. 2008. Acute pancreatitis and thrombotic thrombocytopenic purpura. *European Journal of Medical Research*, 13(10): 481–492. [PMID: 19008177]
- Bernado** A, Ball C, Nolasco L, Moake JF, and Dong J. 2004. Effects of inflammatory cytokines on the release and cleavage of endothelial cell-derived ultralarge von Willebrand factor multimers under flow. *Blood*, 104(1): 100-106. DOI: 10.1182/blood-2004-01-0107.
- Blake** J and Litzi-Davis L. 1992. Evaluation of Peptide Libraries: An Iterative Strategy to Analyze the reactivity of Peptide Mixtures with Antibodies. *Bioconjugate Chemistry*, 3: 510-513. DOI: 10.1021/bc00018a008.
- Blombery** P, Kivivali L, Pepperell D, McQuilten Z, Engelbrecht S, Polizzotto MN, Phillips LE, Wood E, Cooney S. 2016. Diagnosis and management of thrombotic thrombocytopenic purpura (TTP) in Australia: findings from the first 5 years of the Australian TTP/thrombotic microangiopathy registry. *Journal of Internal Medicine* 260(1): 71-79. DOI: 10.1111/imj.12935.
- Bode** W, Fernandez-Catalan C, Tschesche H, Grams F, Nagase H, Maskos K. 1999. Structural properties of matrix metalloproteinase: A Review. *Cellular Molecular Life Sciences*, 55(4): 639-652. <https://doi.org/10.1007/s000180050320>
- Bode** W, Gomis-Ruth FX, Stockler W. 1993. Astacins, serralyins, snake venom and matrix metalloproteinase exhibit identical zinc-binding environments (HEXXHXXGXXH and Met-turn) and topologies and should be grouped into a common family, the 'metzincins'. *Federation of European Biochemical Society Letters*, 331:134-140. [https://doi.org/10.1016/0014-5793\(93\)80312-I](https://doi.org/10.1016/0014-5793(93)80312-I)
- Böhm** S, Kao D, Nimmerjahn F. 2014. Sweet and sour: the role of glycosylation for the anti-inflammatory activity of immunoglobulin G. *Current Topics in Microbiology and Immunology Journal*, 382: 393–417. DOI: 10.1007/978-3-319-07911-0_18
- Boro** J, Pavenski K, Ambler KLS, Leitch HA and Hicks LK. 2011. HIV associated Thrombotic Thrombocytopenic Purpura. *Blood*, 118:4677
- Böttger** V, Böttger A. 2009. Epitope Mapping Using Phage Display Peptide Libraries. In: Schutkowski M., Reineke U. (eds) *Epitope Mapping Protocols. Methods in Molecular Biology™ (Methods and Protocols)*, vol 524. Humana Press. United States of America. https://doi.org/10.1007/978-1-59745-450-6_13
- Bresin** E, Gastoldi S, Daina E, Belotti D, Pogliani E, Perseghin P, Scalzulli PR, Paolini R, Marcenò R, Remuzzi G, Galbusera M. 2009. Rituximab as pre-emptive treatment in patients with thrombotic thrombocytopenic purpura and evidence of anti-ADAMTS13 autoantibodies. *Journal of Thrombosis and Haemostasis*, 101(2):233–238.
- Bustin** M, Robinson RC, Friedman FK. 2003. Immunochemical analysis of Chromatin. *Methods in Enzymology*, 376: 209-220. [https://doi.org/10.1016/S0076-6879\(03\)76014-5](https://doi.org/10.1016/S0076-6879(03)76014-5).
- Camilleri** RS, Cohen H, Mackie IJ, Scully M, Starke RD, Crawley JT, Lane DA, Machin SJ. 2008. Prevalence of the ADAMTS-13 missense mutation R1060W in late onset adult thrombotic thrombocytopenic purpura. *Journal of Thrombosis and Haemostasis*, 6:331–8.
- Cao** W, Krishnaswamy S, Camire R, Lenting PJ, Zheng XL. 2008. Factor VIII accelerates proteolytic cleavage of von Willebrand factor by ADAMTS13. *Proceedings of the National Academy of Sciences of the United States of America*, 105(21): 7416-7421.
- Carson** SD and Johnson DR. 1990. Consecutive enzyme cascades: complement activation at the cell surface triggers increased tissue factor activity. *Blood*, 76(2): 361-367.

Casina VC, Hu W, Mao JH, Lu RN, Hanby HA, Pickens B, Kan ZY, Lim WK, Mayne L, Ostertag EM, Kacir S, Siegel DL, Englander SW, Zheng XL. 2015. High-resolution epitope mapping by HX MS reveals the pathogenic mechanism and a possible therapy for autoimmune TTP syndrome. *Proceedings of the National Academy of Sciences of the United States of America*, 112(31): 9620-9625. DOI:10.1073/pnas.1512561112.

Cataland SR, Holers VM, Geyer S, Yang S, Wu HM. 2014. Biomarkers of terminal complement activation confirm the diagnosis of aHUS and differentiate aHUS from TTP. *Blood*, 123(24): 3733–3738. DOI: <https://doi.org/10.1182/blood-2013-12-547067>

Cataland SR, Jin M, Ferketich AK, Kennedy MS, Kraut EH, George JN, Wu HM. 2007. An evaluation of cyclosporin and corticosteroids individually as adjuncts to plasma exchange in the treatment of thrombotic thrombocytopenic purpura. *British Journal of Haematology*, 136:146-149.

Cataland SR, Jin M, Lin S, Kennedy MS, Kraut EH, George JN, Wu HM. 2007. Cyclosporin and plasma exchange in thrombotic thrombocytopenic purpura: long-term follow-up with serial analysis of ADAMTS13 activity. *British Journal of Haematology*, 139: 486-493.

Cataland SR, Wu HM. 2013. Atypical hemolytic uremic syndrome and thrombotic thrombocytopenic purpura: clinically differentiating the thrombotic microangiopathies. *European Journal of Internal Medicine* 24(6): 486-491.

Chang JC, Naqvi T. 2003. Thrombotic thrombocytopenic purpura associated with bone marrow metastasis and secondary myelofibrosis in cancer. *The Oncologist*, 8: 375-380.

Chen J, Fu X, Wang Y, Ling M, McMullen B, Kulman J, Chung DW, López JA. 2010. Oxidative modification of von Willebrand factor by neutrophil oxidants inhibits its cleavage by ADAMTS13. *Blood*, 115: 706–712.

Chen J, Ling M, Fu X, Lopez JA, Chung DW. 2012. Simultaneous exposure of sites in von Willebrand factor for glycoprotein Ib binding and ADAMTS13 cleavage: studies with ristocetin. *Arteriosclerosis, Thrombosis and Vascular Biology*, 32: 2625–2630.

Chen J, Wang L, Chen JJ, Sahu GK, Tying S, Ramsey K, Indrikovs AJ, Petersen JR, Paar D, Cloyd MW. 2002. Detection of Antibodies to Human Immunodeficiency Virus (HIV) That Recognize Conformational Epitopes of Glycoproteins 160 and 41 Often Allows for Early Diagnosis of HIV Infection. *The Journal of Infectious Diseases*, 186(3): 321–331.

Chirinos JA, Heresi GA, Velasquez H, Jy W, Jimenez JJ, Ahn E, Horstman LL, Soriano AO, Zambrano JP, Ahn YS. 2005. Elevation of Endothelial Microparticles, Platelets, and Leukocyte Activation in Patients With Venous Thromboembolism. *Journal of the American College of Cardiology*, 45(9): 1467-1471. <https://doi.org/10.1016/j.jacc.2004.12.075>.

Chou TW, Wang S, Sakhatskyy PV, Mboudjeka I, Lawrence JM, Huang S, Coley S, Yang B, Li J, Zhu Q, Lu S. 2005. Epitope mapping and biological function analysis of antibodies produced by immunization of mice with an inactivated Chinese isolate of severe acute respiratory syndrome-associated coronavirus (SARS-CoV). *Virology* 337(1): 134–143.

Clinical and Laboratory Standard Institute (CLSI). 2008. *Collection, Transport and Processing of Blood Specimens for testing plasma-based coagulation assays and Molecular Hemostasis assays*; Approved guidelines - fifth edition. Clinical and Laboratory Standard Institute Document H21-A5 (ISBN 1-56238-657-3) 28(5). Clinical and Laboratory Standard Institute. Wayne, Pennsylvania, United States of America. <http://csl.org.h21a5.sample.pdf>

Collen D. 1999. The plasminogen (fibrinolytic) system. *Thrombosis and Haemostasis* 82: 259-270.

- Coppo P**, Bengoufa D, Veyradier A, Wolf M, Bussel A, Millot GA, Malot S, Heshmati F, Mira JP, Boulanger E, Galicier L, Durey-Dragon MA, Fremeaux-Bacchi V, Ramakers M, Pruna A, Bordessoule D, Gouilleux V, Scrobohaci ML, Vernant JP, Moreau D, Azoulay E, Schlemmer B, Guillevin L, Lassoued K. 2004. Severe ADAMTS13 deficiency in adult idiopathic thrombotic microangiopathies defines a subset of patients characterized by various autoimmune manifestations, lower platelet count, and mild renal involvement. *Medicine (Baltimore)*, 83: 233–44. <http://dx.doi.org/10.1097/01.md.0000133622.03370.07>.
- Coppo P**, Busson M, Veyradier A, Wynckel A, Poullin P, Azoulay E, Galicier L, Loiseau P. 2010. HLA-DRB1*11: a strong risk factor for acquired severe ADAMTS13 deficiency-related idiopathic thrombotic thrombocytopenic purpura in Caucasians. *Journal of Thrombosis and Haemostasis*, 8: 856–859.
- Coppo P**, Schwarzinger M, Buffet M, Wynckel A, Clabault K, Presne C, Poullin P, Malot S, Vanhille P, Azoulay E, Galicier L, Lemiale V, Mira JP, Ridel C, Rondeau E, Pourrat J, Girault S, Bordessoule D, Saheb S, Ramakers M, Hamidou M, Vernant JP, Guidet B, Wolf M, Veyradier A, French Reference Center for Thrombotic Microangiopathies. 2010. Predictive features of severe acquired ADAMTS13 deficiency in idiopathic thrombotic microangiopathies: the French TMA reference center experience. *Public Library of Science One*, 5(4): 1-9. DOI:10.1371/journal.pone.0010208
- Coppo P**, Wolf M, Veyradier A, Bussel A, Malot S, Millot GA, Daubin C, Bordessoule D, Pène F, Mira JP, Heshmati F, Maury E, Guidet B, Boulanger E, Galicier L, Parquet N, Vernant JP, Rondeau E, Azoulay E, Schlemmer B; Réseau d'Etude des Microangiopathies Thrombotiques de l'Adulte. 2006. Prognostic value of inhibitory anti-ADAMTS13 antibodies in adult-acquired thrombotic thrombocytopenic purpura. *British Journal of Haematology*, 132: 66–74.
- Crawford A**, Macleod M, Schumacher T, Corlett L, Gray D. 2006. Primary T cell expansion and differentiation in vivo requires antigen presentation by B cells. *Journal of Immunology*, 176: 3498–506.
- Crawley JT**, de Groot R, Xiang Y, Luken BM, Lane DA. 2011. Unravelling the scissile bond: how ADAMTS13 recognizes and cleaves von Willebrand factor – A Review. *Blood*, 118: 3212-3221.
- Crawley JT**, Lam JK, Rance JB, Mollica LR, O'Donnell JS, Lane DA. 2005. Proteolytic inactivation of ADAMTS13 by thrombin and plasmin. *Blood*, 105: 1085-93.
- Crist RA** and Rodgers GM. 2009. A Comparison of Two Commercial ADAMTS13 Activity Assays with a Reference Laboratory Method. *Science Lab Medicine* 40(4): 232-235. <https://academic.oup.com/labmed/article-abstract/40/4/232/2657581>.
- Cruccu V**, Parisio E, Pedretti D, Villa A and Confalonieri F. 1994. HIV-related thrombotic thrombocytopenic purpura as first clinical manifestation of infection. *Haematological*, 79: 277-279.
- De Groot R**, Bardhan A, Ramroop N, Lane DA, Crawley JT. 2009. Essential role of the disintegrin-like domain in ADAMTS13 function. *Blood*, 113: 5609-5616. [PubMed: 19234142]
- De Groot R**, David AL, Crawley TB. 2015. The role of ADAMTS13 cysteine-rich domain in VWF binding and proteolysis. *Blood*, 125(12): 1975-1968.
- De Groot R**, Lane DA, Crawley JT. 2010. The ADAMTS13 metalloprotease domain: roles of subsites in enzyme activity and specificity. *Blood*, 116: 3064-3072.
- De Groot R**, Ryu J-Y, Jaring M, Luken BM, Lane DA, Crawley JT. 2011. VWF proteolysis by ADAMTS13 is dependent on cooperation between the ADAMTS13 cysteine-rich domain loop Q456-Q478 and the spacer domain. (Abstract ISTH 2011). *Journal of Thrombosis and Haemostasis*, 9 (Supplementary 2): 307-317.

- De Maeyer B**, De Meyer SF, Feys HB, Pareyn I, Vandeputte N, Deckmyn H, Vanhoorelbeke K. 2010. The distal carboxyterminal domains of murine ADAMTS13 influence proteolysis of platelet-derived VWF strings *in vivo*. *Journal of Thrombosis and Haemostasis*, 8: 2305-2312. [PubMed: 20695979]
- del Arco A**, Martinez MA, Peña JM, Gamallo C, González JJ, Barbado FJ, Vazquez JJ. 1993. Thrombotic Thrombocytopenic Purpura Associated with Human Immunodeficiency Virus Infection: Demonstration of p24 Antigen in Endothelial Cells. *Clinical Infectious Diseases*, 17(3), 360-363. www.jstor.org/stable/4457307
- Del Fante C**, Perotti C, Viarengo G, Gallini GS, Tinelli C, Salvaneschi L. 2006. Daily plasma-exchange for life threatening class I HELLP syndrome with prevalent pulmonary involvement. *Transfusion and Apheresis Science*, 34: 7-9.
- Dlott JS**, Danielson CFM, Blue-Hnidy DE and McCarthy LJ. 2004. Drug-induced thrombocytopenic purpura/hemolytic uremic syndrome: A concise review. *Therapeutic Apheresis and Dialysis*, 8(2): 102-111.
- Dong J**, Moake JL, Bernardo A, Fujikawa K, Ball C, Nolasco L, López JA, Cruz MA. 2003. ADAMTS-13 Metalloprotease Interacts with the Endothelial Cell-derived Ultra-large von Willebrand Factor. *Journal of Biological Chemistry*, 278: 29633 - 29639. DOI: 10.1074/jbc.M301385200
- Dong JF**, Moake JL, Nolasco L, Bernardo A, Arceneaux W, Shrimpton CN, Schade AJ, McIntire LV, Fujikawa K, Lopez JA. 2002. ADAMTS-13 rapidly cleaves newly secreted ultralarge von Willebrand factor multimers on the endothelial surface under flowing conditions. *Blood*, 100: 4033-9. <http://dx.doi.org/10.1182/blood-2002-05-1401>.
- Dong JF**. 2005. Cleavage of ultra-large von Willebrand factor by ADAMTS-13 under flow conditions. *Journal of Thrombosis and Haemostasis*, 3: 1710-6. <http://dx.doi.org/10.1111/j.1538-7836.2005.01360.x>
- Eckmann CM**, De Laaf RT, van Keulen JM, van Mourik JA, De Laat B. 2007. Bilirubin oxidase as a solution for the interference of hyperbilirubinemia with ADAMTS-13 activity measurement by FRET-VWF73 assay. *Journal of Thrombosis and Haemostasis*, 5: 1330-1.
- Eikenboom J**, Federici AB, Dirven RJ, Castaman G, Rodeghiero F, Budde U, Schneppenheim R, Batlle J, Canciani MT, Goudemand J, Peake I, Goodeve A. 2013. VWF propeptide and ratios between VWF, VWF propeptide, and FVIII in the characterization of type 1 von Willebrand disease. *Blood*, 121(12): 2336-2339. DOI: 10.1182/blood-2012-09-455089.
- Esmon CT**. 2000. Does inflammation contribute to thrombotic events? *Haemostasis, (Supplementary 2)*: 34-40.
- Fakhouri F**, Vernant JP, Veyradier A, Wolf M, Kaplanski G, Binaut R, Rieger M, Scheiflinger F, Poullin P, Deroure B, Delarue R, Lesavre P, Vanhille P, Hermine O, Remuzzi G, Grünfeld JP. 2005. Efficiency of curative and prophylactic treatment with rituximab in ADAMTS13-deficient thrombotic thrombocytopenic purpura: a study of 11 cases. *Blood*, 106: 1932-1937.
- Farhat MH**, de Souza B, and Hanbali A. 2009. Cancer-related TTP: Role of plasma exchange. *Journal of Clinical Oncology, 27(Supplementary 15)*: e13527-e13527. DOI: 10.1200/jco.2009.27.15_suppl.e13527.
- Federici AB**. 2003. The factor VIII/von Willebrand factor complex. Basic and Clinical issues. *Haematologica*, 88: 3-12.
- Ferrari S**, Mudde GC, Rieger M, Veyradier A, Kremer Hovinga JA, Scheiflinger F. 2009. IgG subclass distribution of anti-ADAMTS13 antibodies in patients with acquired thrombotic thrombocytopenic purpura. *Journal of Thrombosis and Haemostasis*, 7: 1703-1710. DOI:10.1111/j.1538-7836.2009.03568.x

Ferrari S, Palavra K, Gruber B, Kremer Hovinga JA, Knöbl P, Caron C, Cromwell C, Aledort L, Plaimauer B, Turecek PL, Rottensteiner H, Scheiflinger F. 2014. Persistence of circulating ADAMTS13-specific immune complexes in patients with acquired thrombotic thrombocytopenic purpura. *Haematologica*, 99: 779–87.

Ferrari S, Scheiflinger F, Rieger M, Mudde G, Wolf M, Coppo P, Girma JP, Azoulay E, Brun-Buisson C, Fakhouri F, Mira JP, Oksenhendler E, Poullin P, Rondeau E, Schleinitz N, Schlemmer B, Teboul JL, Vanhille P, Vernant JP, Meyer D, Veyradier A; French Clinical and Biological Network on Adult Thrombotic Microangiopathies. 2007. Prognostic value of anti-ADAMTS13 antibody features (Ig isotype, titer and inhibitory effect) in a cohort of 35 adult French patients undergoing a first episode of thrombotic microangiopathy with undetectable ADAMTS13 activity. *Blood*, 109(7): 2815-2822.

Feys HB, Anderson PJ, Vanhoorelbeke K, Majerus EM, Sadler JE. 2009. Multi-step binding of ADAMTS-13 to von Willebrand factor. *Journal of Thrombosis and Haemostasis*, 7(12): 2088-2095.

Feys HB, Liu F, Dong N, Pareyn I, Vauterin S, Vandeputte N, Noppe W, Ruan C, Deckmyn H, Vanhoorelbeke K. 2006. ADAMTS-13 plasma level determination uncovers antigen absence in acquired thrombotic thrombocytopenic purpura and ethnic differences. *Journal of Thrombosis and Haemostasis*, 4: 955-962. DOI:10.1111/j.1538-7836.2006.01833.x

Feys HB, Vandeputte N, Palla R, Peyvandi F, Peerlinck K, Deckmyn H, Lijnen HR, Vanhoorelbeke K. 2010. Inactivation of ADAMTS13 by plasmin as a potential cause of thrombotic thrombocytopenic purpura. *Journal of Thrombosis and Haemostasis*, 8: 2053 – 2062. DOI: 10.1111/j.1538-7836.2010.03942.x

Findlay JW, Smith WC, Lee JW, Nordblom GD, Das I, DeSilva BS, Khan MN, Bowsher RR. 2000. Validation of immunoassays for bioanalysis: a pharmaceutical industry perspective. *Journal of Pharmaceutical and Biomedical Analysis*, 21(6): 1249-1273. [PMID: 10708409]

Fontana S, Gerritsen HE, Kremer Hovinga J, Furlan M, Lämmle B. 2001. Microangiopathic haemolytic anaemia in metastasizing malignant tumours is not associated with, a severe deficiency of the von Willebrand factor-cleaving protease. *British Journal of Haematology*, 113: 100–102. DOI:10.1046/j.1365-2141.2001.02704.x

Fritzen A, Risinger C, Korukluoglu G, Christova I, Corli Hitzeroth A, Viljoen N, Burt FJ, Mirazimi A, Blixt O. 2018. Epitope-mapping of the glycoprotein from Crimean-Congo hemorrhagic fever virus using a microarray approach. *Public Library of Science Neglected Tropical Diseases*, 12(7): 1-15. DOI: 10.1371/journal.pntd.0006598.

Fu X, Kassim SY, Parks WC, Heinecke JW. 2001. Hypochlorous acid oxygenates the cysteine switch domain of pro-matrilysin (MMP-7). A mechanism for matrix metalloproteinase activation and atherosclerotic plaque rupture by myeloperoxidase. *Journal Biological Chemistry*, 276: 41279-41287.

Fujimura Y, Matsumoto M. 2010. Registry of 919 patients with thrombotic microangiopathies across Japan: database of Nara Medical University during 1998-2008. *Internal Medicine*, 49: 7-15.

Furie B and Furie BC. 2004. Role of platelet P-selectin and microparticle PSGL-1 in thrombus formation. *Trends in Molecular Medicine*, 10(4): 171-178.

Furlan M, Robles R, Galbusera M, Remuzzi G, Kyrle PA, Brenner B, Krause M, Scharrer I, Aumann V, Mittler U, Solenthaler M, Lämmle B. 1998. von Willebrand Factor-cleaving protease in thrombotic thrombocytopenia purpura and haemolytic-uremic syndrome. *New England Journal of Medicine*, 339: 1578-1584.

Furlan M, Robles R, Lämmle B. 1996. Partial purification and characterization of a protease from human plasma cleaving von Willebrand factor to fragments produced by *in vivo* proteolysis. *Blood*, 87:4223-4234.

Furlan M, Robles R, Morselli B, Sandoz P, Lämmle B. 1999. Recovery and half-life of von Willebrand factor-cleaving protease after plasma therapy in patients with thrombotic thrombocytopenic purpura. *Thrombosis and Haemostasis*, 81: 8-13.

Furlan M, Robles R, Solenthaler M, Wassmer M, Sandoz P and Lämmle B. 1997. Deficient activity of von Willebrand Factor-cleaving protease in chronic relapsing thrombotic thrombocytopenic purpura. *Blood*, 89: 3097-3103.

Fyfe-Brown A, Clarke G, Nerenberg K, Chandra S, Jain V. 2013. Management of pregnancy-associated thrombotic thrombocytopenia purpura. *American Journal of Perinatology Reports*, 3(1): 45-50. DOI: 10.1055/s-0032-1331380

Gao W, Anderson PJ, Majerus EM, Tuley EA, Sadler JE. 2006. Exosite interactions contribute to tension-induced cleavage of von Willebrand factor by the antithrombotic ADAMTS13 metalloprotease. *Proceedings of the National Academy of Sciences of the United States of America*, 103: 19099-19104.

Gao W, Anderson PJ, Sadler JE. 2008. Extensive contacts between ADAMTS13 exosites and von Willebrand factor domain A2 contribute to substrate specificity. *Blood*, 112: 1713-1719. [PubMed: 18492952]

Gardner MD, Chion CK, de Groot, Shah A, Crawley JT and Lane DA. 2009. A functional calcium-binding site in the metalloprotease domain of ADAMTS13. *Blood*, 113: 1149-1157. [PubMed: 19047683]

Garvey B. 2008. Rituximab in the treatment of autoimmune haematological disorders. *British Journal of Haematology*, 141(2): 149-169.

GenBank: Accession number: AAL11095.1. 1988. ADAMTS13 Protein. Bethesda (MD). National Center for Biotechnology Information ADAMTS13 [Homo sapiens]. National Library of Medicine, United States of America. <http://www.ncbi.nlm.nih.gov/protein/AAL11095.1>

Gentric A, Blaschek M, Julien C, Jouquan J, Pennec Y, Berthelot JM, Mottier D, Casburn-Budd R, Youinou P. 1991. Nonorganspecific autoantibodies in individuals infected by type 1 human immunodeficiency virus. *Clinical Immunology and Immunopathology*, 59: 487-494.

George JN, Terell DR, Vesely SK, Kremer Hovinga JA, Lämmle B. 2012. Thrombotic microangiopathic syndromes associated with drugs, HIV infection, hematopoietic stem cell transplantation and cancer. *La Presse Médicale*, 41(3P2): e177 – e188.

George JN. 2010. How I treat patients with thrombotic thrombocytopenic purpura: 2010. *Blood*, 16: 4060-4069.

George JN. 2015. Measuring ADAMTS13 activity in patients with suspected thrombotic thrombocytopenic purpura: when, how, and why? *Transfusion*, 55(1): 11-3. DOI: 10.1111/trf.12885.

George P, Das J, Pawar B, Kakkar N. 2008. Thrombotic thrombocytopenic purpura and systemic lupus erythematosus: Successful management of a rare presentation. *Indian Journal of Critical Care Medicine*, 12(3): 128-131.

Glaser CB, Morser J, Clarke JH, Blasko E, McLean K, Kuhn I, Chang RJ, Lin JH, Vilander L, Andrews WH, Light DR. 1992. Oxidation of a specific methionine in thrombomodulin by activated neutrophil products blocks cofactor activity. A potential rapid mechanism for modulation of coagulation. *Journal of Clinical Investigation*, 90: 2565-2573.

Golding H, Shearer GM, Hillman K, Lucas P, Manischewitz J, Zajac RA, Clerici M, Gress RE, Boswell RN, Golding B. 1989. Common epitope in human immunodeficiency virus (HIV) -gp41 and HLA class II elicits

immunosuppressive autoantibodies capable of contributing to immune dysfunction in HIV I infected individuals. *Journal of Clinical Investigations*, 83: 1430–1435. DOI:10.1172/JCI114034.

Goulabchand R, Vincent T, Batteux F, Eliaou JF, Guilpain P. 2014. Impact of autoantibody glycosylation in autoimmune diseases. *Autoimmunity Reviews*, 13: 742–750.

Grillberger R, Casina VC, Turecek PL, Zheng XL, Rottensteiner H, Scheiflinger F. 2014. Anti-ADAMTS13 IgG autoantibodies present in healthy individuals share linear epitopes with those in patients with thrombotic thrombocytopenia purpura. *Haematological*, 99: e58-e60. DOI:10.3324/haematol.2013.100685.

Gunther K, Garizio D, Dhlamini B. 2006. The pathogenesis of HIV-related thrombotic thrombocytopenic purpura – is it different? *International Society of Blood Transfusion Science Series*, 1: 246–250.

Gunther K, Garizio D, Nesara P. 2007. ADAMTS13 activity and the presence of acquired inhibitors in human immunodeficiency virus-related thrombotic thrombocytopenic purpura. *Transfusion*, 47(9): 1710 – 1716.

Haberichter SL, Balistreri M, Christopherson P, Morateck P, Gav-azova S, Bellissimo DB, Manco-Johnson MJ, Gill JC, Montgomery RR. 2006. Assay of the von Willebrand factor (VWF) propeptide to identify patients with type 1 von Willebrand disease with decreased VWF survival. *Blood*, 108: 3344-3351.

Haberichter SL. 2015. von Willebrand factor propeptide: biology and clinical utility. *Blood*, 126: 1753 – 1761.

Hantgan RR, Hermans J. 1979. Assembly of fibrin. A light scattering study. *Journal of Biological Chemistry*, 254: 11272-11281.

Hart D, Sayer R, Miller R, Edwards S, Kelly A, Baglin T, Hunt B, Benjamin S, Patel R, Machin S, Scully M. 2011. Human immunodeficiency virus associated thrombotic thrombocytopenic purpura--favourable outcome with plasma exchange and prompt initiation of highly active antiretroviral therapy. *British Journal of Haematology*, 153(4): 515-519.

Heidel F, Lipka DB, von Auer C, Huber C, Scharrer I, Hess G. 2007. Addition of rituximab to standard therapy improves response rate and progression-free survival in relapsed or refractory thrombotic thrombocytopenic purpura and autoimmune haemolytic anaemia. *Journal of Thrombosis and Haemostasis*, 97:228-233.

Herbei L and Venugopal P. 2006. Recurrent thrombotic thrombocytopenic purpura treated repeatedly and successfully with the monoclonal antibody rituximab. *Clinical advances in hematology and oncology*, 4:215-217.

Hess C, Winkler A, Lorenz AK, Holeccka V, Blanchard V, Eiglmeier S, Schoen A-L, Bitterling J, Stoehr A, Petzold D, Schommartz T, Mertes M, Schoen C, Tiburzy B, Herrmann A, Köhl J, Manz R, Madaio M, Berger M, Ehlers M. 2013. T cell-independent B cell activation induces immunosuppressive sialylated IgG antibodies. *The Journal of Clinical Investigation*, 123: 3788–96.

Heuzenroeder MW, Barton MD, Vanniasinkam T, Phumoonna T. 2009. Linear B-Cell Epitope Mapping Using Enzyme-Linked Immunosorbent Assay for Libraries of Overlapping Synthetic Peptides. In: Schutkowski M., Reineke U. (eds) *Epitope Mapping Protocols. Methods in Molecular Biology™ (Methods and Protocols)*, vol 524. Humana Press. United States of America.

Hillyer P, Mordelet E, Flynn G, Male D. 2003. Chemokines, chemokine receptors and adhesion molecules on different human endothelia: discriminating the tissue-specific functions that affect leucocyte migration. *Clinical and Experimental Immunology*, 134: 431-441.

Hofmann K, Clauder AK, Manz RA. 2018. Targeting B Cells and Plasma Cells in Autoimmune Diseases. *Frontiers in Immunology*, 9: 835-851. <https://www.frontiersin.org/article/10.3389/fimmu.2018.00835>.

- Hosler** GA, Cusumano AM, Hutchins GM. 2003. Thrombotic thrombocytopenic purpura and hemolytic uremic syndrome are distinct pathologic entities. A review of 56 autopsy cases. *Archives of Pathology and Laboratory Medicine*, 127: 834–839.
- Houghten** RA, Pinilla C, Blondelle SE, Appel JR, Dooley CT, Cuervo JH. 1991. Generation and use of synthetic peptide combinatorial libraries for basic research and drug discovery. *Nature*, 354: 84-86.
- Hrdinová** J, D'Angelo S, Graça, NAG, Ercig B, Vanhoorelbeke K, Veyradier A, Voorberg J, Coppo P. 2018. Dissecting the pathophysiology of immune thrombotic thrombocytopenic purpura: interplay between genes and environmental triggers. *Haematologica*, 103(2): 1099-1109.
- Hughes** C, Mcewan JR, Longair I, Hughes S, Cohen H, Machin S, Scully M. 2009. Cardiac involvement in acute thrombotic thrombocytopenic purpura: association with troponin T and IgG antibodies to ADAMTS 13. *Journal of Thrombosis and Haemostasis*, 7: 529-536. DOI:10.1111/j.1538-7836.2009.03285.x
- Hunt** PW. 2012. HIV and inflammation: mechanisms and consequences. *Current HIV/AIDS Reports*, 9: 139–147.
- Huse** K, Böhme HJ, Scholz GH. 2002. Purification of antibodies by affinity chromatography. *The Journal of Biochemical and Biophysical Methods*, 51: 217–231.
- Hymes** KB, Karpatkin S. 1997. Human immunodeficiency virus infection and thrombotic microangiopathy. *Seminars in Hematology*, 34: 117–25.
- Igari** A, Nakagawa T, Moriki T, Yamaguchi Y, Matsumoto M, Fujimura Y, Soejima K, Murata M. 2012. Identification of epitopes on ADAMTS13 recognized by a panel of monoclonal antibodies with functional or non-functional effects on catalytic activity. *Thrombosis Research*, 130: e79-e83.
- Ikeda** K, Nagasawa K, Horiuchi T, Tsuru T, Nishizaka H, Niho Y. 1997. C5a induces tissue factor activity on endothelial cells. *Journal of Thrombosis and Haemostasis*, 77(2): 394-398.
- Irlam** JH, Siegfried N, Visser ME, Rollins NC. 2013. Micronutrient supplementation for children with HIV infection. *The Cochrane database of systematic reviews*. (10):CD010666. DOI: 10.1002/14651858.CD010666.
- Ito-Habe** N, Wada H, Matsumoto T, Ohishi K, Toyoda H, Ishikawa E, Nomura S, Komada Y, Ito M, Nobori T, Katayama N. 2011. Elevated von Willebrand factor propeptide for the diagnosis of thrombotic microangiopathy and for predicting a poor outcome. *International Journal of Hematology*, 93: 47–52.
- Jackson** SP. 2011. Arterial thrombosis-insidious unpredictable and deadly: A Review. *Nature Medicine*, 17(11): 1423-1436.
- Janeway** CA Jr, Travers P, Walport M, Shlomchik MJ. 2001. *Immunobiology: The immune system in health and disease*. 5th Edition. New York: Garland Sciences. New York, United States of America. <https://www.ncbi.nlm.nih.gov/books/NBK10757/>
- Jang** MJ, Chong SY, Kim IH, Kim JH, Jung CW, Kim JK, Park JC, Lee SM, Kim YK, Lee JE, Jang SS, Kim JS, Jo DY, Zang DY, Lee YY, Yhim HY, Oh D. 2011. Clinical features of severe acquired ADAMTS13 deficiency in thrombotic thrombocytopenic purpura: the Korean TTP registry experience. *International Journal of Hematology*, 93: 163–169.
- Jasti** S, Coyle T, Gentile T, Rosales L, Poiesz B. 2008. Rituximab as an adjunct to plasma exchange in TTP: a report of 12 cases and review of literature. *Journal of Clinical Apheresis*, 23:151-156.
- Jennewein** MF and Alter G. 2017. The Immunoregulatory Roles of Antibody Glycosylation. *Trends in Immunology*, 38(5): 358-372. ISSN 1471-4906. <https://doi.org/10.1016/j.it.2017.02.004>.

- Jimenez JJ, Jy W, Mauro LM, Horstman LL and Ahn YS.** 2001. Elevated endothelial microparticles in thrombotic thrombocytopenic purpura: findings from brain and renal microvascular cell culture and patients with active disease. *British Journal of Haematology*, 112: 81-90.
- Jimenez JJ, Jy W, Mauro LM, Horstman LL, Soderland C, Ahn YS.** 2003. Endothelial microparticles released in thrombotic thrombocytopenic purpura express von Willebrand factor and markers of endothelial activation. *British Journal of Haematology* 123: 896-902
- Jimenez JJ, Jy W, Mauro LM, Mauro AC, Horstman LL, Ahn YS.** 2005. Endothelial Microparticles (EMP) Inhibit ADAMTS13 Activity: Implications in Thrombotic Thrombocytopenic Purpura. *Blood*, 106 (11): 3676. DOI: <https://doi.org/10.1182/blood.V106.11.3676.3676>
- Jin SY, Skipwith CG, Shang D, Zheng XL.** 2009. Von Willebrand factor cleaved from endothelial cells by ADAMTS13 remains ultralarge in size. *Journal of Thrombosis and Haemostasis*, 7:1749-1752. [PubMed: 19682236]
- Jin SY, Skipwith CG, Shang D, Zheng XL.** 2010. Amino acid residues Arg659, Arg660, and Tyr 661 in the spacer domain of ADAMTS13 are critical for cleavage of von Willebrand factor. *Blood*, 115(11): 2300-2310.
- Jokela J, Flynn T, Henry K.** 1987. Thrombotic thrombocytopenia purpura in a human immunodeficiency virus (HIV)-seropositive homosexual man. *American Journal of Haematology*, 25:341-343.
- Joly BS, Coppo P, Veyradier A.** 2017. Thrombotic thrombocytopenic purpura. *Blood*, 129(21): 2836 LP-2846.
- Joseph G, Smith KJ, Hadley TJ, Djulbegovic B, Troup GM, Oldfather J, Barker RL.** 1994. HLADR53 protects against thrombotic thrombocytopenic purpura/adult hemolytic uremic syndrome. *American Journal of Hematology*, 47(3): 189-193.
- Jy W, Jimenez JJ, Mauro LM, Horstman LL, Cheng P, Ahn ER, Bidot CJ, Ahn YS.** 2005. Endothelial microparticles induce formation of platelet aggregates via a von Willebrand factor/ristocetin dependent pathway, rendering them resistant to dissociation. *Journal of Thrombosis and Haemostasis*, 3(6):1301-1308.
- Jy W, Jimenez JJ, Minagar A, Mauro LM, Horstman LL, Bidot CJ, Sheremata WA, Ahn YS.** 2002b. Endothelial microparticles (EMP) enhance adhesion and transmigration of monocytes: EMP-monocyte conjugates as a marker of disease activity in multiple sclerosis (MS). *Blood*, 11(part 2): 460.
- Kasper CK, Aledort LM, Counts RB, Edson JR, Fratantoni J, Green D, Hampton JW, Hilgartner MW, Lazerson J, Levine PH, McMillan CW, Pool JG, Shapiro SS, Shulman NR, Van Eys J.** 1975. A more uniform measurement of factor VIII inhibitors. *Thrombosis et Diathesis Haemorrhagica*, 34: 869–72.
- Keiser SD, Boyd KW, Rehberg JF, Elkins S, Owens MY, Sunesara I, Martin JN Jr.** 2012. A high LDH to AST ratio helps to differentiate pregnancy-associated thrombotic thrombocytopenic purpura (TTP) from HELLP syndrome. *Journal of Maternal-Fetal and Neonatal Medicine*, 25: 1059–1063.
- Khodadadi L, Cheng Q, Alexander T, Sercan-Alp Ö, Klotsche J, Radbruch A, Hiepe F, Hoyer BF, Taddeo A.** 2015. Bortezomib Plus Continuous B Cell Depletion Results in Sustained Plasma Cell Depletion and Amelioration of Lupus Nephritis in NZB/W F1 Mice. *Public Library of Science One*, 10(8): e0135081. DOI: [10.1371/journal.pone.0135081](https://doi.org/10.1371/journal.pone.0135081).
- Klaus C, Plaismauer B, Studt JD, Dorner F, Lämmle B, Mannucci PM, Scheiflinger, F.** 2004. Epitope mapping of ADAMTS13 autoantibodies in acquired thrombocytopenia thrombocytopenic purpura. *Blood*, 103: 4514-4519.

Kokame K, Matsumoto M, Soejima K, Yagi H, Ishizashi H, Funato M, Tamai H, Konno M, Kamide K, Kawano Y, Miyata T, Fujimura Y. 2002. Mutations and common polymorphisms in ADAMTS13 gene responsible for von Willebrand factor-cleaving protease activity. *Proceedings of the National Academy of Sciences of the United States of America*, 99: 11902–11907. <http://dx.doi.org/10.1073/pnas.172277399>.

Kokame K, Nobe Y, Kokubo Y, Okayama A, Miyata T. 2005. FRET-VWF73, a first fluorogenic substrate for ADAMTS13 assay. *British Journal of Haematology*, 129: 93-100. DOI:10.1111/j.1365-2141.2005.05420.x

Kong D, Liu J, Jiang Q, Yu Z, Hu X, Guo D, Huang Q, Jiao M, Qu L. 2016. Production, Characterization, and Epitope Mapping of Monoclonal Antibodies Against Different Subtypes of Rabbit Hemorrhagic Disease Virus (RHDV). *Scientific Reports*, 6: 20857. DOI:10.1038/srep20857.

Kopelman RG, Zola-Pazner S. 1988. Association of human immunodeficiency virus infection and autoimmune phenomena. *American Journal of Medicine*, 84: 82–88.

Kremer-Hovinga JA, Heeb SR, Skowronska M, Schaller, M. 2018. Pathophysiology of thrombotic thrombocytopenic purpura and hemolytic uremic syndrome. *Journal of Thrombosis and Haemostasis*, 16: 618–29.

Kringelum JV, Nielsen M, Padkjær SB, Lund O. 2013. Structural analysis of B-cell epitopes in antibody:protein complexes. *Molecular Immunology*, 53(1–2): 24-34. <https://doi.org/10.1016/j.molimm.2012.06.001>.

Kumar A and Rao AT. 1991. Double-antibody sandwich ELISA for detection of infectious bursal disease virus. *British Veterinary Journal*, 147(3): 251-5.

Laemmler U. 1970. Cleavage of Structural Proteins during the Assembly of the Head of Bacteriophage T4. *Nature*, 227: 680–685. <https://doi.org/10.1038/227680a0>

Lam JK, Chion CK, Zanardelli S, Lane DA, Crawley JT. 2007. Further characterization of ADAMTS-13 inactivation by thrombin. *Journal of Thrombosis and Haemostasis*, 5: 1010–1018.

Lancellotti S, Basso M and De Cristofaro R. 2013. Proteolytic processing of von Willebrand Factor by ADAMTS13 and Leukocyte proteases. *Mediterranean Journal of Haematology and Infectious Diseases*, 5(1): 1-15.

Lattuada A, Rossi E, Calzarossa C, Candolfi R, Mannucci PM. 2003. Mild to moderate reduction of a von Willebrand factor cleaving protease (adamts-13) in pregnant women with HELLP microangiopathic syndrome. *Haematologica*, 88: 1029-1034.

Ledford-Kraemer MR. 2010. Analysis of von Willebrand factor structure by multimer analysis. *American Journal of Hematology*, 85: 510-514.

Lenting PJ, van Mourik JA, Mertens K. 1998. The life cycle of coagulation factor VIII in view of its structure and function. *Blood*, 92: 3983-3996.

Leopold JA. 2013. Chapter 2 - *The Endothelium*. Editor(s): Mark A. Creager, Joshua A. Beckman, Joseph Loscalzo, *Vascular Medicine: A Companion to Braunwald's Heart Disease (second Edition)*. W.B. Saunders. United States of America. <https://doi.org/10.1016/B978-1-4377-2930-6.00002-1>.

Levy GG, Nichols WC, Lian EC, Foroud T, McClintick JN, McGee BM, Yang AY, Siemieniak DR, Stark KR, Gruppo R, Sarode R, Shurin SB, Chandrasekaran V, Stabler SP, Sabio H, Bouhassira EE, Upshaw JD Jr, Ginsburg D, Tsai HM. 2001. Mutations in a member of the ADAMTS gene family cause thrombotic thrombocytopenic purpura. *Nature*, 413(6855): 488 – 94.

- Li A**, Khalighi PR, Wu Q, Garcia DA. 2018. External validation of the PLASMIC score: a clinical prediction tool for thrombotic thrombocytopenic purpura diagnosis and treatment. *Journal of Thrombosis and Haemostasis*, 16(1): 164-169. [DOI: 10.1111/jth.13882].
- Li D**, Xiao J, Paessler M, Zheng XL. 2011. Novel recombinant glycosylphosphatidylinositol (GPI)-anchored ADAMTS13 and variants for assessment of anti-ADAMTS13 autoantibodies in patients with thrombotic thrombocytopenic purpura. *Journal of Thrombosis and Haemostasis*, 106: 947–958. [PubMed: 21901237]
- Liu L**, Choi H, Bernardo A, Bergeron A, Nolasco L, Ruan C, Moake L, Dong J-F. 2005. Platelet-derived VWF-cleaving metalloprotease ADAMTS13. *The Journal of Thrombosis and Haemostasis*, 3: 2536-2544.
- Liu R**, Amanda M. Enstrom, and Kit S. Lam. 2003. Combinatorial peptide library methods for immunobiology research. *Experimental Hematology*, 31: 11–30.
- Liu R**, Enstrom AM, Lam KS. 2003. Combinatorial peptide library methods for immunobiology research. *Experimental Haematology*, 31: 11-30.
- Lopez JA** and Dong JF. 2004. Cleaving of Von Willebrand factor by ADAMTS13 on endothelial cells. *Seminars in Hematology*, 41: 15-23. <http://dx.doi.org/10.1053/j.seminhematol.2003.10.004>.
- Lotta LA**, Lombardi R, Mariani M, Lancellotti S, De Cristofaro R, Hollestelle MJ, Canciani MT, Mannucci PM, Peyvandi F. 2011. Platelet reactive conformation and multimeric pattern of von Willebrand factor in acquired thrombotic thrombocytopenic purpura during acute disease and remission. *Journal of Thrombosis and Haemostasis* 9: 1744-1751.
- Lotta LA**, Valsecchi C, Pontiggia S, Mancini I, Cannavo A, Artoni A, Mikovic D, Meloni G, Peyvandi F. 2014. Measurement and prevalence of circulating ADAMTS13-specific immune complexes in autoimmune thrombotic thrombocytopenic purpura. *Journal of Thrombosis and Haemostasis*, 12: 329-36.
- Louw S**, Gounden R and Mayne ES. 2018. Thrombotic thrombocytopenic purpura (TTP)-like syndrome in the HIV era. *Thrombosis Journal*, 16(35): 1-7.
- Lowe GD**, Woodward M, Rumley A, Morrison CE, Nieuwenhuizen W. 2003. Associations of plasma fibrinogen assays, C-reactive protein and interleukin-6 with previous myocardial infarction. *Journal of Thrombosis and Haemostasis* 1: 2312-2316.
- Lu LL**, Chung AW, Rosebrock TR, Ghebremichael M, Yu WH, Grace PS, Schoen MK, Tafesse F, Martin C, Leung V, Mahan AE. 2016. A functional role for antibodies in tuberculosis. *Cell*, 167(2): 433-443.
- Ludwig RJ**, Vanhoorelbeke K, Leyboldt F, Kaya Z, Bieber K, McLachlan SM, Komorowski L, Luo J, Cabral-Marques O, Hammers CM, Lindstrom JM, Lamprecht P, Fischer A, Riemekasten G, Tersteeg C, Sondermann P, Rapoport B, Wandinger K-P, Probst C, El Beidaq A, Schmidt E, Verkman A, Manz RA, Nimmerjahn F. 2017. Mechanisms of Autoantibody-Induced Pathology. *Frontiers in Immunology*, 8: 1-42. <https://www.frontiersin.org/article/10.3389/fimmu.2017.00603>
- Luken BM**, Kaijen PH, Turenhout EA, Kremer Hovinga JA, van Mourik JA, Fijnheer R, Voorberg J. 2006. Multiple B-cell clones producing antibodies directed to the spacer and disintegrin/thrombospondin type-1 repeat 1 (TSP1) of ADAMTS13 in patients with acquired thrombotic thrombocytopenic purpura. *Journal of Thrombosis and Haemostasis*, 4: 2355-2364.
- Luken BM**, Turenhout EA, Kaijen PH, Fijnheer R, Voorberg J. 2006. Amino acid regions 572-579 and 657-666 of the spacer domain of ADAMTS13 provide a common antigenic core required for binding of antibodies in patients with acquired TTP. *Journal of Thrombosis and Haemostasis*, 96: 295-301.

Luken BM, Winn LY, Emsley J, Lane DA, Crawley JT. 2010. The importance of vicinal cysteines, C1669 and C1670, for von Willebrand factor A2 domain function. *Blood*, 115(23): 4910-4913.

Luken MB, Turenhout EA, Hulstein JJ, Van Mourik JA, Fijnheer R, Voorberg J. 2005. The spacer domain of ADAMTS13 contains a major binding site for antibodies in patients with thrombotic thrombocytopenic purpura. *Journal of Thrombosis and Haemostasis* 93: 267-274.

Majerus EM, Anderson PJ, Sadler JE. 2005. Binding of ADAMTS13 to von Willebrand factor. *Journal of Biological Chemistry*, 280(23): 21773-21778.

Majerus EM, Zheng X, Tuley EA, Sadler JE. 2003. Cleavage of the ADAMTS13 propeptide is not required for protease activity. *Journal of Biological Chemistry*, 278: 46643-46648.

Majumder R, Liang X, Quinn-Allen MA, Kane WH, Lentz BR. 2011. Modulation of prothrombinase assembly and activity by phosphatidylethanolamine. *Journal of Biological Chemistry*, 286(41): 35535–35542. DOI:10.1074/jbc.M111.260141

Mancini I, Ricano-Ponce I, Pappalardo E, Cairo A, Gorski MM, Casoli G, Ferrari B, Alberti M, Mikovic D, Noris M, Wijmenga C, Peyvandi F. 2016. ImmunoChip analysis identifies novel susceptibility loci in the human leukocyte antigen region for acquired thrombotic thrombocytopenic purpura. *Journal of Thrombosis and Haemostasis*, 14: 2356-2367.

Mancini I, Ricano-Ponce I, Pappalardo E, Cairo A, Gorski MM, Casoli G, Ferrari B, Alberti M, Mikovic D, Noris M, Wijmenga C, Peyvandi F, Italian Group of TTP Investigators. 2016. ImmunoChip analysis identifies novel susceptibility loci in the human leukocyte antigen region for acquired thrombotic thrombocytopenic purpura. *Journal of Thrombosis and Haemostasis*, 14 (12): 2356-2367.

Mancini, I, Valsecchi, C, Palla, R, Lotta, LA, Peyvandi, F. 2012. Measurement of anti-ADAMTS13 neutralizing autoantibodies: A comparison between CBA and FRET assays. *Journal of Thrombosis and Haemostasis*, 10(7): 1439-1442. <https://doi.org/10.1111/j.1538-7836.2012.04744.x>

Mannoor K, Xu Y, Chen C. 2013. Natural autoantibodies and associated B cells in immunity and autoimmunity. *Autoimmunity*, 46: 138–147.

Mannucci PM, Vanoli M, Forza I, Canciani MT, Scorza R. 2003. Von Willebrand factor cleaving protease (ADAMTS-13) in 123 patients with connective tissue diseases (systemic lupus erythematosus and systemic sclerosis). *Haematologica*, 88: 914-918.

Mannucci PM, Vanoli M, Forza I, Canciani MT, Scorza R. 2003. Von Willebrand factor cleaving protease (ADAMTS-13) in 123 patients with connective tissue diseases (systemic lupus erythematosus and systemic sclerosis) *Haematologica*, 88: 914–918.

Marincowitz C, Genis A, Goswami N, Boever PD, Nawrot TS, Strijdom H. 2019. Vascular endothelial dysfunction in the wake of HIV and ART. *Federation of European Biochemical Society Journal*, 286(7): 1256–1270. <https://doi.org/10.1111/febs.14657>

Mariotte E, Azoulay E, Galicier L, Rondeau E, Zouiti F, Boisseau P, Poullin P, de Maistre E, Provôt F, Delmas Y, Perez P, Benhamou Y, Stepanian A, Coppo P, Veyradier A. 2016. Epidemiology and pathophysiology of adulthood-onset thrombotic microangiopathy with severe ADAMTS13 deficiency (thrombotic thrombocytopenic purpura): a cross-sectional analysis of the French national registry for thrombotic microangiopathy. *The Lancet Haematology*, 3(5): e237–e245.

- Masoet A**, Bassa F and Chothia MY. 2019. HIV-associated thrombotic thrombocytopenic purpura: A retrospective cohort study during the anti-retroviral therapy era. *Journal of Clinical Apheresis*, 1-7. [DOI: 10.1002/jca.21692]
- Massabki PS**, Accetturi C, Nishie IA, da Silva N, Sato EI, Andrade LEC. 1997. Clinical implications of autoantibodies in HIV infection. *The Journal of Acquired Immune Deficiency Syndromes*, 11: 1845-1850.
- Matsui H**, Sugimoto M, Mizuno T, Tsuji S, Miyata S, Matsuda M, Yoshioka A. 2002. Distinct concerted functions of von Willebrand factor and fibrinogen in mural thrombus growth under high shear flow. *Blood*, 100: 3604-3610.
- McDonald V**, Laffan M, Benjamin S, Bevan D, Machin S, Scully MA. 2009. Thrombotic thrombocytopenic purpura precipitated by acute pancreatitis: A report of seven cases from a regional UK TTP registry. *British Journal of Haematology*, 144: 430-433.
- McHeyzer-Williams LJ**, Pelletier N, Mark L, Fazilleau N, McHeyzer-Williams MG. 2009. Follicular helper T cells as cognate regulators of B cell immunity. *Current Opinion in Immunology*, 21: 266-273.
- McKinnon TA**, Chion AC, Millington AJ, Lane DA, Laffan MA. 2008. N-linked glycosylation of VWF modulates its interaction with ADAMTS13. *Blood*, 111(6): 3042-3049.
- McKinnon TA**, Goode EC, Birdsey GM, Nowak AA, Chan AC, Lane DA, Laffan MA. 2010. Specific N-linked glycosylation sites modulate synthesis and secretion of von Willebrand factor. *Blood*, 116(4): 640-648.
- Medina PJ**, Sipols JM, George JN. 2001. Drug-associated thrombotic thrombocytopenic purpura-hemolytic uremic syndrome. *Current opinion in hematology*, 8: 286-93.
- Meiring SM**, Webb M, Goedhals K and Louw V. 2012. HIV-associated TTP - what we know so far. *European Oncology and Haematology*, 8(20): 89-91.
- Meyer SC**, Sulzer I, Laemmle B, Kremer Hovinga JA. 2007. Hyperbilirubinemia interferes with ADAMTS-13 activity measurement by FRETsvWF73 assay: diagnostic relevance in patients suffering from acute thrombotic microangiopathies. *Journal of Thrombosis and Haemostasis*, 5: 866-870.
- Miyadera H**, Ohashi J, Lernmark Å, Kitamura T, Tokunaga K. 2015. Cell-surface MHC density profiling reveals instability of autoimmunity-associated HLA. *Journal of Clinical Investigation*, 125(1): 275-291.
- Moake JL**, Turner NA, Stathopoulos NA, Nolasco LH, Hellums JD. 1986. Involvement of large plasma von willebrand factor (vWF) multimers and unusually large vWF forms derived from endothelial cells in shear stress-induced platelet aggregation. *Journal of clinical investigations*, 67(6): 1456-1461.
- Moake JL**. 2002. Thrombotic microangiopathies. *The New England Journal of Medicine*, 347: 589-600.
- Moore J**, Wu X, Kulhavy R, Tomana M, Novak J, Moldoveanu Z, Brown R, Goepfert P, Mestecky J. 2005. Increased levels of galactose-deficient IgG in sera of HIV-1-infected individuals. *The Journal of Acquired Immune Deficiency Syndromes*, 19(4):381-389. DOI: 10.1097/01.aids.0000161767.21405.68.
- Morton JM** and George JN. 2016. Microangiopathic hemolytic anemia and thrombocytopenia in patients with cancer. *Journal of Oncology Practice*, 12: 523-530.
- Mounzer K**, DiNardo A, Goldstein K. 2007. Thrombotic thrombocytopenic purpura during immune reconstitution. *The Journal of Acquired Immune Deficiency Syndromes*, 21: 2559-2560.

- Nasiri H**, Valedkarimi Z, Aghebati-Maleki L, Abdolalizadeh J, Kazemi T, Esparvarinha M, Majidi J. 2017. Production and purification of polyclonal antibody against F(ab')₂ fragment of human immunoglobulin G. *Veterinary Research Forum*, 8(4): 307-312.
- Nester CM**, Barbour T, de Cordoba SR, Dragon-Durey MA, Fremeaux-Bacchi V, Goodship TH, Kavanagh D, Noris M, Pickering M, Sanchez-Corral P, Skerka C, Zipfel P, Smith RJ. 2015. Atypical aHUS: State of the art. *Molecular Immunology*, 67(1): 31-42.
- Nimmerjahn F**, Ravetch JV. 2008. Anti-inflammatory actions of intravenous immunoglobulin. *Annual Reviews of Immunology*, 26: 513–533.
- Nishio K**, Anderson PJ, Zheng XL, Sadler JE. 2004. Binding of platelet glycoprotein Iba α to von Willebrand factor domain A1 stimulates the cleavage of the adjacent domain A2 by ADAMTS13. *Proceedings of the National Academy of Sciences of the United States of America*, 101(29): 10578-10583.
- Nossent AY**, VAN Marion V, VAN Tilburg NH, Rosendaal FR, Bertina RM, VAN Mourik JA, Eikenboom HC. 2006. von Willebrand factor and its propeptide: the influence of secretion and clearance on protein levels and the risk of venous thrombosis. *Journal of Thrombosis and Haemostasis*, 4(12): 2556-2562.
- Novitzky N**, Thomson J, Abrahams L, du Toit C, McDonald A. 2005. Thrombotic thrombocytopenic purpura in patients with retroviral infection is highly responsive to plasma infusion therapy. *British Journal of Haematology*, 128: 373-379.
- O'Donnell JS**, McKinnon TA, Crawley JT, Lane DA, Laffan MA. 2005. Bombay phenotype is associated with reduced plasma-VWF levels and an increased susceptibility to ADAMTS13 proteolysis. *Blood*, 106(6):1988-1991.
- Ono T**, Mimuro J, Madoiwa S, Soejima K, Kashiwakura Y, Ishiwata A, Takano K, Ohmori T, Sakata Y. 2006. Severe secondary deficiency of von Willebrand factor-cleaving protease (ADAMTS13) in patients with sepsis-induced disseminated intravascular coagulation: its correlation with development of renal failure. *Blood*, 107: 528-534.
- ONOUE K**, YAGI Y, GROSSBERG AL, PRESSMAN D. 1965. Number of binding sites of rabbit macroglobulin antibody and its subunits. *Immunochemistry*, 2: 401-415.
- Osborne C** and Brooks SA. 2006. SDS-PAGE and Western blotting to detect proteins and glycoproteins of interest in breast cancer research. *Methods In Molecular Medicine*, 120: 217-229.
- Ostertag E**, Bdeir K, Kacir S, Thiboutot M, Gulendran G, Yunk L, Hayes V, Motto D, Poncz M, Zheng XL, Cines D, Siegel D. 2016. ADAMTS13 autoantibodies cloned from patients with acquired thrombotic thrombocytopenic purpura: 2. Pathogenicity in an animal model. *Transfusion*, 56.DOI: 10.1111/trf.13583.
- Ostertag EM**, Kacir S, Thiboutot M, Gulendran G, Zheng XL, Cines DB, Siegel DL. 2016. ADAMTS13 Autoantibodies Cloned from Patients with Acquired Thrombotic Thrombocytopenic Purpura: 1. Structural and functional characterization *in vitro*. *Transfusion*, 56(7): 1763–1774. [DOI:10.1111/trf.13584].
- Ovanesov MV**, Ananyeva NM, Panteleev MA, Ataulakhanov FI, Saenko EL. 2005. Initiation and propagation of coagulation from tissue factor-bearing cell monolayers to plasma: initiator cells do not regulate spatial growth rate. *Journal of Thrombosis and Haemostasis*, 3: 321-331. DOI:10.1111/j.1538-7836.2005.01128.x
- Padilla A**, Moake JL, Bernardo A, Ball C, Wang Y, Arya M, Nolasco L, Turner N, Berndt MC, Anvari B, Lopez JA and Dong JF. 2004. P-selectin anchors newly released ultralarge von Willebrand factor multimers to the endothelial cell surface. *Blood*, 103(6): 2150-2056.

- Page EE**, Kremer Hovinga JA, Terrell DR, Vesely SK, George JN. 2017. Thrombotic thrombocytopenic purpura: diagnostic criteria, clinical features, and longterm outcomes from 1995 through 2015. *Blood Advances*, 1(10): 590–600. DOI:10.1182/bloodadvances.2017005124
- Park YA**, Hay SN, Brecher ME. 2009. ADAMTS13 activity levels in patients with human immunodeficiency virus-associated thrombotic microangiopathy and profound CD4 deficiency. *Journal of Clinical Apheresis*, 24(1): 32-36. DOI: 10.1002/jca.20189.
- Pasquale D**, Vidhya R, DaSilva K, Tsan MF, Lansing L, Chikkappa G. 1998. Chronic relapsing thrombotic thrombocytopenic purpura: role of therapy with cyclosporine. *American Journal of Hematology*, 57: 57–61.
- Patriquin CJ**, Thomas MR, Dutt T, McGuckin S, Blombery PA, Cranfield T, Westwood JP, Scully M. 2016. Bortezomib in the treatment of refractory thrombotic thrombocytopenic purpura. *British Journal of Haematology*, 173: 779-785. DOI:10.1111/bjh.13993
- Perez CA**, Abdo N, Shrestha A, Santos AS. 2011. Systemic Lupus Erythematosus Presenting as Thrombotic Thrombocytopenia Purpura: How Close Is Close Enough? *Case Reports in Medicine*, 267508: 1-3. <http://dx.doi.org/10.1155/2011/267508>
- Peyvandi F**, Ferrari S, Lavoretano S, Canciani MT, Mannucci PM. 2004. Von Willebrand factor cleaving protease (ADAMTS-13) and ADAMTS-13 neutralizing autoantibodies in 100 patients with thrombotic thrombocytopenic purpura. *British Journal of Haematology*, 127(04): 433–439.
- Peyvandi F**, Lavoretano S, Palla R, Feys HB, Vanhoorelbeke K, Battaglioli T, Valsecchi C, Canciani MT, Fabris F, Zver S, Réti M, Mikovic D, Karimi M, Giuffrida G, Laurenti L, Mannucci PM. 2008. ADAMTS13 and anti-ADAMTS13 antibodies as markers for recurrence of acquired thrombotic thrombocytopenic purpura during remission. *Haematologica*, 93(20): 232-239.
- Peyvandi F**, Palla R, Lotta LA, Mackie I, Scully MA, Machin SJ. 2010. ADAMTS-13 assays in thrombotic thrombocytopenic purpura. *Journal of Thrombosis and Haemostasis*, 8: 631-640. DOI:10.1111/j.1538-7836.2010.03761.x
- Peyvandi F**, Scully M, Hovinga JAK, M.D., Cataland S, Knöbl P, Wu H, Artoni A, Westwood JP, Taleghani MM, Jilma B, Callewaert F, Ulrichts H, Duby C, Tersago D. 2016. Caplacizumab for Acquired Thrombotic Thrombocytopenic Purpura. *The New England Journal of Medicine*, 374(6): 511-522.
- Pickens B**, Jin SY, LiD, Zheng XL. 2012. Ectopic expression of ADAMTS13 in platelets as a novel therapeutic approach for arterial thrombosis. *Blood*, 120: 491-499.
- Pikal-Cleland KA**, Cleland JL, Anchordoquy TJ, Carpenter JF. 2002. Effect of glycine on pH changes and protein stability during freeze-thawing in phosphate buffer systems. *Journal of Pharmaceutical Sciences*, 9: 1969-79.
- Pimstone NR**. 1972. Renal degradation of hemoglobin. *Seminars in Hematology*, 9: 31-42.
- Pinilla C**, Appel JR, Houghten RA. 1994. Investigation of antigen-antibody interactions using a soluble, non-support bound synthetic decapeptide library composed of four trillion (4 x 10¹²) sequences. *Biochemistry Journal* 301: 847-853.
- Pinilla C**, Appel JR, Judkowski V, Houghten RA. 2012. Identification of B cell and T cell epitopes using synthetic peptide combinatorial libraries. *Current Protocols in Immunology*. DOI:10.1002/0471142735.im0905s99
- Porta C**, Bobbio-Pallavicini E, Centurioni R, Caporali R, Montecucco CM. 1993. Thrombotic thrombocytopenic purpura in systemic lupus erythematosus. *Journal of Rheumatology*, 20: 1625–1626.

- Pos W**, Crawley JT, Fijnheer R, Voorberg J, Lane DA, Luken BM. 2010. An autoantibody epitope comprising residues R660, Y661, and Y665 in the ADAMTS13 spacer domain identifies a binding site for the A2 domain of VWF. *Blood*, 115: 1640-1649.
- Pos W**, Sorvillo N, Fijnheer R, Feys HB, Kaijen PH, Vidarsson G, Voorberg J. 2011. Residues Arg568 and Phe592 contribute to an antigenic surface for anti-ADAMTS13 antibodies in the spacer domain. *Haematologica* 96: 1670-1677. [PubMed: 21712537]
- Pourrat O**, Coudroy R, Pierre F. 2015. Differentiation between severe HELLP syndrome and thrombotic microangiopathy, thrombotic thrombocytopenic purpura and other imitators. *European Journal of Obstetrics & Gynecology and Reproductive Biology*, 189: 68–72.
- Pudil R**, Krejsek J, Pidman V, Gregor J, Tichy M, Bures J. 2001. Inflammatory response to acute myocardial infarction complicated by cardiogenic shock. *Acta Medica Journal of faculty of Medicine in Hradec.Kralove*, 44: 149-151.
- Raife TJ**, CaoW, Atkinson BS, Bedell B, Montgomery RR, Lentz SR, Johnson GF, Zheng XL. 2009Leukocyte proteases cleave von Willebrand factor at or near the ADAMTS13 cleavage site. *Blood*, 114: 1666–74.
- Reese JA**, Muthurajah DS, Kremer Hovinga JA, Vesely SK, Terrell DR, George JN. 2013. Children and adults with thrombotic thrombocytopenic purpura associated with severe, acquired ADAMTS13 deficiency: comparison of incidence, demographic and clinical features. *Pediatric Blood and Cancer*, 60(10): 1676-1682.
- Regierer AC**, Kuehnhardt D, Schulz C-O, Flath B, Jehn CF, Scholz CW, Possinger K, Eucker J. 2011. Breast Cancer-Associated Thrombotic Microangiopathy. *Breast Care Journal (Basel)* 6(6): 441–445. [DOI: 10.1159/000335201]
- Reineke U**. 2009. Antibody Epitope Mapping Using De Novo Generated Synthetic Peptide Libraries. In: Schutkowski M., Reineke U. (editors) *Epitope Mapping Protocols. Methods in Molecular Biology™ (Methods and Protocols)*, volume 524. Humana Press. Unite States of America. https://doi.org/10.1007/978-1-59745-450-6_14.
- Reineke U**. 2009. Antibody epitope mapping using de novo generated synthetic peptide libraries. *Methods in Molecular Biology*, 524: 203–11.
- Reti M**, Farkas P, Csuka D, Razso K, Schlamadinger A, Udvardy ML, Madach K, Domjan G, Bereczki C, Reusz GS, Szabo AJ, Prohaszka Z. 2012. Complement activation in thrombotic thrombocytopenic purpura. *Journal of Thrombosis and Haemostasis*, 10: 791–798.
- Rieger M**, Ferrari S, Kremer Hovinga JA, Konetschny C, Herzog A, Koller L, Weber A, Remuzzi G, Dockal, M, Plaimauer B, Scheiflinger F. 2006. Relation between ADAMTS13 activity and ADAMTS13 antigen levels in healthy donors and patients with thrombotic microangiopathies (TMA). *Journal of Thrombosis and Haemostasis*, 95: 212–220. [PubMed: 16493480]
- Rieger M**, Mannucci PM, Kremer Hovinga JA, Herzog A, Gerstenbauer G, Konetschny C, Zimmermann K, Scharrer I, Peyvandi F, Galbusera M, Remuzzi G, Bohm M, Plaimauer B, Lammle B, Scheiflinger F. 2005. ADAMTS13 autoantibodies in patients with thrombotic microangiopathies and other immunomediated diseases. *Blood*, 106: 1262-1267. <http://dx.doi.org/10.1182/blood-2004-11-4490>.
- Ripamonti D**, Gregis G, Casari S, Suarfli MG, Chitoni M, Gregorini G, Rossi G, Carosi G. 1996. Prevalence of thrombotic microangiopathy in a cohort of HIV-infected patients. *The Journal of Acquired Immune Deficiency Syndromes*, 1286.

Rock GA, Shumak KH, Buskard NA, Blanchette VS, Kelton JG, Nair RC, Spasoff RA and the Canadian Apheresis study group. 1991. Comparison of plasma exchange with plasma infusion in the treatment of thrombotic thrombocytopenic purpura. *New England Journal of Medicine*, 325: 393-397. DOI:10.1056/NEJM199108083250604.

Rock GA, Shumak KH, Buskard NA, Blanchette VS, Kelton JG, Nair RC, Spasoff RA, Group CAS. 1991. Comparison of plasma exchange with plasma infusion in the treatment of thrombotic thrombocytopenic purpura. *New England Journal of Medicine*, 325: 393–397.

Romani De Wit T, Fijnheer R, Brinkman HJ, Kersting S, Hene RJ, van Mourik JA. 2003. Endothelial cell activation in thrombotic thrombo-cytopenic purpura (TTP): a prospective analysis. *British Journal of Haematology*, 123: 522–527.

Roos A, Bouwman LH, van Gijlswijk-Janssen DJ, Faber-Krol MC, Stahl GL, Daha MR. 2001. Human IgA activates the complement system via the mannan-binding lectin pathway. *Journal of Immunology*, 167(5):2861–2868. DOI:10.4049/jimmunol.167.5.2861

Rubinstein ND, Mayrose I, Halperin D, Yekutieli D, Gershoni JM, Pupko T, 2008. Computational characterization of B-cell epitopes. *Molecular Immunology*, 45: 3477-3489.

Sabatier F, Roux V, Anfosso F, Camoin L, Sampol J, Dignat-George F. 2002b. Interaction of endothelial microparticles with monocytic cells in vitro induces tissue factor-dependent procoagulant activity. *Blood*, 99: 3962–3970.

Sadler JE. 1991. von Willebrand factor. *Journal of Biological Chemistry*, 266: 22777-22780.

Sadler JE. 1998. Biochemistry and genetics of von Willebrand factor. *Annual review of biochemistry*, 67:395-424.

Sadler JE. 2008. Von Willebrand factor, ADAMTS13, and thrombotic thrombocytopenic purpura. *Blood*, 112(1): 11-18.

Schaller M, Vogel M, Kentouche K, Lammler B, Kremer Hovinga JA. 2014. The splenic autoimmune response to ADAMTS13 in thrombotic thrombocytopenic purpura contains recurrent antigen-binding CDR3 motifs. *Blood*, 124(23): 3469–3479. DOI:10.1182/blood-2014-04-561142.

Scheiflinger F, Knobl P, Trattner B, Plaimauer B, Mohr G, Dockal M, Dorner F, Rieger M. 2003. Nonneutralizing IgM and IgG antibodies to von Willebrand factor-cleaving protease (ADAMTS13) in a patient with thrombotic thrombocytopenic purpura. *Blood*, 102:3241-3243.

Schneppenheim R, Kremer Hovinga JA, Becker T, Budde U, Karpman D, Brockhaus W, Hrachovinová I, Korczowski B, Oyen F, Rittich S, Rosen J, Tjønnfjord G, Pimanda J, Wienker T, Lämmle B. 2006. A common origin of the 4143insA ADAMTS13 mutation. *Journal of Thrombosis and Haemostasis*, 96(1): 3-6.

Schulte am EJ 2nd, Robson SC, Knoefel WT, Eisenberger CF, Peiper M, Rogiers X. 2005. Impact of O-linked glycosylation of the VWF-A1-domain flanking regions on platelet interaction. *British Journal of Haematology*, 128(1): 82-90.

Schwameis M, Schörgenhofer C, Assinger A, Steiner MM, Jilka B. 2015. VWF excess and ADAMTS13 deficiency: a unifying pathomechanism linking inflammation to thrombosis in DIC, malaria, and TTP. *Journal of Thrombosis and Haemostasis*, 113(4):708–718. DOI:10.1160/TH14-09-0731

- Scully M**, Brown J, Patel R, McDonald V, Brown CJ, Machin S. 2010. Human leukocyte antigen association in idiopathic thrombotic thrombocytopenic purpura: evidence for an immunogenetic link. *Journal of Thrombosis and Haemostasis*, 8: 257–262.
- Scully M**, Cohen H, Cavenagh J, Benjamin S, Starke R, Killick S, Mackie I, Machin SJ. 2007. Remission in acute refractory and relapsing thrombotic thrombocytopenic purpura following rituximab is associated with a reduction in IgG antibodies to ADAMTS-13. *British Journal of Haematology*, 136(3):451-461.
- Scully M**, Hunt BJ, Benjamin S, Liesner R, Rose P, Peyvandi F, Cheung B, Machin SJ. 2012. Guidelines on the diagnosis and management of thrombotic thrombocytopenic purpura and other thrombotic Microangiopathies. *British Journal of Haematology*, 158(3): 323-35. DOI: 10.1111/j.1365-2141.2012.09167.x.
- Scully M**, Knöbl P, Kentouche K, Rice L, Windyga J, Schneppenheim R, Kremer Hovinga JA, Kajiwara M, Fujimura Y, Maggiore C, Doralt J, Hibbard C, Martell L, Ewenstein B. 2017. Recombinant ADAMTS-13: first-in-human pharmacokinetics and safety in congenital thrombotic thrombocytopenic purpura. *Blood*, 130(19): 2055-2063. DOI: 10.1182/blood-2017-06-788026. [PMID: 28912376; PMCID: PMC5680611].
- Scully M**, Starke R, Lee R, Mackie I, Machin S, Cohen H. 2006. Successful management of pregnancy in women with a history of thrombotic thrombocytopenic purpura. *Blood Coagulation and Fibrinolysis*, 17: 459-463.
- Scully M**, Thomas M, Underwood M, Watson H, Langley K, Camilleri RS, Clark A, Creagh D, Rayment R, McDonald V, Roy A, Evans G, McGuckin S, Ni Ainle F, Maclean R, Lester W, Nash M, Scott R, O'Brien P, collaborators of the UK TTP Registry. 2014. Thrombotic thrombocytopenic purpura and pregnancy presentation, management, and subsequent pregnancy outcomes. *Blood*, 124(2): 211-219.
- Scully M**, Yarranton H, Liesner R, Cavenagh J, Hunt B, Benjamin S, Bevan D, Mackie I, Machin S. 2008. Regional UK TTP registry: correlation with laboratory ADAMTS13 analysis and clinical features. *British Journal of Haematology*, 142: 819-826.
- Scully M**. 2017. Thrombocytopenia in hospitalized patients: approach to the patient with thrombotic microangiopathy. *Hematology-American Society of Hematology Education Program*, 1: 651–659. DOI:10.1182/asheducation-2017.1.651
- Seebach D**, and Gardiner J. 2008. Beta-peptidic peptidomimetics. *Accounts of Chemical Research*, 41: 1366-1375. DOI:10.1021/ar700263g
- Semba R**, Tang A. 1999. Micronutrients and the pathogenesis of human immunodeficiency virus infection. *British Journal of Nutrition*, 81: 181-189.
- Shankaran H**, Neelamegham S. 2004. Hydrodynamic forces applied on intercellular bonds, soluble molecules, and cell-surface receptors. *Biophysical Journal*, 86: 576–588.
- Shelat SG**, Smith P, Ai J, Zheng XL. 2006. Inhibitory autoantibodies against ADAMTS-13 in patients with thrombotic thrombocytopenic purpura bind ADAMTS-13 protease and may accelerate its clearance in vivo. *Journal of Thrombosis and Haemostasis*, 4(8): 1707-1717. DOI:10.1111/j.1538-7836.2006.02025.x
- Shim K**, Anderson PJ, Tuley EA, Wiswall E, Sadler JE. 2007. Platelet-VWF complexes are preferred substrates of ADAMTS13 under fluid shear stress. *Blood*, 111: 651–657.
- Siedlecki CA**, Lestini BJ, Kottke-Marchant KK, Eppell SJ, Wilson DL, Marchant RE. 1996. Shear dependent changes in the three-dimensional structure of human von willebrand factor. *Blood*, 88: 2939-2950. [PubMed: 8874190]

- Sims PJ, Wiedmer T.** 2001. Unravelling the mysteries of phospholipid scrambling. *Journal of Thrombosis and Haemostasis*, 86: 266-275.
- Sinkovits G, Szilágyi Á, Farkas P, Inotai D, Szilvási A, Tordai A, Rázsó K, Réti M, Prohászka Z.** 2018. Concentration and Subclass Distribution of Anti-ADAMTS13 IgG Autoantibodies in Different Stages of Acquired Idiopathic Thrombotic Thrombocytopenic Purpura. *Frontiers in Immunology*, 9(1646): 1-14. <https://www.frontiersin.org/article/10.3389/fimmu.2018.01646>
- Sivalingam GN, Shepherd AJ.** 2012. An analysis of B-cell epitope discontinuity. *Molecular Immunology*, 51(3-4): 304–309. DOI:10.1016/j.molimm.03.030
- Skipwith CG, Cao W, Zheng XL.** 2010. Factor VIII and platelets synergistically accelerate cleavage of von Willebrand factor by ADAMTS13 under fluid shear stress. *Journal of Biological Chemistry*, 285: 28596–28603.
- Slootstra JW, Puijk WC, Ligtoet GJ, Langeveld JP, Meloen RH.** 1996. Structural aspects of antibody–antigen interaction revealed through small random peptide libraries. *Molecular Diversity*, 1: 87–96.
- Soejima K, Matsumoto M, Kokame K, Yagi H, Ishizashi H, Maeda H, Nozaki C, Miyata T, Fujimura Y, Nakagaki T.** 2003. ADAMTS13 cysteine-rich/spacer domains are functionally essential for von Willebrand factor cleavage. *Blood*, 102: 3232-3237.
- Soejima K, Matsumoto M, Kokame K, Yagi H, Ishizashi H, Maeda H, Nozaki C, Miyata T, Fujimura Y, Nakagaki T.** 2003. ADAMTS-13 cysteine-rich/spacer domain are functional essential for von Willebrand factor cleavage. *Blood*, 102: 3232-3237. [PubMed 12869506]
- Soejima K, Mimura N, Hirashima M, Maeda H, Hamamoto T, Nakagaki, T, Nozaki C.** 2001. A novel human metalloprotease synthesized in the liver and secreted into the blood: possibly, the von willebrand factor-cleaving protease? *Journal of Biochemistry*, 130: 475-480.
- Sorvillo N, van Haren SD, Kaijen PH, ten Brinke A, Fijnheer R, Meijer AB, Voorberg J.** 2013. Preferential HLA-DRB1*11-dependent presentation of CUB2-derived peptides by ADAMTS13-pulsed dendritic cells. *Blood*, 121: 3502–3510. <https://doi.org/10.1182/blood-2012-09-456780>.
- South K, Luken BM, Crawley JT, Phillips R, Thomas M, Collins RF, Deforche L, Vanhoorelbeke K, Lane DA.** 2014. Conformational activation of ADAMTS13. *Proceedings of the National Academy of Sciences of the United States of America*, 111: 18578-18583. DOI: 10.073/pnas.1411979112.
- Sporn LA, Chavin SI, Marder VJ, Wagner DD.** 1985. Biosynthesis of von Willebrand protein by human megakaryocytes. *Journal of Clinical Investigation*, 76(3): 1102-1106.
- Statistics South Africa (STAT SA).** 2019. Statistical release P0302: Mid-year population estimates 2019. Pretoria, Republic of South Africa. <http://www.statssa.gov.za/publications/P0302/P03022019.pdf>.
- Strait RT, Posgai MT, Mahler A, Barasa N, Jacob CO, Köhl J, Ehlers M, Stringer K, Shanmukhappa SK, Witte D, Hossain MM, Khodoun M, Herr AB, Finkelman FD.** 2015. IgG1 protects against renal disease in a mouse model of cryoglobulinaemia. *Nature*, 517: 501–504. DOI:10.1038/nature13868.
- Studdt JD, Hovinga JA, Antoine G, Hermann M, Rieger M, Scheiflinger F, Lämmle B.** 2005. Fatal congenital thrombotic thrombocytopenic purpura with apparent ADAMTS13 inhibitor: in vitro inhibition of ADAMTS13 activity by hemoglobin. *Blood*, 105: 542–544.
- Studdt J-D, Hovinga JAK, Antoine G, Hermann M, Rieger M, Scheiflinger F, Lämmle B.** 2004. Fatal congenital thrombotic thrombocytopenic purpura with apparent ADAMTS13 inhibitor: In-vitro inhibition of ADAMTS13 activity by haemoglobin. *Blood*, 1-10.

- Studt** JD, Hovinga JAK, Radonic R, Gasparovic V, Ivanovic D, Merkler M, Wirthmueller U, Dahinden C, Furlan M, Lämmle B. 2004. Familial acquired thrombotic thrombocytopenic purpura: ADAMTS13 inhibitory autoantibodies in identical twins. *Blood*, 103(11): 4195-4197.
- Stufano** F, La Marca S, Pontiggia S, Musallam KM, Peyvandi F. 2012. von Willebrand factor propeptide to antigen ratio in acquired thrombotic thrombocytopenic purpura. *Journal of Thrombosis and Haemostasis*, 10: 728–30.
- Susal** C, Daniel V, Oberg HH, Terness P, Huth-Kuhne A, Zimmerman R, Opelz G. 1992. Striking inverse association of IgG–anti-Fab antibodies and CD4 cell counts in patients with acquired immunodeficiency syndrome (AIDS)/AIDS-related complex. *Blood*, 79: 954-957.
- Suzuki** M, Murata M, Matsubara Y, Uchida, T, Ishihara H, Shibano T, Ashida S-I, Soejima K, Okada Y, Ikeda Y. 2004. Detection of von Willebrand factor-cleaving protease (ADAMTS-13) in human platelets. *Biochemical and Biophysics Research Community*, 313: 212-216.
- Swart** L, Schapkaitz E, Mahlangu JN. 2019. Thrombotic thrombocytopenic purpura: A 5-year tertiary care centre experience. *Journal of Clinical Apheresis*, 34: 44–50.
- Swisher** KK, Doan JT, Vesley SK, Kwaan HC, Kim B, Lämmle B, Kremer Hovinga JA, George JN. 2007. Pancreatitis preceding acute episodes of thrombotic thrombocytopenic purpura-hemolytic uremic syndrome: Report of five patients with a systematic review of published reports. *Haematologica*, 92: 936-943.
- Taddeo** A, Khodadadi L, Voigt C, Mumtaz IM, Cheng Q, Moser K, Alexander T, Manz RA, Radbruch A, Hiepe F, Hoyer BF. 2015. Long-lived plasma cells are early and constantly generated in New Zealand Black/New Zealand White F1 mice and their therapeutic depletion requires a combined targeting of autoreactive plasma cells and their precursors. *Arthritis Research & Therapy*, 17(1):1-12. DOI: 10.1186/s13075-015-0551-3. PMID: 25889236.
- Taggart** C, Cervantes-Laurean D, Kim G, McElvaney NG, Wehr N, Moss J, Levine RL. 2000. Oxidation of either methionine 351 or methionine 358 in α 1-antitrypsin causes loss of anti-neutrophil elastase activity. *Journal of Biological Chemistry*, 275: 27258-27265.
- Tan** EM, Chan EKL, Sullivan KF, Rubin RL. 1988. Antinuclear antibodies: diagnostically specific immune markers and clues toward the understanding of systemic autoimmunity. *Clinical Immunology and Immunopathology*, 47: 121-141.
- Tang** BL. 2001. ADAMTS: a novel family of extracellular matrix proteases. *International Journal of Biochemical Cell Biology*, 33: 33-44. [PubMed: 11167130]
- Tao** Z, Peng Y, Nolasco L, Cal S, Lopez-Otin C, Li R, Moake JL, López JA, Dong JF. 2005. Recombinant CUB-1 domain polypeptide inhibits the cleavage of ULVWF strings by ADAMTS13 under flow conditions. *Blood*, 106(13): 4139–4145.
- Tao** Z, Peng Y, Nolasco L, Cal S, Lopez-Otin C, Li R, Moake JL, Lopez JA, Dong JF. 2005. Role of the CUB-1 domain in docking ADAMTS-13 to unusually large Von Willebrand factor in flowing blood. *Blood*, 106: 4139–4145. [PubMed: 16141351]
- Tao** Z, Wang Y, Choi H, Bernardo A, Nishio K, Sadler JE, Lopez JA, Dong JF. 2005. Cleavage of ultralarge multimers of von Willebrand factor by C-terminal-truncated mutants of ADAMTS-13 under flow. *Blood*, 106: 141-143. [PubMed: 15774619]

- Tati R**, Kristoffersson AC, Ståhl AL, Mörgelin M, Motto D, Satchell S, Mathieson P, Manea-Hedström M, Karpman D. 2011. Phenotypic expression of ADAMTS13 in glomerular endothelial cells. *Public Library of Science One*, 6(6): 1 – 11.e21587. DOI: 10.1371/journal.pone.0021587.
- Tauchi R**, Imagama S, Ohgomori T, Natori T, Shinjo R, Ishiguro N, Kadomatsu K. 2012. ADAMTS-13 is produced by glial cells and upregulated after spinal cord injury. *Neuroscience Letter* 23, 517(1): 1-6. [PMID: 22425718].
- Tedesco F**, Pausa M, Nardon E, Introna M, Mantovani A, Dobrina A. 1997. The cytolytically inactive terminal complement complex activates endothelial cells to express adhesion molecules and tissue factor procoagulant activity. *Journal of Experimental Medicine*, 185(9): 1619-1627.
- Terrell DR**, Vesely SK, Kremer Hovinga JA, Lämmle B, George JN. 2010. Different disparities of gender and race among the thrombotic thrombocytopenic purpura and haemolytic-uremic syndromes. *American Journal of Haematology*, 85(11): 844-847.
- Thomas MR**, de Groot R, Scully MA, Crawley JTB. 2015. Pathogenicity of Anti-ADAMTS13 Autoantibodies in Acquired Thrombotic Thrombocytopenic Purpura. *EBioMedicine*, 2: 942-952. <http://dx.doi.org/10.1016/j.ebiom.2015.06.007>.
- Thornton JM**, Edwards MS, Taylor WR, Barlow, DJ. 1986. Location of “continuous” antigenic determinants in the protruding regions of proteins. *The EMBO Journal*, 5: 409–413. <https://doi.org/10.1002/j.1460-2075.1986.tb04226.x>
- Tiller T**, Tsuiji M, Yurasov S, Velinzon K, Nussenzweig MC, Wardemann H. 2007. Autoreactivity in human IgG+ memory B cells. *Immunity*, 26: 205–213.
- Toong C**, Adelstein S, Phan TG. 2011. Clearing the complexity: immune complexes and their treatment in lupus nephritis. *The International Journal of Nephrology and Renovascular Disease*, 4: 17-28
- Tousoulis D**, Davies G, Stefanadis C, Toutouzas P, Ambrose JA. 2003. Inflammatory and thrombotic mechanisms in coronary atherosclerosis. *Heart*, 89: 993-997.
- Trimarchi H**, Freixas E, Rabinovich O, Schropp J, Pereyra H, Bullorsky E. 2001. Cyclosporine-associated thrombotic microangiopathy during daclizumab induction: a suggested therapeutic approach. *Nephron*, 87: 361–364.
- Trivedi MV**, Laurence JS and Siahaan TJ. 2009. The role of thiols and disulfides in protein chemical and physical stability. *Current Protein and Peptide Science*, 10(6): 614-625. [PMC3319691]
- Tsai HM** and Lian EC. 1998. Antibodies to von Willebrand factor-cleaving protease in acute thrombotic thrombocytopenic purpura. *New England Journal of Medicine*, 339(22): 1585 – 1594.
- Tsai HM**, Li A, Rock G. 2001. Inhibitors of von Willebrand factor-cleaving protease in thrombotic thrombocytopenic purpura. *Clinical Laboratory Journal*, 47: 387-392.
- Tsai HM**, Raoufi M, Zhou W, Guinto E, Grafos N, Ranzurmal S, Greenfield RS, Rand JH. 2006. ADAMTS13-binding IgG are present in patients with thrombotic thrombocytopenic purpura. *Journal of Thrombosis and Haemostasis*, 95: 886–892. [PubMed: 16676082]
- Tsai HM**, Rice L, Sarode R, Chow TW, Moake JL. 2000. Antibody inhibitors to von Willebrand factor metalloproteinase and increased binding of von Willebrand factor to platelets in ticlopidine-associated thrombotic thrombocytopenic purpura. *Annals of Internal Medicine*, 132: 794–799.

- Tsai** HM, Sussman II, Ginsburg D, Lankhof H, Sixma JJ, and Nagel RL. 1997. Proteolytic Cleavage of Recombinant Type 2A von Willebrand Factor Mutants R834W and R834Q: Inhibition by Doxycycline and by Monoclonal Antibody VP-1. *Blood*, 89: 1954–1962.
- Tsai** HM, Sussman II, Nagel RL. 1994. Shear stress enhances the proteolysis of Von Willebrand factor in normal plasma. *Blood*, 83: 2171-2179. PMID: 8161783.
- Tsai** HM. 1996. Physiological cleavage of von Willebrand factor by a plasma protease is dependent on its conformation and requires calcium ion. *Blood*, 87: 4235-4244. (PMID: 8639782).
- Tsai** HM. 2003. Shear stress and von Willebrand factor in health and diseases. *Seminars in Thrombosis and Hemostasis*, 29: 479-488. [PubMed: 14631548]
- Turner** NA, Nolasco L, Tao Z, Dong JF, Moake J. 2006. Human endothelial cells synthesize and release ADAMTS13. *Journal of Thrombosis and Haemostasis*, 4: 1396-1404.
- Turner** NA, Nolasco L, Ruggeri ZM, Moake JL. 2009. Endothelial cell ADAMTS-13 and VWF: production, release, and VWF string cleavage. *Blood*, 114(24): 5102–5111. DOI: 10.1182/blood-2009-07-231597
- Ueda** S, Nishio K, Minamino N, Kubo A, Akai Y, Kangawa K, Matsuo H, Fujimura Y, Yoshioka A, Masiu K, Doi N, Murao Y, Miyamoto S. 1999. Increased plasma levels of adrenomedullin in patients with systemic inflammatory response syndrome. *American Journal of Respiratory and Critical Care Medicine*, 160: 132-136. DOI: 10.1164/ajrccm.160.1.9810006.
- van Mourik** JA, Boertjes R, Huisveld IA, Fijnvandraat K, Pajkrt D, van Genderen PJ, Fijnheer R. 1999. Von Willebrand factor propeptide in vascular disorders: a tool to distinguish between acute and chronic endothelial cell perturbation. *Blood*, 94: 179-185.
- Van Regenmortel** MHV. 2009. What is a B-cell epitope? *Methods in Molecular Biology*, 524: 3-20.
- Vendramin** C, Thomas M, Westwood J-P, Scully M. 2018. Bethesda Assay for Detecting Inhibitory Anti-ADAMTS13 Antibodies in Immune-Mediated Thrombotic Thrombocytopenic Purpura. *Thrombosis and Haemostasis Open*, 02: e329-e333. DOI:10.1055/s-0038-1672187.
- Verbij** FC, Turksma AW, de Heij F, Kaijen P, Lardy N, Fijnheer R, Sorvillo N, ten Brinke A, Voorberg J. 2016. CD4+ T cells from patients with acquired thrombotic thrombocytopenic purpura recognize CUB2 domain-derived peptides. *Blood*, 127: 1606–1609.
- Vesely** SK, George JN, Lammle B, Studt J-D, Alberio L, El-Harake MA, Raskob GE. 2003. ADAMTS13 activity in thrombotic thrombocytopenic purpura–hemolytic uremic syndrome: relation to presenting features and clinical outcomes in a prospective cohort of 142 patients. *Blood*, 102: 60–68.
- Vesely** SK, Li X, McMinn JR, Terrell DR, George JN. 2004. Pregnancy outcomes after recovery from thrombotic thrombocytopenic purpura-hemolytic uremic syndrome. *Transfusion*, 44: 1149-1158.
- Veyradier** A, Lavergne JM, Ribba AS, Obert B, Loirat C, Meyer D, Girma JP. 2004. Ten candidate ADAMTS13 mutations in six French families with congenital thrombotic thrombocytopenic purpura (Upshaw-Schulman syndrome). *Journal of Thrombosis and Haemostasis*, 2:424–429. <http://dx.doi.org/10.1111/j.1538-7933.2004.00623.x>.
- Vincentelli** A, Susen S, Le Tourneau T, Six I, Fabre O, Juthier F, Bauters A, Decoene C, Goudemand J, Prat A, Jude B. 2003. Acquired von Willebrand syndrome in aortic stenosis. *New England Journal of Medicine*, 349: 343-349. [PubMed: 12878741]

- Visagie** GL and Louw VJ. 2010. Myocardial injury in HIV-associated thrombotic thrombocytopenic purpura (TTP). *Transfusion Medicine*, 20(4): 258 – 264.
- Vomund** AN and Majerus EM. 2009. ADAMTS13 bound to endothelial cell exhibits enhanced cleavage of von Willebrand factor. *Journal of Biological Chemistry*, 284: 30925-30932. [PubMed: 19729451].
- von Krogh** AS, Quist-Paulsen P, Waage A, Langseth ØO, Thorstensen K, Brudevold R, Tjønnfjord GE, Largiadèr CR, Lämmle B, Kremer Hovinga JA. 2016. High prevalence of hereditary thrombotic thrombocytopenic purpura in central Norway: from clinical observation to evidence. *Journal of Thrombosis and Haemostasis*, 14(1): 73-82.
- Wada** H, Matsumoto T, Suzuki K, Imai H, Katayama N, Iba T, Matsumoto M. 2018. Differences and similarities between disseminated intravascular coagulation and thrombotic microangiopathy. *Thrombosis Journal*, 16(14). <https://doi.org/10.1186/s12959-018-0168-2>.
- Wada** H, Thachil J, Di Nisio M, Mathew P, Kurosawa S, Gando S, Kim HK, Nielsen JD, Dempfle CE, Levi M, Toh CH. 2013. The scientific standardization committee on DIC of the international society on thrombosis Haemostasis: guidance for diagnosis and treatment of DIC from harmonization of the recommendations from three guidelines. *Journal of Thrombosis and Haemostasis*, 11: 761–767.
- Wada** H. 2004. Disseminated intravascular coagulation. *Clinica Chimica Acta*, 344: 13–21
- Wagner** DD, Olmsted JB, Marder VJ. 1982. Immunolocalization of von Willebrand protein in Weibel-Palade bodies of human endothelial cells. *Journal of Cell Biology*, 95(1): 355-360.
- Wagner** DD, Saffari-pour S, Bonfanti R, Sadler JE, Cramer EM, Chapman B, Mayadas TN. 1991. Induction of specific storage organelles by von Willebrand factor propolypeptide. *Cell*, 64(2): 403-413.
- Wang** Y, Chen J, Ling M, López JA, Chung DW, Fu X. 2015. Hypochlorous acid generated by neutrophils inactivates ADAMTS13: an oxidative mechanism for regulating ADAMTS13 proteolytic activity during inflammation. *Journal of Biological Chemistry*, 290(3): 1422-1431.
- Wang** Y, Rosen H, Madtes DK, Shao B, Martin TR, Heinecke JW, Fu X. 2007. Myeloperoxidase inactivates TIMP-1 by oxidizing its N-terminal cysteine residue. An oxidative mechanism for regulating proteolysis during inflammation. *Journal of Biological Chemistry*, 282: 31826-31834.
- Wardemann** H, Yurasov S, Schaefer A, Young JW, Meffre E, Nussenzweig MC. 2003. Predominant autoantibody production by early human B cell precursors. *Science*, 301: 1374-1377.
- Waritani** T, Chang J, McKinney B and Terato K. 2017. An ELISA protocol to improve the accuracy and reliability of serological antibody assay. *Methods*, 4: 153-165.
- Weinstein** L. 1982. Syndrome of hemolysis, elevated liver enzymes, and low platelet count: a severe consequence of hypertension. *American Journal of Obstetrics and Gynecology*, 142: 159–167.
- Weisel** JW. 1986. Fibrin assembly. Lateral aggregation and the role of the two pairs of fibrinopeptides. *Biophysical Journal*, 50: 1079-1093.
- Weissmann** G. 2009. Rheumatoid arthritis and systemic lupus erythematosus as immune complex diseases. *Bulletin of the NYU Hospital Joint Diseases*, 67(3): 251-253.
- Wilfinger** WW, Mackey K and Chomczynski P. 1997. The effect of pH and ionic strength on the Spectrophotometric assessment of nucleic acid purity. *BioTechniques*, 22: 474-481.

- Wolff B**, Burns AR, Middleton J, Rot A. 1998. Endothelial cell “memory” of inflammatory stimulation: human venular endothelial cells store interleukin 8 in Weibel-Palade bodies. *Journal of Experimental Medicine*, 188: 1757-1762.
- Woodhams B**, Girardot O, Blanco MJ, Colesse G, Gourmelin Y. 2001. Stability of coagulation proteins in frozen plasma. *Blood Coagulation and Fibrinolysis*, 12 (4): 229-236. DOI:10.1097/00001721-200106000-00002.
- Wu JJ**, Fujikawa K, McMullen BA, Chung DW. 2006. Characterization of a core binding site for ADAMTS-13 in the A2 domain of von Willebrand factor. *Proceedings of the National Academy of Sciences of the United States of America*, 103(49): 18470-18474.
- Xiang Y**, de Groot R, Crwaley JT Lane DA. 2011. Mechanisms of von Willebrand factor scissile bond cleavage by a disintegrin and metalloprotease with thrombospondin type 1 motif, member 13 (ADAMTS13). *Proceedings of the National Academy of Sciences of the United States of America*, 108: 11602-11607. [PubMed: 21705658]
- Xiao J** and Zheng XL. 2011. Carboxyl-Terminal Thrombospondin-type 1 (TSP-1) Repeats of ADAMTS13 inhibits platelet adhesion to collagen-coated surface under shear stress, Independent of Proteolysis Activity. *Blood*, 118: 195-200.
- Xiao J**, Jin SY, Xue J, Sorvillo N, Voorberg J, Zheng XL. 2011. Essential domains of a disintegrin and metalloprotease with thrombospondin type 1 repeats -13 metalloprotease required for modulation of arterial thrombosis. *Arteriosclerosis, Thrombosis, and Vascular Biology*, 31: 2261 – 2269. [PubMed: 21799176]
- Xu AJ** and Springer TA. 2013. Mechanisms by which von Willebrand disease mutations destabilizes the A2 domain. *Journal of Biological Chemistry*, 288(9): 6317-6324.
- Yamaguchi Y**, Moriki T, Igari A, Nakagawa T, Wada H, Matsumota M, Fujimura Y, Murata M. 2011. Epitope analysis of autoantibody to ADAMTS13 in patients with thrombotic thrombocytopenic purpura. *Thrombosis Research*, 128: 169-173.
- Yamaguchi Y**, Moriki T, Igari A, Nakagawa T, Wada H, Matsumoto M, Fujimura Y, Murata M. 2011. Epitope analysis of autoantibody to ADAMTS13 in patients with thrombotic thrombocytopenic purpura. *Thrombosis Research*, 128: 169-173.
- Yau JW**, Teoh H and Verma S. 2015. Endothelial cell control of thrombosis. *BMC Cardiovascular Disorders*, 15(130): 1-11.
- Yeh HC**, Zhou Z, Choi H, Tekeoglu S, May W III, Wang C, Turner N, Scheiflinger F, Moake JL, Dong JF. 2010. Disulfide bond reduction of von Willebrand factor by ADAMTS-13. *Journal of Thrombosis and Haemostasis*, 8: 2778-2788.
- Yewdall AW**, Drutman SB, Jinwala F, Bahjat KS, Bhardwaj N. 2010. CD8+ T cell priming by dendritic cell vaccines requires antigen transfer to endogenous antigen presenting cells. *Public Library of Science (PLOS) One*, 5(6): e11144. DOI :10.1371/journal.pone.0011144
- Zanardelli S**, Chion ACK, Groot E, Lenting PJ, McKinnon TAJ, Laffan MA, Tseng M, and Lane DA. 2009. A novel binding site for ADAMTS13 constitutively exposed on the surface of globular VWF. *Blood*, 114(13): 2819–2828.
- Zhang C**. 2008. The role of inflammatory cytokines in endothelial dysfunction. *Basic Research in Cardiology*, 103: 398–406.

- Zhang Q**, Zhou YF, Zhang CZ, Zhang X, Lu C, Springer TA. 2009. Structural specializations of A2, a force-sensing domain in the ultralarge vascular protein von Willebrand factor. *Proceedings of the National Academy of Sciences of the United States of America*, 106(23): 9226-9231.
- Zhang XL**, Halvorsen K, Zhang CZ, Wong WP, Springer TA. 2009. Mechanoenzymatic cleavage of the ultralarge vascular protein von Willebrand factor. *Science*, 324(5932): 1330-1334.
- Zheng XL**, Chung D, Takayama TK, Majerus E, Sadler J, Fujikawa K. 2001. Structure of von Willebrand factor cleaving protease (ADAMTS13), a metalloprotease involved in thrombotic thrombocytopenic purpura. *The Journal of Biological Chemistry*, 276: 41059-41063. [PubMed: 11557746]
- Zheng XL**, Kaufman RM, Goodnough LT, Sadler JE. 2004. Effects of plasma exchange on plasma ADAMTS13 metalloprotease activity, inhibitor level, and clinical outcome in patients idiopathic and nonidiopathic thrombotic thrombocytopenic purpura. *Blood*, 103: 4043-4049.
- Zheng XL**, Nishio K, Majerus EM, Sadler JE. 2003. Cleavage of von Willebrand factor requires the spacer domain of the metalloprotease ADAMTS13. *Journal of Biological Chemistry*, 278: 30136-30141. [PubMed:12791682]
- Zheng XL**, Wu HM, Shang D, Falls E, Skipwith CG, Cataland SR, Bennett CL, Kwaan HC. 2010. Multiple domains of ADAMTS13 are targeted by autoantibodies against ADAMTS13 in patients with acquired idiopathic thrombotic thrombocytopenic purpura. *Haematologica*, 95: 1555-1562.
- Zheng XL**. 2013. Structure-function and regulation of ADAMTS13 protease. *Journal of Thrombosis and Haematology*, 11(01): 11-23.
- Zheng XL**. 2015. ADAMTS13 and von Willebrand factor in thrombotic thrombocytopenic purpura. *Annual Review of Medicine*, 66: 211–225. DOI:10.1146/annurev-med-061813-013241
- Zheng XL**. 2015. ADAMTS13, lucky to have a hydrophobic pocket. *Blood*, 125(12): 1852-1853.
- Zhou W**, Inada M, Lee TP, Benten D, Lyubsky S, Bouhassira EE, Gupta S, Tsai HM. 2005. ADAMTS13 is expressed in hepatic stellate cells. *Laboratory Investigation*, 85: 780-768.
- Zhou YF**, Eng ET, Nishida N, Lu C, Walz T, Springer TA. 2011. A pH-regulated dimeric bouquet in the structure of von Willebrand factor. *The EMBO Journal*, 30(19): 4098-4111. <http://dx.doi.org/10.1038/emboj.2011.297>.

Appendix A: The full-length ADAMTS13 nucleotide sequence

ADAMTS13 amino acid sequence

1 MHQRHPRARC PPLCVAGILA CGFLLGCWGP SHFQQSCLQA LEPQAVSSYL SPGAPLKGRP
61 PSPGFQRQRQ RQRRAAGGIL HLELLVAVGP DVFQAHQEDT ERYVLTNLNI GAELLRDPSL
121 GAQFRVHLVK MVILTEPEGA PNITANLTSS LLSVCGWSQT INPEDDTPDG HADLVLYITR
181 FDLELPDGNR QVRGVTQLGG ACSPTWSCLI TEDTGFDLGV TIA**HEIGHSF** **GLEHD**GAPGS
241 GCGPSGHVMA SDGAAPRAGL AWSPCSRRL LSLLSAGRAR C'VWDPPRPQP GSAGHPPDAQ
301 PGLYYSANEQ CRVAFGPKAV ACTFAREHL DMCQALSCHTD PLDQSSCSRL LVPLLDGTEC
361 GVEKWCSKGR CRSLVELTPI AAV**HGRWSSW** **GPRSPCSRSC** **GGGVVTRRRQ** **CNNPRPAFGG**
421 **RACVGADLQA** **EMCNTQACE****K** TQLEFMSQQC ARTDGOPLRS SPGGASFYHW GAAVPHSQGD
481 ALCRHMCRAI GESFIMKRGD SFLDGTRCMP SGPREDGTL LCVSGS CRTF GCDGRMDSQQ
541 VWDRQCQVCGG DNSTCSPR**KG** **SFTAGRAREY** **VTFLT VTPNL** **TSVYIANHRP** **LFTHLAVRIG**
601 **GRYV VAGKMS** **ISPNTTYP****SL** **LEDGRVEYRV** **ALTEDRLPRL** **EEIRIWG****PLO** **EDADIQVYRR**
661 **YGEEYGNLTR** **PDITFTYFQ****P** **K****PRQAWVWAA** **VRGPCSVSCG** **AGLRWVNYSC** **LDQARKELVE**
721 **TVQCQGSQOP** **PAWPEACVLE** **P****CPPYWAVGD** **FGPCSASC****GG** **GLRERPVR****CV** **EAQGSLLKTL**
781 **PPARC RAGA Q** **QPAVALET****CN** **POPC****PAR****WEV** **SEPSSCTSAG** **GAGLAL****ENET** **CVPGADGLEA**
841 **PVTEGPGSVD** **EKLPAPEP****CV** **GMSCPPG****WGH** **LDATSAGEKA** **PSPWGS****SIRTG** **AQAAH****VWTPA**
901 **AGSCSVSCGR** **GLMELRFL****CM** **DSALRVPVQ****E** **ELCGLASKPG** **SRREVCQAVP** **CPARWQYKLA**
961 **ACSVSCGRGV** **VRRILYCARA** **HGEDDGE****EIL** **LDTQCQGLPR** **PEPQEAC****SL****E** **PCPPRWKVMS**
1021 **LGPCSASCGL** **GTARRSVACV** **QLDQGD****VEV** **DEAACAALVR** **PEASVPC****LIA** **D****CTYRWHVGT**
1081 **WMECSVSCGD** **GIQRRRDT****CL** **GPQAQAPVPA** **DFCQHL****PKPV** **TVRGCWAGPC** **V****GQGT****PSLVP**
1141 HEEAAAPGRT TATPAGASLE WSQARGLLFS PAPQPRLLP GPQENSVQSS A**CGRQHLEPT**
1201 **GTIDMRGPGQ** **ADCAVAIGRP** **LGEVVTLRVL** **ESSLNCSAGD** **MLLLWGRLTW** **RKMCRKLLDM**
1261 **TFSSKTNTLV** **VRQRCGRP****GG** **GVLLRYGS****QL** **APETFYRECD** **MQLFGPWGEI** **VSPSLSPATS**
1321 **NAGGCR****LFIN** **VAPHARIAI****H** **ALATNMGAGT** **EGANASYILI** **RDTHSLRTTA** **FHGQQVLYWE**
1381 **SESSQAEMEF** **SEGFLKAQAS** **LRGQYWT****LQS** **WVPEMQDPQS** **WKGKEGT**

Figure 1: The full ADAMTS13 nucleotide sequence. (<https://www.ncbi.nlm.nih.gov/nucore/525313726>). Mature ADAMTS13 aa sequence underlined (75-1427) with amino acid sequences of selected domains for peptide library highlighted at different positions. The Metalloprotease (MP) domain (75-286, red) with active site sequence (light blue); Disintegrin-like domain (Dis-like) (287-383, yellow); Thrombospondin motif 1 number 1 (TSP1-1) (384-439, green); Cysteine-rich (Cys-rich) (440-558, grey); and the Spacer domain (spacer) (559-680, magenta); TSP1 repeats 2-8 respectively (682-1131, green); CUB-1-2 (1192-1427, dark red) domains (GenBank:AAL110951).

Domains selected for designed an overlapping peptide library (GenScript)

Overlapping linear peptide sequences. Length 20aa long/ 15aa overlapping/ 5 offset. The number of sequences = 105.

Metalloprotease and Disitergrin-like domains (aa sequence: 75-383)

```
61      XXXXXXXXXXXX XXXXAAGGIL HLELLVAVGP DVFQAHQEDT ERYVLTNLNI GAELLRDPSL
121     GAQFRVHLVK MVILTEPEGA PNITANLTSS LLSVCGWSQT INPEDDTPG HADLVLYITR
181     FDLELPDGNR QVRGVTQLGG ACSPTWSCLI TEDTGFDLGV TIAHEIGHSF GLEHDGAPGS
241     GCGPSGHVMA SDGAAPRAGL AWSPCSRRQL LSLLSAGRAR CVWDPPRPQP GSAGHPPDAQ
301     PGLYYSANEQ CRVAFGPKAV ACTFAREHLD MCQALSCHTD PLDQSSCSRL LVPLLDGTEC
361     GVEKWCSKGR CRSLVELTPI AAVXXXXXXXXX XXXXXXXXXXXX XXXXXXXXXXXX XXXXXXXXXXXX
```

Cysteine-rich and Spacer domains (aa sequence: 440-680)

```
421     XXXXXXXXXXXX XXXXXXXXXXXX TQLEFMSQQC ARTDGOPLRS SPGGASFYHW GAAVPHSQGD
481     ALCRHMCRAIGESFIMKRGD SFLDGTRCMP SGPREDTLS LCVSGSCRTF GCDGRMDSQQ
541     VWDRQVCGG DNSTCSPRKG SFTAGRAREY VTFLTVPNL TSVYIANHRP LFTHLAVRIG
601     GRYVVAGKMS ISPNTTYPST LEDGRVEYRV ALTEDRLPRL EEIRIWGPLQ EDADIQVYRR
661     YGEEYGNLTR PDITFTYFQP XXXXXXXXXXXX XXXXXXXXXXXX XXXXXXXXXXXX XXXXXXXXXXXX
```

Appendix B: Laboratory data of HIV-associated TTP patients at initial disease presentation.

| No.: | Sample No.: | Laboratory parameters | | | | | | | | | | | |
|------|-------------|-------------------------------|--------------------------------------|------------------|------------------|--------------------------|--------------------|------------------------------------|------------------------------|-----------------------|-------------------------------|--|-----------------------------------|
| | | <i>Schistocytes fragments</i> | <i>Plt count (x10⁹/L)</i> | <i>Hb (g/dL)</i> | <i>LDH (U/L)</i> | <i>Creatinine (µg/L)</i> | <i>Coombs test</i> | <i>ADAMTS13 Antigen levels (%)</i> | <i>ADAMTS13 Activity (%)</i> | <i>HIV status P/N</i> | <i>Viral load (Copies/mL)</i> | <i>CD4+ T cell counts (Cells/mm³)</i> | <i>ART at presentation Yes/No</i> |
| 1. | TTP 1 | Present | 17 | 7.6 | 1683 | 113 | Negative | 13 | 3 | P | LDL | 383 | Yes |
| 2. | TTP 5 | Present | 6 | 5.5 | 1768 | 73 | Negative | 0 | 0 | P | ND | 585 | Yes |
| 3. | TTP 6 | Present | 5 | 6.7 | 2708 | 129 | Negative | 2 | 6 | P | 9800000 | 187 | No |
| 4. | TTP 7 | Present | 6 | 5.6 | 3399 | 112 | Negative | 43 | 2 | P | LDL | 180 | Yes |
| 5. | TTP 8 | Present | 5 | 6 | 2404 | 110 | Negative | 26 | 5 | P | 562 635 | 421 | No |
| 6. | TTP 9 | Present | 9 | 6.7 | 1053 | 122 | Negative | 18 | 8 | P | 653000 | 120 | No |
| 7. | TTP 10 | Present | 6 | 5.1 | 2148 | 102 | Negative | 4 | 2 | P | 241000 | 175 | Yes |
| 8. | TTP 11 | Present | 17 | 6.2 | 1537 | 113 | Negative | 12 | 2 | P | 1105000 | 138 | No |
| 9. | TTP 12 | Present | 13 | 5.3 | 3430 | 99 | Negative | 1 | 2 | P | LDL | 247 | No |
| 10. | TTP 13 | Present | 13 | 5.8 | 1857 | 72 | Negative | 15 | 2 | P | 435000 | 193 | No |
| 11. | TTP 14 | Present | 17 | 6.2 | 1537 | 113 | Negative | 16 | 0 | P | 72905 | 138 | No |
| 12. | TTP 15 | Present | 6 | 5.1 | 2148 | 102 | Negative | 0 | 0 | P | 241000 | 175 | No |
| 13. | TTP 16 | Present | 13 | 5.3 | 3430 | 99 | Negative | 0 | 0 | P | LDL | 347 | No |
| 14. | TTP 17 | Present | 7 | 4.1 | 3958 | 99 | Negative | 9 | 0 | P | 121000 | 547 | Yes |
| 15. | TTP 18 | Present | 6 | 6.6 | 575 | 87 | Negative | 0 | 0 | P | 769536 | 101 | No |
| 16. | TTP 19 | Present | 13 | 5.2 | 1983 | 207 | Negative | 14 | 0 | P | 1920 | 258 | No |

Table continues...

| No.: | Sample No.: | Laboratory parameters | | | | | | | | | | | |
|------|-------------|-------------------------------|--------------------------------------|------------------|------------------|--------------------------|--------------------|------------------------------------|------------------------------|-----------------------|-------------------------------|--|-------------------------------------|
| | | <i>Schistocytes fragments</i> | <i>Plt count (x10⁹/L)</i> | <i>Hb (g/dL)</i> | <i>LDH (U/L)</i> | <i>Creatinine (µg/L)</i> | <i>Coombs test</i> | <i>ADAMTS13 Antigen levels (%)</i> | <i>ADAMTS13 Activity (%)</i> | <i>HIV status P/N</i> | <i>Viral load (Copies/mL)</i> | <i>CD4+ T cell counts (Cells/mm³)</i> | <i>HAART at presentation Yes/No</i> |
| 17. | TTP 20 | Present | 4 | 6 | 2939 | 109 | Negative | 0 | 0 | P | 367000 | 102 | No |
| 18. | TTP 21 | Present | 11 | 5.3 | 921 | 88 | Negative | 0 | 0 | P | 367000 | 276 | No |
| 19. | TTP 22 | Present | 5 | 6.9 | 2038 | 62 | Negative | 3 | 0 | P | LDL | 78 | Yes |
| 20. | TTP 23 | Present | 11 | 4.6 | 2948 | 245 | Negative | 11 | 5 | P | 64852 | 243 | No |
| 21. | TTP 24 | Present | 15 | 4.3 | 1652 | 36 | Negative | 3 | 0 | P | 12458 | 396 | Yes |
| 22. | TTP 25 | Present | 12 | 3.1 | 4775 | 116 | Negative | 26 | 8 | P | 375000 | 198 | No |
| 23. | TTP 27 | Present | 22 | 5.9 | 4982 | 98 | Negative | 9 | 0 | P | 197800 | 89 | No |
| 24. | TTP 28 | Present | 10 | 5.2 | 3962 | 106 | Negative | 48 | 4 | P | 8452 | 382 | Yes |
| 25. | TTP 29 | Present | 9 | 6.1 | 898 | 140 | Negative | 28 | 1 | P | ND | 162 | No |
| 26. | TTP 31 | Present | 11 | 5.2 | 1025 | 80 | Negative | 5 | 1 | P | ND | 441 | Yes |
| 27. | TTP 33 | Present | 15 | 6.9 | 1335 | 77 | Negative | 4 | 0 | P | LDL | 831 | Yes |
| 28. | TTP 34 | Present | 4 | 9.1 | 1052 | 56 | Negative | 3 | 0 | P | 8974 | 304 | Yes |
| 29. | TTP 35 | Present | 6 | 6.1 | 3166 | 38 | Negative | 3 | 0 | P | 125458 | 189 | No |
| 30. | TTP 37 | Present | 9 | 4.8 | 8675 | 98 | Negative | 2 | 1 | P | ND | 84 | No |
| 31. | TTP 38 | Present | 8 | 4.7 | 8436 | 79 | Negative | 10 | 0 | P | 7523 | 201 | No |
| 32. | TTP 39 | Present | 15 | 6.5 | 1254 | 90 | Negative | 1 | 0 | P | 9875 | 211 | Yes |
| 33. | TTP 40 | Present | 17 | 6.5 | 2335 | 95 | Negative | 4 | 0 | P | 123654 | 102 | No |
| 34. | TTP 42 | Present | 36 | 7.7 | 4121 | 100 | Negative | 14 | 0 | P | ND | 189 | No |

Table continues...

| No.: | Sample No.: | Laboratory parameters | | | | | | | | | | | |
|------|-------------|-------------------------------|--------------------------------------|------------------|------------------|--------------------------|--------------------|------------------------------------|------------------------------|-----------------------|-------------------------------|--|-----------------------------------|
| | | <i>Schistocytes fragments</i> | <i>Plt count (x10⁹/L)</i> | <i>Hb (g/dL)</i> | <i>LDH (U/L)</i> | <i>Creatinine (µg/L)</i> | <i>Coombs test</i> | <i>ADAMTS13 Antigen levels (%)</i> | <i>ADAMTS13 Activity (%)</i> | <i>HIV status P/N</i> | <i>Viral load (Copies/mL)</i> | <i>CD4+ T cell counts (Cells/mm³)</i> | <i>ART at presentation Yes/No</i> |
| 35. | TTP 43 | Present | 22 | 4.2 | 873 | 152 | Negative | 6 | 0 | P | 258679 | 187 | No |
| 36. | TTP 45 | Present | 37 | 5.4 | 890 | 130 | Negative | 5 | 0 | P | 748752 | 50 | No |
| 37. | TTP 48 | Present | 10 | 4.6 | 956 | 87 | Negative | 37 | 5 | P | ND | 180 | No |
| 38. | TTP 49 | Present | 10 | 5.2 | 1089 | 56 | Negative | 2 | 0 | P | 197857 | 113 | No |
| 39. | TTP 50 | Present | 5 | 5.8 | 2145 | 45 | Negative | 1 | 0 | P | 97852 | 182 | Yes |
| 40. | TTP 51 | Present | 19 | 5.7 | 5487 | 50 | Negative | 9 | 10 | P | 684257 | 80 | No |
| 41. | TTP 52 | Present | 15 | 5.2 | 6665 | 95 | Negative | 0 | 0 | P | 26897 | 135 | No |
| 42. | TTP 53 | Present | 15 | 6.3 | 3400 | 298 | Negative | 15 | 1 | P | 547860 | 191 | Yes |
| 43. | TTP 55 | Present | 5 | 8.3 | 9852 | 119 | Negative | 13 | 1 | P | 1500987 | 68 | No |
| 44. | TTP 56 | Present | 6 | 7.7 | 2365 | 187 | Negative | 16 | 1 | P | 4879 | 289 | No |
| 45. | TTP 57 | Present | 13 | 5.9 | 1857 | 75 | Negative | 5 | 1 | P | 587 | 415 | Yes |
| 46. | TTP 58 | Present | 14 | 4.1 | 1248 | 48 | Negative | 16 | 6 | P | 487521 | 171 | No |
| 47. | TTP 59 | Present | 71 | 6.6 | 903 | 58 | Negative | 24 | 8 | P | 998000 | 108 | No |
| 48. | TTP 60 | Present | 8 | 4.3 | 1409 | 70 | Negative | 4 | 0 | P | 1978522 | 71 | No |
| 49. | TTP 61 | Present | 17 | 5.8 | 2393 | 66 | Negative | 30 | 5 | P | 875551 | 97 | No |
| 50. | TTP 62 | Present | 42 | 6.6 | 1499 | 142 | Negative | 14 | 0 | P | 65427 | 144 | No |
| 51. | TTP 63 | Present | 36 | 4.9 | 1207 | 60 | Negative | 10 | 0 | P | 1587820 | 28 | No |
| 52. | TTP 64 | Present | 28 | 8.2 | 1596 | 74 | Negative | 0 | 0 | P | 15874 | 258 | No |

Table continues...

| No.: | Sample No.: | Laboratory parameters | | | | | | | | | | | |
|------|-------------|-------------------------------|--------------------------------------|------------------|------------------|--------------------------|--------------------|------------------------------------|------------------------------|-----------------------|-------------------------------|--|-------------------------------------|
| | | <i>Schistocytes fragments</i> | <i>Plt count (x10⁹/L)</i> | <i>Hb (g/dL)</i> | <i>LDH (U/L)</i> | <i>Creatinine (µg/L)</i> | <i>Coombs test</i> | <i>ADAMTS13 Antigen levels (%)</i> | <i>ADAMTS13 Activity (%)</i> | <i>HIV status P/N</i> | <i>Viral load (Copies/mL)</i> | <i>CD4+ T cell counts (Cells/mm³)</i> | <i>HAART at presentation Yes/No</i> |
| 53 | TTP 65 | Present | 55 | 7.6 | 1930 | 83 | Negative | 15 | 2 | P | ND | 347 | Yes |
| 54. | TTP 66 | Present | 16 | 5.8 | 1740 | 91 | Negative | 1 | 0 | P | ND | 209 | No |
| 55. | TTP 67 | Present | 19 | 5.8 | 2486 | 124 | Negative | 41 | 1 | P | 352847 | 55 | No |
| 56. | TTP 69 | Present | 21 | 6.7 | 3096 | 113 | Negative | 13 | 5 | P | LDL | 800 | Yes |
| 57. | TTP 70 | Present | 24 | 4.3 | 4812 | 81 | Negative | 1 | 6 | P | 557825 | 65 | No |
| 58. | TTP 71 | Present | 32 | 6.3 | 1121 | 101 | Negative | 9 | 3 | P | 1569536 | 10 | No |
| 59. | TTP 72 | Present | 16 | 4.2 | 1092 | 142 | Negative | 8 | 0 | P | 1587465 | 17 | No |

All 59 HIV-associated TTP study samples were collected before plasma therapy. The HIV positive status was confirmed on all samples. Abbreviations: PLT– platelet count, Hb – Haemaglobulin, LDH – Lactate dehydrogenase, HIV status: P – Positive, N – Negative, CD4+ lymphocyte count, HAART – Highly active antiretroviral therapy, LDL – Lower than the detectable limit, ND – Not done.

Appendix C: Laboratory data of HIV positive control plasma samples

| No.: | Study Sample No.: | HIV status P/N | Viral load (copies/mL) | CD4+ count (cell/mm3) | ART (Yes/No) |
|------|-------------------|-------------------|---------------------------|--------------------------|-----------------|
| 1. | 1/ | P | 500 | 117 | Yes |
| 2. | 37/ | P | 170000 | 430 | Yes |
| 4. | 186/ | P | 27188 | 285 | Yes |
| 5. | 30/ | P | 1090000 | 181 | Yes |
| 6. | 195/ | P | 12999 | 574 | Yes |
| 7. | 192/ | P | 48717 | 377 | Yes |
| 8. | 32/ | P | 99600 | 148 | Yes |
| 9. | 33/ | P | 105000 | 367 | Yes |
| 10. | 34/ | P | 77817 | 325 | Yes |
| 11. | 28/ | P | 16015 | 375 | Yes |
| 12. | 194/ | P | 10472 | 633 | Yes |
| 13. | 191/ | P | LDL | 311 | Yes |
| 14. | 185/ | P | 31562 | 468 | Yes |
| 15. | 200/ | P | LDL | 484 | Yes |
| 16. | 148/ | P | 22356 | 563 | Yes |
| 17. | 112/ | P | 18255 | 323 | Yes |
| 18. | 115/ | P | 3172 | 545 | Yes |
| 19. | 119/ | P | 135597 | 285 | Yes |
| 20. | 120/ | P | 17398 | 493 | Yes |
| 21. | 122/ | P | 22864 | 487 | Yes |
| 22. | 124/ | P | 36055 | 548 | Yes |
| 23. | 125/ | P | LDL | 789 | Yes |
| 24. | 126/ | P | 106593 | 187 | Yes |
| 25. | 127/ | P | 520 | 242 | Yes |
| 26. | 129/ | P | LDL | 589 | Yes |
| 27. | 130/ | P | 347 | 656 | Yes |
| 28. | 131/ | P | 48 | 271 | Yes |
| 29. | 133/ | P | 157000 | 213 | Yes |
| 30. | 134/ | P | LDL | 631 | Yes |
| 31. | 135/ | P | 2154 | 472 | Yes |
| 32. | 137/ | P | 854 | 482 | Yes |
| 33. | 141/ | P | 10248 | 365 | Yes |
| 34. | 142/ | P | LDL | 256 | Yes |
| 35. | 143/ | P | LDL | 334 | Yes |
| 36. | 145/ | P | 952 | 477 | Yes |
| 37. | 146/ | P | LDL | 374 | Yes |
| 38. | 147/ | P | 21548 | 244 | Yes |
| 39. | 149/ | P | LDL | 752 | Yes |
| 40. | 151/ | P | LDL | 582 | Yes |
| 41. | 152/ | P | LDL | 521 | Yes |
| 42. | 153/ | P | 176000 | 321 | Yes |
| 43. | 154/ | P | LDL | 431 | Yes |
| 44. | 155/ | P | 157455 | 254 | Yes |
| 45. | 156/ | P | 187000 | 264 | Yes |
| 46. | 157/ | P | 64785 | 234 | Yes |
| 47. | 160/ | P | 4578 | 321 | Yes |
| 48. | 161/ | P | LDL | 443 | Yes |
| 49. | 162/ | P | 585 | 238 | Yes |

Table continues...

| Table continues... | | | | | |
|--------------------|-------------------|-------------------|---------------------------|--------------------------|-----------------|
| No.: | Study Sample No.: | HIV status P/N | Viral load (copies/mL) | CD4+ count (cell/mm3) | ART (Yes/No) |
| | | | | | |
| 50. | 163/ | P | LDL | 745 | Yes |
| 51. | 164/ | P | LDL | 642 | Yes |
| 52. | 165/ | P | LDL | 607 | Yes |
| 53. | 167/ | P | 597 | 245 | Yes |
| 54. | 169/ | P | LDL | 623 | Yes |
| 55. | 173/ | P | 587 | 542 | Yes |
| 56. | 174/ | P | 10074 | 574 | Yes |
| 57. | 175/ | P | LDL | 159 | Yes |
| 58. | 177/ | P | LDL | 575 | Yes |
| 59. | 76/ | P | LDL | 785 | Yes |
| 60. | 80/ | P | LDL | 547 | Yes |
| 61. | 81/ | P | <20 | 365 | Yes |
| 62. | 84/ | P | 110 | 457 | Yes |
| 63. | 87/ | P | 987 | 464 | Yes |
| 64. | 88/ | P | <20 | 354 | Yes |
| 65. | 89/ | P | LDL | 760 | Yes |
| 66. | 91/ | P | 185 | 285 | Yes |
| 67. | 94/ | P | 8451 | 290 | Yes |
| 68. | 97/ | P | LDL | 802 | Yes |
| 69. | 98/ | P | 543 | 371 | Yes |
| 70. | 99/ | P | 9875 | 245 | Yes |
| 71. | 103/ | P | LDL | 524 | Yes |
| 72. | 104/ | P | 8745 | 230 | Yes |
| 73. | 106/ | P | 7895 | 296 | Yes |
| 74. | 108/ | P | 6987 | 275 | Yes |
| 75. | 111/ | P | 48200 | 115 | Yes |
| 76. | 38/ | P | LDL | 586 | Yes |
| 77. | 42/ | P | 8785 | 258 | Yes |
| 78. | 43/ | P | 2750 | 615 | Yes |
| 79. | 44/ | P | LDL | 352 | Yes |
| 80. | 45/ | P | 8647 | 348 | Yes |
| 81. | 46/ | P | LDL | 387 | Yes |
| 82. | 47/ | P | LDL | 565 | Yes |
| 83. | 48/ | P | LDL | 742 | Yes |
| 84. | 49/ | P | 18967 | 250 | Yes |
| 85. | 50/ | P | 273 | 516 | Yes |
| 86. | 52/ | P | <50 | 472 | Yes |
| 87. | 54/ | P | 1025 | 542 | Yes |
| 88. | 55/ | P | LDL | 491 | Yes |
| 89. | 56/ | P | 728 | 567 | Yes |
| 90. | 59/ | P | LDL | 588 | Yes |
| 91. | 60/ | P | LDL | 856 | Yes |
| 92. | 64/ | P | LDL | 522 | Yes |
| 93. | 66/ | P | 71 | 344 | Yes |
| 94. | 68/ | P | 37 | 479 | Yes |
| 95. | 6/ | P | LDL | 519 | Yes |
| 96. | 14/ | P | <20 | 267 | Yes |
| Table continues... | | | | | |

| Table continues... | | | | | |
|---------------------------|--------------------------|---------------------------|-----------------------------------|----------------------------------|-------------------------|
| No.: | Study Sample No.: | HIV status P/N | Viral load (copies/mL) | CD4+ count (cell/mm3) | ART (Yes/No) |
| | | | | | |
| 97. | 18/ | P | 16500 | 417 | Yes |
| 98. | 19/ | P | LDL | 457 | Yes |
| 99. | 22/ | P | LDL | 771 | Yes |
| 100. | 23/ | P | LDL | 453 | Yes |

HIV status: P – positive/ or N-negative, CD4+ - CD4+ lymphocyte count, HAART – Highly active antiretroviral therapy, LDL – Lower than detectable limit

Supplementary data 2:

Table 4: The HIV status results.

| HIV-associated TTP samples (n=59) | | | | HIV positive samples (n=100) | | |
|-----------------------------------|-------------------|----------------------------------|---------------------------|------------------------------|----------------------------------|---------------------------|
| No.: | Study sample no.: | OD values obtained at 450/630 nm | Interpretation of Results | Study sample no.: | OD values obtained at 450/630 nm | Interpretation of Results |
| 1. | TTP 1 | 1,271 | Positive | 1/ | 1,643 | Positive |
| 2. | TTP 5 | 1,317 | Positive | 37/ | 1,732 | Positive |
| 3. | TTP 6 | 1,735 | Positive | 186/ | 1,505 | Positive |
| 4. | TTP 7 | 1,898 | Positive | 30/ | 2,71 | Positive |
| 5. | TTP 8 | 1,719 | Positive | 195/ | 1,887 | Positive |
| 6. | TTP 9 | 1,822 | Positive | 192/ | 1,425 | Positive |
| 7. | TTP 10 | 1,509 | Positive | 32/ | 1,371 | Positive |
| 8. | TTP 11 | 2,731 | Positive | 33/ | 1,397 | Positive |
| 9. | TTP 12 | 2,177 | Positive | 36/ | 1,502 | Positive |
| 10. | TTP 13 | 1,577 | Positive | 28/ | 1,323 | Positive |
| 11. | TTP 14 | 1,645 | Positive | 194/ | 1,506 | Positive |
| 12. | TTP 15 | 1,652 | Positive | 191/ | 1,628 | Positive |
| 13. | TTP 16 | 1,474 | Positive | 185/ | 1,217 | Positive |
| 14. | TTP 17 | 1,849 | Positive | 200/ | 1,471 | Positive |
| 15. | TTP 18 | 1,447 | Positive | 148/ | 1,25 | Positive |
| 16. | TTP 19 | 1,596 | Positive | 112/ | 1,223 | Positive |
| 17. | TTP 20 | 1,703 | Positive | 115/ | 1,335 | Positive |
| 18. | TTP 21 | 1,529 | Positive | 119/ | 1,803 | Positive |
| 19. | TTP 22 | 1,526 | Positive | 120/ | 1,263 | Positive |
| 20. | TTP 23 | 1,618 | Positive | 122/ | 1,419 | Positive |
| 21. | TTP 24 | 1,955 | Positive | 124/ | 1,675 | Positive |
| 22. | TTP 25 | 1,909 | Positive | 125/ | 1,411 | Positive |
| 23. | TTP 27 | 1,683 | Positive | 126/ | 1,244 | Positive |
| 24. | TTP 28 | 1,63 | Positive | 127/ | 1,601 | Positive |
| 25. | TTP 29 | 1,161 | Positive | 129/ | 1,52 | Positive |
| 26. | TTP 31 | 0,787 | Positive | 130/ | 1,283 | Positive |
| 27. | TTP 33 | 1,203 | Positive | 131/ | 2,364 | Positive |
| 28. | TTP 34 | 1,225 | Positive | 133/ | 1,674 | Positive |
| 29. | TTP 35 | 1,172 | Positive | 134/ | 1,255 | Positive |
| 30. | TTP 37 | 1,856 | Positive | 135/ | 1,156 | Positive |
| 31. | TTP 38 | 1,097 | Positive | 137/ | 1,177 | Positive |
| 32. | TTP 39 | 3,797 | Positive | 141/ | 1,006 | Positive |
| 33. | TTP 40 | 3,189 | Positive | 142/ | 1,07 | Positive |
| 34. | TTP 42 | 1,883 | Positive | 143/ | 1,036 | Positive |
| 35. | TTP 43 | 1,236 | Positive | 145/ | 1,54 | Positive |
| 36. | TTP 45 | 1,503 | Positive | 146/ | 1,16 | Positive |
| 37. | TTP 48 | 2,125 | Positive | 147/ | 1,042 | Positive |
| 38. | TTP 49 | 1,315 | Positive | 149/ | 1,256 | Positive |
| 39. | TTP 50 | 1,631 | Positive | 151/ | 1,862 | Positive |
| 40. | TTP 51 | 2,743 | Positive | 152/ | 1,121 | Positive |
| 41. | TTP 52 | 1,76 | Positive | 153/ | 1,977 | Positive |
| 42. | TTP 53 | 1,57 | Positive | 154/ | 1,336 | Positive |
| 43. | TTP 55 | 1,586 | Positive | 155/ | 1,096 | Positive |

Table continues...

Table continues...

| HIV-associated TTP samples (n=59) | | | | HIV positive samples (n=100) | | |
|-----------------------------------|-------------------|----------------------------------|---------------------------|------------------------------|----------------------------------|---------------------------|
| No.: | Study sample no.: | OD values obtained at 450/630 nm | Interpretation of Results | Study sample no.: | OD values obtained at 450/630 nm | Interpretation of Results |
| 44. | TTP 56 | 1,679 | Positive | 156/ | 1,828 | Positive |
| 45. | TTP 57 | 2,012 | Positive | 157/ | 1,145 | Positive |
| 46. | TTP 58 | 1,966 | Positive | 160/ | 1,197 | Positive |
| 47. | TTP 59 | 1,744 | Positive | 161/ | 1,206 | Positive |
| 48. | TTP 60 | 1,705 | Positive | 162/ | 1,115 | Positive |
| 49. | TTP 61 | 1,625 | Positive | 163/ | 1,261 | Positive |
| 50. | TTP 62 | 1,599 | Positive | 164/ | 1,135 | Positive |
| 51. | TTP 63 | 1,594 | Positive | 165/ | 1,598 | Positive |
| 52. | TTP 64 | 2,186 | Positive | 167/ | 1,161 | Positive |
| 53. | TTP 65 | 2,48 | Positive | 169/ | 1,893 | Positive |
| 54. | TTP 66 | 1,671 | Positive | 173/ | 1,524 | Positive |
| 55. | TTP 67 | 1,893 | Positive | 174/ | 1,539 | Positive |
| 56. | TTP 69 | 1,652 | Positive | 175/ | 1,523 | Positive |
| 57. | TTP 70 | 2,037 | Positive | 177/ | 1,498 | Positive |
| 58. | TTP 71 | 2,778 | Positive | 76/ | 1,883 | Positive |
| 59. | TTP 72 | 2,437 | Positive | 80/ | 1,483 | Positive |
| 60. | | | | 81/ | 1,597 | Positive |
| 61. | | | | 84/ | 1,795 | Positive |
| 62. | | | | 87/ | 1,59 | Positive |
| 63. | | | | 88/ | 1,506 | Positive |
| 64. | | | | 89/ | 2,424 | Positive |
| 65. | | | | 91/ | 1,803 | Positive |
| 66. | | | | 94/ | 1,537 | Positive |
| 67. | | | | 97/ | 1,466 | Positive |
| 68. | | | | 98/ | 1,432 | Positive |
| 69. | | | | 99/ | 1,592 | Positive |
| 70. | | | | 103/ | 1,602 | Positive |
| 71. | | | | 104/ | 1,375 | Positive |
| 72. | | | | 106/ | 1,32 | Positive |
| 73. | | | | 108/ | 1,354 | Positive |
| 74. | | | | 111/ | 1,448 | Positive |
| 75. | | | | 38/ | 1,288 | Positive |
| 76. | | | | 42/ | 1,452 | Positive |
| 77. | | | | 43/ | 1,541 | Positive |
| 78. | | | | 44/ | 1,53 | Positive |
| 79. | | | | 45/ | 1,331 | Positive |
| 80. | | | | 46/ | 1,213 | Positive |
| 81. | | | | 47/ | 1,188 | Positive |
| 82. | | | | 48/ | 1,246 | Positive |
| 83. | | | | 49/ | 1,561 | Positive |
| 84. | | | | 50/ | 1,202 | Positive |
| 85. | | | | 52/ | 1,26 | Positive |
| 86. | | | | 54/ | 1,341 | Positive |
| 87. | | | | 55/ | 1,327 | Positive |
| 88. | | | | 56/ | 1,209 | Positive |

Table continue...

| Table continues... | | | | | | | |
|-----------------------------------|-------------------|----------------------------------|---------------------------|------------------------------|-------------------|----------------------------------|---------------------------|
| HIV-associated TTP samples (n=59) | | | | HIV positive samples (n=100) | | | |
| No.: | Study sample no.: | OD values obtained at 450/630 nm | Interpretation of Results | | Study sample no.: | OD values obtained at 450/630 nm | Interpretation of Results |
| 87. | | | | | 55/ | 1,327 | Positive |
| 89. | | | | | 59/ | 1,285 | Positive |
| 90. | | | | | 60/ | 1,483 | Positive |
| 91. | | | | | 64/ | 1,225 | Positive |
| 92. | | | | | 66/ | 1,967 | Positive |
| 93. | | | | | 68/ | 1,644 | Positive |
| 94. | | | | | 6/ | 1,221 | Positive |
| 95. | | | | | 14/ | 1,261 | Positive |
| 96. | | | | | 18/ | 1,202 | Positive |
| 97. | | | | | 19/ | 0,385 | Positive |
| 98. | | | | | 22/ | 1,433 | Positive |
| 99. | | | | | 23/ | 1,263 | Positive |
| 100. | | | | | 25/ | 1,24 | Positive |

n, number of samples.

Positive control OD value: 1.523

Negative controls OD values: 0.065, 0.06, and 0.56

Mean OD450 of Negative control = $(0.065+0.06+0.056)/3$

$$= 0.060$$

Calculation of the Cut-off value = 0.060 + 0.12 = 0.180

Samples with OD450 value greater than the cut-off value of 0.180 are considered positive for the presence of HIV.

Samples with OD450 cut-off value less than 0.180 are considered negative for HIV.

Table 4.1: ADAMTS13 antigen levels and ADAMTS13 activity of HIV-associated TTP and HIV positive individual plasma samples.

| HIV-associated TTP samples (n=59) | | | | HIV positive samples (n=100) | | |
|-----------------------------------|-------------------|--|--|------------------------------|--|--|
| No.: | Study Sample No.: | ADAMTS13 antigen levels (Normal ranges 50%-150%) | ADAMTS13 activity (Normal ranges 50%-150%) | Study Sample No.: | ADAMTS13 antigen levels (Normal ranges 50%-150%) | ADAMTS13 activity (Normal ranges 50%-150%) |
| 1. | TTP 1 | 13 | 3 | 1/ | 55 | 86 |
| 2. | TTP 5 | 0 | 0 | 37/ | 38 | 49 |
| 3. | TTP 6 | 2 | 6 | 186/ | 42 | 42 |
| 4. | TTP 7 | 43 | 2 | 30/ | 121 | 101 |
| 5. | TTP 8 | 26 | 5 | 195/ | 65 | 71 |
| 6. | TTP 9 | 18 | 8 | 192/ | 36 | 51 |
| 7. | TTP 10 | 4 | 2 | 32/ | 100 | 65 |
| 8. | TTP 11 | 12 | 2 | 33/ | 57 | 100 |
| 9. | TTP 12 | 1 | 2 | 36/ | 64 | 68 |
| 10. | TTP 13 | 15 | 2 | 28/ | 55 | 68 |
| 11. | TTP 14 | 16 | 0 | 194/ | 70 | 100 |
| 12. | TTP 15 | 0 | 0 | 191/ | 46 | 57 |
| 13. | TTP 16 | 0 | 0 | 185/ | 50 | 63 |
| 14. | TTP 17 | 9 | 0 | 200/ | 129 | 66 |
| 15. | TTP 18 | 0 | 0 | 148/ | 43 | 52 |
| 16. | TTP 19 | 14 | 0 | 112/ | 63 | 113 |
| 17. | TTP 20 | 0 | 0 | 115/ | 68 | 65 |
| 18. | TTP 21 | 0 | 0 | 119/ | 114 | 51 |
| 19. | TTP 22 | 3 | 0 | 120/ | 130 | 77 |
| 20. | TTP 23 | 11 | 5 | 122/ | 103 | 67 |
| 21. | TTP 24 | 3 | 0 | 124/ | 73 | 82 |
| 22. | TTP 25 | 26 | 8 | 125/ | 64 | 77 |
| 23. | TTP 27 | 9 | 0 | 126/ | 24 | 43 |
| 24. | TTP 28 | 48 | 4 | 127/ | 91 | 81 |
| 25. | TTP 29 | 28 | 1 | 129/ | 123 | 98 |
| 26. | TTP 31 | 5 | 1 | 130/ | 125 | 87 |
| 27. | TTP 33 | 4 | 0 | 131/ | 93 | 100 |
| 28. | TTP 34 | 3 | 0 | 133/ | 77 | 108 |
| 29. | TTP 35 | 3 | 0 | 134/ | 42 | 50 |
| 30. | TTP 37 | 2 | 1 | 135/ | 91 | 100 |
| 31. | TTP 38 | 10 | 0 | 137/ | 60 | 80 |
| 32. | TTP 39 | 1 | 0 | 141/ | 58 | 68 |
| 33. | TTP 40 | 4 | 0 | 142/ | 72 | 67 |
| 34. | TTP 42 | 14 | 0 | 143/ | 89 | 49 |
| 35. | TTP 43 | 6 | 0 | 145/ | 107 | 100 |
| 36. | TTP 45 | 5 | 0 | 146/ | 47 | 77 |
| 37. | TTP 48 | 37 | 5 | 147/ | 52 | 82 |
| 38. | TTP 49 | 2 | 0 | 149/ | 46 | 89 |
| 39. | TTP 50 | 1 | 0 | 151/ | 21 | 53 |
| 40. | TTP 51 | 9 | 10 | 152/ | 45 | 37 |
| 41. | TTP 52 | 0 | 0 | 153/ | 52 | 101 |

Table continues....

| Table continues... | | | | | | | |
|-----------------------------------|-------------------|--|--|------------------------------|--|--|--|
| HIV-associated TTP samples (n=53) | | | | HIV positive samples (n=100) | | | |
| No.: | Study sample No.: | ADAMTS13 antigen levels (Normal ranges 50%-150%) | ADAMTS13 activity (Normal ranges 50%-150%) | Study Sample No.: | ADAMTS13 antigen levels (Normal ranges 50%-150%) | ADAMTS13 activity (Normal ranges 50%-150%) | ADAMTS13 activity (Normal ranges 50%-150%) |
| 42. | TTP 53 | 15 | 1 | 154/ | 100 | 100 | |
| 43. | TTP 55 | 13 | 1 | 155/ | 79 | 100 | |
| 44. | TTP 56 | 16 | 1 | 156/ | 53 | 66 | |
| 45. | TTP 57 | 5 | 1 | 157/ | 37 | 100 | |
| 46. | TTP 58 | 16 | 6 | 160/ | 54 | 91 | |
| 47. | TTP 59 | 24 | 8 | 161/ | 36 | 75 | |
| 48. | TTP 60 | 4 | 0 | 162/ | 62 | 90 | |
| 49. | TTP 61 | 30 | 5 | 163/ | 70 | 90 | |
| 50. | TTP 62 | 14 | 0 | 164/ | 77 | 90 | |
| 51. | TTP 63 | 10 | 0 | 165/ | 100 | 89 | |
| 52. | TTP 64 | 0 | 0 | 167/ | 58 | 61 | |
| 53. | TTP 65 | 15 | 2 | 169/ | 47 | 54 | |
| 54. | TTP 66 | 1 | 0 | 173/ | 130 | 63 | |
| 55. | TTP 67 | 41 | 1 | 174/ | 120 | 85 | |
| 56. | TTP 69 | 13 | 5 | 175/ | 59 | 68 | |
| 57. | TTP 70 | 1 | 6 | 177/ | 120 | 28 | |
| 58. | TTP 71 | 9 | 3 | 76/ | 55 | 25 | |
| 59. | TTP 72 | 8 | 0 | 80/ | 104 | 57 | |
| 60. | | | | 81/ | 115 | 100 | |
| 61. | | | | 84/ | 54 | 31 | |
| 62. | | | | 87/ | 53 | 116 | |
| 63. | | | | 88/ | 64 | 100 | |
| 64. | | | | 89/ | 116 | 109 | |
| 65. | | | | 91/ | 55 | 70 | |
| 66. | | | | 94/ | 67 | 68 | |
| 67. | | | | 97/ | 58 | 78 | |
| 68. | | | | 98/ | 54 | 77 | |
| 69. | | | | 99/ | 62 | 57 | |
| 70. | | | | 103/ | 48 | 60 | |
| 71. | | | | 104/ | 100 | 100 | |
| 72. | | | | 106/ | 57 | 100 | |
| 73. | | | | 108/ | 74 | 94 | |
| 74. | | | | 111/ | 53 | 100 | |
| 75. | | | | 38/ | 125 | 78 | |
| 76. | | | | 42/ | 130 | 60 | |
| 77. | | | | 43/ | 71 | 61 | |
| 78. | | | | 44/ | 130 | 67 | |
| 79. | | | | 45/ | 121 | 80 | |
| 80. | | | | 46/ | 85 | 78 | |
| 81. | | | | 47/ | 62 | 49 | |
| 82. | | | | 48/ | 74 | 64 | |
| 83. | | | | 49/ | 57 | 54 | |
| 84. | | | | 50/ | 60 | 44 | |
| 85. | | | | 52/ | 53 | 50 | |
| 86. | | | | 54/ | 69 | 60 | |

Table continues...

Supplementary data 4

Table 4.2: Anti-ADAMTS13 IgG antibody titer of HIV-associated TTP and HIV positive individual plasma samples.

| HIV-associated TTP samples (n=59) | | | | HIV Positive samples (n=100) | | |
|-----------------------------------|-------------------|---|----------------|------------------------------|---|----------------|
| No.: | Study sample No.: | ADAMTS13: IgG (Technozyme® ADAMTS13 ELISA) (Negative <12ug/mL; Positive >15ug/mL) | Interpretation | Study sample No.: | ADAMTS13: IgG (Technozyme® ADAMTS13 ELISA) (Negative <12ug/mL; Positive >15ug/mL) | Interpretation |
| 1. | TTP 1 | 175 | Positive | 1/ | 12 | Negative |
| 2. | TTP 5 | 64 | Positive | 37/ | 8 | Negative |
| 3. | TTP 6 | 97 | Positive | 186/ | 4 | Negative |
| 4. | TTP 7 | 7 | Negative | 30/ | 13 | Negative |
| 5. | TTP 8 | 40 | Positive | 195/ | 4 | Negative |
| 6. | TTP 9 | 223 | Positive | 192/ | 2 | Negative |
| 7. | TTP 10 | 77 | Positive | 32/ | 65 | Positive |
| 8. | TTP 11 | 42 | Positive | 33/ | 18 | Positive |
| 9. | TTP 12 | 32 | Positive | 36/ | 5 | Negative |
| 10. | TTP 13 | 59 | Positive | 28/ | 8 | Negative |
| 11. | TTP 14 | 57 | Positive | 194/ | 4 | Negative |
| 12. | TTP 15 | 94 | Positive | 191/ | 4 | Negative |
| 13. | TTP 16 | 78 | Positive | 185/ | 2 | Negative |
| 14. | TTP 17 | 107 | Positive | 200/ | 3 | Negative |
| 15. | TTP 18 | 96 | Positive | 148/ | 7 | Negative |
| 16. | TTP 19 | 25 | Positive | 112/ | 3 | Negative |
| 17. | TTP 20 | 77 | Positive | 115/ | 5 | Negative |
| 18. | TTP 21 | 28 | Positive | 119/ | 8 | Negative |
| 19. | TTP 22 | 96 | Positive | 120/ | 9 | Negative |
| 20. | TTP 23 | 57 | Positive | 122/ | 18 | Positive |
| 21. | TTP 24 | 103 | Positive | 124/ | 4 | Negative |
| 22. | TTP 25 | 26 | Positive | 125/ | 13 | Negative |
| 23. | TTP 27 | 54 | Positive | 126/ | 3 | Negative |
| 24. | TTP 28 | 42 | Positive | 127/ | 4 | Negative |
| 25. | TTP 29 | 48 | Positive | 129/ | 8 | Negative |
| 26. | TTP 31 | 111 | Positive | 130/ | 32 | Positive |
| 27. | TTP 33 | 21 | Positive | 131/ | 5 | Negative |
| 28. | TTP 34 | 28 | Positive | 133/ | 14 | Negative |
| 29. | TTP 35 | 13 | Negative | 134/ | 9 | Negative |
| 30. | TTP 37 | 2 | Negative | 135/ | 5 | Negative |
| 31. | TTP 38 | 105 | Positive | 137/ | 17 | Positive |
| 32. | TTP 39 | 102 | Positive | 141/ | 13 | Negative |
| 33. | TTP 40 | 18 | Positive | 142/ | 12 | Negative |
| 34. | TTP 42 | 33 | Positive | 143/ | 5 | Negative |
| 35. | TTP 43 | 14 | Negative | 145/ | 9 | Negative |
| 36. | TTP 45 | 32 | Positive | 146/ | 7 | Negative |
| 37. | TTP 48 | 30 | Positive | 147/ | 6 | Negative |
| 38. | TTP 49 | 37 | Positive | 149/ | 7 | Negative |
| 39. | TTP 50 | 131 | Positive | 151/ | 9 | Negative |
| 40. | TTP 51 | 3 | Negative | 152/ | 6 | Negative |

| HIV-associated TTP samples (n=59) | | | | HIV positive samples (n=100) | | |
|-----------------------------------|-------------------|---|----------------|------------------------------|---|----------------|
| No.: | Study sample No.: | ADAMTS13: IgG (Technozyme® ADAMTS13 ELISA) (Negative <12ug/mL; Positive >15ug/mL) | Interpretation | Study sample No.: | ADAMTS13: IgG (Technozyme® ADAMTS13 ELISA) (Negative <12ug/mL; Positive >15ug/mL) | Interpretation |
| 41. | TTP 52 | 86 | Positive | 153/ | 10 | Negative |
| 42. | TTP 53 | 6 | Negative | 154/ | 9 | Negative |
| 43. | TTP 55 | 80 | Positive | 155/ | 5 | Negative |
| 44. | TTP 56 | 23 | Positive | 156/ | 24 | Positive |
| 45. | TTP 57 | 71 | Positive | 157/ | 4 | Negative |
| 46. | TTP 58 | 18 | Positive | 160/ | 5 | Negative |
| 47. | TTP 59 | 21 | Positive | 161/ | 70 | Positive |
| 48. | TTP 60 | 21 | Positive | 162/ | 6 | Negative |
| 49. | TTP 61 | 55 | Positive | 163/ | 16 | Positive |
| 50. | TTP 62 | 28 | Positive | 164/ | 40 | Positive |
| 51. | TTP 63 | 17 | Positive | 165/ | 29 | Positive |
| 52. | TTP 64 | 23 | Positive | 167/ | 8 | Negative |
| 53. | TTP 65 | 26 | Positive | 169/ | 7 | Negative |
| 54. | TTP 66 | 18 | Positive | 173/ | 14 | Negative |
| 55. | TTP 67 | 22 | Positive | 174/ | 10 | Negative |
| 56. | TTP 69 | 18 | Positive | 175/ | 6 | Negative |
| 57. | TTP 70 | 82 | Positive | 177/ | 4 | Negative |
| 58. | TTP 71 | 92 | Positive | 76/ | 4 | Negative |
| 59. | TTP 72 | 47 | Positive | 80/ | 11 | Negative |
| 60. | | | | 81/ | 4 | Negative |
| 61. | | | | 84/ | 5 | Negative |
| 62. | | | | 87/ | 7 | Negative |
| 63. | | | | 88/ | 6 | Negative |
| 64. | | | | 89/ | 2 | Negative |
| 65. | | | | 91/ | 5 | Negative |
| 66. | | | | 94/ | 19 | Positive |
| 67. | | | | 97/ | 3 | Negative |
| 68. | | | | 98/ | 24 | Positive |
| 69. | | | | 99/ | 8 | Negative |
| 70. | | | | 103/ | 3 | Negative |
| 71. | | | | 104/ | 5 | Negative |
| 72. | | | | 106/ | 21 | Positive |
| 73. | | | | 108/ | 38 | Positive |
| 74. | | | | 111/ | 9 | Negative |
| 75. | | | | 38/ | 5 | Negative |
| 76. | | | | 42/ | 7 | Negative |
| 77. | | | | 43/ | 21 | Positive |
| 78. | | | | 44/ | 8 | Negative |
| 79. | | | | 45/ | 6 | Negative |
| 80. | | | | 46/ | 72 | Positive |
| 81. | | | | 47/ | 5 | Negative |
| 82. | | | | 48/ | 4 | Negative |
| 83. | | | | 49/ | 7 | Negative |
| 84. | | | | 50/ | 6 | Negative |
| 85. | | | | 52/ | 8 | Negative |

| HIV-associated TTP samples (n=59) | | | | HIV positive samples (n=100) | | |
|-----------------------------------|-------------------|---|----------------|------------------------------|---|----------------|
| No.: | Study sample No.: | ADAMTS13: IgG (Technozyme® ADAMTS13 ELISA) (Negative <12ug/mL; Positive >15ug/mL) | Interpretation | Study sample No.: | ADAMTS13: IgG (Technozyme® ADAMTS13 ELISA) (Negative <12ug/mL; Positive >15ug/mL) | Interpretation |
| 86. | | | | 54/ | 4 | Negative |
| 87. | | | | 55/ | 8 | Negative |
| 88. | | | | 56/ | 13 | Negative |
| 89. | | | | 59/ | 7 | Negative |
| 90. | | | | 60/ | 87 | Positive |
| 91. | | | | 64/ | 2 | Negative |
| 92. | | | | 66/ | 4 | Negative |
| 93. | | | | 68/ | 29 | Positive |
| 94. | | | | 6/ | 6 | Negative |
| 95. | | | | 14/ | 7 | Negative |
| 96. | | | | 18/ | 10 | Negative |
| 97. | | | | 19/ | 6 | Negative |
| 98. | | | | 22/ | 6 | Negative |
| 99. | | | | 23/ | 6 | Negative |
| 100. | | | | 25/ | 1 | Negative |

n, number of samples

Table 4.3: Mixing studies results and the inhibitory Bethesda units for individual HIV-associated TTP plasma samples.

| No.: | Study sample No.: | Mixing studies (50:50 mix) ADAMTS13 activity (Normal ranges: 50%-150%) | Interpretation of mixing studies results (<50% - no correction; >50% - correction) | Residual ADAMTS13 Activity (25%-75%) | Bethesda Units (Normal ranges <0.5 BU/mL) |
|------|-------------------|--|--|--------------------------------------|---|
| 1. | TTP 1 | 12% | No correction | 38% | 11.17 |
| 2. | TTP 5 | 28% | No correction | 39% | 4.54 |
| 3. | TTP 6 | 29% | No correction | 46% | 17.92 |
| 4. | TTP 8 | 60% | Correction | >75% | <0.5 |
| 5. | TTP 9 | 59% | Correction | >75% | <0.5 |
| 6. | TTP 10 | 12% | No correction | 57% | 3.04 |
| 7. | TTP 11 | 14% | No correction | 42% | 1.25 |
| 8. | TTP 12 | 12% | No correction | 55% | 1.72 |
| 9. | TTP 13 | 6% | No correction | 38% | 5.58 |
| 10. | TTP 14 | 6% | No correction | 25% | 8.0 |
| 11. | TTP 15 | 7% | No Correction | 30% | 13.90 |
| 12. | TTP 16 | 4% | No Correction | 43% | 9.74 |
| 13. | TTP 17 | 9% | No Correction | 41% | 10.29 |
| 14. | TTP 18 | 6% | No correction | 46% | 8.96 |
| 15. | TTP 19 | 61% | Correction | >75% | <0.5 |
| 16. | TTP 20 | 68% | Correction | >75% | <0.5 |
| 17. | TTP 21 | 57% | Correction | >75% | <0.5 |
| 18. | TTP 22 | 9% | No correction | 38% | 16.50 |
| 19. | TTP 23 | 68% | Correction | >75% | <0.5 |
| 20. | TTP 24 | 9% | No correction | 45% | 9.21 |
| 21. | TTP 25 | 79% | Correction | >75% | <0.5 |
| 22. | TTP 27 | 42% | No correction | 39% | 1.40 |
| 23. | TTP 28 | 21% | No correction | 34% | 6.23 |
| 24. | TTP 29 | 10% | No correction | 47% | 2.18 |
| 25. | TTP 31 | 8% | No correction | 47% | 8.71 |
| 26. | TTP 33 | 51% | Correction | >75% | <0.5 |
| 27. | TTP 34 | 65% | Correction | >75% | <0.5 |
| 28. | TTP 38 | 4% | No Correction | 21% | 9.0 |
| 29. | TTP 39 | 4% | No Correction | 27% | 14.80 |
| 30. | TTP 40 | 98% | Correction | >75% | <0.5 |
| 31. | TTP 42 | 26% | No Correction | 46% | 1.12 |
| 32. | TTP 45 | 2% | No Correction | 46% | 8.96 |
| 33. | TTP 48 | 30% | No Correction | 54% | 3.60 |
| 34. | TTP 49 | 36% | No Correction | 64% | 0.64 |
| 35. | TTP 50 | 10% | No Correction | 36% | 11.79 |
| 36. | TTP 52 | 50% | No correction | 39% | 2.7 |
| 37. | TTP 55 | 31% | No Correction | 51% | 3.90 |
| 38. | Pre 56 | 68% | Correction | >75% | <0.5 |
| 39. | TTP 57 | 48% | No correction | 68% | 1.11 |
| 40. | TTP 58 | 73% | Correction | >75% | <0.5 |
| 41. | TTP 59 | 55% | Correction | >75% | <0.5 |
| 42. | TTP 60 | 14% | No Correction | 25% | 2.0 |

| No.: | Study sample No.: | Mixing studies (50:50 mix) ADAMTS13 activity (Normal ranges 50%-150%) | Interpretation of mixing studies results (<50% - no correction; >50% - correction) | Residual ADAMTS13 Activity (25%-75%) | Bethesda Units (Normal ranges <0.5 BU/mL) |
|------|-------------------|---|--|--------------------------------------|---|
| 43. | TTP 61 | 40% | No Correction | 55% | 0.86 |
| 44. | TTP 62 | 50% | Correction | >75% | <0.5 |
| 45. | TTP 63 | 54% | Correction | >75% | <0.5 |
| 46. | TTP 64 | 23% | No Correction | 31% | 1.70 |
| 47. | TTP 65 | 71% | Correction | >75% | <0.5 |
| 48. | TTP 66 | 22% | No Correction | 32% | 2.12 |
| 49. | TTP 67 | 36% | No Correction | 28% | 1.85 |
| 50. | TTP 69 | 54% | Correction | >75% | <0.5 |
| 51. | TTP 70 | 9% | No Correction | 37% | 11.48 |
| 52. | TTP 71 | 5% | No Correction | 31% | 13.52 |
| 53. | TTP 72 | 13% | No Correction | 27% | 7.56 |

(Number of samples = 53).

Supplementary data 6

Table 4.4: The concentrations of IgM and IgA antibodies in plasma samples of HIV-associated TTP and HIV positive patients.

| HIV-associated TTP samples (n=53) | | | HIV positive samples (n=18) | | |
|-----------------------------------|---|--|-----------------------------|---|--|
| Study sample No.: | Plasma IgM antibody Normal ranges: 0.23-1.4 mg/mL | Plasma IgA antibody Normal ranges: 1.1-2.6 mg/mL | Study sample No.: | Plasma IgM antibody Normal ranges: 0.23-1.4 mg/mL | Plasma IgA antibody Normal ranges: 1.1-2.6 mg/mL |
| TTP 1 | 1,75 | 2,67 | 32/ | 0,61 | 1.64 |
| TTP 5 | 1,36 | 2,85 | 33/ | 0,68 | 1.84 |
| TTP 6 | 1,46 | 1,97 | 122/ | 1,70 | 1.63 |
| TTP 8 | 1,71 | 1,19 | 130/ | 0,56 | 1.52 |
| TTP 9 | 1,33 | 2,95 | 137/ | 0,85 | 1.78 |
| TTP 10 | 1,72 | 1,06 | 156/ | 0,85 | 1.71 |
| TTP 11 | 1,54 | 1,53 | 161/ | 0,58 | 1.54 |
| TTP 12 | 1,36 | 2,82 | 163/ | 1.2 | 1.92 |
| TTP 13 | 1,4 | 2,93 | 164/ | 1,29 | 1.84 |
| TTP 14 | 2,16 | 2,81 | 165/ | 0,58 | 1.53 |
| TTP 15 | 1,2 | 1,89 | 94/ | 0,61 | 1.55 |
| TTP 16 | 1,47 | 1,9 | 98/ | 0,47 | 1.41 |
| TTP 17 | 1,53 | 1,72 | 106/ | 0,21 | 1.78 |
| TTP 18 | 1,6 | 1,11 | 108/ | 1,08 | 1.87 |
| TTP 19 | 1,05 | 1,7 | 43/ | 0,60 | 1.55 |
| TTP 20 | 1,37 | 1,82 | 46/ | 0,59 | 1.57 |
| TTP 21 | 1,62 | 2,93 | 60/ | 2.0 | 1.56 |
| TTP 22 | 1,53 | 1,76 | 68/ | 0,61 | 1.56 |
| TTP 23 | 2,02 | 1,77 | | | |
| TTP 24 | 1,66 | 2,85 | | | |
| TTP 25 | 2,35 | 2,89 | | | |
| TTP 27 | 1,1 | 1,16 | | | |
| TTP 28 | 1,59 | 1,91 | | | |
| TTP 29 | 1,63 | 1,87 | | | |
| TTP 31 | 1,35 | 1,8 | | | |
| TTP 33 | 2,1 | 1,78 | | | |
| TTP 34 | 1,78 | 1,78 | | | |
| TTP 38 | 1,39 | 2,76 | | | |
| TTP 39 | 1,55 | 1,84 | | | |
| TTP 40 | 1,75 | 2,7 | | | |
| TTP 42 | 1,38 | 2,82 | | | |
| TTP 45 | 1,15 | 2,98 | | | |
| TTP 48 | 1,12 | 1,82 | | | |
| TTP 49 | 1,27 | 1,9 | | | |
| TTP 50 | 1,69 | 1,7 | | | |
| TTP 52 | 1,08 | 2,8 | | | |
| TTP 55 | 1,7 | 2,65 | | | |
| TTP 56 | 1,67 | 1,61 | | | |
| TTP 57 | 1,69 | 1,63 | | | |
| TTP 58 | 1,83 | 1,7 | | | |
| TTP 59 | 1,63 | 1,58 | | | |
| TTP 60 | 1,81 | 2,71 | | | |

| HIV-associated TTP samples (n=53) | | | HIV positive samples (n=18) | | |
|-----------------------------------|---|--|-----------------------------|---|--|
| Study sample No.: | Plasma IgM antibody Normal ranges: 0.23-1.4 mg/mL | Plasma IgA antibody Normal ranges: 1.1-2.6 mg/mL | Study sample No.: | Plasma IgM antibody Normal ranges: 0.23-1.4 mg/mL | Plasma IgA antibody Normal ranges: 1.1-2.6 mg/mL |
| TTP 61 | 1,94 | 2,8 | | | |
| TTP 62 | 1,91 | 2,75 | | | |
| TTP 63 | 1,68 | 1,68 | | | |
| TTP 64 | 1,57 | 1,53 | | | |
| TTP 65 | 1,54 | 1,51 | | | |
| TTP 66 | 1,6 | 1,58 | | | |
| TTP 67 | 1,88 | 2,97 | | | |
| TTP 69 | 1,55 | 1,54 | | | |
| TTP 70 | 1,61 | 1,64 | | | |
| TTP 71 | 1,68 | 1,85 | | | |
| TTP 72 | 1,7 | 2,64 | | | |

n, number of samples

Supplementary data 1**Table 4.5 A: Anti-ADAMTS13 IgM and anti-ADAMTS13 IgA in HIV-associated TTP and HIV positive plasma samples.**

The cut-off OD value for anti-ADAMTS13 IgM obtained is 0.134 and for anti-ADAMTS13 IgA is 0.114. The results are interpreted as either positive (+) for the presence and negative (-) for the absence of anti-ADAMTS13 IgM and IgA antibodies.

| HIV-associated TTP plasma samples (n=53) | | | | | |
|---|--------------------------|---|--|---|--|
| Number | Study sample No.: | Anti-ADAMTS13 IgM antibody (ELISA) Cut-off value >0.134 | Interpretation Positive (+)/ Negative (-) | Anti-ADAMTS13 IgA antibody (ELISA) Cut-off value >0.114 | Interpretation Positive (+)/ Negative (-) |
| 1. | TTP 1 | 0.103 | - | 0.106 | - |
| 2. | TTP 5 | 0.119 | - | 0.221 | + |
| 3. | TTP 6 | 0.251 | + | 0.208 | + |
| 4. | TTP 8 | 0.126 | - | 0.103 | - |
| 5. | TTP 9 | 0.262 | + | 0.208 | + |
| 6. | TTP 10 | 0.087 | - | 0.105 | - |
| 7. | TTP 11 | 0.119 | - | 0.252 | + |
| 8. | TTP 12 | 0.276 | + | 0.294 | + |
| 9. | TTP 13 | 0.095 | - | 0.25 | + |
| 10. | TTP 14 | 0.239 | + | 0.265 | + |
| 11. | TTP 15 | 0.093 | - | 0.084 | - |
| 12. | TTP 16 | 0.264 | + | 0.298 | + |
| 13. | TTP 17 | 0.267 | + | 0.215 | + |
| 14. | TTP 18 | 0.241 | + | 0.285 | + |
| 15. | TTP 19 | 0.12 | - | 0.233 | + |
| 16. | TTP 20 | 0.11 | - | 0.239 | + |
| 17. | TTP 21 | 0.246 | + | 0.243 | + |
| 18. | TTP 22 | 0.251 | + | 0.273 | + |
| 19. | TTP 23 | 0,053 | - | 0,211 | + |
| 20. | TTP 24 | 0,248 | + | 0,243 | + |
| 21. | TTP 25 | 0,069 | - | 0,216 | + |
| 22. | TTP 27 | 0,068 | - | 0,261 | + |
| 23. | TTP 28 | 0,073 | - | 0,082 | - |
| 24. | TTP 29 | 0,073 | - | 0,089 | - |
| 25. | TTP 31 | 0,201 | + | 0,203 | + |
| 26. | TTP 33 | 0.109 | - | 0.221 | + |
| 27. | TTP 34 | 0.083 | - | 0.241 | + |
| 28. | TTP 38 | 0.083 | - | 0.112 | - |
| 29. | TTP 39 | 0.078 | - | 0.215 | + |
| 30. | TTP 40 | 0.105 | - | 0.103 | - |
| 31. | TTP 42 | 0.243 | + | 0.103 | - |
| 32. | TTP 45 | 0.285 | + | 0.227 | + |
| 33. | TTP 48 | 0.265 | + | 0.23 | + |
| 34. | TTP 49 | 0.277 | + | 0.217 | + |
| 35. | TTP 50 | 0.072 | - | 0.066 | - |
| 36. | TTP 52 | 0.102 | - | 0.339 | + |
| 37. | TTP 55 | 0.124 | - | 0.26 | + |

| HIV-associated TTP samples (n=53) | | | | | |
|------------------------------------|-------------------|--|--|--|--|
| Number | Study sample No.: | Anti-ADAMTS13 IgM antibody (ELISA) Cut-off value >0.143 | Interpretation Positive (+)/ Negative (-) | Anti-ADAMTS13 IgA antibody (ELISA) Cut-off value >0.114 | Interpretation Positive (+)/ Negative (-) |
| 38. | TTP 56 | 0.092 | - | 0.092 | - |
| 39. | TTP 57 | 0.12 | - | 0.261 | + |
| 40. | TTP 58 | 0.119 | - | 0.075 | - |
| 41. | TTP 59 | 0.063 | - | 0.112 | - |
| 42. | TTP 60 | 0.096 | - | 0.105 | - |
| 43. | TTP 61 | 0.088 | - | 0.098 | - |
| 44. | TTP 62 | 0.108 | - | 0.085 | - |
| 45. | TTP 63 | 0.132 | - | 0.259 | + |
| 46. | TTP 64 | 0.103 | - | 0.07 | - |
| 47. | TTP 65 | 0.107 | - | 0.237 | + |
| 48. | TTP 66 | 0.076 | - | 0.108 | - |
| 49. | TTP 67 | 0.088 | - | 0.11 | - |
| 50. | TTP 69 | 0.076 | - | 0.251 | + |
| 51. | TTP 70 | 0.127 | - | 0.339 | + |
| 52. | TTP 71 | 0.067 | - | 0.247 | + |
| 53. | TTP 72 | 0.281 | + | 0.211 | + |
| HIV positive plasma samples (n=18) | | | | | |
| Number | Study sample No.: | Anti-ADAMTS13 IgM antibody (ELISA) Cut-off value >0.134 | Interpretation Positive (+)/ Negative (-) | Anti-ADAMTS13 IgA antibody (ELISA) Cut-off value >0.114 | Interpretation Positive (+)/ Negative (-) |
| 1. | 32/ | 0.095 | - | 0.094 | - |
| 2. | 33/ | 0.078 | - | 0.067 | - |
| 3. | 122/ | 0.077 | - | 0.101 | - |
| 4. | 130/ | 0.08 | - | 0.083 | - |
| 5. | 137/ | 0.103 | - | 0.061 | - |
| 6. | 156/ | 0.107 | - | 0.095 | - |
| 7. | 161/ | 0.079 | - | 0.083 | - |
| 8. | 163/ | 0.075 | - | 0.067 | - |
| 9. | 164/ | 0.204 | + | 0.147 | + |
| 10. | 165/ | 0.108 | - | 0.105 | - |
| 11. | 94/ | 0.114 | - | 0.087 | - |
| 12. | 98/ | 0.076 | - | 0.059 | - |
| 13. | 106/ | 0.075 | - | 0.086 | - |
| 14. | 108/ | 0.289 | + | 0.347 | + |
| 15. | 43/ | 0.25 | + | 0.093 | - |
| 16. | 46/ | 0.204 | + | 0.189 | + |
| 17. | 60/ | 0.278 | + | 0.192 | + |
| 18. | 68/ | 0.08 | - | 0.064 | - |

Table 4.5 B: Anti-ADAMTS13 IgM and IgA ELISA assay precision calculation results

1. Anti-ADAMTS13 IgM antibody Precision results

| Negative sample (PNP) | | | | Positive IgM sample | | | |
|---|-----------|-----------|------------------|-----------------------------------|-----------|-----------|------------------|
| Plate | Results 1 | Results 2 | Mean OD490 value | Plate | Results 1 | Results 2 | Mean OD490 value |
| 1. | 0.108 | 0.104 | 0.106 | 1. | 0.425 | 0.438 | 0.4315 |
| 2. | 0.106 | 0.108 | 0.107 | 2. | 0.404 | 0.408 | 0.406 |
| 3. | 0.099 | 0.097 | 0.098 | 3. | 0.42 | 0.424 | 0.422 |
| 4. | 0.089 | 0.091 | 0.09 | 4. | 0.392 | 0.408 | 0.4 |
| 5. | 0.105 | 0.109 | 0.107 | 5. | 0.371 | 0.409 | 0.39 |
| Means | | | 0.102 | Means | | | 0.410 |
| Standard deviation | | | 0.0075 | Standard deviation | | | 0.0167 |
| % Coefficient of variation | | | 7.36% | % Coefficient of variation | | | 4.09% |
| <i>Inter-assay CV (n=5) = average of positive and negative control CV = (7.36+ 4.09)/2 = 5.74%</i> | | | | | | | |

2. Anti-ADAMTS13 IgA antibody precision results

| Negative sample (PNP) | | | | Positive IgA sample | | | |
|---|-----------|-----------|------------------|-----------------------------------|-----------|-----------|------------------|
| Plate | Results 1 | Results 2 | Mean OD490 value | Plate | Results 1 | Results 2 | Mean OD490 value |
| 1. | 0.089 | 0.082 | 0.0855 | 1. | 0.235 | 0.239 | 0.237 |
| 2. | 0.093 | 0.092 | 0.0925 | 2. | 0.257 | 0.257 | 0.257 |
| 3. | 0.096 | 0.098 | 0.097 | 3. | 0.268 | 0.265 | 0.267 |
| 4. | 0.089 | 0.089 | 0.089 | 4. | 0.241 | 0.24 | 0.241 |
| 5. | 0.082 | 0.08 | 0.081 | 5. | 0.27 | 0.275 | 0.273 |
| Means | | | 0.089 | Means | | | 0.255 |
| Standard deviation | | | 0.0062 | Standard deviation | | | 0.0156 |
| % Coefficient of variation | | | 6.94% | % Coefficient of variation | | | 6.13% |
| <i>Inter-assay CV (n=5) = average of positive and negative control CV = (6.94+ 6.13)/2 = 6.54%</i> | | | | | | | |

Table 4.5 C: Determining the cut-off values for anti-ADAMTS13 IgM and anti-ADAMTS13 IgA

The cut-off value for ELISA system was determined using the mean absorbance of a negative control plus 2x times the standard deviation, as described by Kumar & Rao (1991). Samples with OD value at 490 nm greater than the cut-off value were considered as positive and samples with the OD value at 490 nm less than the cut-off value were considered as negative.

- For anti-ADAMTS13 IgM: Calculation was as follow: mean value plus 2 (Standard deviation) = 0.1075 + 2(0.01584) = 0.139.

| No.: | Negative OD value | Mean | SD | 2SD | Cut-off value |
|------|-------------------|--------|---------|---------------------------|--------------------------------------|
| 1. | 0.097 | 0.1075 | 0.01584 | $(2*0.01584)$ = 0.0317 | $(0.016 + 0.0317)$ = 0.139 |
| 2. | 0.13 | | | | |
| 3. | 0.113 | | | | |
| 4. | 0.09 | | | | |
| 5. | 0.097 | | | | |
| 6. | 0.13 | | | | |
| 7. | 0.113 | | | | |
| 8. | 0.09 | | | | |
| 9. | 0.097 | | | | |
| 10. | 0.13 | | | | |
| 11. | 0.113 | | | | |
| 12. | 0.09 | | | | |
| 13. | 0.097 | | | | |
| 14. | 0.13 | | | | |
| 15. | 0.113 | | | | |
| 16. | 0.09 | | | | |
| 17. | 0.097 | | | | |
| 18. | 0.13 | | | | |
| 19. | 0.113 | | | | |
| 20. | 0.09 | | | | |

- For anti-ADAMTS13 IgA: Calculation was as follow: mean value plus 2 (Standard deviation) = 0.0977 + 2(0.00818) = 0.114.

| No.: | Negative OD value | Mean | SD | 2SD | Cut-off value |
|------|-------------------|--------|---------|---------------------------|---------------------------------------|
| 1. | 0,097 | 0.0977 | 0.00818 | $(2*0.00818)$ = 0.0164 | $(0.0979 + 0.0164)$ = 0.114 |
| 2. | 0,113 | | | | |
| 3. | 0,099 | | | | |
| 4. | 0,103 | | | | |
| 5. | 0,099 | | | | |
| 6. | 0,095 | | | | |
| 7. | 0,092 | | | | |
| 8. | 0,085 | | | | |
| 9. | 0,112 | | | | |
| 10. | 0,099 | | | | |
| 11. | 0,097 | | | | |
| 12. | 0,095 | | | | |
| 13. | 0,115 | | | | |
| 14. | 0,087 | | | | |
| 15. | 0,098 | | | | |
| 16. | 0,097 | | | | |
| 17. | 0,09 | | | | |
| 18. | 0,096 | | | | |
| 19. | 0,087 | | | | |
| 20. | 0,097 | | | | |

Supplementary data 7

Table 4.6: VWF antigen levels of HIV-associated TTP plasma samples and HIV positive samples.

| HIV-associated TTP samples (n=59) | | | HIV positive samples (n=100) | |
|-----------------------------------|-------------------|--|------------------------------|--|
| No.: | Study sample no.: | VWF:Ag levels (ELISA) Normal ranges: 50% - 150% | Study sample no.: | VWF:Ag levels (ELISA) Normal ranges: 50% - 150% |
| 1. | TTP 1 | 152 | 1/ | 538 |
| 2. | TTP 5 | 177 | 37/ | 102 |
| 3. | TTP 6 | 217 | 186/ | 287 |
| 4. | TTP 7 | 250 | 30/ | 234 |
| 5. | TTP 8 | 158 | 195/ | 112 |
| 6. | TTP 9 | 217 | 192/ | 318 |
| 7. | TTP 10 | 226 | 32/ | 211 |
| 8. | TTP 11 | 174 | 33/ | 318 |
| 9. | TTP 12 | 178 | 36/ | 87 |
| 10. | TTP 13 | 243 | 28/ | 170 |
| 11. | TTP 14 | 154 | 194/ | 184 |
| 12. | TTP 15 | 185 | 191/ | 222 |
| 13. | TTP 16 | 211 | 185/ | 114 |
| 14. | TTP 17 | 227 | 200/ | 253 |
| 15. | TTP 18 | 318 | 148/ | 374 |
| 16. | TTP 19 | 158 | 112/ | 141 |
| 17. | TTP 20 | 217 | 115/ | 210 |
| 18. | TTP 21 | 226 | 119/ | 239 |
| 19. | TTP 22 | 174 | 120/ | 163 |
| 20. | TTP 23 | 381 | 122/ | 322 |
| 21. | TTP 24 | 80 | 124/ | 199 |
| 22. | TTP 25 | 180 | 125/ | 269 |
| 23. | TTP 27 | 170 | 126/ | 146 |
| 24. | TTP 28 | 260 | 127/ | 251 |
| 25. | TTP 29 | 280 | 129/ | 187 |
| 26. | TTP 31 | 286 | 130/ | 226 |
| 27. | TTP 33 | 281 | 131/ | 379 |
| 28. | TTP 34 | 136 | 133/ | 213 |
| 29. | TTP 35 | 207 | 134/ | 117 |
| 30. | TTP 37 | 278 | 135/ | 291 |
| 31. | TTP 38 | 134 | 137/ | 138 |
| 32. | TTP 39 | 170 | 141/ | 219 |
| 33. | TTP 40 | 124 | 142/ | 155 |
| 34. | TTP 42 | 270 | 143/ | 358 |
| 35. | TTP 43 | 124 | 145/ | 133 |
| 36. | TTP 45 | 217 | 146/ | 471 |
| 37. | TTP 48 | 157 | 147/ | 354 |
| 38. | TTP 49 | 158 | 149/ | 183 |
| 39. | TTP 50 | 190 | 151/ | 173 |
| 40. | TTP 51 | 405 | 152/ | 220 |
| 41. | TTP 52 | 201 | 153/ | 206 |
| 42. | TTP 53 | 700 | 154/ | 286 |
| 43. | TTP 55 | 289 | 155/ | 69 |
| 44. | TTP 56 | 70 | 156/ | 317 |

| HIV-associated TTP samples (n=59) | | | HIV positive samples (n=100) | |
|-----------------------------------|-------------------|--|------------------------------|--|
| No.: | Study sample no.: | VWF:Ag levels (ELISA) Normal ranges: 50% - 150% | Study sample no.: | VWF:Ag levels (ELISA) Normal ranges: 50% - 150% |
| 45. | TTP 57 | 348 | 157/ | 136 |
| 46. | TTP 58 | 183 | 160/ | 139 |
| 47. | TTP 59 | 668 | 161/ | 164 |
| 48. | TTP 60 | 292 | 162/ | 168 |
| 49. | TTP 61 | 176 | 163/ | 239 |
| 50. | TTP 62 | 293 | 164/ | 233 |
| 51. | TTP 63 | 408 | 165/ | 141 |
| 52. | TTP 64 | 163 | 167/ | 110 |
| 53. | TTP 65 | 523 | 169/ | 125 |
| 54. | TTP 66 | 109 | 173/ | 149 |
| 55. | TTP 67 | 162 | 174/ | 173 |
| 56. | TTP 69 | 201 | 175/ | 175 |
| 57. | TTP 70 | 157 | 177/ | 123 |
| 58. | TTP 71 | 214 | 76/ | 150 |
| 59. | TTP 72 | 85 | 80/ | 129 |
| 60. | | | 81/ | 158 |
| 61. | | | 84/ | 272 |
| 62. | | | 87/ | 102 |
| 63. | | | 88/ | 271 |
| 64. | | | 89/ | 193 |
| 65. | | | 91/ | 184 |
| 66. | | | 94/ | 201 |
| 67. | | | 97/ | 220 |
| 68. | | | 98/ | 209 |
| 69. | | | 99/ | 61 |
| 70. | | | 103/ | 107 |
| 71. | | | 104/ | 135 |
| 72. | | | 106/ | 401 |
| 73. | | | 108/ | 349 |
| 74. | | | 111/ | 203 |
| 75. | | | 38/ | 90 |
| 76. | | | 42/ | 331 |
| 77. | | | 43/ | 240 |
| 78. | | | 44/ | 218 |
| 79. | | | 45/ | 260 |
| 80. | | | 46/ | 158 |
| 81. | | | 47/ | 399 |
| 82. | | | 48/ | 228 |
| 83. | | | 49/ | 199 |
| 84. | | | 50/ | 105 |
| 85. | | | 52/ | 107 |
| 86. | | | 54/ | 292 |
| 87. | | | 55/ | 149 |
| 88. | | | 56/ | 261 |
| 89. | | | 59/ | 235 |
| 90. | | | 60/ | 181 |
| 91. | | | 64/ | 155 |

| HIV-associated TTP samples (n=59) | | | HIV positive samples (n=100) | |
|-----------------------------------|-------------------|--|------------------------------|--|
| No.: | Study sample no.: | VWF:Ag levels (ELISA) Normal ranges: 50% - 150% | Study sample no.: | VWF:Ag levels (ELISA) Normal ranges: 50% - 150% |
| 92. | | | 66/ | 127 |
| 93. | | | 68/ | 210 |
| 94. | | | 6/ | 173 |
| 95. | | | 14/ | 209 |
| 96. | | | 18/ | 160 |
| 97. | | | 19/ | 124 |
| 98. | | | 22/ | 142 |
| 99. | | | 23/ | 149 |
| 100. | | | 25/ | 157 |

Supplementary data 8

Table 4.7: The VWF propeptide levels and VWFpp/VWF:Ag ratio of HIV-associated TTP and HIV positive plasma samples.

| HIV-associated TTP samples (n=59) | | | | HIV positive samples (n=100) | | |
|-----------------------------------|-------------------|---|--------------------|------------------------------|---|--------------------|
| No.: | Study sample no.: | VWFpp levels (ELISA) Normal ranges: (60%-140)% | VWFpp/VWF:Ag ratio | Study sample no.: | VWFpp levels (ELISA) Normal ranges: (60%-140)% | VWFpp/VWF:Ag ratio |
| 1. | TTP 1 | 118 | 0,78 | 1/ | 1258 | 2,34 |
| 2. | TTP 5 | 350 | 1,98 | 37/ | 270 | 2,65 |
| 3. | TTP 6 | 1275 | 5,88 | 186/ | 162 | 0,56 |
| 4. | TTP 7 | 214 | 0,86 | 30/ | 409 | 1,75 |
| 5. | TTP 8 | 603 | 3,82 | 195/ | 484 | 4,32 |
| 6. | TTP 9 | 518 | 2,34 | 192/ | 207 | 0,65 |
| 7. | TTP 10 | 913 | 4,94 | 32/ | 910 | 4,31 |
| 8. | TTP 11 | 321 | 1,36 | 33/ | 371 | 1,17 |
| 9. | TTP 12 | 701 | 3,88 | 36/ | 270 | 3,10 |
| 10. | TTP 13 | 224 | 1,03 | 28/ | 460 | 2,71 |
| 11. | TTP 14 | 527 | 2,33 | 194/ | 234 | 1,27 |
| 12. | TTP 15 | 478 | 2,75 | 191/ | 368 | 1,66 |
| 13. | TTP 16 | 889 | 4,99 | 185/ | 167 | 1,46 |
| 14. | TTP 17 | 822 | 3,38 | 200/ | 604 | 2,39 |
| 15. | TTP 18 | 372 | 2,42 | 148/ | 913 | 2,44 |
| 16. | TTP 19 | 205 | 1,11 | 112/ | 229 | 1,62 |
| 17. | TTP 20 | 271 | 1,28 | 115/ | 235 | 1,12 |
| 18. | TTP 21 | 397 | 1,75 | 119/ | 260 | 1,09 |
| 19. | TTP 22 | 789 | 2,48 | 120/ | 540 | 3,31 |
| 20. | TTP 23 | 764 | 4,03 | 122/ | 424 | 1,32 |
| 21. | TTP 24 | 322 | 1,02 | 124/ | 345 | 1,73 |
| 22. | TTP 25 | 183 | 1,18 | 125/ | 126 | 0,47 |
| 23. | TTP 27 | 201 | 1,62 | 126/ | 308 | 2,11 |
| 24. | TTP 28 | 422 | 1,52 | 127/ | 511 | 2,04 |
| 25. | TTP 29 | 425 | 2,44 | 129/ | 223 | 1,20 |
| 26. | TTP 31 | 697 | 1,35 | 130/ | 436 | 1,93 |
| 27. | TTP 33 | 380 | 1,35 | 131/ | 721 | 1,90 |
| 28. | TTP 34 | 77 | 0,57 | 133/ | 1075 | 5,05 |
| 29. | TTP 35 | 205 | 0,99 | 134/ | 491 | 4,20 |
| 30. | TTP 37 | 294 | 1,06 | 135/ | 931 | 3,20 |
| 31. | TTP 38 | 59 | 0,44 | 137/ | 205 | 1,49 |
| 32. | TTP 39 | 294 | 1,72 | 141/ | 503 | 2,30 |
| 33. | TTP 40 | 30 | 0,24 | 142/ | 570 | 3,68 |
| 34. | TTP 42 | 188 | 0,70 | 143/ | 609 | 1,70 |
| 35. | TTP 43 | 324 | 2,61 | 145/ | 205 | 1,54 |
| 36. | TTP 45 | 581 | 2,68 | 146/ | 211 | 0,45 |
| 37. | TTP 48 | 225 | 1,43 | 147/ | 269 | 0,76 |
| 38. | TTP 49 | 205 | 1,29 | 149/ | 552 | 3,02 |
| 39. | TTP 50 | 182 | 0,96 | 151/ | 323 | 1,87 |
| 40. | TTP 51 | 700 | 1,72 | 152/ | 390 | 1,77 |
| 41. | Pre 52 | 946 | 4,71 | 153/ | 491 | 2,38 |
| 42. | Pre 53 | 354 | 0,51 | 154/ | 862 | 3,01 |

| HIV-associated TTP samples (n=59) | | | | HIV positive samples (n=100) | | |
|-----------------------------------|-------------------|---|--------------------|------------------------------|---|--------------------|
| No.: | Study sample no.: | VWFpp levels (ELISA) Normal ranges: (60%-140)% | VWFpp/VWF:Ag ratio | Study sample no.: | VWFpp levels (ELISA) Normal ranges: (60%-140)% | VWFpp/VWF:Ag ratio |
| 43. | TTP 55 | 480 | 1,66 | 155/ | 104 | 1,51 |
| 44. | TTP 56 | 194 | 2,77 | 156/ | 488 | 1,54 |
| 45. | TTP 57 | 368 | 1,06 | 157/ | 205 | 1,51 |
| 46. | TTP 58 | 342 | 1,87 | 160/ | 278 | 2 |
| 47. | TTP 59 | 394 | 0,59 | 161/ | 424 | 2,56 |
| 48. | TTP 60 | 292 | 1 | 162/ | 546 | 3,25 |
| 49. | TTP 61 | 133 | 0,76 | 163/ | 1002 | 4,19 |
| 50. | TTP 62 | 104 | 0,35 | 164/ | 461 | 1,98 |
| 51. | TTP 63 | 144 | 0,35 | 165/ | 345 | 2,45 |
| 52. | TTP 64 | 84 | 0,52 | 167/ | 269 | 2,45 |
| 53. | TTP 65 | 293 | 0,56 | 169/ | 369 | 2,95 |
| 54. | TTP 66 | 253 | 2,32 | 173/ | 351 | 2,36 |
| 55. | TTP 67 | 199 | 1,23 | 174/ | 533 | 3,08 |
| 56. | TTP 69 | 156 | 0,78 | 175/ | 131 | 0,75 |
| 57. | TTP 70 | 220 | 1,40 | 177/ | 558 | 4,54 |
| 58. | TTP 71 | 76 | 0,35 | 76/ | 168 | 1,12 |
| 59. | TTP 72 | 115 | 1,35 | 80/ | 290 | 2,25 |
| 60. | | | | 81/ | 105 | 0,66 |
| 61. | | | | 84/ | 235 | 0,86 |
| 62. | | | | 87/ | 83 | 0,81 |
| 63. | | | | 88/ | 278 | 1,03 |
| 64. | | | | 89/ | 384 | 1,99 |
| 65. | | | | 91/ | 253 | 1,38 |
| 66. | | | | 94/ | 430 | 2,14 |
| 67. | | | | 97/ | 314 | 1,42 |
| 68. | | | | 98/ | 436 | 2,09 |
| 69. | | | | 99/ | 217 | 3,56 |
| 70. | | | | 103/ | 113 | 1,06 |
| 71. | | | | 104/ | 150 | 1,11 |
| 72. | | | | 106/ | 1331 | 3,32 |
| 73. | | | | 108/ | 826 | 2,37 |
| 74. | | | | 111/ | 193 | 0,95 |
| 75. | | | | 38/ | 162 | 1,8 |
| 76. | | | | 42/ | 238 | 0,72 |
| 77. | | | | 43/ | 745 | 3,10 |
| 78. | | | | 44/ | 346 | 1,59 |
| 79. | | | | 45/ | 137 | 0,53 |
| 80. | | | | 46/ | 232 | 1,47 |
| 81. | | | | 47/ | 270 | 0,68 |
| 82. | | | | 48/ | 327 | 1,43 |
| 83. | | | | 49/ | 276 | 1,39 |
| 84. | | | | 50/ | 150 | 1,43 |
| 85. | | | | 52/ | 289 | 2,70 |
| 86. | | | | 54/ | 473 | 1,62 |
| 87. | | | | 55/ | 238 | 1,60 |
| 88. | | | | 56/ | 428 | 1,64 |

| HIV-associated TTP samples (n=59) | | | | HIV positive samples (n=100) | | |
|-----------------------------------|-------------------|---|---------------------|------------------------------|---|---------------------|
| No.: | Study sample no.: | VWFpp levels (ELISA) Normal ranges: (60%-140)% | VWFpp/ VWF:Ag ratio | Study sample no.: | VWFpp levels (ELISA) Normal ranges: (60%-140)% | VWFpp/ VWF:Ag ratio |
| 89. | | | | 59/ | 498 | 2,12 |
| 90. | | | | 60/ | 131 | 0,72 |
| 91. | | | | 64/ | 290 | 1,87 |
| 92. | | | | 66/ | 174 | 1,37 |
| 93. | | | | 68/ | 253 | 1,20 |
| 94. | | | | 6/ | 188 | 1,09 |
| 95. | | | | 14/ | 644 | 3,08 |
| 96. | | | | 18/ | 276 | 1,73 |
| 97. | | | | 19/ | 289 | 2,33 |
| 98. | | | | 22/ | 327 | 2,30 |
| 99. | | | | 23/ | 169 | 1,13 |
| 100. | | | | 25/ | 156 | 0,99 |

n, number of samples.

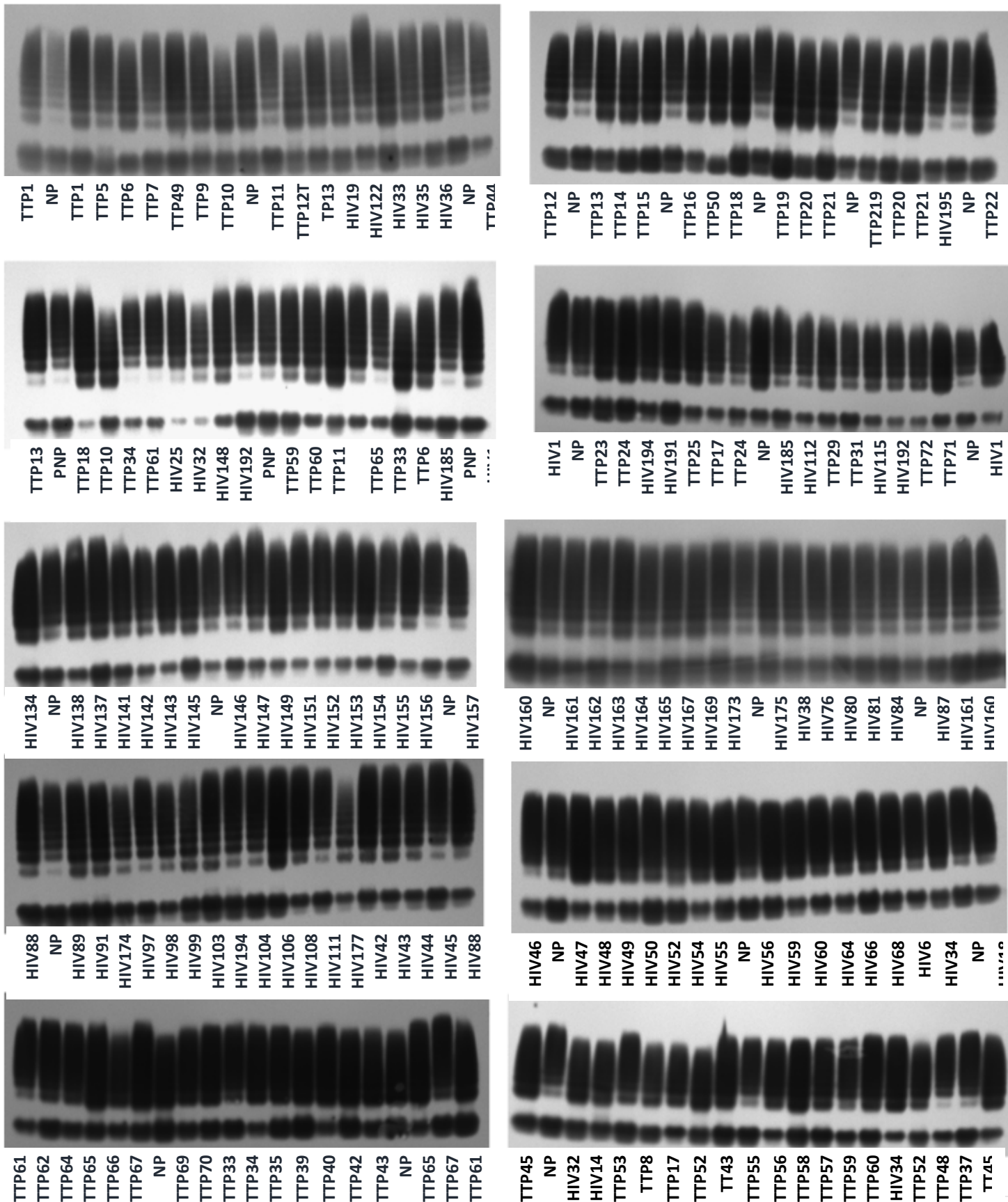


Figure 4.5.1: VWF multimer patterns obtained by 1% SDS agarose gel electrophoresis.
 Numbers in each lane identifies VWF multimeric patterns of individual plasma samples from the HIV-associated TTP, HIV positive and pooled normal plasma samples.

Table 4.8: Obtained concentrations of purified IgG from individual plasma samples.

| HIV-associated TTP samples (n=53) | | | | HIV positive samples (n=18) | | |
|-----------------------------------|-------------------|---|---------------|-----------------------------|---|---------------|
| No.: | Study sample no.: | Quantified purities of IgG antibodies (mg/mL) | 260/280 ratio | Study sample no.: | Quantified purities of IgG antibodies (mg/mL) | 260/280 ratio |
| 1. | TTP 1 | 10,49 | 0,598 | 32/ | 5,028 | 0,550 |
| 2. | TTP 5 | 4,544 | 0,552 | 33/ | 1,437 | 0,585 |
| 3. | TTP 6 | 9,762 | 0,553 | 122/ | 1,36 | 0,597 |
| 4. | TTP 8 | 2,376 | 0,583 | 130/ | 3,715 | 0,531 |
| 5. | TTP 9 | 14,79 | 0,526 | 137/ | 1,265 | 0,554 |
| 6. | TTP 10 | 3,702 | 0,572 | 156/ | 1,4 | 0,558 |
| 7. | TTP 11 | 3,545 | 0,563 | 161/ | 7,63 | 0,514 |
| 8. | TTP 12 | 4,311 | 0,570 | 163/ | 1,312 | 0,583 |
| 9. | TTP 13 | 5,168 | 0,548 | 164/ | 4,152 | 0,540 |
| 10. | TTP 14 | 1,315 | 0,567 | 165/ | 3,138 | 0,543 |
| 11. | TTP 15 | 6,870 | 0,538 | 94/ | 1,265 | 0,554 |
| 12. | TTP 16 | 7,572 | 0,544 | 98/ | 2,045 | 0,544 |
| 13. | TTP 17 | 10,58 | 0,541 | 106/ | 1,735 | 0,595 |
| 14. | TTP 18 | 9,413 | 0,540 | 108/ | 3,78 | 0,547 |
| 15. | TTP 19 | 6,622 | 0,563 | 43/ | 3,906 | 0,580 |
| 16. | TTP 20 | 4,969 | 0,587 | 46/ | 6,701 | 0,570 |
| 17. | TTP 21 | 11,08 | 0,545 | 60/ | 6,803 | 0,512 |
| 18. | TTP 22 | 7,200 | 0,568 | 68/ | 2,997 | 0,534 |
| 19. | TTP 23 | 4,027 | 0,534 | | | |
| 20. | TTP 24 | 7,507 | 0,525 | | | |
| 21. | TTP 25 | 14,79 | 0,526 | | | |
| 22. | TTP 27 | 9,91 | 0,535 | | | |
| 23. | TTP 28 | 9,488 | 0,578 | | | |
| 24. | TTP 29 | 13,243 | 0,537 | | | |
| 25. | TTP 31 | 14,256 | 0,546 | | | |
| 26. | TTP 33 | 8,876 | 0,500 | | | |
| 27. | TTP 34 | 3,293 | 0,524 | | | |
| 28. | TTP 38 | 14,57 | 0,508 | | | |
| 29. | TTP 39 | 2,591 | 0,531 | | | |
| 30. | TTP 40 | 2,997 | 0,534 | | | |
| 31. | TTP 42 | 8,893 | 0,509 | | | |
| 32. | TTP 45 | 4,69 | 0,510 | | | |
| 33. | TTP 48 | 6,614 | 0,596 | | | |
| 34. | TTP 49 | 2,977 | 0,234 | | | |
| 35. | TTP 50 | 10,03 | 0,515 | | | |
| 36. | TTP 52 | 7,538 | 0,527 | | | |
| 37. | TTP 55 | 10,98 | 0,512 | | | |
| 38. | TTP 56 | 5,273 | 0,504 | | | |
| 39. | TTP 57 | 6,507 | 0,516 | | | |
| 40. | TTP 58 | 6,351 | 0,515 | | | |
| 41. | Pre-59 | 5,400 | 0,528 | | | |
| 42. | TTP 60 | 6,800 | 0,527 | | | |

| HIV-associated TTP samples (n=53) | | | | HIV positive samples (n=18) | | |
|-----------------------------------|-------------------|---|---------------|-----------------------------|---|---------------|
| No.: | Study sample no.: | Quantified purities of IgG antibodies (mg/mL) | 260/280 ratio | Study sample no.: | Quantified purities of IgG antibodies (mg/mL) | 260/280 ratio |
| 43. | TTP 61 | 4,215 | 0,543 | | | |
| 44. | TTP 62 | 3,977 | 0,589 | | | |
| 45. | TTP 63 | 2,879 | 0,531 | | | |
| 46. | TTP 64 | 3,715 | 0,531 | | | |
| 47. | TTP 65 | 2,638 | 0,543 | | | |
| 48. | TTP 66 | 3,297 | 0,584 | | | |
| 49. | TTP 67 | 3,578 | 0,586 | | | |
| 50. | TTP 69 | 3,763 | 0,586 | | | |
| 51. | TTP 70 | 3,671 | 0,544 | | | |
| 52. | TTP 71 | 2,312 | 0,577 | | | |
| 53. | TTP 72 | 5,682 | 0,538 | | | |

n, number of samples.

Peptide ELISA Optimization raw data results

A. The results of the plate viability assay.

| dilutions | Absorbance results at 450 nm | | | | | | Mean OD at 450 nm | | |
|-----------|------------------------------|-------|-------|-------|-------|----------------|-------------------|----------|----------|
| | | 1 | 2 | 3 | 4 | | Dilutions | Positive | Negative |
| 1:10000 | A | 1,541 | 1,513 | 0,111 | 0,098 | Absorbance:490 | 1:10000 | 1,4855 | 0,064 |
| 1:20000 | B | 1,291 | 1,2 | 0,083 | 0,081 | Absorbance:490 | 1:20000 | 1,204 | 0,0415 |
| 1:30000 | C | 0,972 | 0,962 | 0,06 | 0,065 | Absorbance:490 | 1:30000 | 0,9255 | 0,022 |
| 1:40000 | D | 0,759 | 0,76 | 0,053 | 0,056 | Absorbance:490 | 1:40000 | 0,718 | 0,014 |
| 1:50000 | E | 0,536 | 0,549 | 0,045 | 0,049 | Absorbance:490 | 1:50000 | 0,501 | 0,0065 |
| Blank | F | 0,041 | 0,042 | 0,041 | 0,04 | Absorbance:490 | | Blank | 0.041 |

Positive control results in blue, negative control results in orange, and the blank results in green.

B. Optimization raw data results

i. Checkerboard titration results of peptide antigen and Positive control sample

| Antibody Dilution | Peptide Dilution | Absorbance readings at 450 nm | | | | | | | |
|-------------------|------------------|-------------------------------|--------|--------|--------|--------|----------|--------|----------------|
| | | 16µg/mL | 8µg/mL | 4µg/mL | 2µg/mL | 1µg/mL | 0.5µg/mL | 0µg/mL | |
| | | 1 | 2 | 3 | 4 | 5 | 6 | 7 | |
| 24µg/mL | A | 1,861 | 1,699 | 1,476 | 1,301 | 1,225 | 1,117 | 0,964 | Absorbance:450 |
| 20µg/mL | B | 1,594 | 1,368 | 1,254 | 1,134 | 1,18 | 0,877 | 0,612 | Absorbance:450 |
| 16µg/mL | C | 1,211 | 1,191 | 1,015 | 0,964 | 0,724 | 0,562 | 0,497 | Absorbance:450 |
| 12µg/mL | D | 1,065 | 1,028 | 0,997 | 0,642 | 0,515 | 0,454 | 0,148 | Absorbance:450 |
| 8µg/mL | E | 0,972 | 0,741 | 0,615 | 0,514 | 0,42 | 0,32 | 0,142 | Absorbance:450 |
| 4µg/mL | F | 0,691 | 0,687 | 0,567 | 0,462 | 0,396 | 0,267 | 0,123 | Absorbance:450 |
| 1µg/mL | G | 0,274 | 0,271 | 0,174 | 0,155 | 0,159 | 0,158 | 0,147 | Absorbance:450 |
| 0µg/mL | H | 0,095 | 0,095 | 0,094 | 0,093 | 0,092 | 0,092 | 0,092 | Absorbance:450 |

Peptide dilution of 4µg/mL showed suitable reading indicating that enough antigen is available for binding antibodies maximally. The antibody concentration of 12µg/mL also produced low background at D7 and was chosen as the optimal concentration for detection of epitopes. With this dilution ratio of 1:4, a good color development from antibody binding was observed, while low background was produced.

ii. Checkerboard titration results of antigen and negative control sample

| sample dilution | peptide dilution | Absorbance reading at 450 nm | | | | | | | |
|-----------------|------------------|------------------------------|--------|--------|--------|--------|----------|--------|----------------|
| | | 16µg/mL | 8µg/mL | 4µg/mL | 2µg/mL | 1µg/mL | 0.5µg/mL | 0µg/mL | |
| | | 1 | 2 | 3 | 4 | 5 | 6 | 7 | |
| 1:50 | A | 0,578 | 0,524 | 0,519 | 0,527 | 0,528 | 0,521 | 0,514 | Absorbance:450 |
| 1:100 | B | 0,449 | 0,423 | 0,429 | 0,442 | 0,443 | 0,461 | 0,413 | Absorbance:450 |
| 1:200 | C | 0,312 | 0,323 | 0,35 | 0,333 | 0,354 | 0,352 | 0,172 | Absorbance:450 |
| 1:400 | D | 0,247 | 0,265 | 0,267 | 0,282 | 0,264 | 0,281 | 0,127 | Absorbance:450 |
| 1:800 | E | 0,203 | 0,21 | 0,231 | 0,222 | 0,215 | 0,228 | 0,117 | Absorbance:450 |
| 1:1600 | F | 0,157 | 0,173 | 0,192 | 0,163 | 0,19 | 0,185 | 0,106 | Absorbance:450 |
| 1:3200 | G | 0,132 | 0,148 | 0,151 | 0,156 | 0,147 | 0,145 | 0,103 | Absorbance:450 |
| 0 | H | 0,097 | 0,095 | 0,094 | 0,092 | 0,092 | 0,09 | 0,09 | Absorbance:450 |

The slight color observed in A7 and B7 shows background binding, although there was no peptide coat, indicating that dilution 1:50 and 1:100 produces non-specific binding of plasma proteins. Therefore, a 1:200 dilution was chosen as the optimal dilution for the negative control that produces low background.

iii. Checkerboard titration results of HRP-conjugated anti-human IgG detection antibody in blocking buffer.

| Conjugate dilution | | Absorbance reading at 450 nm | | | | | | |
|--------------------|---|------------------------------|-------|------------------|-------|--------------|-------|----------------|
| | | Negative control | | Positive control | | Blank values | | |
| | | 1 | 2 | 3 | 4 | 5 | 6 | |
| 1:500 | A | 0,617 | 0,582 | 1,18 | 1,254 | 0,577 | 0,573 | Absorbance:450 |
| 1:1000 | B | 0,516 | 0,501 | 1,028 | 0,997 | 0,36 | 0,352 | Absorbance:450 |
| 1:2000 | C | 0,349 | 0,338 | 0,962 | 0,954 | 0,127 | 0,131 | Absorbance:450 |
| 1:4000 | D | 0,238 | 0,224 | 0,835 | 0,842 | 0,116 | 0,109 | Absorbance:450 |
| 1:8000 | E | 0,223 | 0,209 | 0,613 | 0,625 | 0,096 | 0,095 | Absorbance:450 |
| 1:16000 | F | 0,203 | 0,2 | 0,583 | 0,593 | 0,096 | 0,095 | Absorbance:450 |
| 1:32000 | G | 0,167 | 0,161 | 0,164 | 0,179 | 0,096 | 0,095 | Absorbance:450 |
| 0 | H | 0,098 | 0,098 | 0,096 | 0,097 | 0,096 | 0,095 | Absorbance:450 |

A dilution 1:2000 of the conjugate was chosen as the optimal dilution able to detect bound antibodies, while minimizing background interference. A dilution of 1:500 has an absorbance reading of >0.5 in raw A5 and A6, which indicates a non-specific binding of the conjugate detection antibody with the coated peptides. However, the OD values decrease from raw B, although B5 and B6 still indicates high background at a dilution of 1:1000. Background remains constant for the rest of the dilutions (from raw E6-and raw H), and may suggest minimum background for the plate.

iv. Checkerboard titration results of blocking conditions.

Blocking conditions were maintained at 37°C for 2 hours, with BSA protein diluted to 0.5%, 1% and 2% percent concentrations in PBS (pH 7.4) containing 0.05% Tween-20. A 1% BSA concentration was chosen as the optimal blocking buffer.

| BSA dilution | Peptide coated wells | | | | | | Peptide non-coated wells | | | | | | | |
|--------------|----------------------|-------|-------|-------|-------|-------|--------------------------|-------|-------|-------|-------|-------|-------|----------------|
| | 1 | 2 | 3 | 4 | 5 | 6 | 7 | 8 | 9 | 10 | 11 | 12 | | |
| 0,5% | A | 0,998 | 0,996 | 0,201 | 0,191 | 0,083 | 0,079 | 0,137 | 0,139 | 0,057 | 0,052 | 0,045 | 0,049 | Absorbance:450 |
| 1% | C | 0,696 | 0,675 | 0,161 | 0,131 | 0,065 | 0,068 | 0,098 | 0,092 | 0,055 | 0,057 | 0,046 | 0,043 | Absorbance:450 |
| 2% | E | 0,342 | 0,351 | 0,098 | 0,098 | 0,049 | 0,047 | 0,065 | 0,06 | 0,052 | 0,051 | 0,04 | 0,04 | Absorbance:450 |

The OD values obtained from wells coated with peptides and peptide non-coated wells clearly indicates that background noise influences the results. Blocking with BSA protein reduced background noise, while still allowing antibodies to bind. However, the concentrated BSA at 2% affected the ELISA assay by the time it takes for clear color development to be observed thus affecting antibody binding maximally to peptides. Thus, a 1% BSA concentration was chosen for making up blocking buffer.

C. Assay precision calculation results

| Negative sample (PNP) | | | | Positive sample | | | |
|--|-----------|-----------|------------------|-----------------------------------|-----------|-----------|------------------|
| Plate | Results 1 | Results 2 | Mean OD490 value | Plate | Results 1 | Results 2 | Mean OD490 value |
| 1. | 0.168 | 0.171 | 0.169 | 1. | 0.536 | 0.525 | 0.530 |
| 2. | 0.138 | 0.134 | 0.136 | 2. | 0.548 | 0.557 | 0.552 |
| 3. | 0.117 | 0.124 | 0.121 | 3. | 0.576 | 0.525 | 0.550 |
| 4. | 0.180 | 0.179 | 0.180 | 4. | 0.536 | 0.523 | 0.530 |
| 5. | 0.091 | 0.086 | 0.089 | 5. | 0.459 | 0.423 | 0.441 |
| Means | | | 0.139 | Means | | | 0.521 |
| Standard deviation | | | 0.0081 | Standard deviation | | | 0.0301 |
| % Coefficient of variation | | | 6.09% | % Coefficient of variation | | | 5.77% |
| Inter-assay CV (n=5) = average of positive and negative control CV = (6.09 + 5.77)/2 = 5.93% | | | | | | | |

D. Determining the cut-off value calculated from OD results of negative control

| No.: | Negative OD value | Mean | SD | 2SD | Cut-off value |
|------|-------------------|-------|--------|------------------------------|--|
| 1. | 0.137 | 0.149 | 0.0285 | $(2 * 0.0285)$ $= 0.0571$ | $(0.149 + 0.0571)$ $= \mathbf{0.206}$ |
| 2. | 0.128 | | | | |
| 3. | 0.129 | | | | |
| 4. | 0.195 | | | | |
| 5. | 0.186 | | | | |
| 6. | 0.133 | | | | |
| 7. | 0.14 | | | | |
| 8. | 0.108 | | | | |
| 9. | 0.152 | | | | |
| 10. | 0.199 | | | | |
| 11. | 0.134 | | | | |
| 12. | 0.128 | | | | |
| 13. | 0.182 | | | | |
| 14. | 0.195 | | | | |
| 15. | 0.153 | | | | |
| 16. | 0.132 | | | | |
| 17. | 0.14 | | | | |
| 18. | 0.152 | | | | |
| 19. | 0.15 | | | | |
| 20. | 0.102 | | | | |

Supplementary data 12

Table 4.10: The details of reactive peptides and OD values obtained for each patient IgG antibody sample.

Refer to Excel spreadsheet.

Supplementary data 12

Table 4.10: The details of reactive peptides and OD values obtained for

Linear peptide sequenc

| Sample number | Cys 1 | Cys 2 | Cys 3 |
|-------------------|-------------------------------|-------------------------------|-------------------------------|
| | <i>KTQLEFMSQQCA RTDG QPLR</i> | <i>FMSQQCA RTDG QPLRSSPGG</i> | <i>CA RTDG QPLRSSPGGASFYH</i> |
| TTP Pre 1 | 0,079 | 0,054 | 0,488 |
| TTP Pre 5 | 0,066 | 0,046 | 0,432 |
| TTP Pre 6 | 0,135 | 0,435 | 0,443 |
| TTP Pre 8 | 0,547 | 0,55 | 0,576 |
| TTP Pre 9 | 0,329 | 0,329 | 0,311 |
| TTP Pre 10 | 0,084 | 0,477 | 0,5 |
| TTP Pre 11 | 0,109 | 0,453 | 0,462 |
| TTP Pre 12 | 0,035 | 0,361 | 0,368 |
| TTP Pre 13 | 0,106 | 0,23 | 0,232 |
| TTP Pre 14 | 0,055 | 0,599 | 0,517 |
| TTP Pre 15 | 0,072 | 0,426 | 0,42 |
| TTP Pre 16 | 0,053 | 0,358 | 0,372 |
| TTP Pre 17 | 0,078 | 0,477 | 0,465 |
| TTP Pre 18 | 0,097 | 0,234 | 0,278 |
| TTP Pre 19 | 0,036 | 0,046 | 0,077 |
| TTP Pre 20 | 0,156 | 0,148 | 0,246 |
| TTP Pre 21 | 0,112 | 0,385 | 0,369 |
| TTP Pre 22 | 0,07 | 0,477 | 0,5 |
| TTP Pre 23 | 0,046 | 0,047 | 0,398 |
| TTP Pre 24 | 0,081 | 0,074 | 0,308 |
| TTP Pre 25 | 0,057 | 0,049 | 0,165 |
| TTP Pre 27 | 0,066 | 0,057 | 0,146 |
| TTP Pre 28 | 0,095 | 0,084 | 0,172 |
| TTP Pre 29 | 0,045 | 0,034 | 0,106 |
| TTP Pre 31 | 0,123 | 0,306 | 0,399 |
| TTP Pre 33 | 0,078 | 0,367 | 0,31 |
| TTP Pre 34 | 0,085 | 0,061 | 0,411 |
| TTP Pre 38 | 0,082 | 0,067 | 0,097 |
| TTP Pre 39 | 0,09 | 0,096 | 0,101 |
| TTP Pre 40 | 0,107 | 0,093 | 0,392 |
| TTP Pre 42 | 0,103 | 0,095 | 0,391 |
| TTP Pre 45 | 0,094 | 0,084 | 0,388 |
| TTP Pre 48 | 0,087 | 0,089 | 0,107 |
| TTP Pre 49 | 0,116 | 0,121 | 0,302 |
| TTP Pre 50 | 0,133 | 0,115 | 0,297 |
| TTP Pre 52 | 0,066 | 0,045 | 0,062 |
| TTP Pre 55 | 0,041 | 0,021 | 0,334 |
| TTP Pre 56 | 0,078 | 0,547 | 0,55 |
| TTP Pre 57 | 0,086 | 0,473 | 0,477 |
| TTP Pre 58 | 0,112 | 0,519 | 0,525 |
| TTP Pre 59 | 0,123 | 0,123 | 0,237 |
| TTP Pre 60 | 0,127 | 0,106 | 0,338 |

| | | | |
|----------------------|-------|-------|-------|
| TTP Pre 61 | 0,038 | 0,031 | 0,504 |
| TTP Pre 62 | 0,081 | 0,079 | 0,511 |
| TTP Pre 63 | 0,091 | 0,076 | 0,393 |
| TTP Pre 64 | 0,059 | 0,043 | 0,466 |
| TTP Pre 65 | 0,115 | 0,093 | 0,235 |
| TTP Pre 66 | 0,127 | 0,294 | 0,327 |
| TTP Pre 67 | 0,152 | 0,253 | 0,364 |
| TTP Pre 69 | 0,127 | 0,547 | 0,55 |
| TTP Pre 70 | 0,099 | 0,094 | 0,117 |
| TTP Pre 71 | 0,113 | 0,295 | 0,326 |
| TTP Pre 72 | 0,088 | 0,082 | 0,1 |
| HIV - samples | | | |
| 32/ | 0,238 | 0,24 | 0,287 |
| 33/ | 0,028 | 0,024 | 0,047 |
| 122/ | 0,277 | 0,266 | 0,262 |
| 130/ | 0,006 | 0,002 | 0,026 |
| 137/ | 0,275 | 0,266 | 0,296 |
| 156/ | 0,028 | 0,022 | 0,039 |
| 161/ | 0,049 | 0,042 | 0,071 |
| 163/ | 0,076 | 0,085 | 0,094 |
| 164/ | 0,058 | 0,075 | 0,097 |
| 165/ | 0,062 | 0,086 | 0,084 |
| 94/ | 0,069 | 0,067 | 0,085 |
| 98/ | 0,05 | 0,051 | 0,094 |
| 106/ | 0,267 | 0,265 | 0,297 |
| 108/ | 0,069 | 0,052 | 0,095 |
| 43/ | 0,049 | 0,035 | 0,055 |
| 46/ | 0,107 | 0,097 | 0,123 |
| 60/ | 0,07 | 0,07 | 0,083 |
| 68/ | 0,088 | 0,073 | 0,318 |

for each patient IgG antibody sample.

Peptides: 20 amino acid long. 15aa overlapping and 5aa offset.

| Cys 4 | Cys 5 | Cys 6 | Cys 7 |
|---------------------------------------|--|---|--|
| <i>G</i> QPLRSSPGGASFYHW <i>GAA</i> V | SSPGGASFYHW <i>GAA</i> VPH SQ <i>G</i> | ASFYHW <i>GAA</i> VPH SQ <i>GDALC</i> R | W <i>GAA</i> VPH SQ <i>GDALC</i> RHMCR A |
| 0,555 | 0,532 | 0,544 | 0,063 |
| 0,428 | 0,439 | 0,445 | 0,052 |
| 0,443 | 0,437 | 0,102 | 0,388 |
| 0,607 | 0,063 | 0,047 | 0,045 |
| 0,325 | 0,017 | 0,182 | 0,263 |
| 0,498 | 0,506 | 0,038 | 0,04 |
| 0,474 | 0,474 | 0,067 | 0,066 |
| 0,38 | 0,378 | 0,036 | 0,041 |
| 0,284 | 0,248 | 0,1 | 0,309 |
| 0,581 | 0,504 | 0,053 | 0,051 |
| 0,489 | 0,511 | 0,065 | 0,065 |
| 0,466 | 0,393 | 0,053 | 0,049 |
| 0,467 | 0,494 | 0,077 | 0,084 |
| 0,3 | 0,225 | 0,108 | 0,219 |
| 0,097 | 0,071 | 0,054 | 0,063 |
| 0,269 | 0,28 | 0,262 | 0,372 |
| 0,365 | 0,38 | 0,09 | 0,383 |
| 0,498 | 0,506 | 0,15 | 0,579 |
| 0,395 | 0,382 | 0,344 | 0,353 |
| 0,357 | 0,353 | 399 | 0,085 |
| 0,11 | 0,087 | 0,068 | 0,081 |
| 0,101 | 0,079 | 0,059 | 0,069 |
| 0,122 | 0,103 | 0,079 | 0,098 |
| 0,082 | 0,094 | 0,099 | 0,097 |
| 0,457 | 0,422 | 0,114 | 0,416 |
| 0,348 | 0,322 | 0,08 | 0,087 |
| 0,498 | 0,411 | 0,214 | 0,095 |
| 0,099 | 0,082 | 0,065 | 0,066 |
| 0,115 | 0,092 | 0,088 | 0,077 |
| 0,412 | 0,386 | 0,104 | 0,102 |
| 0,403 | 0,381 | 0,098 | 0,092 |
| 0,405 | 0,384 | 0,089 | 0,088 |
| 0,125 | 0,102 | 0,083 | 0,082 |
| 0,314 | 0,332 | 0,306 | 0,345 |
| 0,327 | 0,301 | 0,117 | 0,107 |
| 0,068 | 0,06 | 0,048 | 0,049 |
| 0,339 | 0,317 | 0,21 | 0,307 |
| 0,576 | 0,607 | 0,081 | 0,086 |
| 0,481 | 0,524 | 0,083 | 0,08 |
| 0,557 | 0,521 | 0,101 | 0,098 |
| 0,237 | 0,229 | 0,099 | 0,087 |
| 0,35 | 0,372 | 0,128 | 0,103 |

| | | | |
|-------|-------|-------|-------|
| 0,514 | 0,488 | 0,555 | 0,047 |
| 0,446 | 0,506 | 0,481 | 0,074 |
| 0,411 | 0,362 | 0,465 | 0,076 |
| 0,538 | 0,458 | 0,391 | 0,24 |
| 0,227 | 0,254 | 0,085 | 0,102 |
| 0,347 | 0,324 | 0,198 | 0,583 |
| 0,37 | 0,366 | 0,139 | 0,457 |
| 0,576 | 0,607 | 0,121 | 0,306 |
| 0,122 | 0,106 | 0,095 | 0,095 |
| 0,33 | 0,329 | 0,113 | 0,324 |
| 0,115 | 0,096 | 0,099 | 0,092 |
| | | | |
| 0,294 | 0,278 | 0,072 | 0,329 |
| 0,053 | 0,044 | 0,069 | 0,029 |
| 0,29 | 0,309 | 0,089 | 0,279 |
| 0,035 | 0,023 | 0,035 | 0,005 |
| 0,301 | 0,287 | 0,08 | 0,273 |
| 0,046 | 0,039 | 0,066 | 0,016 |
| 0,061 | 0,043 | 0,079 | 0,024 |
| 0,091 | 0,078 | 0,07 | 0,071 |
| 0,09 | 0,072 | 0,061 | 0,051 |
| 0,076 | 0,07 | 0,06 | 0,054 |
| 0,088 | 0,076 | 0,061 | 0,06 |
| 0,08 | 0,06 | 0,042 | 0,04 |
| 0,255 | 0,273 | 0,059 | 0,306 |
| 0,098 | 0,073 | 0,052 | 0,061 |
| 0,062 | 0,035 | 0,029 | 0,03 |
| 0,132 | 0,103 | 0,082 | 0,092 |
| 0,088 | 0,073 | 0,067 | 0,081 |
| 0,317 | 0,308 | 0,321 | 0,321 |

| Cys 8 | Cys 9 | Cys 10 | Cys 11 |
|---------------------------------|-------------------------------|-----------------------------|-----------------------------|
| <i>PH SQ GDALC RHMCRAI GESF</i> | <i>DALC RHMCR AIGESFIMKRG</i> | <i>HMCRAIGESFIMKRGDSFLD</i> | <i>IGESFIMKRGDSFLDGTRCM</i> |
| 0,049 | 0,076 | 0,066 | 0,099 |
| 0,044 | 0,052 | 0,045 | 0,046 |
| 0,393 | 0,333 | 0,342 | 0,055 |
| 0,05 | 0,075 | 0,073 | 0,05 |
| 0,276 | 0,265 | 0,281 | 0,051 |
| 0,048 | 0,057 | 0,064 | 0,075 |
| 0,072 | 0,087 | 0,099 | 0,039 |
| 0,046 | 0,048 | 0,049 | 0,092 |
| 0,306 | 0,343 | 0,342 | 0,06 |
| 0,062 | 0,052 | 0,048 | 0,074 |
| 0,071 | 0,071 | 0,059 | 0,081 |
| 0,066 | 0,147 | 0,087 | 0 |
| 0,091 | 0,08 | 0,072 | 0,066 |
| 0,299 | 0,276 | 0,284 | 0,016 |
| 0,06 | 0,188 | 0,132 | 0,01 |
| 0,351 | 0,327 | 0,338 | 0,069 |
| 0,335 | 0,272 | 0,231 | 0,068 |
| 0,571 | 0,574 | 0,615 | 0,092 |
| 0,365 | 0,371 | 0,365 | 0,082 |
| 0,092 | 0,165 | 0,095 | 0,031 |
| 0,109 | 0,122 | 0,085 | 0,05 |
| 0,109 | 0,121 | 0,069 | 0,044 |
| 0,117 | 0,135 | 0,086 | 0,17 |
| 0,102 | 0,105 | 0,048 | 0,074 |
| 0,435 | 0,458 | 0,412 | 0,087 |
| 0,078 | 0,089 | 0,083 | 0,02 |
| 0,086 | 0,152 | 0,109 | 0,087 |
| 0,077 | 0,076 | 0,08 | 0,052 |
| 0,081 | 0,086 | 0,077 | 0,013 |
| 0,102 | 0,115 | 0,104 | 0,067 |
| 0,099 | 0,107 | 0,108 | 0,104 |
| 0,09 | 0,103 | 0,089 | 0,113 |
| 0,085 | 0,091 | 0,081 | 0,199 |
| 0,392 | 0,387 | 0,328 | 0,006 |
| 0,105 | 0,109 | 0,103 | 0,042 |
| 0,045 | 0,057 | 0,06 | 0,033 |
| 0,314 | 0,322 | 0,321 | 0,009 |
| 0,077 | 0,08 | 0,131 | 0,056 |
| 0,074 | 0,092 | 0,081 | 0,083 |
| 0,091 | 0,098 | 0,143 | 0,053 |
| 0,085 | 0,105 | 0,092 | 0,009 |
| 0,126 | 0,15 | 0,116 | 0,01 |

| | | | |
|-------|-------|-------|-------|
| 0,055 | 0,123 | 0,091 | 0,064 |
| 0,082 | 0,147 | 0,126 | 0,023 |
| 0,075 | 0,088 | 0,166 | 0 |
| 0,239 | 0,248 | 0,249 | 0,03 |
| 0,081 | 0,097 | 0,087 | 0,025 |
| 0,584 | 0,592 | 0,585 | 0,078 |
| 0,411 | 0,486 | 0,464 | 0,002 |
| 0,302 | 0,321 | 0,328 | 0,065 |
| 0,098 | 0,111 | 0,097 | 0,076 |
| 0,326 | 0,393 | 0,342 | 0,054 |
| 0,107 | 0,106 | 0,09 | 0,03 |
| | | | |
| 0,312 | 0,32 | 0,33 | 0,055 |
| 0,033 | 0,048 | 0,075 | 0,028 |
| 0,287 | 0,292 | 0,31 | 0,071 |
| 0,006 | 0,022 | 0,031 | 0,018 |
| 0,283 | 0,285 | 0,29 | 0,09 |
| 0,017 | 0,025 | 0,042 | 0,024 |
| 0,03 | 0,039 | 0,046 | 0,075 |
| 0,084 | 0,107 | 0,097 | 0,128 |
| 0,066 | 0,083 | 0,069 | 0,056 |
| 0,067 | 0,09 | 0,063 | 0,085 |
| 0,072 | 0,089 | 0,07 | 0,021 |
| 0,071 | 0,086 | 0,049 | 0,077 |
| 0,333 | 0,395 | 0,266 | 0,10 |
| 0,036 | 0,057 | 0,059 | 0,08 |
| 0,032 | 0,04 | 0,037 | 0,10 |
| 0,097 | 0,109 | 0,111 | 0,07 |
| 0,093 | 0,135 | 0,096 | 0,013 |
| 0,354 | 0,375 | 0,332 | 0,173 |

| Cys 12 | Cys 13 | Cys 14 | Cys 15 |
|-----------------------------|----------------------------|----------------------------|------------------------------|
| <i>IMKRGDSFLDGTRCMPSPGR</i> | <i>DSFLDGTRCMPSPREDGTL</i> | <i>GTRCMPSPREDGTLSLCVS</i> | <i>PSGPREDGTLSLCVSGS CRT</i> |
| 0,098 | 0,077 | 0,04 | 0,04 |
| 0,048 | 0,048 | 0,05 | 0,09 |
| 0,072 | 0,063 | 0,062 | 0,073 |
| 0,053 | 0,047 | 0,053 | 0,062 |
| 0,053 | 0,511 | 0,531 | 0,544 |
| 0,07 | 0,064 | 0,088 | 0,081 |
| 0,044 | 0,037 | 0,062 | 0,076 |
| 0,062 | 0,093 | 0,092 | 0,082 |
| 0,059 | 0,059 | 0,049 | 0,076 |
| 0,074 | 0,067 | 0,067 | 0,071 |
| 0,086 | 0,054 | 0,101 | 0,093 |
| 0,025 | 0,008 | 0,002 | 0,026 |
| 0,055 | 0,029 | 0,004 | 0,043 |
| 0,013 | 0,084 | 0,087 | 0,1 |
| 0,047 | 0,083 | 0,021 | 0,066 |
| 0,135 | 0,515 | 0,537 | 0,609 |
| 0,04 | 0,036 | 0,069 | 0,079 |
| 0,045 | 0,039 | 0,043 | 0,094 |
| 0,093 | 0,05 | 0,081 | 0,071 |
| 0,036 | 0,072 | 0,076 | 0,082 |
| 0,04 | 0,002 | 0,01 | 0,017 |
| 0,035 | 0,077 | 0,022 | 0,005 |
| 0,145 | 0,065 | 0,058 | 0,072 |
| 0,049 | 0,089 | 0,089 | 0,01 |
| 0,08 | 0,511 | 0,531 | 0,544 |
| 0,08 | 0,004 | 0,01 | 0,009 |
| 0,097 | 0,033 | 0,042 | 0,027 |
| 0,079 | 0,018 | 0,013 | 0,013 |
| 0,095 | 0,054 | 0,046 | 0,047 |
| 0,076 | 0,095 | 0,118 | 0,066 |
| 0,089 | 0,043 | 0,028 | 0,057 |
| 0,115 | 0,051 | 0,052 | 0,048 |
| 0,199 | 0,042 | 0,04 | 0,011 |
| 0,032 | 0,149 | 0,143 | 0,162 |
| 0,07 | 0,023 | 0,016 | 0,025 |
| 0,032 | 0,02 | 0,032 | 0,038 |
| 0,049 | 0,043 | 0,056 | 0,017 |
| 0,063 | 0,005 | 0,003 | 0,023 |
| 0,082 | 0,374 | 0,38 | 0,398 |
| 0,05 | 0,07 | 0,023 | 0,032 |
| 0,031 | 0,02 | 0,06 | 0,03 |
| 0,013 | 0,04 | 0,043 | 0,042 |

| | | | |
|-------|-------|-------|-------|
| 0,009 | 0,002 | 0,002 | 0,027 |
| 0,003 | 0,021 | 0,005 | 0,085 |
| 0,026 | 0,041 | 0,046 | 0,015 |
| 0,01 | 0,079 | 0,072 | 0,068 |
| 0,024 | 0,051 | 0,026 | 0,029 |
| 0,068 | 0,548 | 0,539 | 0,529 |
| 0,024 | 0,006 | 0,009 | 0,006 |
| 0,098 | 0,569 | 0,535 | 0,538 |
| 0,062 | 0,518 | 0,488 | 0,503 |
| 0,022 | 0,021 | 0,025 | 0,057 |
| 0,004 | 0,006 | 0,048 | 0,032 |

| | | | |
|-------|-------|-------|-------|
| 0,034 | 0,036 | 0,05 | 0,065 |
| 0,024 | 0,02 | 0,021 | 0,031 |
| 0,062 | 0,072 | 0,07 | 0,078 |
| 0,014 | 0,012 | 0,019 | 0,019 |
| 0,085 | 0,079 | 0,087 | 0,086 |
| 0,026 | 0,02 | 0,023 | 0,025 |
| 0,077 | 0,062 | 0,07 | 0,078 |
| 0,072 | 0,065 | 0,069 | 0,071 |
| 0,055 | 0,044 | 0,048 | 0,045 |
| 0,085 | 0,074 | 0,07 | 0,064 |
| 0,015 | 0,013 | 0,008 | 0,007 |
| 0,084 | 0,066 | 0,063 | 0,064 |
| 0,09 | 0,10 | 0,10 | 0,10 |
| 0,09 | 0,08 | 0,09 | 0,08 |
| 0,09 | 0,08 | 0,09 | 0,08 |
| 0,06 | 0,06 | 0,07 | 0,05 |
| 0,009 | 0,005 | 0,008 | 0,011 |
| 0,169 | 0,163 | 0,17 | 0,158 |

| Cys 16 | Cys 17 | Cys 18 | Cys 19 |
|-----------------------------|-----------------------------|-----------------------------|------------------------------|
| <i>EDGTLSLCVSGSCRTFGCDG</i> | <i>SLCVSGSCRTFGCDGRMDSQ</i> | <i>GSCRTFGCDGRMDSQQVWDR</i> | <i>FGCDGRMDSQQVWDRQCQVCG</i> |
| 0,041 | 0,081 | 0,061 | 0,063 |
| 0,089 | 0,096 | 0,048 | 0,05 |
| 0,068 | 0,042 | 0,056 | 0,059 |
| 0,051 | 0,037 | 0,041 | 0,052 |
| 0,541 | 0,059 | 0,053 | 0,053 |
| 0,071 | 0,051 | 0,074 | 0,057 |
| 0,05 | 0,032 | 0,046 | 0,026 |
| 0,093 | 0,084 | 0,095 | 0,095 |
| 0,072 | 0,058 | 0,074 | 0,057 |
| 0,062 | 0,06 | 0,063 | 0,076 |
| 0,047 | 0,052 | 0,075 | 0,057 |
| 0,01 | 0,005 | 0,438 | 0,423 |
| 0,008 | 0,493 | 0,549 | 0,546 |
| 0,063 | 0,452 | 0,484 | 0,487 |
| 0,008 | 0,445 | 0,356 | 0,369 |
| 0,539 | 0,539 | 0,531 | 0,515 |
| 0,042 | 0,085 | 0,069 | 0,065 |
| 0,022 | 0,371 | 0,363 | 0,366 |
| 0,089 | 0,547 | 0,55 | 0,576 |
| 0,074 | 0,473 | 0,477 | 0,481 |
| 0,005 | 0,448 | 0,45 | 0,475 |
| 0,001 | 0,488 | 0,481 | 0,496 |
| 0,065 | 0,579 | 0,571 | 0,574 |
| 0,074 | 0,061 | 0,064 | 0,074 |
| 0,541 | 0,548 | 0,536 | 0,55 |
| 0,02 | 0,273 | 0,282 | 0,286 |
| 0,037 | 0,301 | 0,325 | 0,333 |
| 0,003 | 0,264 | 0,276 | 0,28 |
| 0,052 | 0,353 | 0,336 | 0,349 |
| 0,092 | 0,374 | 0,378 | 0,383 |
| 0,012 | 0,307 | 0,32 | 0,349 |
| 0,03 | 0,35 | 0,363 | 0,357 |
| 0,028 | 0,262 | 0,267 | 0,282 |
| 0,172 | 0,463 | 0,465 | 0,467 |
| 0,027 | 0,314 | 0,342 | 0,332 |
| 0,036 | 0,314 | 0,308 | 0,316 |
| 0,086 | 0,444 | 0,454 | 0,446 |
| 0,014 | 0,28 | 0,288 | 0,298 |
| 0,393 | 0,367 | 0,364 | 0,398 |
| 0,032 | 0,303 | 0,302 | 0,308 |
| 0,04 | 0,486 | 0,485 | 0,484 |
| 0,045 | 0,432 | 0,428 | 0,439 |

| | | | |
|-------|-------|-------|-------|
| 0,008 | 0,374 | 0,366 | 0,393 |
| 0,018 | 0,423 | 0,428 | 0,414 |
| 0,045 | 0,456 | 0,451 | 0,451 |
| 0,096 | 0,41 | 0,424 | 0,427 |
| 0,036 | 0,353 | 0,365 | 0,367 |
| 0,557 | 0,454 | 0,487 | 0,464 |
| 0,008 | 0,387 | 0,42 | 0,419 |
| 0,547 | 0,477 | 0,5 | 0,498 |
| 0,543 | 0,453 | 0,462 | 0,474 |
| 0,051 | 0,361 | 0,368 | 0,38 |
| 0,064 | 0,069 | 0,071 | 0,06 |
| | | | |
| 0,062 | 0,062 | 0,063 | 0,056 |
| 0,024 | 0,024 | 0,03 | 0,025 |
| 0,073 | 0,072 | 0,082 | 0,078 |
| 0,015 | 0,018 | 0,034 | 0,012 |
| 0,083 | 0,088 | 0,103 | 0,091 |
| 0,025 | 0,027 | 0,033 | 0,028 |
| 0,063 | 0,069 | 0,078 | 0,063 |
| 0,069 | 0,065 | 0,08 | 0,094 |
| 0,042 | 0,043 | 0,054 | 0,064 |
| 0,067 | 0,076 | 0,081 | 0,098 |
| 0,003 | 0,005 | 0,01 | 0,025 |
| 0,053 | 0,058 | 0,073 | 0,078 |
| 0,10 | 0,10 | 0,10 | 0,11 |
| 0,08 | 0,08 | 0,08 | 0,09 |
| 0,09 | 0,08 | 0,09 | 0,10 |
| 0,06 | 0,05 | 0,05 | 0,06 |
| 0,008 | 0,015 | 0,019 | 0,027 |
| 0,16 | 0,165 | 0,148 | 0,205 |

| Cys/Spa 20 | Cys/Spa 21 | Cys/Spa 22 | Cys/Spa 23 |
|-----------------------------|-----------------------------|------------------------------|------------------------------|
| <i>RMDSQQVWDRQCVCGGDNST</i> | <i>QVWDRQCVCGGDNSTCSPRK</i> | <i>CQVCG DNSTCSPRKG SFTA</i> | <i>GDNSTCSPRKG SFTAGRARE</i> |
| 0,052 | 0,015 | 0,039 | 0,062 |
| 0,057 | 0,133 | 0,116 | 0,09 |
| 0,058 | 0,09 | 0,082 | 0,091 |
| 0,066 | 0,159 | 0,142 | 0,159 |
| 0,06 | 0,118 | 0,121 | 0,131 |
| 0,15 | 0,121 | 0,116 | 0,124 |
| 0,072 | 0,109 | 0,101 | 0,098 |
| 0,062 | 0,055 | 0,069 | 0,046 |
| 0,066 | 0,046 | 0,096 | 0,078 |
| 0,072 | 0,057 | 0,061 | 0,042 |
| 0,062 | 0,082 | 0,145 | 0,079 |
| 0,49 | 0,057 | 0,095 | 0,058 |
| 0,655 | 0,103 | 0,16 | 0,128 |
| 0,562 | 0,119 | 0,133 | 0,11 |
| 0,358 | 0,091 | 0,069 | 0,078 |
| 0,526 | 0,149 | 0,152 | 0,114 |
| 0,038 | 0,089 | 0,099 | 0,08 |
| 0,367 | 0,088 | 0,115 | 0,095 |
| 0,607 | 0,07 | 0,09 | 0,117 |
| 0,524 | 0,025 | 0,049 | 0,062 |
| 0,483 | 0,041 | 0,066 | 0,05 |
| 0,532 | 0,061 | 0,064 | 0,1 |
| 0,615 | 0,057 | 0,069 | 0,131 |
| 0,103 | 0,06 | 0,04 | 0,048 |
| 0,6 | 0,072 | 0,076 | 0,09 |
| 0,285 | 0,045 | 0,051 | 0,069 |
| 0,321 | 0,055 | 0,076 | 0,07 |
| 0,301 | 0,051 | 0,041 | 0,042 |
| 0,373 | 0,084 | 0,049 | 0,052 |
| 0,395 | 0,081 | 0,081 | 0,075 |
| 0,344 | 0,002 | 0,048 | 0,032 |
| 0,346 | 0,041 | 0,048 | 0,061 |
| 0,27 | 0,032 | 0,008 | 0,021 |
| 0,444 | 0,029 | 0,009 | 0,017 |
| 0,322 | 0,096 | 0,046 | 0,042 |
| 0,315 | 0,073 | 0,058 | 0,072 |
| 0,447 | 0,066 | 0,081 | 0,055 |
| 0,285 | 0,036 | 0,031 | 0,024 |
| 0,372 | 0,095 | 0,033 | 0,034 |
| 0,321 | 0,074 | 0,25 | 0,22 |
| 0,5 | 0,013 | 0,017 | 0,017 |
| 0,445 | 0,062 | 0,082 | 0,323 |

| | | | |
|-------|-------|-------|-------|
| 0,37 | 0,125 | 0,13 | 0,137 |
| 0,418 | 0,156 | 0,152 | 0,152 |
| 0,435 | 0,153 | 0,149 | 0,153 |
| 0,429 | 0,047 | 0,03 | 0,057 |
| 0,37 | 0,131 | 0,142 | 0,145 |
| 0,469 | 0,028 | 0,024 | 0,036 |
| 0,411 | 0,051 | 0,068 | 0,071 |
| 0,506 | 0,044 | 0,082 | 0,079 |
| 0,474 | 0,092 | 0,088 | 0,103 |
| 0,378 | 0,044 | 0,063 | 0,071 |
| 0,088 | 0,015 | 0,016 | 0 |
| <hr/> | | | |
| 0,046 | 0,062 | 0,058 | 0,062 |
| 0,02 | 0,058 | 0,053 | 0,058 |
| 0,069 | 0,05 | 0,049 | 0,054 |
| 0,016 | 0,055 | 0,036 | 0,025 |
| 0,096 | 0,072 | 0,06 | 0,065 |
| 0,031 | 0,063 | 0,057 | 0,057 |
| 0,072 | 0,122 | 0,089 | 0,093 |
| 0,093 | 0,076 | 0,051 | 0,077 |
| 0,06 | 0,078 | 0,069 | 0,08 |
| 0,103 | 0,09 | 0,081 | 0,077 |
| 0,02 | 0,079 | 0,075 | 0,069 |
| 0,073 | 0,079 | 0,066 | 0,061 |
| 0,10 | 0,086 | 0,082 | 0,075 |
| 0,08 | 0,083 | 0,078 | 0,06 |
| 0,10 | 0,074 | 0,09 | 0,068 |
| 0,06 | 0,102 | 0,118 | 0,079 |
| 0,011 | 0,049 | 0,042 | 0,045 |
| 0,185 | 0,122 | 0,121 | 0,128 |

| Spa 24 | Spa 25 | Spa 26 | Spa 27 |
|----------------------------|------------------------|------------------|---------------|
| <i>CSPRKGSTAGRARREYVTF</i> | <i>GSFTAGRARREYVTF</i> | <i>GRAREYVTF</i> | <i>YVTF</i> |
| 0,06 | 0,056 | 0,019 | 0,075 |
| 0,056 | 0,091 | 0,046 | 0,033 |
| 0,07 | 0,091 | 0,056 | 0,024 |
| 0,089 | 0,077 | 0,099 | 0,081 |
| 0,581 | 0,504 | 0,514 | 0,488 |
| 0,094 | 0,073 | 0,103 | 0,07 |
| 0,096 | 0,051 | 0,064 | 0,032 |
| 0,105 | 0,058 | 0,092 | 0,074 |
| 0,08 | 0,032 | 0,063 | 0,047 |
| 0,08 | 0,048 | 0,058 | 0,05 |
| 0,114 | 0,072 | 0,075 | 0,088 |
| 0,069 | 0,021 | 0,032 | 0,025 |
| 0,115 | 0,082 | 0,104 | 0,084 |
| 0,093 | 0,055 | 0,068 | 0,086 |
| 0,068 | 0,055 | 0,039 | 0,03 |
| 0,138 | 0,103 | 0,12 | 0,099 |
| 0,064 | 0,098 | 0,04 | 0,04 |
| 0,15 | 0,108 | 0,122 | 0,103 |
| 0,121 | 0,121 | 0,152 | 0,107 |
| 0,107 | 0,096 | 0,113 | 0,103 |
| 0,021 | 0,047 | 0,08 | 0,06 |
| 0,104 | 0,088 | 0,131 | 0,071 |
| 0,094 | 0,088 | 0,141 | 0,083 |
| 0,009 | 0,056 | 0,02 | 0,036 |
| 0,127 | 0,096 | 0,125 | 0,092 |
| 0,076 | 0,068 | 0,068 | 0,034 |
| 0,07 | 0,094 | 0,118 | 0,158 |
| 0,162 | 0,119 | 0,166 | 0,175 |
| 0,039 | 0,022 | 0,05 | 0,064 |
| 0,085 | 0,094 | 0,069 | 0,097 |
| 0,077 | 0,169 | 0,013 | 0,117 |
| 0,064 | 0,05 | 0,009 | 0,08 |
| 0,053 | 0,069 | -0,014 | 0,059 |
| 0,216 | 0,139 | 0,149 | 0,123 |
| 0,124 | 0,146 | 0,081 | 0,141 |
| 0,101 | 0,028 | 0,046 | -0,003 |
| 0,135 | 0,101 | 0,173 | 0,093 |
| 0,104 | 0,091 | 0,091 | 0,025 |
| 0,017 | 0,022 | 0,066 | 0,043 |
| 0,049 | 0,065 | 0,093 | 0,049 |
| 0,079 | 0,088 | 0,096 | 0,101 |
| 0,098 | 0,124 | 0,113 | 0,133 |

| | | | |
|-------|-------|-------|-------|
| 0,078 | 0,03 | 0,075 | 0,057 |
| 0,115 | 0,076 | 0,09 | 0,088 |
| 0,136 | 0,094 | 0,109 | 0,098 |
| 0,018 | 0,064 | 0,075 | 0,07 |
| 0,042 | 0,09 | 0,123 | 0,102 |
| 0,058 | 0,057 | 0,063 | 0,067 |
| 0,037 | 0,012 | 0,014 | 0,021 |
| 0,035 | 0,016 | 0,039 | 0,032 |
| 0,054 | 0,048 | 0,036 | 0,057 |
| 0,051 | 0,005 | 0,016 | 0,012 |
| 0,057 | 0,012 | 0,032 | 0,022 |

| | | | |
|-------|-------|-------|-------|
| 0,067 | 0,058 | 0,052 | 0,062 |
| 0,056 | 0,055 | 0,054 | 0,061 |
| 0,066 | 0,042 | 0,05 | 0,049 |
| 0,032 | 0,021 | 0,03 | 0,028 |
| 0,056 | 0,043 | 0,048 | 0,052 |
| 0,062 | 0,055 | 0,07 | 0,05 |
| 0,097 | 0,087 | 0,05 | 0,083 |
| 0,129 | 0,069 | 0,072 | 0,08 |
| 0,087 | 0,067 | 0,075 | 0,07 |
| 0,08 | 0,066 | 0,08 | 0,076 |
| 0,074 | 0,056 | 0,055 | 0,066 |
| 0,072 | 0,055 | 0,064 | 0,064 |
| 0,089 | 0,069 | 0,067 | 0,069 |
| 0,082 | 0,055 | 0,068 | 0,062 |
| 0,084 | 0,081 | 0,095 | 0,102 |
| 0,07 | 0,076 | 0,093 | 0,09 |
| 0,054 | 0,045 | 0,034 | 0,066 |
| 0,136 | 0,123 | 0,13 | 0,128 |

| Spa 28 | Spa 29 | Spa 30 | Spa 31 |
|-----------------------------|-----------------------------|-----------------------------|-----------------------------|
| <i>TVTPNLTSVYIANHRPLFTH</i> | <i>LTSVYIANHRPLFTHLAVRI</i> | <i>IANHRPLFTHLAVRIGGRYV</i> | <i>PLFTHLAVRIGGRYVVAGKM</i> |
| 0,066 | 0,082 | 0,099 | 0,175 |
| 0,023 | 0,078 | 0,031 | 0,248 |
| 0,005 | 0,089 | 0,012 | 0,175 |
| 0,055 | 0,063 | 0,014 | 0,272 |
| 0,555 | 0,165 | 0,091 | 0,287 |
| 0,057 | 0,058 | 0,064 | 0,207 |
| 0,025 | 0,064 | 0,019 | 0,383 |
| 0,054 | 0,058 | 0,001 | 0,444 |
| 0,011 | 0,043 | 0 | 0,191 |
| 0,036 | 0,063 | 0,062 | 0,103 |
| 0,043 | 0,064 | -0,035 | 0,159 |
| 0,001 | 0,019 | 0,061 | 0,132 |
| 0,071 | 0,104 | 0,024 | 0,142 |
| 0,05 | 0,067 | -0,013 | 0,228 |
| 0,033 | 0,061 | 0,006 | 0,098 |
| 0,082 | 0,115 | 0,015 | 0,278 |
| 0,04 | 0,022 | 0,016 | 0,098 |
| 0,088 | 0,1 | 0,017 | 0,078 |
| 0,106 | 0,175 | 0,068 | 0,519 |
| 0,096 | 0,134 | 0,046 | 0,472 |
| 0,076 | 0,045 | 0,066 | 0,402 |
| 0,098 | 0,094 | 0,025 | 0,575 |
| 0,107 | 0,142 | 0,045 | 0,598 |
| 0,02 | 0,049 | 0,041 | 0,316 |
| 0,13 | 0,107 | 0,049 | 0,535 |
| 0,044 | 0,021 | 0,04 | 0,413 |
| 0,13 | 0,099 | 0,065 | 0,462 |
| 0,138 | 0,14 | 0,17 | 0,495 |
| 0,05 | 0,057 | 0,045 | 0,519 |
| 0,076 | 0,101 | 0,098 | 0,472 |
| 0,057 | 0,01 | 0,068 | 0,402 |
| 0,062 | 0,014 | 0,045 | 0,508 |
| 0,007 | 0,038 | 0,038 | 0,598 |
| 0,19 | 0,167 | 0,044 | 0,569 |
| 0,116 | 0,11 | 0,049 | 0,535 |
| 0,1 | 0,056 | 0,054 | 0,444 |
| 0,026 | 0,153 | 0,123 | 0,467 |
| 0,057 | 0,071 | 0,16 | 0,493 |
| 0,029 | 0,026 | 0,041 | 0,459 |
| 0,023 | 0,091 | 0,058 | 0,376 |
| 0,101 | 0,11 | 0,118 | 0,488 |
| 0,048 | 0,063 | 0,132 | 0,575 |

| | | | |
|-------|-------|-------|-------|
| 0,047 | 0,054 | 0,097 | 0,498 |
| 0,071 | 0,083 | 0,121 | 0,408 |
| 0,105 | 0,1 | 0,151 | 0,403 |
| 0,049 | 0,072 | 0,087 | 0,403 |
| 0,076 | 0,101 | 0,04 | 0,388 |
| 0,021 | 0,033 | 0,099 | 0,464 |
| 0,012 | 0,021 | 0,049 | 0,484 |
| 0,021 | 0,019 | 0,044 | 0,519 |
| 0,036 | 0,049 | 0,083 | 0,562 |
| 0,005 | 0,065 | 0,041 | 0,441 |
| 0,024 | 0,012 | 0,059 | 0,362 |

| | | | |
|-------|-------|-------|-------|
| 0,055 | 0,057 | 0,072 | 0,097 |
| 0,055 | 0,061 | 0,082 | 0,07 |
| 0,018 | 0,051 | 0,049 | 0,109 |
| 0,014 | 0,024 | 0,029 | 0,104 |
| 0,033 | 0,05 | 0,051 | 0,096 |
| 0,029 | 0,036 | 0,055 | 0,095 |
| 0,063 | 0,062 | 0,075 | 0,015 |
| 0,071 | 0,079 | 0,081 | 0,115 |
| 0,073 | 0,068 | 0,062 | 0,123 |
| 0,082 | 0,092 | 0,087 | 0,224 |
| 0,076 | 0,06 | 0,067 | 0,079 |
| 0,063 | 0,061 | 0,07 | 0,09 |
| 0,086 | 0,054 | 0,085 | 0,047 |
| 0,063 | 0,055 | 0,085 | 0,093 |
| 0,065 | 0,095 | 0,081 | 0,058 |
| 0,099 | 0,051 | 0,079 | 0,051 |
| 0,065 | 0,046 | 0,023 | 0,062 |
| 0,12 | 0,113 | 0,13 | 0,059 |

| Spa 32 | Spa 33 | Spa 34 | Spa 35 |
|-----------------------------|----------------------------|------------------------------|------------------------------|
| <i>LAVRIGGRYVVAGKMSISPN</i> | <i>GGRYVVAGKMSISPNTTYP</i> | <i>VAGKMSISPNTTYPSSLLEDG</i> | <i>SISPNTTYPSSLLEDGRVEYR</i> |
| 0,198 | 0,213 | 0,2 | 0,195 |
| 0,274 | 0,287 | 0,272 | 0,062 |
| 0,19 | 0,196 | 0,185 | 0,171 |
| 0,285 | 0,29 | 0,283 | 0,27 |
| 0,287 | 0,296 | 0,294 | 0,271 |
| 0,21 | 0,227 | 0,216 | 0,191 |
| 0,377 | 0,384 | 0,377 | 0,133 |
| 0,413 | 0,43 | 0,405 | 0,042 |
| 0,115 | 0,11 | 0,098 | 0,092 |
| 0,202 | 0,186 | 0,193 | 0,176 |
| 0,191 | 0,17 | 0,18 | 0,168 |
| 0,103 | 0,09 | 0,085 | 0,084 |
| 0,159 | 0,154 | 0,141 | 0,149 |
| 0,132 | 0,113 | 0,119 | 0,174 |
| 0,142 | 0,113 | 0,112 | 0,112 |
| 0,228 | 0,256 | 0,297 | 0,123 |
| 0,06 | 0,076 | 0,076 | 0,077 |
| 0,069 | 0,055 | 0,063 | 0,061 |
| 0,516 | 0,496 | 0,486 | 0,093 |
| 0,472 | 0,462 | 0,484 | 0,159 |
| 0,4 | 0,503 | 0,381 | 0,076 |
| 0,56 | 0,593 | 0,576 | 0,069 |
| 0,572 | 0,586 | 0,573 | 0,075 |
| 0,302 | 0,311 | 0,304 | 0,89 |
| 0,515 | 0,486 | 0,458 | 0,182 |
| 0,396 | 0,385 | 0,406 | 0,083 |
| 0,444 | 0,423 | 0,467 | 0,044 |
| 0,473 | 0,451 | 0,476 | 0,067 |
| 0,516 | 0,496 | 0,486 | 0,083 |
| 0,472 | 0,462 | 0,484 | 0,049 |
| 0,4 | 0,376 | 0,381 | 0,126 |
| 0,492 | 0,474 | 0,493 | 0,078 |
| 0,572 | 0,586 | 0,573 | 0,165 |
| 0,563 | 0,496 | 0,486 | 0,088 |
| 0,515 | 0,486 | 0,458 | 0,072 |
| 0,413 | 0,43 | 0,405 | 0,032 |
| 0,464 | 0,46 | 0,425 | 0,033 |
| 0,498 | 0,491 | 0,49 | 0,081 |
| 0,47 | 0,462 | 0,454 | 0,064 |
| 0,386 | 0,356 | 0,38 | 0,049 |
| 0,484 | 0,496 | 0,486 | 0,088 |
| 0,56 | 0,593 | 0,576 | 0,159 |

| | | | |
|-------|-------|-------|-------|
| 0,503 | 0,296 | 0,27 | 0,06 |
| 0,386 | 0,38 | 0,396 | 0,058 |
| 0,364 | 0,35 | 0,34 | 0,022 |
| 0,386 | 0,377 | 0,398 | 0,041 |
| 0,372 | 0,347 | 0,342 | 0,024 |
| 0,462 | 0,467 | 0,464 | 0,049 |
| 0,468 | 0,493 | 0,491 | 0,077 |
| 0,491 | 0,502 | 0,492 | 0,065 |
| 0,537 | 0,569 | 0,543 | 0,118 |
| 0,416 | 0,438 | 0,459 | 0,027 |
| 0,34 | 0,34 | 0,372 | 0,04 |
| | | | |
| 0,068 | 0,065 | 0,068 | 0,095 |
| 0,075 | 0,061 | 0,065 | 0,065 |
| 0,052 | 0,058 | 0,089 | 0,057 |
| 0,049 | 0,054 | 0,095 | 0,086 |
| 0,049 | 0,098 | 0,105 | 0,054 |
| 0,088 | 0,095 | 0,084 | 0,082 |
| 0,054 | 0,056 | 0,063 | 0,087 |
| 0,134 | 0,131 | 0,118 | 0,078 |
| 0,136 | 0,139 | 0,139 | 0,096 |
| 0,216 | 0,228 | 0,231 | 0,078 |
| 0,094 | 0,099 | 0,083 | 0,068 |
| 0,085 | 0,082 | 0,081 | 0,064 |
| 0,061 | 0,053 | 0,087 | 0,063 |
| 0,097 | 0,08 | 0,081 | 0,088 |
| 0,056 | 0,057 | 0,069 | 0,052 |
| 0,062 | 0,051 | 0,046 | 0,044 |
| 0,047 | 0,045 | 0,062 | 0,059 |
| 0,06 | 0,051 | 0,049 | 0,05 |

| Spa 36 | Spa 37 | Spa 38 | Spa 39 |
|------------------------------|------------------------------|------------------------------|------------------------------|
| <i>TTYP</i> SLLEDGRVEYRVALTE | <i>LLED</i> GRVEYRVALTEDRLPR | <i>RVEYR</i> VALTEDRLPRLEEIR | <i>VAL</i> TEDRLPRLEEIRIWGPL |
| 0,14 | 0,16 | 0,149 | 0,159 |
| 0,09 | 0,035 | 0,028 | 0,037 |
| 0,145 | 0,143 | 0,143 | 0,146 |
| 0,255 | 0,245 | 0,224 | 0,262 |
| 0,248 | 0,247 | 0,235 | 0,257 |
| 0,171 | 0,173 | 0,184 | 0,174 |
| 0,124 | 0,14 | 0,138 | 0,133 |
| 0,177 | 0,186 | 0,175 | 0,183 |
| 0,08 | 0,086 | 0,09 | 0,094 |
| 0,179 | 0,177 | 0,186 | 0,175 |
| 0,164 | 0,158 | 0,161 | 0,142 |
| 0,071 | 0,07 | 0,072 | 0,071 |
| 0,135 | 0,117 | 0,119 | 0,17 |
| 0,133 | 0,09 | 0,115 | 0,086 |
| 0,11 | 0,104 | 0,087 | 0,085 |
| 0,16 | 0,184 | 0,186 | 0,078 |
| 0,073 | 0,083 | 0,099 | 0,028 |
| 0,06 | 0,056 | 0,047 | 0,094 |
| 0,098 | 0,091 | 0,09 | 0,091 |
| 0,147 | 0,162 | 0,154 | 0,074 |
| 0,086 | 0,086 | 0,08 | 0,09 |
| 0,063 | 0,096 | 0,086 | 0,098 |
| 0,06 | 0,093 | 0,076 | 0,069 |
| 0,083 | 0,096 | 0,087 | 0,081 |
| 0,181 | 0,183 | 0,181 | 0,007 |
| 0,077 | 0,084 | 0,077 | 0,091 |
| 0,043 | 0,43 | 0,405 | 0,442 |
| 0,064 | 0,46 | 0,425 | 0,443 |
| 0,088 | 0,491 | 0,49 | 0,491 |
| 0,22 | 0,462 | 0,454 | 0,474 |
| 0,136 | 0,356 | 0,38 | 0,349 |
| 0,074 | 0,496 | 0,486 | 0,498 |
| 0,15 | 0,593 | 0,576 | 0,569 |
| 0,093 | 0,296 | 0,27 | 0,311 |
| 0,071 | 0,483 | 0,481 | 0,507 |
| 0,01 | 0,291 | 0,286 | 0,276 |
| 0,046 | 0,362 | 0,353 | 0,343 |
| 0,067 | 0,278 | 0,276 | 0,284 |
| 0,057 | 0,303 | 0,315 | 0,314 |
| 0,085 | 0,268 | 0,265 | 0,278 |
| 0,093 | 0,338 | 0,313 | 0,335 |
| 0,153 | 0,274 | 0,29 | 0,294 |

| | | | |
|-------|-------|-------|-------|
| 0,053 | 0,35 | 0,361 | 0,387 |
| 0,072 | 0,385 | 0,389 | 0,395 |
| 0,013 | 0,334 | 0,346 | 0,37 |
| 0,061 | 0,399 | 0,382 | 0,407 |
| 0,007 | 0,355 | 0,378 | 0,376 |
| 0,043 | 0,459 | 0,467 | 0,467 |
| 0,086 | 0,477 | 0,453 | 0,475 |
| 0,064 | 0,454 | 0,476 | 0,453 |
| 0,119 | 0,499 | 0,518 | 0,544 |
| 0,045 | 0,425 | 0,433 | 0,45 |
| 0,036 | 0,329 | 0,318 | 0,335 |

| | | | |
|-------|-------|-------|-------|
| 0,041 | 0,12 | 0,123 | 0,111 |
| 0,057 | 0,118 | 0,101 | 0,096 |
| 0,086 | 0,136 | 0,144 | 0,128 |
| 0,078 | 0,097 | 0,103 | 0,108 |
| 0,078 | 0,105 | 0,105 | 0,103 |
| 0,073 | 0,077 | 0,103 | 0,067 |
| 0,094 | 0,105 | 0,087 | 0,124 |
| 0,051 | 0,245 | 0,244 | 0,241 |
| 0,054 | 0,232 | 0,261 | 0,253 |
| 0,081 | 0,244 | 0,269 | 0,222 |
| 0,077 | 0,152 | 0,16 | 0,151 |
| 0,073 | 0,244 | 0,266 | 0,248 |
| 0,077 | 0,078 | 0,108 | 0,093 |
| 0,099 | 0,101 | 0,099 | 0,098 |
| 0,047 | 0,051 | 0,052 | 0,054 |
| 0,042 | 0,047 | 0,049 | 0,052 |
| 0,044 | 0,072 | 0,088 | 0,07 |
| 0,048 | 0,044 | 0,039 | 0,051 |

| Spa 40 | Spa 41 | Spa 42 | Spa 43 |
|----------------------------|-----------------------------|--------------------------------|----------------------------------|
| <i>DRLPREEIRIWGPLQEDAD</i> | <i>LEEIRIWGPLQEDADIQVYR</i> | <i>IWGPLQEDADIQVY RRY G EE</i> | <i>QEDADIQVY RRY G EEY G NLT</i> |
| 0,135 | 0,047 | 0,504 | 0,514 |
| 0,022 | 0,096 | 0,511 | 0,446 |
| 0,138 | 0,036 | 0,544 | 0,411 |
| 0,192 | 0,039 | 0,449 | 0,538 |
| 0,117 | 0,052 | 0,454 | 0,382 |
| 0,248 | 0,039 | 0,523 | 0,306 |
| 0,142 | 0,309 | 0,459 | 0,453 |
| 0,182 | 0,337 | 0,487 | 0,496 |
| 0,096 | 0,09 | 0,475 | 0,474 |
| 0,183 | 0,182 | 0,528 | 0,529 |
| 0,161 | 0,15 | 0,437 | 0,455 |
| 0,079 | 0,058 | 0,634 | 0,636 |
| 0,154 | 0,12 | 0,467 | 0,464 |
| 0,103 | 0,092 | 0,493 | 0,498 |
| 0,092 | 0,074 | 0,459 | 0,47 |
| 0,203 | 0,173 | 0,376 | 0,386 |
| 0,061 | 0,061 | 0,488 | 0,484 |
| 0,085 | 0,085 | 0,575 | 0,56 |
| 0,077 | 0,098 | 0,498 | 0,503 |
| 0,167 | 0,13 | 0,333 | 0,323 |
| 0,05 | 0,07 | 0,546 | 0,547 |
| 0,093 | 0,174 | 0,596 | 0,597 |
| 0,063 | 0,068 | 0,329 | 0,342 |
| 0,084 | 0,081 | 0,595 | 0,585 |
| 0,15 | 0,117 | 0,317 | 0,313 |
| 0,089 | 0,096 | 0,346 | 0,346 |
| 0,42 | 0,109 | 0,359 | 0,353 |
| 0,456 | 0,116 | 0,366 | 0,353 |
| 0,477 | 0,134 | 0,384 | 0,359 |
| 0,467 | 0,131 | 0,381 | 0,37 |
| 0,385 | 0,106 | 0,356 | 0,358 |
| 0,503 | 0,112 | 0,362 | 0,351 |
| 0,563 | 0,085 | 0,368 | 0,363 |
| 0,304 | 0,07 | 0,389 | 0,388 |
| 0,5 | 0,097 | 0,681 | 0,705 |
| 0,284 | 0,044 | 0,351 | 0,343 |
| 0,344 | 0,092 | 0,353 | 0,358 |
| 0,262 | 0,069 | 0,346 | 0,348 |
| 0,3 | 0,087 | 0,361 | 0,363 |
| 0,252 | 0,098 | 0,351 | 0,356 |
| 0,332 | 0,09 | 0,38 | 0,37 |
| 0,278 | 0,12 | 0,368 | 0,366 |

| | | | |
|-------|-------|-------|-------|
| 0,367 | 0,11 | 0,39 | 0,39 |
| 0,392 | 0,12 | 0,4 | 0,364 |
| 0,365 | 0,096 | 0,376 | 0,382 |
| 0,414 | 0,145 | 0,425 | 0,438 |
| 0,356 | 0,124 | 0,404 | 0,408 |
| 0,451 | 0,14 | 0,42 | 0,424 |
| 0,448 | 0,112 | 0,392 | 0,408 |
| 0,482 | 0,091 | 0,371 | 0,409 |
| 0,538 | 0,102 | 0,382 | 0,39 |
| 0,45 | 0,034 | 0,314 | 0,339 |
| 0,327 | 0,125 | 0,559 | 0,563 |
| | | | |
| 0,109 | 0,192 | 0,073 | 0,095 |
| 0,098 | 0,07 | 0,064 | 0,074 |
| 0,125 | 0,081 | 0,074 | 0,084 |
| 0,1 | 0,057 | 0,048 | 0,046 |
| 0,099 | 0,092 | 0,093 | 0,092 |
| 0,066 | 0,095 | 0,105 | 0,096 |
| 0,085 | 0,081 | 0,099 | 0,11 |
| 0,239 | 0,043 | 0,07 | 0,068 |
| 0,251 | 0,053 | 0,067 | 0,041 |
| 0,223 | 0,075 | 0,087 | 0,088 |
| 0,159 | 0,072 | 0,126 | 0,139 |
| 0,248 | 0,079 | 0,092 | 0,105 |
| 0,107 | 0,094 | 0,094 | 0,103 |
| 0,104 | 0,051 | 0,053 | 0,049 |
| 0,058 | 0,06 | 0,061 | 0,053 |
| 0,052 | 0,118 | 0,217 | 0,219 |
| 0,088 | 0,047 | 0,273 | 0,295 |
| 0,046 | 0,081 | 0,099 | 0,11 |

| Spa 44 | Spa 45 | Spa/TSP1-2 46 |
|-----------------------------------|----------------------------------|--------------------------------|
| <i>IQVY RRY G EEY G NLT RPDIT</i> | <i>RY G EEY G NLT RPDITFTYFQ</i> | <i>Y G NLT RPDITFTYFQPKPRQ</i> |
| 0,488 | 0,555 | 0,532 |
| 0,506 | 0,481 | 0,475 |
| 0,362 | 0,465 | 0,421 |
| 0,458 | 0,391 | 0,518 |
| 0,385 | 0,404 | 0,375 |
| 0,315 | 0,301 | 0,28 |
| 0,498 | 0,503 | 0,253 |
| 0,482 | 0,481 | 0,227 |
| 0,442 | 0,42 | 0,291 |
| 0,443 | 0,456 | 0,255 |
| 0,491 | 0,477 | 0,283 |
| 0,64 | 0,647 | 0,634 |
| 0,563 | 0,568 | 0,249 |
| 0,516 | 0,512 | 0,201 |
| 0,517 | 0,513 | 0,219 |
| 0,345 | 0,345 | 0,369 |
| 0,33 | 0,315 | 0,598 |
| 0,542 | 0,527 | 0,531 |
| 0,544 | 0,359 | 0,333 |
| 0,326 | 0,331 | 0,312 |
| 0,531 | 0,529 | 0,533 |
| 0,599 | 0,593 | 0,598 |
| 0,331 | 0,335 | 0,332 |
| 0,578 | 0,592 | 0,585 |
| 0,318 | 0,309 | 0,303 |
| 0,353 | 0,332 | 0,346 |
| 0,371 | 0,352 | 0,345 |
| 0,353 | 0,356 | 0,348 |
| 0,364 | 0,359 | 0,362 |
| 0,381 | 0,374 | 0,379 |
| 0,346 | 0,37 | 0,353 |
| 0,34 | 0,335 | 0,34 |
| 0,356 | 0,398 | 0,371 |
| 0,393 | 0,406 | 0,409 |
| 0,685 | 0,659 | 0,634 |
| 0,338 | 0,352 | 0,355 |
| 0,344 | 0,388 | 0,367 |
| 0,34 | 0,347 | 0,39 |
| 0,36 | 0,368 | 0,375 |
| 0,354 | 0,348 | 0,361 |
| 0,385 | 0,373 | 0,393 |
| 0,356 | 0,351 | 0,375 |

| | | |
|-------|-------|-------|
| 0,365 | 0,357 | 0,359 |
| 0,365 | 0,347 | 0,353 |
| 0,362 | 0,346 | 0,353 |
| 0,444 | 0,428 | 0,44 |
| 0,393 | 0,388 | 0,406 |
| 0,44 | 0,411 | 0,455 |
| 0,413 | 0,383 | 0,4 |
| 0,391 | 0,367 | 0,394 |
| 0,388 | 0,379 | 0,38 |
| 0,319 | 0,313 | 0,293 |
| 0,524 | 0,526 | 0,534 |

| | | |
|-------|-------|-------|
| 0,021 | 0,018 | 0,026 |
| 0,092 | 0,098 | 0,105 |
| 0,087 | 0,104 | 0,107 |
| 0,079 | 0,078 | 0,073 |
| 0,1 | 0,07 | 0,072 |
| 0,101 | 0,079 | 0,057 |
| 0,136 | 0,113 | 0,117 |
| 0,056 | 0,075 | 0,075 |
| 0,065 | 0,076 | 0,073 |
| 0,114 | 0,119 | 0,118 |
| 0,153 | 0,148 | 0,153 |
| 0,137 | 0,155 | 0,151 |
| 0,105 | 0,096 | 0,082 |
| 0,05 | 0,052 | 0,049 |
| 0,057 | 0,056 | 0,062 |
| 0,216 | 0,225 | 0,226 |
| 0,221 | 0,218 | 0,206 |
| 0,136 | 0,113 | 0,117 |



=====

=====

Supplementary data 13

Predicting potential epitope regions from reactive linear overlapping peptide sequences of the Metalloprotease and Disintegrin-like domains using mapping studies.

Linear overlapping amino acid sequences with potential epitopes are highlighted yellow in mapping studies. Peptide names are derived from relevant domain name and the relevant amino acid position relative to the coding region of full-length ADAMTS13 protein.

Mapping 1:

IgG autoantibodies isolated from individual plasma samples of HIV-associated TTP and HIV positive groups all showed reactivity to peptide MP1 only and not to adjacent overlapping linear peptides.

| Peptide sequence | amino acid position |
|-------------------------|----------------------------|
| AAGGI LHLELLVAVGPDVFQ | 75-94 |
| LHLELLVAVGPDVFQAHQED | 80-99 |
| LVAVGPDVFQAHQEDTERYV | 85-104 |
| PDVFQAHQEDTERYVLTNLN | 90-109 |
| AHQEDTERYVLTNLNIGAEL | 95-114 |

A potential epitope with amino acid residue sequence “AAGGI” from the N-terminal side of the Metalloprotease domain is suggestive. The amino acid sequence “AAGGI” is found at the proximal part of the ADAMTS13 Metalloprotease domain at position 75 – 80.

Mapping 2:

IgG autoantibodies reacted to linear peptide MP9 and MP10.

| Peptide sequence | amino acid position |
|-------------------------|----------------------------|
| LGAQFRVHLVKMVLTEPEG | 115-134 |
| RVHLVKMVLTEPEGAPNIT | 120-139 |

A potential epitopic region lies in the amino acid sequence “RVHLVKMVLTEPEG” at position 125-139 on the full ADAMTS13 nucleotide sequence in the region coding the Metalloprotease domain. No binding of IgG’s was observed from adjacent peptides, suggesting that an IgG antibody may possibly recognize and bind to this fragment.

IgG antibodies isolated from individual plasma samples of both groups shared linearity to this epitope.

Mapping 3:

Two HIV positive samples showed IgG antibody binding to linear overlapping peptides MP1-MP10. If we consider the possibility that IgG's from this samples also bound to the peptide MP1 amino acid sequence "AAGGI", similar to antibodies in mapping one and "RVHLVKMVLTEPEG" in mapping 2, sharing linearity with the rest of the samples. Then linear overlapping peptides MP2 – MP8 may contain another potential epitope region.

| Peptide sequence (MP2-MP8) | amino acid position |
|-----------------------------------|----------------------------|
| LHLELLVAVGPDVFQAHQED | 88 - 99 |
| LVAVGPDVFQAHQEDTERYV | 85 - 104 |
| PDVFQAHQEDTERYVLTNLN | 90 - 109 |
| AHQEDTERYVLTNLNIGAEL | 95 - 114 |
| TERYVLTNLNIGAELLRDP | 100 - 119 |
| LTNLNIGAELLRDP | 105 - 124 |
| IGAELLRDP | 110 - 129 |

Amino acid sequence "LVAVGPDVFQAHQEDTERYVLTNLNIGAELLRDP" from position 80 – 124 contains potential epitopic region for binding IgG antibodies.

Mapping 4:

IgG autoantibody binding to linear overlapping peptides MP18 – MP21 and MP19-MP20 and MP19-MP21.

| Peptide sequence (MP19-MP20) | amino acid position |
|-------------------------------------|----------------------------|
| DDTDPGHADLVLYITRFDLE | 165 - 184 |
| GHADLVLYITRFDLELPDGN | 170 - 194 |

| Peptide sequence (MP18-MP21) | amino acid position |
|-------------------------------------|----------------------------|
| TINPEDDTDPGHADLVLYIT | 160 - 179 |
| DDTDPGHADLVLYITRFDLE | 165 - 184 |
| GHADLVLYITRFDLELPDGN | 170 - 189 |
| VLYITRFDLELPDGNRQVRG | 175 - 194 |

| Peptide sequence (MP19-MP21) | amino acid position |
|-------------------------------------|----------------------------|
| DDTDPGHADLVLYITRFDLE | 165 - 184 |
| GHADLVLYITRFDLELPDGN | 170 - 189 |
| VLYITRFDLELPDGNRQVRG | 175 - 194 |

Epitopic region lies in the amino acid sequence "DDTDPGHADLVLYITRFDLELPDGN" from position 169-189. About 37 HIV-associated TTP samples had IgG autoantibodies binding peptide MP19 and MP20 only with overlapping residues "GHADLVLYITRFDLE" as potential epitopic region. While 16 HIV-associated TTP samples and 5 HIV positive samples had IgG autoantibodies binding to peptide

MP18/19 - MP21 with potential epitopic region “VLYITRFDLE”. Interesting is that this potential epitope region lies in close proximity with possible subsites of ADAMTS13 Metalloprotease domain that interact with VWF (Xiang *et al.* 2011).

Mapping 5:

Reactive peptides MP25 – MP28.

| Peptide sequence | amino acid position |
|---------------------------------------|----------------------------|
| VTQLG GACSPTWSCLITEDT | 195 - 214 |
| GACSPTWSCLITEDTGFDLG | 200 - 219 |
| TWSCLITEDTGFDLGV TIAH | 205 - 224 |
| ITEDTGFDLGV TIAH HEIGHS | 210 - 229 |

The linear peptides overlap with amino acid sequence “GACSPTWSCLITEDTGFDLGV**TIAH**” which suggest a potential epitope lies in this region. This sequence is located at position 200-224, which lies in close proximity to the active site cleft responsible for proteolysis of VWF. The histidine amino acid in this epitopic region is also reported to play a part in coordinating the Zn²⁺ ion in the sequence. An epitope consist predominantly of hydrophobic amino acids in the center flanked by charged residues often found close to the surface (Rubinstein *et al.* 2008). Considering this characteristic, amino acid sequence “**ITEDTGFDLGV**TIAH” may be the potential epitope.

10 HIV-associated TTP plasma samples and 10 HIV positive plasma samples had IgG antibodies binding this region,

Mapping 6:

Reactive peptides MP29-MP34.

| Peptide sequence | amino acid position |
|--|----------------------------|
| GFDL GV TIAHEIGHS F GLEH | 215 – 234 |
| VTIA HEIGHS F GLEHDGAPG | 220 - 239 |
| EIGHS FGLEHDGAPG SGCGP | 225 - 244 |
| FGLE HDGAPG SGCGP SGHVM | 230 - 249 |
| DGAP SGCGP SGHVM ASDGA | 235 - 254 |
| SGCGP SGHVMASDGA APRAG | 240 - 259 |

A potential epitopic region lies in the overlapping amino acid sequence “VTIAHEIGHS**F**GLEHDGAPG**SGCGP**SGHVMASDGA” from position 220 – 244. This region contains the catalytic amino acid sequence, which is necessary for ADMATS13 Metalloprotease domain to

perform its proteolysis function. Only 2 HIV positive samples had IgG antibodies binding this region, No antibody binding was observed from the HIV-associated TTP group.

Mapping 7:

Reactive peptides MP33 – MP36.

| Peptide sequence | amino acid position |
|-------------------------|----------------------------|
| DGAPGSGCGPSGHVMASDGA | 235 – 245 |
| SGCGPSGHVMASDGAAPRAG | 240 - 259 |
| SGHVMASDGAAPRAGLAWSP | 245 - 264 |
| ASDGAAPRAGLAWSPCSRQ | 250 - 269 |

A potential epitopic region is located in amino acid sequence “SGCGPSGHVMASDGAAPRAGLAWSP” located at position 240 – 264 on the full ADAMTS13 nucleotide sequence. Only 3 HIV-associated TTP samples had IgG antibodies binding to these peptides, No binding was observed in the HIV positive group.

Mapping 8:

Reactive peptides MP37 – MP39 and MP37 – MP/Dis40.

| Peptide sequence | amino acid position |
|-------------------------|----------------------------|
| APRAGLAWSPCSRQLLSLL | 255 - 274 |
| LAWSPCSRQLLSLLSAGRA | 260 - 279 |
| CSRQLLSLLSAGRARCVD | 265 - 284 |
| LLSLLSAGRARCVDPPRPQ | 270 - 289 |

96% of HIV-associated TTP samples had IgG antibodies binding linear overlapping peptides with a potential epitope region with amino acid sequence “LAWSPCSRQLLSLLSAGRARCVD” from position 260 – 284 on the full ADAMTS13 nucleotide sequence. With potential epitope residues, “CSRQLLSLL” for antibodies binding MP37-MP39 and epitope “LLSLLSAGRA” for samples with antibodies to MP37-MP/Dis40. 51 plasma samples from the HIV-associated TTP group had IgG antibodies to this epitope region, while only 1 HIV positive had antibody binding. This sequence also contains the ADAMTS13 subsite at position 274, which is important for ADAMTS13 interactions with VWF (Xiang *et al.* 2011).

Mapping 9:

Reactive peptide MP40/MP41 – MP/Dis44.

| Peptide sequence | amino acid position |
|-------------------------|----------------------------|
| LLSLLSAGRARCWDPDRPQ | 270 - 289 |
| SAGRARCWDPDRPQGSAG | 275 - 294 |
| RCWDPDRPQGSAGHPPDA | 280 - 299 |
| DRPQGSAGHPPDAQGLY | 285 - 304 |
| GSAGHPPDAQGLYYSANE | 290 - 309 |

Antibodies from 2 HIV positive sample reacted with this peptides, with a potential epitope in the amino acid sequence “SAGRARCWDPDRPQGSAGHPPDAQGLY” at position 275 – 304 of the ADAMTS13 nucleotide sequence.

Mapping 10:

Reactive peptides MP/Dis43 – Dis48.

| Peptide sequence | amino acid position |
|-------------------------|----------------------------|
| DRPQGSAGHPPDAQGLY | 285 - 304 |
| GSAGHPPDAQGLYYSANE | 290 - 309 |
| HPPDAQGLYYSANEQCRVA | 295 - 314 |
| QGLYYSANEQCRVAFGPKA | 300 - 319 |
| YSANEQCRVAFGPKAVACTF | 305 - 324 |
| QCRVAFGPKAVACTFAREHL | 310 – 334 |

A potential epitopic region in the amino acid sequence was detected by binding IgG antibodies from 4 HIV-associated TTP plasma samples. The epitopic sequence “GSAGHPPDAQGLYYSANEQCRVAFGPKAVACTF” is located from position 290 – 324 on the full ADAMTS13 nucleotide sequence,

Mapping 11:

The IgG antibody binding to various linear overlapping peptides of the Disintegrin-like domain was observed from individual HIV-associated TTP and HIV positive plasma samples. Several potential epitope regions were identified in 53% of the HIV-associated TTP plasma samples having IgG antibody binding various sections of linear overlapping peptides from Dis49 – Dis/TSP1-1 59. While 83% of the HIV positive plasma samples also showed IgG antibody binding to these various section. Antigenic linear peptides are listed below.

Reactive peptides Dis49 – Dis52.

| Peptide sequence | amino acid position |
|-------------------------|----------------------------|
| FGPKA VACTFAREHLDMCQA | 315 - 334 |
| VACTFAREHLDMCQALSCHT | 320 - 339 |
| AREHLDMCQALSCHTDPLDQ | 325 - 345 |
| DMCQALSCHTDPLDQSSCSR | 330 - 349 |

A potential epitope sequence “VACTFAREHLDMCQALSCHTDPLDQ” with IgG antibodies binding from 4 HIV-associated TTP samples. This amino acid sequence is located from position 320 – 345 on the full ADAMTS13 nucleotide sequence.

Reactive peptides Dis55 – Dis/TSP1-1 59.

| Peptide sequence (Dis55-Dis/TSP1-1 59) | amino acid position |
|---|----------------------------|
| SSCSR LLVPLLDGTECGVEK | 345 - 364 |
| LLVPLLDGTECGVEKWCSKG | 350 - 369 |
| LDGTECGVEKWCSKGRCRSL | 355 - 374 |
| CGVEKWCSKGRCRSLVELTP | 360 - 379 |
| WCSKGRCRSLVELTPIAAVH | 365 - 383 |

A potential epitopic region lies in the amino acid sequence “LLVPLLDGTECGVEKWCSKGRCRSLVELTP” located from 350 – 379 on the full ADAMTS13 nucleotide sequence. Two HIV-associated TTP samples and 1 HIV-positive sample showed IgG autoantibody binding.

Reactive peptide Dis56 – Dis/TSP1-1 59.

| Peptide sequence (Di56-Dis/TSP1-1 59) | amino acid position |
|--|----------------------------|
| LLVPLLDGTECGVEKWCSKG | 350 - 369 |
| LDGTECGVEKWCSKGRCRSL | 355 - 374 |
| CGVEKWCSKGRCRSLVELTP | 360 - 379 |
| WCSKGRCRSLVELTPIAAVH | 365 - 383 |

A potential epitopic region lies in the amino acid sequence “LDGTECGVEKWCSKGRCRSLVELTP” located from 355– 379 on the full ADAMTS13 nucleotide sequence. IgG autoantibodies from 2 HIV-associated TTP plasma samples showed reactivity.

Reactive peptide Dis57 – Dis/TSP1-1 59.

| Peptide sequence (Dis57 – Dis/TSP1-1 59) | amino acid position |
|---|----------------------------|
| LDGTECGVEK WCSKGRCRSL | 355 - 374 |
| CGVEK WCSKGRCRSL VELTP | 360 - 379 |
| WCSKGRCRSL VELTPIAAVH | 365 - 383 |

Amino acid sequence “WCSKGRCRSL” is identified as a potential epitope for binding IgG antibodies. This sequence is located from 365 – 374 in the coding the Disintegrin-like domain of ADAMTS13 nucleotide sequence. Only one HIV-associated TTP plasma sample showed IgG antibody binding this linear peptide.

Reactive peptide Dis58 – Dis/TSP1-1 59.

| Peptide sequence (Dis58 – Dis/TSP1-1 59) | amino acid position |
|---|----------------------------|
| CGVEK WCSKGRCRSLVELTP | 360 - 379 |
| WCSKGRCRSLVELTP IAAVH | |

Two HIV-associated TTP samples showed IgG antibody binding to these peptides, with a potential epitope identified by amino acid sequence “WCSKGRCRSLVELTP” located from position 365 – 374.

Reactive peptide Dis53 – Dis/TSP1-1 59.

| Peptide sequence (Dis53 – Dis/TSP1-1 59) | amino acid position |
|---|----------------------------|
| LSCHT DPLDQSSCSRLLVPL | 335 - 354 |
| DPLDQSSCSRLLVPLLDGTEC | 340 - 359 |
| SSCSRLLVPLLDGTECGVEK | 345 - 364 |
| LLVPLLDGTECGVEKWCSKG | 350 - 369 |
| LDGTECGVEKWCSKGRCRSL | 355 - 374 |
| CGVEKWCSKGRCRSLVELTP | 360 - 379 |
| WCSKGRCRSLVELTP IAAVH | 365 – 383, |

Five (5) HIV-associated TTP plasma samples and 4 HIV positive plasma samples had IgG antibodies binding linear overlapping peptide Dis53 – Dis/TSP1-1 59 of the Disintegrin-like domain. A potential epitopic region with the amino acid sequence “SSCSRLLVPLLDGTECGVEKWCSKGRCRSLVELTP was identified, This sequence is located from position 340 – 379 on the full ADAMTS13 nucleotide sequence.

Amino acid sequence “WCSKGRCRSLVELTP” was constantly involved in antibody binding.

Locating potential antibody binding amino acid sequences on the full ADAMTS13 nucleotide sequence from position: 1 - 421

MHQRHPRARCPLCVAGILACGFLGCGWGPSHFQQSCLQALEPQAVSSYLSPGAPLKGRPPSPGFQRQRQRRAAGGILHLELLVAVGPDVFAQHQEDT
ERYVLTNLNIGAELLRDP SLGAQFRVHLVKMVLTEPEGAPNITANLTSSL SVCGWSQTINPEDD TDPGHADLVLYITRFDELELPDGNRQVRGVTQLGG
ACSP TWSCLITEDTGFDLGVTIAHEIGH SFLEH DGAPSGCGPSGHVMSDGAAPRAGLAWSPCSRRLLSLLSAGRARCWWDPPRPQPGSAGHPPDAQ
PGLYY SANEQRVAFGPKAVACTFAREHLDMCQALSCHTDPLDQSSCSRLLVPLLDGTECGVEKWCSKGRCRSLVELTPIAAVHGRWSSWGPRSPCSRSCG
GGVTRRRQCNNPRPAFGGRACVGADLQAEMCNTQACEKTQLEFMSQQCARTDGP LRSPPGGASFYHWGA AVPHSQGD

The ADAMTS13 Metalloprotease domain and the Disintegrin-like domain (1-421) with potential epitope regions highlighted yellow.

Predicting potential epitope regions from reactive linear overlapping peptide sequences of the Cysteine-rich domain and Spacer domain.

Anti-DAMTS13 IgG antibodies isolated from HIV-associated TTP plasma samples target major binding sites on the Cysteine-rich and the Spacer domains. Less reactivity was observed from IgG antibodies isolated from the HIV positive plasma samples.

Mapping 1:

Reactive linear overlapping peptides Cys1-Cys6, with the majority of HIV-associated TTP samples (23/53) having IgG antibodies binding to peptides Cys2-Cys5, followed by reactivity to peptides Cys3-Cys6 (10/53) and Cys3-Cys5. About 5 HIV positive samples also had IgG autoantibodies binding to the same peptide sequences.

| Peptide sequence Cys1 – Cys6 | amino acid position |
|-------------------------------------|----------------------------|
| KTQLEFMSQQCARTDGQPLR | 440 - 459 |
| FMSQQCARTDGQPLRSPGG | 445 - 464 |
| CARTDGQPLRSPGGASFYH | 450 - 469 |
| GQPLRSPGGASFYHWGAAV | 455 - 474 |
| SSPGGASFYHWGAAVPHSQG | 460 - 479 |
| ASFYHWGAAVPHSQGDALCR | 465 – 484 |

A potential epitopic region lies in the amino acid sequence “FMSQQCARTDGQPLRSPGGASFYHWGAAVPHSQG located from position 445 – 479 of the full ADAMTS13 nucleotide sequence. With a common epitopic region for these samples located at position 455-469 with amino acid sequence “GQPLRSPGGASFYH”.

Mapping 2:

Reactive peptide Cys7 – Cys10.

| Peptide sequence | amino acid position |
|-------------------------|----------------------------|
| WGAAVPHSQGDALCRHMCRA | 470 - 489 |
| PHSQGDALCRHMCRAIGESF | 475 - 494 |
| DALCRHMCRAIGESFIMKRG | 480 - 504 |
| HMCRAIGESFIMKRGDSFLD | 485 - 504 |

About 16/53 HIV-associated TTP samples and 5 HIV positive samples showed IgG antibody binding to peptide sequence Cys7-Cy10 with a potential epitopic residues “PHSQGDALCRHMCRAIGESFIMKRG” located from position 475-504. All sharing a common amino acid residue “HMCRA” in the overlapping region.

Mapping 3:

A potential epitopic region is identified from reactive peptides Cys13- Cys/Spa20 with overlapping amino acid sequence “GTRCMPSPGPRE~~DTL~~SLCVSGSCRTFGCDGRMDSQQVWDR~~CQVCG~~” by IgG antibodies from the HIV-associated TTP group only. No binding was detected from IgG antibodies of individual HIV positive plasma samples.

About 7/53 samples showed IgG binding to Cys13-Cys16.

| <u>Peptide sequence (Cys13-Cys16)</u> | <u>amino acid position</u> |
|--|-----------------------------------|
| DSFLD GTRCMPSPGPREDTL | 500 - 519 |
| GTRCMPSPGPREDTLSLCVS | 505 - 524 |
| PSGPREDTLSLCVSGSCRT | 510 - 529 |
| EDGTLSLCVSGSCRT FGCDG | 515 – 534 |

A potential epitope region with amino acid sequence “GTRCMPSPGPRE~~DTL~~SLCVSGSCRT” located from position 505-529 on the full ADAMTS13 nucleotide sequence is identified.

About 35/53 samples showed IgG binding to Cys17-Cys/Spa20.

| <u>Peptide sequence (Cys17-Cys/Spa20)</u> | <u>amino acid position</u> |
|--|-----------------------------------|
| SLCVS GSCRTFGCDGRMDSQ | 535 - 554 |
| GSCRTFGCDGRMDSQQVWDR | 540 - 559 |
| FGCDGRMDSQQVWDRCQVCG | 545 - 564 |
| RMDSQQVWDRCQVCG GDNST | 550 - 554 |

A potential epitope region with amino acid sequence “GSCRTFGCDGRMDSQQVWDR~~CQVCG~~” located from position 540-564 on the full ADAMTS13 nucleotide sequence is identified.

Mapping 4:

Only 1 plasma sample from the HIV-associated TTP group showed IgG antibody binding to peptides Spa24-Spa28.

| <u>Peptide sequence</u> | <u>amino acid sequence</u> |
|---|-----------------------------------|
| CSPRK GSFTAGRAREYVTFL | 555 - 574 |
| GSFTAGRAREYVTFLTVTPN | 560 - 579 |
| GRAREYVTFLTVTPNLTSVY | 565 - 584 |
| YVTFLTVTPNLTSVYIANHR | 570 - 589 |
| TVTPNLTSVYIANHR PLFTH | 575 - 604 |

The IgG autoantibodies binding identified a potential epitope region in amino acid sequence “GSFTAGRAREYVTF~~L~~TVTPN~~L~~TSVYIANHR” located from position 560–586 on the full ADAMTS13 nucleotide sequence coding the Spacer domain.

Mapping 5:

About 42 HIV-associated TTP samples and 1 HIV positive samples showed IgG antibody binding to linear overlapping peptides Spa31-Spa34.

| <u>Peptide sequence</u> | <u>amino acid position</u> |
|--------------------------------|-----------------------------------|
| PLFTHLAVRIGGRYVVAGKM | 590 - 609 |
| LAVRIGGRYVVAGKMSISP | 595 - 614 |
| GGRYVVAGKMSISPNTTYP | 600 - 619 |
| VAGKMSISPNTTYP | 605 - 624 |

The IgG autoantibodies binding revealed a potential epitopic region with overlapping amino acid sequence “LAVRIGGRYVVAGKMSISPNTTYP” located at position 595 – 619 on the full ADAMTS13 nucleotide sequence coding the Spacer domain.

Mapping 6:

Reactive peptides Spa37-Spa40.

| <u>Peptide sequence</u> | <u>amino acid position</u> |
|--------------------------------|-----------------------------------|
| LLEDGRVEYRVALTEDRLPR | 620 - 639 |
| RVEYRVALTEDRLPRLEEIR | 625 - 644 |
| VALTEDRLPRLEEIRIWGPL | 630 - 649 |
| DRLPRLEEIRIWGPLQEDAD | 635 - 654 |

The IgG autoantibodies binding from 27 HIV-associated TTP plasma samples and 4 HIV positive plasma samples revealed a potential epitopic region with overlapping amino acid sequence “RVEYRVALTEDRLPRLEEIRIWGPL” located at position 625-649 on the full ADAMTS13 nucleotide sequence.

IgG autoantibodies from 2 HIV-associated TTP plasma samples also showed reactivity to peptide Spa31-Spa39, probably sharing same epitopic regions with IgG’s in mapping 4 and 5.

Mapping 7:

All HIV-associated TTP plasma samples and only 1 HIV positive sample showed IgG autoantibody binding to linear overlapping peptides Spa42 – Spa/TSP1-2 46.

| Peptide sequence | amino acid position |
|-------------------------|----------------------------|
| IWGPLQEDADIQVYRRYGEE | 645 - 664 |
| QEDADIQVYRRYGEEYGNLT | 650 - 669 |
| IQVYRRYGEEYGNLTRPDIT | 655 - 674 |
| RYGEEYGNLTRPDITFTYFQ | 660 - 669 |
| YGNLTRPDITFTYFQPKPRQ | 665 - 684 |

A potential epitopic region with amino acid sequence “QEDADIQVYRRYGEEYGNLTRPDITFTYFQ” is identified and is located at position 650-669 on the full ADAMTS13 nucleotide sequence in the region coding the Spacer domain.

Locating potential antibody binding amino acid sequences on the full ADAMTS13 nucleotide sequence from position 440-680

VWDRQCQVCGG DNSTCSPRK**G SFTAGRAREY VTFLTVPNL TSVYIANHRP LFTHLAVRIG GRYVVAGKMS ISPNTTYP**SL
 LEDGR**VEYRV** **ALTEDRLPRL EEIRIWGPLQ EDADIQVYRR YGEEYGNLTR PDITFTYFQ**P KPRQAWVWAA VRGPCSVSCG
 AGLRWVNYSC LDQARKELVE

The ADAMTS13 Cysteine-rich domain and the Spacer domain (440-680) with potential epitope regions highlighted yellow.